

**THE DYNAMIC TUMOUR MICROENVIRONMENT:
FROM TUMOUR PERFUSION TO DIFFERENTIAL GENE EXPRESSION**

by

KEVIN LESLIE BENNEWITH

B.Sc. (Chemistry), The University of British Columbia, 1997

A THESIS SUBMITTED IN PARTIAL FULFILMENT OF THE
REQUIREMENTS FOR THE DEGREE OF DOCTOR OF PHILOSOPHY

in

THE FACULTY OF GRADUATE STUDIES
(Department of Pathology and Laboratory Medicine)

We accept this thesis as conforming to the required ~~st~~andard

THE UNIVERSITY OF BRITISH COLUMBIA

September 2004

© Kevin Leslie Bennewith, 2004

ABSTRACT

Solid tumours can contain areas of poor oxygenation and nutrient status, and tumour cells in these regions can limit tumour response to therapy. Increasing evidence suggests that the tumour microenvironment can be dynamic, with temporally varying blood flow and oxygen tensions in different tumour regions inducing a variety of gene expression profiles in populations of cells. Cellular hypoxia that varies over time is a poorly understood feature of many tumours, but is thought to represent a key factor contributing to therapy failure.

This thesis investigated the solid tumour microenvironment by demonstrating the therapeutic relevance of transient tumour perfusion and transiently hypoxic tumour cells, while developing methods to specifically identify and quantify these cells in human tumour xenografts. During the course of these studies, a number of interesting and novel insights into tumour hypoxia and the dynamic tumour microenvironment became evident, which may have far-reaching implications for clinical cancer therapy.

The therapeutic relevance of dynamic tumour perfusion was established by pharmaceutically manipulating tumour blood flow to increase the radiation sensitivity of specific tumour cell subpopulations. Changes in tumour cell hypoxia over time were studied by sequentially administering two exogenous “markers” of hypoxia followed by quantification of tumour cells containing bound marker by flow cytometry. Tumour hypoxia was measured continuously (i.e. was “integrated”) over periods of time ranging from hours to days using multiple injections or oral administration of the hypoxia marker pimonidazole, indicating temporal changes in the hypoxic status of some tumour cells.

Tumour hypoxia was also studied more implicitly *in vitro*, using multicellular spheroids to mimic the disparate tumour microenvironments associated with tumour hypoxia. Global gene expression patterns of cells from different microenvironmental conditions were compared using serial analysis of gene expression, and a number of genes were significantly differentially

expressed. Products of these differentially expressed genes may provide a means to selectively study the therapeutic implications of transiently hypoxic tumour cells *in vivo*.

Overall, improving our understanding of the dynamic tumour microenvironment (from temporally varying tumour perfusion and hypoxia to differential gene expression) has important implications for the strategic improvement of clinical cancer therapy.

TABLE OF CONTENTS

ABSTRACT.....	ii
TABLE OF CONTENTS.....	iv
LIST OF TABLES.....	vii
LIST OF FIGURES.....	viii
LIST OF ABBREVIATIONS.....	x
ACKNOWLEDGEMENTS.....	xii
CHAPTER 1: INTRODUCTION.....	1
1.1 THE MICROENVIRONMENT OF SOLID TUMOURS.....	2
1.1.1 Physiology of Normal and Pathological Tissues.....	2
1.1.2 Structure and Function of Tumour Blood Vessels.....	3
1.2 CLASSIFICATION OF TUMOUR HYPOXIA.....	8
1.2.1 "Chronic" and "Diffusion-Limited" Hypoxia.....	9
1.2.1.1 Nomenclature.....	10
1.2.1.2 Variables affecting diffusion-limited hypoxia.....	12
1.2.2 "Transient" and "Intermittent" Hypoxia.....	13
1.3 TUMOUR PHYSIOLOGY AND CANCER THERAPY.....	17
1.3.1 Radiotherapy.....	17
1.3.2 Chemotherapy.....	20
1.4 TUMOUR MICROENVIRONMENT AND GENE EXPRESSION.....	23
1.4.1 Hypoxia-Induced Gene Expression.....	23
1.4.2 Tumour Metabolism.....	25
1.4.3 Carbonic Anhydrases.....	25
1.5 METHODS FOR MEASURING TUMOUR HYPOXIA.....	28
1.5.1 Physical Measurements of Tumour Oxygenation.....	28
1.5.2 Exogenous Hypoxia Markers.....	30
1.5.2.1 Radiolabeled misonidazole.....	31
1.5.2.2 Binding of 2-nitroimidazoles.....	33
1.5.2.3 CCI-103F.....	36
1.5.2.4 Pimonidazole.....	38
1.5.2.5 EF5.....	40
1.5.2.6 Quantification of pimonidazole and EF5.....	41
1.5.3 Endogenous Hypoxia Markers.....	43
1.5.3.1 Hypoxia inducible factor-1 α	43
1.5.3.2 Carbonic anhydrase 9.....	45
1.6 RESEARCH OBJECTIVES.....	48
1.6.1 Specific Aims.....	48
1.6.2 Thesis Overview.....	49

CHAPTER 2: MODIFYING TUMOUR PERFUSION TO IMPROVE TUMOUR RADIOSENSITIVITY	50
2.1 INTRODUCTION	51
2.2 MATERIALS AND METHODS.....	54
2.2.1 Tumours	54
2.2.2 Reagents.....	54
2.2.3 Rubidium-86 (Rb ⁸⁶) Extraction.....	54
2.2.4 Dual Stain Mismatch.....	55
2.2.5 Fluorescence Activated Cell Sorting	59
2.2.6 <i>In Vivo-In Vitro</i> Cloning Assay	60
2.2.7 Statistics	61
2.3 RESULTS	62
2.3.1 Drug-Induced Changes in Net Tumour Perfusion	62
2.3.2 Pentoxifylline-Induced Changes in Microregional Tumour Perfusion.....	62
2.3.3 Impact of Tumour Perfusion Modification on Tumour Cell Radiosensitivity	65
2.4 DISCUSSION	67
 CHAPTER 3: QUANTIFYING TRANSIENT TUMOUR HYPOXIA BY FLOW CYTOMETRY.....	 71
3.1 INTRODUCTION	72
3.2 MATERIALS AND METHODS.....	77
3.2.1 Tumours and Reagents.....	77
3.2.2 Fluorescence Activated Cell Sorting	77
3.2.3 Antibodies	78
3.2.4 Flow Cytometry	78
3.2.5 Statistics	79
3.3 RESULTS	80
3.3.1 “Time-Integrated” Pimonidazole Labeling in SiHa Tumours	80
3.3.2 Evidence of Transient Hypoxia in SiHa Tumours	82
3.3.3 Transient Hypoxia in WiDr Tumours	86
3.4 DISCUSSION	91
 CHAPTER 4: ORALLY ADMINISTERED PIMONIDAZOLE TO LABEL HYPOXIC TUMOUR CELLS	 100
4.1 INTRODUCTION	101
4.2 MATERIALS AND METHODS.....	103
4.2.1 Common Materials and Methods.....	103
4.2.2 Iododeoxyuridine	103
4.2.3 Pimonidazole Pharmacokinetics	103
4.3 RESULTS	105
4.3.1 SiHa Tumour Cells Labeled with Oral Pimonidazole	105
4.3.2 Relative Fluorescence Intensity of Oral Pimonidazole-Labeled Tumour Cells ..	105
4.3.3 Oral Pimonidazole and Transiently Hypoxic SiHa Tumour Cells.....	109
4.3.4 Oral Pimonidazole and Proliferative Capacity of SiHa Tumour Cells	111
4.3.5 Oral Pimonidazole to Label Hypoxic WiDr Tumour Cells	111
4.3.6 Pimonidazole Pharmacokinetics	116
4.4 DISCUSSION	120

CHAPTER 5: MICROENVIRONMENT-INDUCED DIFFERENTIAL GENE	
EXPRESSION	124
5.1 INTRODUCTION	125
5.2 MATERIALS AND METHODS.....	130
5.2.1 Multicellular Spheroids.....	130
5.2.2 Fluorescence Activated Cell Sorting	130
5.2.3 Modeling Tumour Hypoxia with Spheroids	131
5.2.4 Serial Analysis of Gene Expression.....	133
5.2.5 DISCOVERYspace.....	135
5.3 RESULTS	137
5.3.1 Summary of SAGE Data.....	137
5.3.2 SAGE Tags Differentially Expressed Between Chronic and Transient Hypoxia.....	137
5.4 DISCUSSION.....	145
5.4.1 Metallothionein IIA and RTP801	146
5.4.2 Indications of Microenvironmentally-Influenced Differential Gene Expression.....	147
5.4.3 CD151	149
CHAPTER 6: SUMMARY AND FUTURE DIRECTIONS.....	153
6.1 SUMMARY.....	154
6.2 FUTURE DIRECTIONS	158
REFERENCES	162

LIST OF TABLES

5.1	Summary of abundance classes for SAGE libraries.	136
5.2	Identification of selected tags from Figures 5.4-5.6.	140
5.3	Identification of selected tags from Figure 5.7.	144

LIST OF FIGURES

1.1	Illustration of vasculature in normal and tumour tissue.....	5
1.2	Diffusion-limited hypoxia.....	11
1.3	Cellular metabolism in the presence and absence of oxygen.	26
1.4	Structures of exogenous hypoxia markers.	32
1.5	Mechanism of 2-nitroimidazole binding in hypoxic cells.	34
2.1	Diagram of the Rb ⁸⁶ extraction method.	56
2.2	Illustration of dual stain mismatch experiments.	58
2.3	Relative net tumour perfusion measured by Rb ⁸⁶ extraction.	63
2.4	Dual stain mismatch data showing changes in the microregional distribution of tumour blood flow 15 and 30 minutes after administration of pentoxifylline.....	64
2.5	Radiosensitivity data for SiHa and WiDr tumours with pentoxifylline administered prior to tumour irradiation.....	66
3.1	SiHa tumour cells labeled with pimonidazole.	81
3.2	Sorted SiHa tumour cells labeled with CCI-103F and/or pimonidazole.	83
3.3	Representative flow cytometry dot plots showing hypoxic SiHa tumour cells labeled with pimonidazole and CCI-103F.....	85
3.4	WiDr tumour cells labeled with pimonidazole.	87
3.5	Sorted WiDr tumour cells labeled with CCI-103F and/or pimonidazole.	89
3.6	Representative flow cytometry dot plots showing hypoxic WiDr tumour cells labeled with pimonidazole and CCI-103F.....	90
3.7	Comparison of different pimonidazole doses on the relative fluorescence intensity of pimonidazole-labeled cells and the fraction of pimonidazole-labeled cells.	93
3.8	Dual stain mismatch data for untreated WiDr and SiHa human tumour xenografts.	94
4.1	SiHa tumour cells labeled with oral pimonidazole.	106

4.2	Relative fluorescence intensity of SiHa tumour cells labeled with oral pimonidazole. ...	108
4.3	Sorted SiHa tumour cells labeled with CCI-103F and/or oral pimonidazole.	110
4.4	Sorted SiHa tumour cells labeled with IdUrd and/or oral pimonidazole.	112
4.5	WiDr tumour cells labeled with oral pimonidazole.	113
4.6	Sorted WiDr tumour cells labeled with CCI-103F and/or oral pimonidazole.	114
4.7	Sorted WiDr tumour cells labeled with IdUrd and/or oral pimonidazole.	117
4.8	Pimonidazole pharmacokinetics.	118
5.1	Multicellular spheroid model.	127
5.2	Illustration of different subpopulations of cells within multicellular spheroids.	132
5.3	Diagram of serial analysis of gene expression.	134
5.4	SAGE tags differentially expressed between chronically hypoxic and aerobic cells.	138
5.5	SAGE tags differentially expressed between transiently hypoxic and aerobic cells.	139
5.6	SAGE tags differentially expressed between chronically hypoxic and transiently hypoxic cells.	141
5.7	Selected genes of interest significantly differentially expressed between chronically and transiently hypoxic cells.	143
5.8	Section of SiHa human tumour xenograft showing proximity of CD151 to perfused blood vessels and diffusion-limited hypoxia.	151

LIST OF ABBREVIATIONS

ADP	Adenosine Diphosphate
ARNT	Aryl Hydrocarbon Receptor Nuclear Translocator
ATP	Adenosine Triphosphate
bp	Base Pair
CA	Carbonic Anhydrase
cDNA	Complementary DNA
CI	Confidence Interval
CO	Cardiac Output
DiOC ₇	Carbocyanine
DMSO	Dimethyl Sulfoxide
ds	Double-Stranded
dT	Deoxythymidine
<i>E. coli</i>	<i>Escherichia coli</i>
ELISA	Enzyme-Linked Immunosorbent Assay
FACS	Fluorescence Activated Cell Sorter
FBS	Fetal Bovine Serum
FIH	Factor Inhibiting Hypoxia Inducible Factor-1
Glut	Glucose Transporter
Gy	Gray
HCl	Hydrochloric Acid
HIF	Hypoxia Inducible Factor
HPLC	High-Performance Liquid Chromatography
IdUrd	Iododeoxyuridine
i.d.	Inner Diameter
IFP	Interstitial Fluid Pressure
i.m.	Intramuscular
i.p.	Intraperitoneal
i.v.	Intravenous
keV	10 ³ Electron Volts
MAPK	Mitogen-Activated Protein Kinase
MBq	Megabecquerel

MEM	Minimal Essential Medium
MGC	Mammalian Gene Collection
mmHg	Millimeters of Mercury
mRNA	Messenger RNA
M10	Minimal Essential Medium Containing 10% Fetal Bovine Serum
OER	Oxygen Enhancement Ratio
PBS	Phosphate Buffered Saline
Pento	Pentoxifylline
PETA-3	Platelet-Endothelial Tetraspan Antigen-3; CD151
P _i	Inorganic Phosphate
Pimo	Pimonidazole; Ro 03-8799
PI3K	Phosphatidylinositol 3-Kinase
pO ₂	Partial Pressure of Oxygen; Oxygen Tension
ppm	Parts Per Million
Rb ⁸⁶	Rubidium-86
Rb ⁸⁶ Cl	Rubidium-86 Chloride
rpm	Rotations per Minute
RT-PCR	Reverse Transcriptase-Polymerase Chain Reaction
S100P	S100 Calcium Binding Protein P
SAGE	Serial Analysis of Gene Expression
s.c.	Subcutaneous
SCID	Severe Combined Immunodeficient
SiHa	Human Cervical Squamous Cell Carcinoma
VEGF	Vascular Endothelial Growth Factor
VHL	Von Hippel-Lindau Tumour Suppressor Protein
WiDr	Human Colon Adenocarcinoma

ACKNOWLEDGEMENTS

I have been extremely fortunate in my graduate studies to be trained by a very skilled group of people, and this work could not have been completed without their assistance. Firstly, I would like to thank my supervisor Dr. Ralph Durand for giving me the opportunity to work in his lab and on this project. His enormous knowledge base was an invaluable resource, and he was never “too busy” to talk about the project, despite the mountain of papers, data, blueprints, and/or grants that were constantly awaiting his attention.

Thank you to Denise McDougal for enduring the countless days of cell sorting and never-ending flow cytometry samples. Thank you to Nancy LePard for showing me how to analyze data from the aforementioned never-ending flow cytometry samples, and for running the cell sorter during our “double-up” days. Thanks to Darrell Trendall for implanting mice, plating cells, and for not complaining (too loudly) when I needed to “steal” a mouse from time to time. I should also thank you for showing me which end of the mouse was the biting end, and for demonstrating a stunning variety of ways to (not) get things into the garbage can. Thank you to Angie Nicol for teaching me how to work with spheroids, and about the intricacies (and occasional frustrations) of antibody work. Without all of you I would have no data (and this thesis would have been a lot shorter).

I was also fortunate to have a number of other laboratories nearby containing extremely helpful people (and items). Thank you to Dr. Peggy Olive for always having time to talk science, for accepting me as an “adopted” lab member (especially when food was involved), and for your valuable input into my training. Thank you to Susan MacPhail for sharing your remarkable practical knowledge about every technique I could come up with, and for all the things you do to keep the lab equipment in tip-top shape; I shudder to think how many beers I must owe you by now. Thank you to Dr. Judit Banáth for looking the other way every time I came in to the lab to borrow something, and to Laura Sinnott (dude!) for letting me take your

clean cages and for not treating me the way you treated Darrell. I must also thank Alastair Kyle and Lynsey Huxham from Dr. Andrew Minchinton's lab for enduring my barrage of questions and constant need for assistance with the pharmacokinetics experiments.

I should also thank Dr. Peter Johnston (formerly of Dr. Peggy Olive's lab) for training me in the proper use of radioactive isotopes when I first arrived; I don't glow in the dark nearly as much anymore (at least not the last time I checked). I'm sure my future children thank you too.

My sincere gratitude to our departmental administrative assistant Wil Cottingham. Thank you for all the things you do to make life easier for all of us, and for your support during life's little curveballs. You really do make the world go around.

I would also like to thank Dr. Jim Raleigh of the University of North Carolina for his invaluable expertise with exogenous hypoxia markers and for providing a seemingly endless supply of CCI-103F and CCI-103F antiserum. Our collaborators at Canada's Michael Smith Genome Sciences Centre were critical contributors to the work presented in Chapter 5. Thank you to Dr. Marco Marra and Jas Khattra for their enthusiasm and support on the SAGE project, to Jenn Asano and Pawan Pandoh for constructing the SAGE libraries, and to Dr. Agnes Baross for helping to guide me through the darkness that is SAGE data analysis. I also thank Drs. Aly Karsan, Andrew Minchinton, Cal Roskelley, and Wan Lam from my Ph.D. Supervisory Committee for their valuable input and expertise during my training.

I feel fortunate to have met and shared time with a number of other people during my graduate studies that have made the time go by very quickly! The beer went down a lot easier and tasted a lot better while sharing it with (any of) a number of people. So thanks to Graeme, Chad, Arek, Chris, Farrell, Jason, Ed, Michela, Nancy, Jenn, and a variety of others that have stopped by for a drink and/or a chat over the years. To Sheela, thank you for the countless laughs, good advice, and for "forcing" me into various Christmas parties and sumo wrestling tournaments. To Michelle, thank you for your support through a variety of "life-altering"

decisions, and for putting up with my constant teasing, mood swings, and horrendously messy desk. I also want to thank Colin and the rest of my “non-science” friends for always being willing to spend free-time watching and playing hockey, throwing a disc around, or finding new ways to beat each other to a pulp.

I would like to thank my parents (all four of them!). You have been a constant inspiration in both my professional and personal life, and your love and support have helped to make me what I am today. I hope I have made you proud.

And finally, to my wife Lauren. Thank you for believing in my ability, and for the sacrifices you have made for my career. It’s been a long road to get to this point, but it’s been so much easier with you by my side. I dedicate this thesis to you.

CHAPTER 1: INTRODUCTION

1.1 THE MICROENVIRONMENT OF SOLID TUMOURS

Tumour cells live in a rather unusual environment, typically containing malformed tumour blood vessels and chaotic vascular patterns that contribute to regions of poor perfusion, nutrient, and oxygenation status (Vaupel *et al.*, 1989). The resulting microenvironment in solid tumours can be particularly heterogeneous compared to the more structured and regulated cellular environment found in most normal tissues.

1.1.1 Physiology of Normal and Pathological Tissues

In the majority of tissues in the body, the supply of oxygen and nutrients through the bloodstream is normally sufficient to satisfy the metabolic demands of the tissue cells, and to maintain the functional capacity and general health of the tissue. Blood vessels in normal (healthy) tissues are structurally and functionally sound, spaced regularly, and are close enough together to ensure adequate diffusion of oxygen and nutrients to tissue regions that are several cell diameters away from the vasculature. The amount of oxygen and nutrients delivered to a given cell therefore depends on the oxygen and nutrient levels in the bloodstream, and the flow of blood through tissue vasculature. Some pathological conditions can lead to decreased oxygen or nutrient delivery to various tissues or organs, with serious consequences if left unchecked. Perfusion disorders, for example, resulting from partial or complete blockages of blood vessels can restrict blood flow to tissues, which is especially problematic if the tissue has a high nutrient and oxygen demand (e.g. heart and brain).

The demand for oxygen and nutrients depends on the functional and proliferative activity of the cells in question. Increases in the demand for oxygen and/or nutrients to levels greater than the blood can supply results in a net imbalance in tissue oxygen and/or nutrient status. Some tissues have inherent mechanisms to survive (temporary) periods of increased metabolic demand; skeletal muscle, for example, is capable of anaerobic energy metabolism (Section 1.4.2) during periods of rigorous exercise. When coupled with the increases in blood flow (heart rate) and

blood oxygenation (breathing rate) associated with exercise, the tissue adaptations help to maintain tissue function and health until “normal” conditions are restored. However, if increases in metabolic demand are longer-term, or occur in a tissue less able to adapt to the metabolic changes, pathological conditions can develop. This is the case with chronic alcoholism, where increased oxygen consumption by the liver (to detoxify alcohol) can result in relatively poorly oxygenated liver tissue, a factor that is thought to contribute to the development of liver cirrhosis (Arteel *et al.*, 1996; Arteel *et al.*, 1997).

A high demand for the delivery of oxygen and nutrients is also created by the uncontrolled cell proliferation associated with the growth of many solid tumours. Newly formed tumours use host vasculature initially for their nutritional supply, but this is typically insufficient to support continued growth of a tumour beyond ~1mm in diameter. Continued tumour growth therefore requires the recruitment and formation of new blood vessels (angiogenesis) to provide additional nourishment. However, blood vessels that form in and around tumours tend to have significant abnormalities in terms of both their structure and their functional capacity. When coupled with the continually high metabolic demands of a growing tumour, the poorly functioning tumour vasculature contributes to a tumour microenvironment that is typically deficient in oxygen and nutrients.

1.1.2 Structure and Function of Tumour Blood Vessels

The majority of observations regarding tumour vasculature have been made in animal systems, using either murine (rodent) tumours or human tumours xenografted into murine hosts. As with most cancer research, the reasons for using animal-based tumour systems are primarily dictated by ethics, technical feasibility, expense, and convenience. Experimental tumour systems represent a venue for novel experimentation, and the resultant data provide insights into the development and treatment of cancer that is largely unattainable in the clinic. These data provide directions of further study for clinical research, but caution is warranted in directly applying

observations made in experimental tumour systems to tumours in the clinic. It is therefore worth noting that the remainder of this Chapter will focus on observations made in experimental tumour systems (typically with murine hosts/vasculature); tumour characteristics observed in the clinic will be indicated where appropriate.

Blood vessels in many solid tumours tend to be malformed and irregularly spaced in comparison to vasculature in “normal” tissues (Figure 1.1). Tumour vascular networks typically lack hierarchy, contain tortuous blood vessels with varying diameter and blind ends, and can have shunts that bypass portions of tumour tissue and mix out-flowing with in-flowing blood. Tumour blood vessels can also be spaced irregularly and relatively far apart, producing areas of tumour necrosis at a distance from vasculature when diffusion of oxygen and/or nutrients is insufficient to sustain tumour cells (Thomlinson and Gray, 1955). Interestingly, vascular casting experiments suggest that the seemingly chaotic patterns of tumour vasculature may actually possess characteristics that are specific to the type of tumour under study, despite being implanted in the same host mouse strain (Konerding *et al.*, 1999).

From a structural point of view, tumour blood vessels can be lined with a disorganized collection of endothelial cells which may include overlapping cells, cellular projections into the vessel lumen, and relatively large intracellular gaps or pores (Hashizume *et al.*, 2000; McDonald and Foss, 2000). It is thought that the presence of these intracellular gaps contributes to tumour blood vessels that are “leaky” in comparison to well-formed vasculature. The leakiness of tumour vasculature, coupled with the relative lack of functional lymphatic drainage in many tumours, can produce areas of high interstitial fluid pressure (IFP). The high IFP essentially counteracts the normal hydrostatic gradient responsible for the movement of macromolecules from the lumen of blood vessels to the interstitial space, thereby limiting the delivery of blood-borne macromolecules to a less efficient passive diffusion mechanism (McDonald and Baluk, 2002).

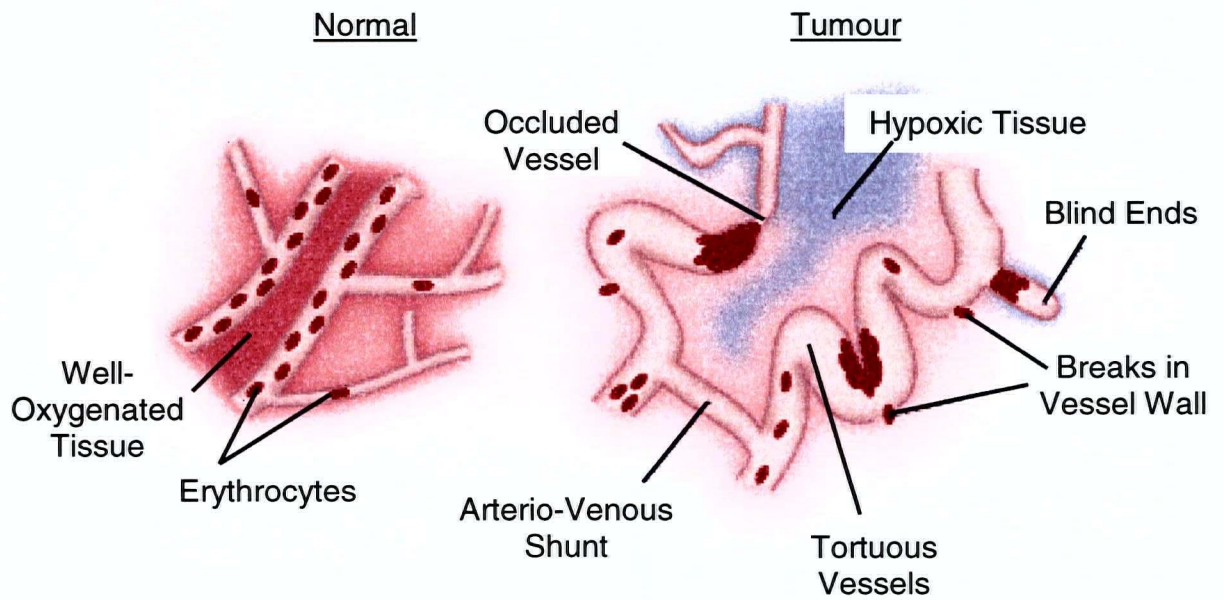


Figure 1.1 Illustration of vasculature in normal and tumour tissue.

Primary differences between vasculature in normal and tumour tissue are indicated. Pink shading indicates well-oxygenated, well-nourished tissue; blue shading indicates poorly-oxygenated, poorly-nourished tissue. Figure adapted from Brown and Giaccia, 1998.

The majority of newly formed blood vessels in tumours appear to originate from venules of host or tumour tissue (Vaupel *et al.*, 1989; Konerding *et al.*, 1999), with implications for the oxygen and nutrient content of the blood provided to the tumour. While some tumour blood vessels can have flow rates on par with normal tissues, a proportion of vasculature in many tumours are subject to sluggish or intermittent blood flow, with episodes of flow reversal or stasis (Vaupel *et al.*, 1989). Modeling studies have indicated that the characteristics of many tumour blood vessels, including abnormal vascular spacing (Secomb *et al.*, 1993; Baish *et al.*, 1996) and impaired blood flow (Baish *et al.*, 1996), can limit effective oxygen and nutrient delivery to some tumour regions independent of the intravascular oxygen and nutrient content.

Overall, the structural and functional abnormalities associated with tumour blood vessels can contribute to a highly heterogeneous tumour microenvironment, and to tumour cells with typically poor nutrient and oxygenation status. However, despite these conditions, populations of tumour cells must be able to survive (and proliferate in) the tumour microenvironment since tumours are capable of continued growth. The solid tumour microenvironment therefore represents a complex interplay between the characteristics of tumour vasculature discussed in this Section, the formation of tumour microregions of heterogeneous oxygen and nutrient status, and the response of individual tumour cells to an environment that may not be particularly conducive to cell survival. The recruitment and formation of new blood vessels (angiogenesis) can increase the perfusion and nutrient status of some tumour regions, while other areas can be subject to increased extracellular lactic acid and decreased extracellular pH due to changes in tumour cell metabolism (Section 1.4). Different tumour regions can also contain diffusion gradients of oxygen and nutrients, including areas of necrotic tissue (Section 1.2) presumably resulting from severe and/or prolonged deprivation of oxygen and nutrients.

Of all the microenvironmental characteristics of solid tumours, the tumour oxygenation status has received the most attention. This is largely due to observations that “poorly oxygenated”

tumours (and tumour cells) are typically more refractory to treatment with various cancer therapies (Section 1.3), and to the availability and development of a number of methods to directly or indirectly measure tissue oxygenation levels (Section 1.5). The oxygenation status of tumour cells also affects the expression of a variety of genes involved in tumour cell metabolism, pH regulation, and angiogenesis (Section 1.4), providing an attractive mechanism for the formation of the myriad of microenvironmental characteristics common to many tumours. However, before any of these topics can be discussed in detail, a brief overview of terminology regarding “poorly oxygenated” tumour cells is necessary.

1.2 CLASSIFICATION OF TUMOUR HYPOXIA

The first issue that should be addressed in any discussion of poorly oxygenated (i.e. hypoxic) cells is the degree of oxygen deprivation intended. While there has been a great deal of work invested in studying “hypoxic” tumour cells and their impact on tumour therapy, there is surprisingly little standardization in terminology. This subtle, but potentially important, consideration has led to confusion and ambiguity in the literature, particularly when attempts have been made to model tumour hypoxia *in vitro*.

The practice of describing cells as “poorly oxygenated” or “hypoxic” is ambiguous without reference to the oxygenation level that one considers “oxic”. Indeed, one could potentially argue that most tissues in the body contain cells that are hypoxic relative to the 21% oxygen found in air! While this example is extreme, it is interesting to note that many groups studying the molecular impact of hypoxia describe tumour cells *in vitro* as being at “normal” oxygen levels (in culture medium equilibrated with air) when the cells are more precisely “hyperoxic” relative to their “normal” environment in the human body (particularly in tumours). Indeed, tumour oxygenation measurements indicate that maximal oxygenation levels can be less than 5% O₂ for cells in some murine tumours (~27 mmHg; Dewhirst *et al.*, 1992) and human tumour xenografts (~30 mmHg; Helmlinger *et al.*, 1997). Other groups have estimated that maximally oxygenated cells may be at levels as low as 2% O₂ in some murine tumours (Pogue *et al.*, 2001), human tumour xenografts (Olive *et al.*, 2002), and even clinical tumours (Urtasun *et al.*, 1986b). While there is likely considerable heterogeneity in the absolute values of maximally oxygenated cells in different tumours (and in different regions of the same tumour), these values highlight the importance of proper *in vitro* modeling of tumour hypoxia.¹

¹ Most *in vitro* studies cite the oxygen concentration in the gas phase above culture medium as either parts per million (ppm), a percentage, or the partial pressure of oxygen (pO₂) in millimetres of mercury (mmHg). Thus 20,000 ppm O₂ = 2% O₂ = ~15 mmHg pO₂. Assuming equilibration of culture medium with the gas phase above it, this corresponds to a dissolved oxygen concentration of 21 μM at 37°C.

An additional consideration when discussing “hypoxic” tumour cells is context; the levels of oxygen deprivation required to induce changes in gene or protein expression are typically different from those necessary to adversely affect tumour response to treatment (Horsman, 1998; Hockel and Vaupel, 2001). Moreover, low levels of oxygenation can limit the therapeutic efficacy of various treatment modalities to different extents (Hockel and Vaupel, 2001). It is therefore important to precisely define what is meant by “hypoxia” in a given situation. Thus for the purposes of this thesis, “hypoxia” will refer to cellular oxygenation levels that are sufficiently low so as to decrease cellular sensitivity to ionizing radiation ($pO_2 < 10$ mmHg; see Section 1.3.1).

Hypoxic tumour cells have traditionally been classified into one of two discrete categories: “chronic” or “acute”. These definitions primarily presume one of two specific mechanisms of oxygen deprivation leading to hypoxia (as will be covered below), but also inherently imply a non-specific duration of hypoxia. As more work has gone into identifying and characterizing different sources of hypoxia in solid tumours, it has become apparent that classifying tumour hypoxia in this binary way is imprecise and insufficient. What follows are descriptions of the different processes that are thought to give rise to poorly oxygenated tumour cells, and justification for the terminology that will be used throughout this thesis when discussing tumour hypoxia.

1.2.1 “Chronic” and “Diffusion-Limited” Hypoxia

The historical model of tumour hypoxia originated from histological observations of clinical tumour tissue with areas of necrosis running parallel to vascularized stroma, with apparently viable tumour tissue in between. The width of the tumour tissue (~ 120 μm) closely matched calculated diffusion distances of oxygen, and cells adjacent to the necrosis were thought to be hypoxic (Thomlinson and Gray, 1955). Histological observations in rodent tumours indicated an alternative version of this model, consisting of necrotic areas surrounding ring-like “cords” of

apparently viable tumour tissue that surrounded individual tumour blood vessels (Tannock, 1968). Since then, many experimental and clinical tumours have been found to contain regions of necrosis at varying distances from tumour vasculature, implying that this form of hypoxia is a relatively common feature of many solid tumours.

1.2.1.1 Nomenclature

Tumour tissue that is adjacent to tumour vasculature tends to contain large fractions of proliferating cells (Tannock, 1968). As these tumour cells continue to proliferate, other populations of cells are progressively “pushed” farther away from the nutrient source, and eventually beyond the diffusion distance of oxygen. These cells become subject to “chronic” or “diffusion-limited” hypoxia in the periphery of tumour cords, and eventually enter into the necrotic compartment themselves (Figure 1.2). However, the word “chronic” implies a process that does not vary over time and is indefinite in duration. In actuality, this mechanism of hypoxia formation is more “steady-state” in that these cells had been exposed to decreasing levels of oxygen over time as they “progressed” down the oxygen diffusion gradient (away from the blood vessel) to become hypoxic, and eventually anoxic (and necrotic). Thus “diffusion-limited” is the more accurate (and less time-sensitive) description of this form of tumour hypoxia, and will be used throughout this thesis to describe hypoxia ($pO_2 < 10$ mmHg) derived from this mechanism.

It is worth reiterating that diffusion-limited hypoxic cells are the result of a continuous radial diffusion gradient of oxygen away from tumour vasculature. It therefore follows that diffusion-limited hypoxia is not a binary phenomenon, and that populations of cells situated at “intermediate” distances from tumour blood vessels are at “intermediate” levels of oxygenation. These cells are thought to have important implications for tumour response to clinical radiation therapy regimens (Wouters and Brown, 1997; Evans *et al.*, 1997; Olive *et al.*, 2002), and will be discussed further in Section 1.3.1.

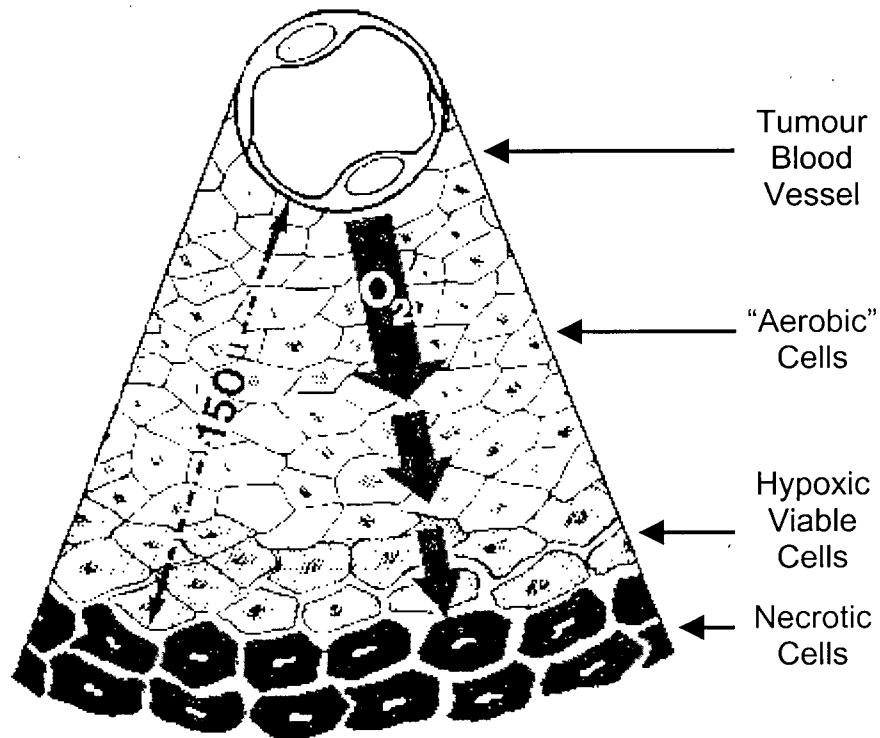


Figure 1.2 Diffusion-limited hypoxia.

Poorly oxygenated tumour cells are typically found at a radial distance of $\sim 100\text{-}150\ \mu\text{m}$ from functional tumour vasculature, and can be adjacent to regions of tumour necrosis. Poor vascular delivery of oxygen combined with a relatively high oxygen consumption of cells near the vasculature can further limit the diffusion distance of oxygen.

1.2.1.2 Variables affecting diffusion-limited hypoxia

The amount of tumour tissue between tumour blood vessels and necrosis can be quite variable (typically on the order of 100-150 μm), depending on the heterogeneity of the tumour vascular network (Secomb *et al.*, 1993; Baish *et al.*, 1996), the oxygen consumption of tumour tissue adjacent to a given blood vessel (Dewhirst *et al.*, 1994; Secomb *et al.*, 1995), and the oxygen content and flow of blood through that vessel (Jain, 1988; Vaupel *et al.*, 1989; Baish *et al.*, 1996). Each of these variables can contribute to levels of hypoxia that vary between different tumour types, different tumours of the same type, and different regions of the same tumour.

Oxygenation levels and perfusion rates in tumour blood vessels can vary over a relatively wide range, suggesting that some areas of tumour vasculature may provide only low levels of oxygen to adjacent tumour cells. Indeed, murine tumours implanted in a skin-fold window chamber model (Huang *et al.*, 1999) can contain blood vessels with relatively rapid blood flow, but low pO_2 of the perivascular tissue (Dewhirst *et al.*, 1992; Helmlinger *et al.*, 1997). These observations indicate apparently “functional” blood vessels that contain non-nutritive blood flow, and therefore would more appropriately be classified as “non-functional”. The presence of these vessels in other tumour types has been supported by theoretical studies modeling low intravascular pO_2 as a result of the abnormal vascular structures prevalent in many solid tumours (Baish *et al.*, 1996; Pogue *et al.*, 2001). Longitudinal gradients of pO_2 (i.e. along tumour blood vessels) have also been observed in murine window chamber tumours, suggesting intravascular oxygenation levels may decrease as blood vessels traverse through a tumour (Dewhirst *et al.*, 1999). In addition, some tumour vasculature in the same model system has been shown to contain plasma flow with very little erythrocyte flux (Dewhirst *et al.*, 1996), with implications for intravascular oxygen content.

It is worth noting that most of these studies involved murine tumours and need to be verified in human tumour xenografts and spontaneous tumours (if possible). However, the principle that tumour blood vessels can contain non-nutritive blood flow appears to be reasonable, and would be thought to decrease the tumour cord radius in some tumour areas. Indeed, heterogeneous tumour cord radii have been observed in many human tumours, and a small fraction of cells adjacent to tumour blood vessels can bind exogenous hypoxia markers (Chapter 3-4) or display some resistance to ionizing radiation (Chapter 2). These data effectively illustrate that the mere presence of tumour vasculature does not indicate a well-perfused tumour region without also considering the functionality of the blood vessels.

In extreme cases, blood vessels containing poorly oxygenated blood or poor blood flow may produce areas of tumour hypoxia adjacent to tumour vasculature. Thus tumour hypoxia derived from limited oxygen delivery (as distinct from limited oxygen diffusion through tissue) may also be considered “chronic” in nature, assuming no significant changes in nutritive blood flow over time. Therefore for the purposes of this thesis, “chronic” hypoxia will pertain to oxygen deprivation ($pO_2 < 10$ mmHg) resulting from limitations of oxygen diffusion and/or delivery that are thought to be irreversible over time in the absence of treatment or other intervention.

1.2.2 “Transient” and “Intermittent” Hypoxia

As discussed in Section 1.1.2, tumour vasculature tends to be highly irregular and tumour blood flow can be chaotic, with some areas exhibiting relatively rapid blood flow while other areas may have sluggish blood flow or flow stasis (Vaupel *et al.*, 1989). Blood flow in a given tumour blood vessel can also vary over time, and real-time fluctuations in erythrocyte flux through tumour vasculature have been measured with laser Doppler flowmetry both in experimental tumours (Hill *et al.*, 1996; Braun *et al.*, 1999) and in the clinic (Hill *et al.*, 1996; Pigott *et al.*, 1996). It therefore follows that tumour oxygenation may vary over time as well, and that the non-constant tumour blood flow observed in both experimental and clinical tumours

may also indicate temporally variable tumour oxygenation in both systems. If fluctuations in tumour oxygenation were to affect cells at sufficiently low oxygen levels, then changes in the degree and duration of tumour hypoxia would occur over time. Hypothetically, if regional tumour oxygen tensions change significantly and frequently over time, it is conceivable that hypoxia that is truly “chronic” in nature may be relatively infrequent (Dewhirst, 1998). Moreover, since diffusion-limited hypoxic tumour cells may be destined to enter the necrotic compartment and die in the absence of treatment or intervention, the potential therapeutic relevance of these cells may be questionable.

Suggestions of a more dynamic form of tumour hypoxia (i.e. “acute” hypoxia) were originally made over two decades ago from observations in animal tumours (Brown, 1979). However, surprisingly little is known about tumour cells with a hypoxic status that changes over time, particularly the relative numbers of these cells, their proximity to tumour vasculature, and their influence on cancer therapy. Furthermore, efforts to observe changes in tumour oxygenation (and/or hypoxia) over time in the clinic have been limited by current hypoxia detection methodology (as will be discussed further in Section 1.5).

Hypoxia that changes over time is thought to occur in tumour cells that are nutritionally dependent on tumour blood vessels subject to partial and/or intermittent decreases in functionality. Blood vessels that have temporary flow reductions or complete flow stasis are likely involved, as well as blood vessels with relatively stable blood flow and transient decreases in intravascular oxygenation. Importantly, changes in the hypoxic status of some tumour cells is thought to occur in the absence of any sort of intervention or treatment (as will be discussed further in Chapter 3). A great deal of confusion and ambiguity is prevalent in the literature when it comes to describing hypoxia derived from these mechanisms. Different groups have used names that include: “acute”, “perfusion-limited”, “cyclic”, “transient”, and “intermittent”, none of which are entirely appropriate. Each description has a few underlying implications as to the

degree of hypoxia and/or the duration of the changing cellular hypoxic status in question, that have typically not been derived from experimental data. As methods for studying changes in tumour hypoxia improve, it will be necessary to modify these descriptions to better reflect current understanding and to facilitate comparisons of this phenomenon between different tumours and different laboratories.

The word “acute” to describe tumour hypoxia either implies relatively low levels of static oxygenation (i.e. not as low as “chronic” hypoxia), or that a hypoxic episode is short-lived and may or may not recur. “Perfusion-limited” hypoxia is a more descriptive term, although it merely implies that perfusion is limiting tumour cell oxygenation and does not suggest a dynamic process. For example, poorly perfused tumour vasculature (including blood vessels containing plasma flow) can limit oxygen delivery to tumour cords and reduce the diffusion distance of oxygen. Perfusion limitations would therefore affect diffusion-limited hypoxia in this case, leading to confusion and potential overlap between definitions for “perfusion-limited” and “diffusion-limited” hypoxia. “Cyclic” hypoxia implies a process that is capable of repeating itself, but also suggests some form of regularity and/or regulation. Fluctuations in tumour blood flow and perivascular tumour pO_2 (Dewhirst *et al.*, 1996; Kimura *et al.*, 1996; Dewhirst *et al.*, 1998; Braun *et al.*, 1999) in murine tumours can appear to be cyclic, but the application of these observations to changes in tumour hypoxia is inferential. While cyclic regimens of hypoxia and reoxygenation may represent useful strategies for modeling dynamic tumour hypoxia *in vitro* (Cairns *et al.*, 2001; Cairns and Hill, 2004), describing tumour hypoxia as “cyclic” should perhaps be avoided until such time as a cyclic regularity has been established *in vivo*.

“Transient” or “intermittent” hypoxia implies a process that can occur sporadically, at different points in time, and may or may not recur. While these descriptions are somewhat vague on their own, they convey the sense of irregularity thought to be prevalent in the blood flow of many tumours, and have the potential to be informative if coupled with an indication of the

degree and duration of hypoxia being discussed. This terminology is perhaps the best at this point, although the actual degree and duration of transiently hypoxic episodes are rarely explicitly mentioned, largely due to inadequate knowledge and methodology to study the process. Therefore for the purposes of this thesis, “transient” or “intermittent” hypoxia will be used interchangeably to describe hypoxia ($pO_2 < 10$ mmHg) that changes over time in the absence of any intervention or treatment.

1.3 TUMOUR PHYSIOLOGY AND CANCER THERAPY

The microenvironment of solid tumours can adversely impact the efficacy of clinical cancer therapy in a number of ways. The oxygenation status, proliferative capacity, and DNA repair capacity of tumour cells are a few of the factors directly related to the tumour microenvironment that provide unique challenges for cancer therapy.

1.3.1 Radiotherapy

Ionizing radiation causes damage to DNA in the form of DNA strand breaks, and the sensitivity of a given cell to radiation (i.e. its *radiosensitivity*) can be influenced directly or indirectly by the tumour microenvironment. Almost 100 years ago, the radiation response of skin was found to decrease when the area was compressed during irradiation, thereby reducing blood flow to the region and providing the first evidence that perfusion status could affect cellular radiosensitivity (Overgaard and Horsman, 1996). It was later hypothesized that poorly oxygenated tumour cells may represent a major source of resistance to ionizing radiation (Gray *et al.*, 1953), and histological observations of presumably hypoxic cells adjacent to necrosis in clinical tumours (Thomlinson and Gray, 1955) led to a plausible explanation for radiation therapy failure in the clinic.

Since that time, oxygen has been identified as a potent enhancer of DNA damage induced by ionizing radiation. Tumour cells are considered radiobiologically hypoxic when they are more resistant to killing by a given dose of ionizing radiation (i.e. are more *radioresistant*) than aerobic cells. Cells at oxygen tensions below that of venous blood (20-40 mmHg; Vaupel *et al.*, 1989; Bussink *et al.*, 2003) require progressively higher doses of radiation for the same biological effect (i.e. the same level of cell kill). A 2-fold or greater reduction in radiosensitivity can occur at pO_2 values less than 3-4 mmHg (Vaupel *et al.*, 1989), and cells that are fully anoxic can require up to three-times the radiation dose as aerobic cells for equivalent levels of cell kill from a single, large dose of radiation (Gray *et al.*, 1953; Dasu and Denekamp, 1998). The

enhancement of radiation damage by oxygen is expressed as the oxygen enhancement ratio (OER) and stems from the high electron affinity of oxygen and its propensity to interact with DNA free radicals formed by radiation damage. This process acts to “fix” (i.e. make permanent) DNA strand breaks induced by ionizing radiation, leading to decreased efficacy of DNA repair and increased levels of mitotic cell death in oxygenated cells.

In addition to the direct enhancement of radiation damage induced by oxygen during irradiation, the radiation response of tumour cells can also be indirectly influenced by the tumour microenvironment. In some cases, aspects of the tumour microenvironment can actually make some populations of hypoxic cells *more* sensitive to killing by ionizing radiation. For example, cells maintained in hypoxic conditions *in vitro* (simulating chronic hypoxia) tend to accumulate in the radiosensitive G₁ phase of the cell cycle (Berry *et al.*, 1970; Spiro *et al.*, 1984; Shrieve and Begg, 1985). Different tumour cell types also have varying inherent abilities to repair DNA damage, and these repair processes require energy derived from nutrients that can be limited by the perfusion status of different tumour regions. Cells that are chronically nutrient-deprived have a lower cellular energy status and are less able to repair DNA damage compared to well-nourished cells *in vitro* (Ling *et al.*, 1988; Gerweck *et al.*, 1993), indicating that nutrient-deprived cells would be more radiosensitive. These observations are intriguing when considered with the diffusion-limited hypoxia model, since cells on the periphery of tumour cords may lack nutrients as well as oxygen. Although the diffusion distance of nutrients such as glucose through tissue may be greater than that of oxygen in some cases (Groebe *et al.*, 1994), areas of insufficient nutritive blood flow may restrict the nutritive status of diffusion-limited hypoxic cells with a resultant decrease in cellular energy status. Thus low levels of oxygenation at the time of irradiation enhances cellular radioresistance, while a prolonged period of oxygen and/or nutrient deprivation can confer a level of radiosensitivity to these cells (Hall *et al.*, 1966; Berry *et al.*, 1970; Shrieve and Harris, 1985; Spiro *et al.*, 1985; Pettersen and Wang, 1996; Zolzer and

Streffer, 2002). However, chronically hypoxic tumour cells and cells made acutely hypoxic *in vivo* have been shown to display similar radiation sensitivities for at least one human tumour xenograft line (Vordermark *et al.*, 2003).

The traditional dogma prevalent in the radiation oncology field was that tumour cells subject to diffusion-limited hypoxia were preferentially able to survive a given dose of radiation and were largely responsible for tumour repopulation after (or during) therapy. A reasonable mechanistic explanation was that since most therapies were more effective against better oxygenated, proliferating cells closer to tumour blood vessels, the killing (or damaging) of these more sensitive cells could conceivably reduce oxygen consumption and increase the oxygen diffusion distance. Treatment may therefore effectively increase the oxygenation of diffusion-limited hypoxic cells near the periphery of tumour cords and essentially “rescue” cells that would otherwise have “progressed” into necrosis, thereby allowing these cells to contribute to tumour repopulation. Thus the presence of tumour cords and the detection of diffusion-limited hypoxic cells in many experimental and clinical tumours has provided indirect evidence to support the role of diffusion-limited hypoxia in reducing tumour response to cancer therapy. However, cells that are hypoxic only transiently (in the absence of treatment) may represent equally or even more important limitations to the efficacy of tumour therapy.

Theoretically, transiently hypoxic tumour cells may have better access to nutrients (albeit periodically), may not be preferentially concentrated in a radiosensitive phase of the cell cycle, and may be better able to repair DNA damage than chronically hypoxic cells (Denekamp and Dasu, 1999). Moreover, transiently hypoxic cells are capable of retaining some proliferative capacity during the temporary reduction (or absence) of oxygen (Durand and Raleigh, 1998), and therefore could potentially proliferate upon reoxygenation of a tumour region. Tumour cells at intermediate levels of oxygenation (i.e. $pO_2 = 0.5-10$ mmHg) have also been suggested as important limiting factors in tumour radiotherapy (Wouters and Brown, 1997; Evans *et al.*, 1997;

Olive *et al.*, 2002) since they may also be better nourished and able to repair radiation-induced DNA damage more readily than diffusion-limited hypoxic cells. Direct testing of these hypotheses has been limited, however, by a lack of methods available for distinguishing between different “types” of hypoxic cell *in vivo*. If hypoxia detection methodology could be improved to allow distinction between disparate hypoxic cells, appropriate assessments could be made of the relative importance of diffusion-limited, intermediately oxygenated, and transiently hypoxic tumour cells in tumour response to clinical radiotherapy regimens.

1.3.2 Chemotherapy

Features of the tumour microenvironment likely play important roles in the response of tumour cells to chemotherapy agents, although the role of the tumour microenvironment in tumour response to chemotherapy has received less attention than in the radiotherapy field. Chemotherapeutic agents that are directly cytotoxic must reach the target cells in sufficient concentration in order to be effective. Thus the delivery and diffusion limitations associated with oxygen and nutrients may also apply to blood-borne chemotherapy drugs, and cells with limited oxygenation or nutrient status would tend to receive the least amount of drug.

Drug delivery can be limited by tumour perfusion (Baish *et al.*, 1996), particularly in regions that may exhibit non-constant blood flow during the circulation lifetime of the agent. This potential problem could be limited with the use of chemotherapeutics with longer circulation lifetimes or by administering the agent in multiple or continuous low doses (Durand, 2001; Colleoni *et al.*, 2002; Kerbel *et al.*, 2002; Man *et al.*, 2002). These strategies may increase the delivery of chemotherapy agents to poorly perfused tumour regions, but may also increase normal tissue toxicity.

A further consideration in the treatment of solid tumours with chemotherapeutics is that different agents have different abilities to diffuse through tumour tissue, limiting the amount of drug that reaches tumour cells at a distance from the vasculature. Drug diffusion through tumour

tissue can be limited if the drug is bound, metabolized, or otherwise retained in cells near the vasculature, thereby reducing the amount of drug available for further diffusion. The diffusion characteristics of a variety of chemotherapy agents have been studied using *in vitro* models such as multicellular spheroids (Durand, 1989; Durand, 1991) and multilayered cell cultures (Cowan *et al.*, 1996; Minchinton *et al.*, 1997; Phillips *et al.*, 1998; Tannock *et al.*, 2002), indicating a relatively wide range of diffusion distances for different drugs.

In terms of the mechanism of action of chemotherapy agents, tumour cell oxygenation can be directly limiting for drugs that require the generation of reactive oxygen free radical species for their cytotoxicity. The tumour microenvironment can also indirectly influence the efficacy of chemotherapy in a similar fashion as previously discussed for radiation treatment, including accumulation of tumour cells in a particularly resistant or sensitive cell cycle phase, and differences in the DNA repair capacity of tumour cells related to nutrient status and cell type. Furthermore, many chemotherapy drugs preferentially target actively cycling cells, and the decreased proliferation associated with tumour cells subject to poor oxygen and/or nutrient delivery (Tannock, 1968) can enhance cellular resistance to these agents. Thus the tumour microenvironment may represent a relatively effective barrier to the delivery, diffusion, and cytotoxicity of many chemotherapeutic agents.

Novel strategies to use the tumour microenvironment as an advantage for chemotherapy have more recently been devised, including agents that require intracellular enzymatic reduction to be converted from a pro-drug into an actively cytotoxic form (Brown and Siim, 1996). Enzyme-catalyzed reduction of exogenous agents occurs preferentially in cells at low oxygen tensions (see Section 1.5.2.2), and diffusion of the pro-drug is therefore not limited by consumption or accumulation in relatively well-oxygenated cells adjacent to tumour vasculature. Bioreductive drugs such as tirapazamine (Zeman *et al.*, 1986; Brown, 1993), and others (Sartorelli, 1988; Brown and Siim, 1996), are therefore designed to target hypoxic cells regardless of the

mechanism of hypoxia induction. The use of agents to specifically target hypoxic cells complements the cytotoxicity of many standard cancer therapies, and tirapazamine has shown promising clinical results in combination with radiation and/or chemotherapy (Craighead *et al.*, 2000; von Pawel *et al.*, 2000; Rischin *et al.*, 2001). Thus hypoxic cell-specific targeting may prove to be a valuable strategy for tumour therapy, particularly as methods for detecting tumour hypoxia are improved to identify patients that could potentially benefit from the intervention.

1.4 TUMOUR MICROENVIRONMENT AND GENE EXPRESSION

Patients with poorly oxygenated tumours have been found to respond poorly to therapy (see Section 1.5), even if the primary treatment consisted of surgical resection of the tumour (Hockel *et al.*, 1996a). These intriguing observations suggest that hypoxia itself, or a microenvironment that favors hypoxic cells, may be related to the inherent aggressiveness of some tumours. Although it is unknown whether a microenvironment containing a large number of hypoxic cells is a cause, effect, or coincidence of a more aggressive tumour phenotype (Coleman *et al.*, 2002), investigations continue into the relationship between low oxygen levels and the expression of a variety of genes involved in promoting aggressive tumour characteristics.

1.4.1 Hypoxia-Induced Gene Expression

Studies involving gene expression induced by hypoxia have largely revolved around a hypoxia responsive transcription factor, appropriately named hypoxia inducible factor-1 (HIF-1), that is a heterodimer consisting of an α - and a β -subunit. HIF-1 β (or aryl hydrocarbon receptor nuclear translocator; ARNT) is a constitutively expressed nuclear protein, while levels of HIF-1 α are hypoxia-responsive and therefore mediate the transcriptional activity of the HIF-1 complex. HIF-1 α levels are primarily controlled at the protein level, and under non-hypoxic conditions HIF-1 α is bound to the von Hippel-Lindau (VHL) tumour suppressor protein (Maxwell *et al.*, 1999). VHL is the recognition component of an E3 ubiquitin-protein ligase complex, and acts to target HIF-1 α for proteasomal degradation under non-hypoxic conditions (Cockman *et al.*, 2000; Kamura *et al.*, 2000; Ohh *et al.*, 2000; Tanimoto *et al.*, 2000). Hydroxylation of two proline residues on HIF-1 α is required for interaction with VHL (Ivan *et al.*, 2001; Jaakkola *et al.*, 2001; Masson *et al.*, 2001; Yu *et al.*, 2001), and this reaction is catalyzed by one of three prolyl hydroxylases (Bruick and McKnight, 2001; Epstein *et al.*, 2001) that require oxygen and 2-oxoglutarate for the reaction. Thus in the absence of oxygen, HIF-1 α is not hydroxylated, does not interact with VHL, and is not targeted for degradation. This effective stabilization of HIF-1 α

protein levels (half-maximal response at cellular oxygenation levels of 1.5-2% O₂) is responsible for the oxygen-dependent regulation of HIF-1 α expression (Wang *et al.*, 1995; Jiang *et al.*, 1996).

The transcriptional activity of HIF-1 is also regulated by oxygen (Jiang *et al.*, 1997; Pugh *et al.*, 1997) through the co-repressor “factor inhibiting HIF-1” (FIH-1; Mahon *et al.*, 2001). FIH-1 hydroxylates HIF-1 α in the presence of oxygen, preventing its interaction with transcriptional co-activators necessary for the up-regulation of many hypoxia-induced genes (Hewitson *et al.*, 2002; Lando *et al.*, 2002a; Lando *et al.*, 2002b). Thus the post-translational modifications of HIF-1 α protein by various hydroxylation reactions limit both the intracellular level and the transcriptional activity of the protein via inherently oxygen-dependent processes.

HIF-1 α protein levels can also be increased in a non-oxygen dependent manner in some cases. Depending on the cell type, stimulation by a variety of growth factors can increase synthesis of HIF-1 α protein (Semenza, 2003) via activation of the phosphatidylinositol 3-kinase (PI3K) or mitogen activated protein kinase (MAPK) pathways (Zhong *et al.*, 2000; Laughner *et al.*, 2001; Fukuda *et al.*, 2002; Fukuda *et al.*, 2003). Moreover, cells that have loss-of-function mutations in VHL can have constitutively high levels of HIF-1 α since the protein is not ubiquitinated and targeted for degradation under non-hypoxic conditions (Maxwell *et al.*, 1999). Increases in HIF-1 α levels that are oxygen-independent can lead to increased transcription of HIF-1 responsive genes when the levels of HIF-1 α protein are higher than can be repressed by the oxygen-dependent action of FIH-1.

HIF-1 was first identified as a regulator of erythropoietin expression (Semenza and Wang, 1992), and since then has been shown to regulate the transcription of over 60 genes related to glycolysis, angiogenesis, vascular remodeling, cell proliferation, and cell viability (Semenza, 2003). Rather than present an exhaustive list of genes regulated by HIF-1, specific examples that are relevant to this thesis will be discussed in Sections 1.4.2, 1.4.3, 1.5.3, and also in Chapter 5.

1.4.2 Tumour Metabolism

HIF-1 regulates transcription of glucose transporters 1 and 3 (Ebert *et al.*, 1996; Behrooz and Ismail-Beigi, 1997) and a number of enzymes involved in glucose metabolism by glycolysis (Figure 1.3A). Under well-oxygenated conditions, cells get the majority of their energy in the form of adenosine triphosphate (ATP) from the efficient, oxygen-dependent process of oxidative phosphorylation downstream of glycolysis (Figure 1.3B). Under conditions of reduced oxygenation however, up-regulation of glucose transporters and glycolytic enzymes indicate a metabolic switch from oxidative phosphorylation to glycolysis as the primary source of ATP generation (Seagroves *et al.*, 2001; Williams *et al.*, 2002). Glycolysis is a less efficient energy producing process than oxidative phosphorylation, and increased glucose transporter and glycolytic enzyme levels are necessary to increase the rate of glycolysis to maintain adequate cellular energy levels. The terminal phase of glycolysis can be completely anaerobic (Figure 1.3C), producing lactic acid as a primary waste product that typically dissociates into hydrogen ions and lactate anions. Both the lactic acid and/or the hydrogen ions are transported out of the cell to maintain a neutral intracellular pH (Griffiths, 1991), and a (variable) pH gradient across the cell membrane (Gerweck and Seetharaman, 1996; Prescott *et al.*, 2000). The production of lactic acid is therefore thought to contribute to the acidic extracellular pH commonly associated with the tumour microenvironment, although low pH values have also been found in tumours unable to produce lactic acid (Newell *et al.*, 1993; Yamagata *et al.*, 1998; Helmlinger *et al.*, 2002). These latter observations suggest the involvement of an additional mechanism of pH modification in some tumours, and carbonic anhydrases are thought to play a role (Potter and Harris, 2003).

1.4.3 Carbonic Anhydrases

Carbonic anhydrases are a family of enzymes that catalyze the reversible hydration of CO₂ to carbonic acid (H₂CO₃). Carbonic anhydrase 9 and 12 (CAIX and CAXII) are transmembrane

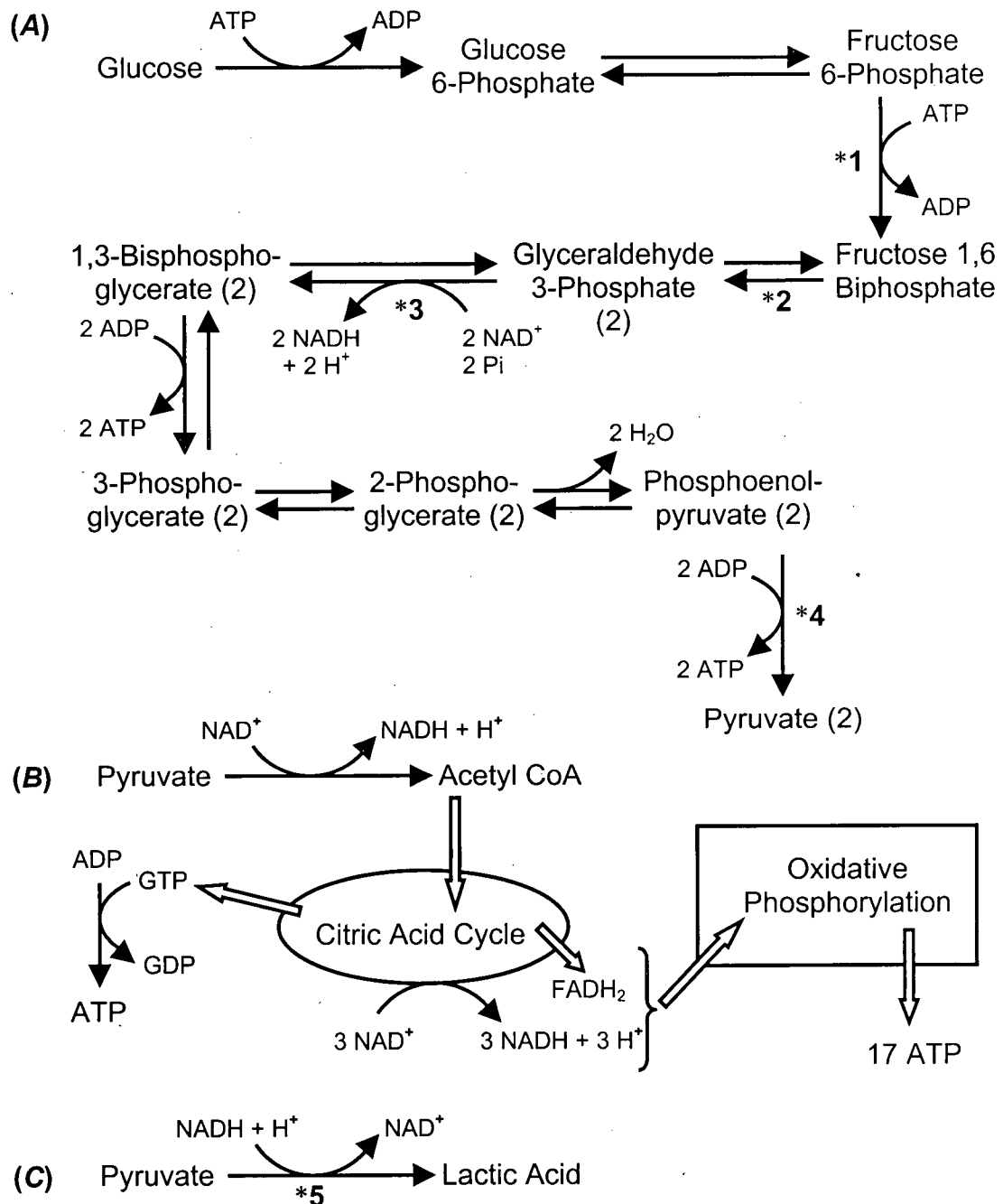


Figure 1.3 Cellular metabolism in the presence and absence of oxygen.

(A) Glycolysis. All steps are enzyme-catalyzed, but only selected enzymes relevant to Chapter 5 are identified: *1 = phosphofructokinase L; *2 = aldolase A; *3 = glyceraldehyde 3-phosphate dehydrogenase; *4 = pyruvate kinase M.

(B) In the presence of oxygen, pyruvate is converted into acetyl CoA for entry into the citric acid cycle. Reducing equivalents of NADH enter oxidative phosphorylation to produce ATP.

(C) In the absence of oxygen, pyruvate is converted to lactic acid; *5 = lactate dehydrogenase.

proteins that are transcriptionally regulated by HIF-1 (Wykoff *et al.*, 2000) and have major roles in maintaining intracellular pH homeostasis (Potter and Harris, 2004). The removal of intracellular hydrogen ions produced during anaerobic glycolysis is facilitated by combination with bicarbonate anions followed by carbonic anhydrase-catalyzed dehydration to form freely diffusible CO₂. CAIX (or CAXII) can convert CO₂ back to bicarbonate outside of the cell, creating a diffusion gradient that removes CO₂ from the cell and maintains a more neutral intracellular pH (Potter and Harris, 2003). In normal tissues, extracellular hydrogen ions are typically removed from the interstitial space by blood or lymphatic drainage to maintain a neutral pH between 7.0 and 7.4. Conceivably, the hypoxia-induced up-regulation of CAIX coupled with increased anaerobic glycolysis (and lactic acid production) in hypoxic tumour cells produces a net increase in hydrogen ions in the extracellular space (Ivanov *et al.*, 2001), particularly with the insufficient interstitial drainage commonly found in many tumours. Extracellular pH values can be as low as 6.2 in some tumours (Vaupel *et al.*, 1989), and an acidic extracellular microenvironment is commonly associated with hypoxia in many tumours.

Thus there are a variety of genes up-regulated in hypoxic tumour cells, some of which can directly or indirectly influence various characteristics of the tumour microenvironment. Increased expression levels of some hypoxia-inducible proteins have even been used as indicators of hypoxic tumour cells *in vivo*, as will be discussed in Section 1.5.3.

1.5 METHODS FOR MEASURING TUMOUR HYPOXIA

The oxygenation status of a tumour is thought to have potential prognostic value in cancer treatment, and many methods for measuring tumour oxygenation have been developed (Raleigh *et al.*, 1996; Horsman, 1998; Dewhirst *et al.*, 2000; Bussink *et al.*, 2003). Techniques vary in terms of convenience, resolution, relevance of the information obtained, and applicability to measuring tumour oxygenation or hypoxia in the clinic. Methods that have already been used in the clinic with varying degrees of success include: 1.) insertion of physical probes to directly measure tumour oxygenation, 2.) detection of exogenous agents that are modified and bound under hypoxic conditions, and 3.) detection of endogenous gene products expressed as surrogate markers of hypoxia. This thesis primarily deals with the latter two methods of hypoxia detection, and therefore exogenous and endogenous hypoxia markers will be discussed in the most detail.

1.5.1 Physical Measurements of Tumour Oxygenation

Polarographic oxygen electrodes (Cater and Silver, 1960; Whalen *et al.*, 1967) have been used most often in the clinic to directly measure tumour oxygenation, and provided the majority of oxygen tensions cited in the preceding Sections. The electrode is introduced into a tissue of interest, and electrochemical reduction of oxygen at the probe tip produces a current that is proportional to the oxygen tension (pO_2) surrounding the tip. The sensitivity of the probe therefore decreases at lower oxygen tensions, which can be problematic for the accurate determination of absolute pO_2 values in poorly oxygenated tumour regions. However, this effect is minimized in practice since tissue pO_2 values are typically cited as the median of multiple measurements or the fraction of measurements below a given threshold value (usually 5 or 10 mmHg). The electrochemical reaction at the probe tip consumes oxygen that could potentially induce oxygen gradients in the tissue, although this effect can be minimized by using a smaller, recessed probe tip with a decreased sampling volume (Schneiderman and Goldstick, 1978;

Linsenmeier and Yancey, 1987). Commercially available Eppendorf pO_2 microelectrodes are housed in 300 μm needles with a probe tip of 12-17 μm and include computer automated linear repositioning of the probe after each measurement (Kallinowski *et al.*, 1990; Hockel *et al.*, 1991; Vaupel *et al.*, 1991). Polarographic electrodes have been used in a variety of clinical studies for measuring oxygen tensions, primarily in cancers of the uterine cervix or of the head and neck. Low levels of tumour oxygenation have correlated with reduced local control after radiotherapy, decreased disease free and overall survival (Hockel *et al.*, 1993; Hockel *et al.*, 1996b; Nordmark *et al.*, 1996; Brizel *et al.*, 1997; Fyles *et al.*, 1998; Brizel *et al.*, 1999; Nordmark *et al.*, 2001), and increased distant metastases (Brizel *et al.*, 1996; Pitson *et al.*, 2001; Fyles *et al.*, 2002). These clinical correlations with therapeutic outcome have led to consideration of Eppendorf pO_2 measurements as the “gold standard” of clinical oxygen detection to which other methods are often compared (Stone *et al.*, 1993). Recessed tip micro-electrodes with smaller tip sizes (3-10 μm) have been used to monitor changes in tumour pO_2 for up to 2 hours at a single location in murine tumours (Dewhirst *et al.*, 1996; Kimura *et al.*, 1996; Dewhirst *et al.*, 1998; Braun *et al.*, 1999), but these types of studies have not been replicated in the clinic.

The Oxylite fibre-optic microprobe (Griffiths and Robinson, 1999) is a more recent alternative to the polarographic pO_2 microelectrode, but has not yet been used in the clinic. The Oxylite system uses fibre-optic detection of short-lived fluorescent pulses induced from a substrate in the probe tip, with lifetimes that are inversely proportional to the surrounding oxygen tension (Young *et al.*, 1996; Griffiths and Robinson, 1999). Oxylite probes therefore have improved sensitivity in areas of low pO_2 , and produce oxygen distributions that are generally similar to polarographic probes (Collingridge *et al.*, 1997; Braun *et al.*, 2001; Seddon *et al.*, 2001). Importantly, Oxylite probes do not consume significant amounts of oxygen during pO_2 measurements, which has facilitated the continuous monitoring of pO_2 over time (with or

without hypoxia manipulation) in a variety of experimental tumours (Bussink *et al.*, 2000a; Urano *et al.*, 2002; Brurberg *et al.*, 2003; Brurberg *et al.*, 2004).

Taken together, studies monitoring tumour pO₂ over time using polarographic or Oxylite probes have provided evidence that significant, yet highly heterogeneous changes in tumour pO₂ can occur with different periodicities and different magnitudes in many tumour types. While pO₂ probes provide real-time tissue oxygenation measurements, direct measurements of tumour pO₂ are limited in that both the number and the viability of tumour cells being measured are unknown, and therefore the functional significance of observed temporal changes in pO₂ must be inferred. Furthermore, physical probes are most easily used in superficially accessible tumours, and there is a large dependence on operator experience for reliable and reproducible pO₂ readings (Stone *et al.*, 1993; Nozue *et al.*, 1997; Brown and Le, 2002). Importantly, the probes are unable to distinguish between viable tumour tissue and areas of necrosis, potentially leading to spuriously low pO₂ readings depending on the intra-tumour placement of the probe and the degree of necrosis in the tumour. Moreover, the mechanical introduction of one or more probes into a tumour is invasive, and can significantly perturb or damage tumour tissue. Many of the issues associated with using physical probes for measuring tumour oxygenation can be avoided through the use of exogenous agents as “markers” of tumour hypoxia.

1.5.2 Exogenous Hypoxia Markers

Exogenous hypoxia markers are chemical agents that can be introduced into a tumour system to label cells that are below a given level of oxygenation. Typically these agents undergo enzyme-catalyzed chemical modification in cells at low oxygen tensions, resulting in binding of drug adducts to intracellular macromolecules and retention within the cells. Various methods have been developed for qualitatively and quantitatively assessing the amount of drug bound within a tumour, and hence the fraction of a tumour below a given oxygenation level. In terms of resolution, tumour hypoxia can be expressed as a function of drug retained by whole tumours,

or as the fraction of tumour area or tumour cells containing bound drug adducts. Importantly, exogenous markers have been used clinically to assess hypoxia in a variety of tumours, including non-superficial tumours that are largely inaccessible to solid pO_2 probes.

1.5.2.1 Radiolabeled misonidazole

Among the earliest exogenous markers of poorly oxygenated cells were radiolabeled derivatives of 2-nitroimidazole compounds, such as the hypoxic cell radiosensitizer misonidazole (Figure 1.4A). Early studies into the cytotoxic mechanism of misonidazole demonstrated that the drug was converted to a reduced form under conditions of hypoxia (Varghese *et al.*, 1976), and that the reduced drug was capable of binding to intracellular RNA and/or protein (Varghese and Whitmore, 1980; Miller *et al.*, 1982). Since misonidazole binding apparently occurred selectively in poorly oxygenated cells, it was proposed that 2-nitroimidazole binding could be used as an indication of hypoxia in solid tumours, provided that a detection method could be devised for the bound adducts (Chapman, 1979; Chapman, 1984).

Bound adducts of radiolabeled misonidazole were first detected in fixed tissue sections using autoradiography. These studies demonstrated that misonidazole adducts were bound and retained in the interior of multicellular spheroids and adjacent to necrosis in solid tumours (Chapman *et al.*, 1981), both of which were assumed to be sites of diffusion-limited hypoxia. By sequentially modifying the external oxygen concentration of spheroids, it was subsequently confirmed that the binding rate of radiolabeled misonidazole increased several-fold in response to relatively small changes in cellular oxygenation (Franko and Chapman, 1982; Miller *et al.*, 1982). The binding process itself was largely oxygen-dependent, and gradients of other nutrients or catabolites were found to have minimal effects on misonidazole binding patterns (Franko *et al.*, 1987). Further studies demonstrated the amount of misonidazole bound within hypoxic cells depended on intracellular misonidazole concentration, the duration of misonidazole contact, and the cell type (Franko *et al.*, 1982; Chapman *et al.*, 1983; Franko and Koch, 1984; Koch *et al.*,

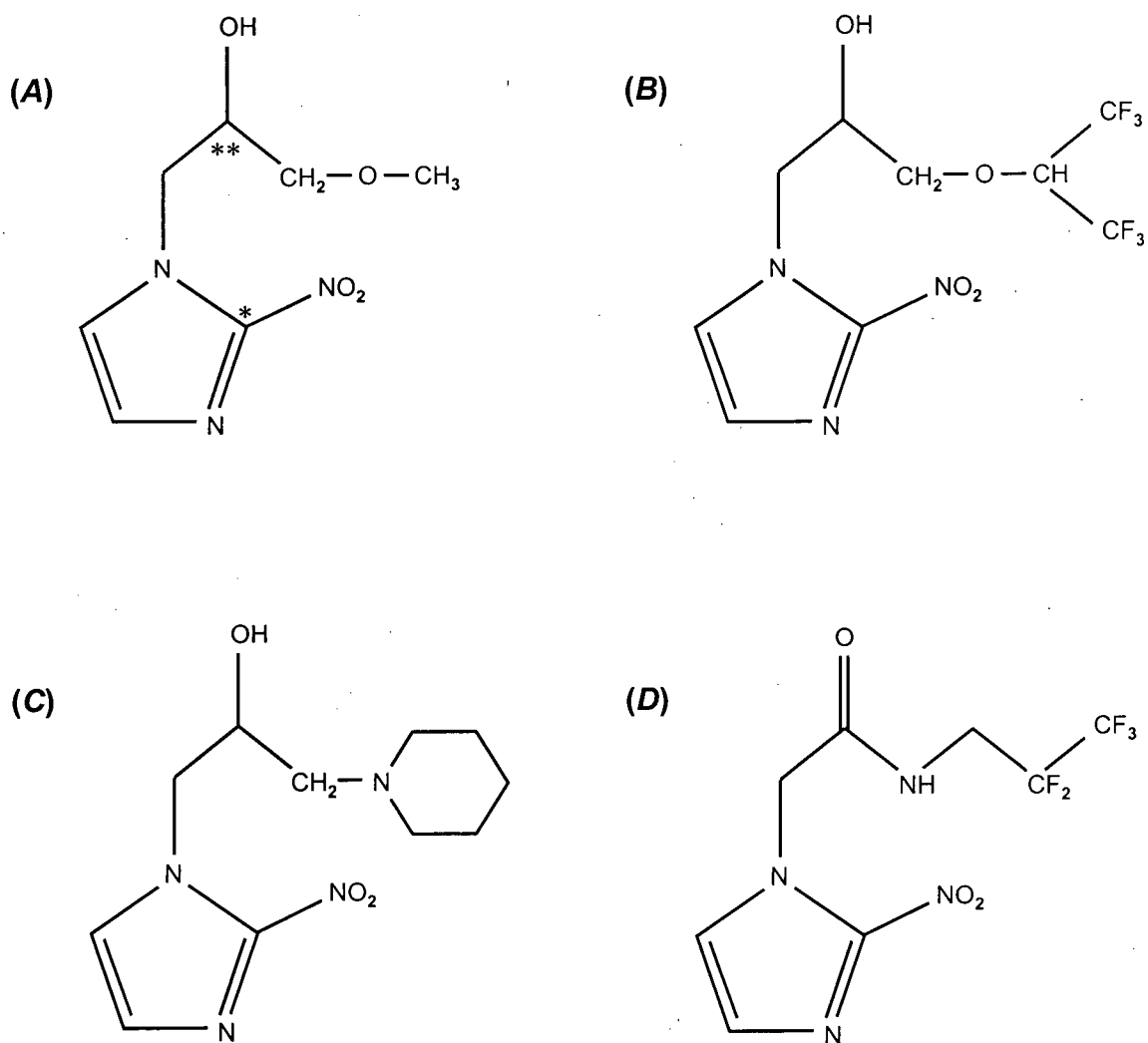


Figure 1.4 Structures of exogenous hypoxia markers.

(A) Misonidazole; sites of C^{14} (*) or H^3 (**) also indicated for radiolabeled misonidazole.

(B) CCI-103F.

(C) Pimonidazole.

(D) EF5.

1984; Van Os-Corby *et al.*, 1987). Importantly, the drug diffused rapidly through tissue (Franko *et al.*, 1987) and remained preferentially bound within the cell in which it was reduced (Franko *et al.*, 1982; Chapman *et al.*, 1983; Franko and Koch, 1984). Moreover, a relatively large (and easily detectable) number of adducts could be bound per cell without observable effects on cellular proliferative capacity or survival (Miller *et al.*, 1982; Chapman *et al.*, 1983). The fraction of tissue area containing bound radiolabeled misonidazole was also comparable to the radiobiologically hypoxic fraction of spheroids (Franko, 1985) and tumours (Hirst *et al.*, 1985).

Radiolabeled misonidazole was subsequently used in the clinic and provided evidence of hypoxic tumour cells, albeit with a great deal of inter- and intra-tumour heterogeneity (Urtasun *et al.*, 1986a; Urtasun *et al.*, 1986b; Chapman, 1991). Hypoxic cells were found primarily adjacent to necrosis, although misonidazole binding was also observed surrounding tumour vasculature (Urtasun *et al.*, 1986b), providing the first clinical suggestion that hypoxia could result from limited nutritive blood flow in some tumour regions.

Despite indications that misonidazole displayed promising characteristics as a marker of tumour hypoxia, the mechanism of 2-nitroimidazole binding was largely unknown and there were observations of presumably non-oxygen dependent binding in some tissues (Cobb *et al.*, 1990; Cobb *et al.*, 1992). Studies into the nature of misonidazole binding reconciled some of these observations, and led to the improved design of 2-nitroimidazole derivatives as exogenous hypoxia markers.

1.5.2.2 Binding of 2-nitroimidazoles

The current model for 2-nitroimidazole binding is depicted in Figure 1.5. When intracellular oxygen concentrations decrease to a sufficient level (binding occurs below 14 μM O_2 *in vitro*; Arteel *et al.*, 1995), reducing equivalents of NADH (or NADPH) normally involved in oxidative phosphorylation donate electrons to the intracellular 2-nitroimidazole. Nitroreductase enzyme activity is required for the “bioreductive activation” of 2-nitroimidazole into a nitro radical anion

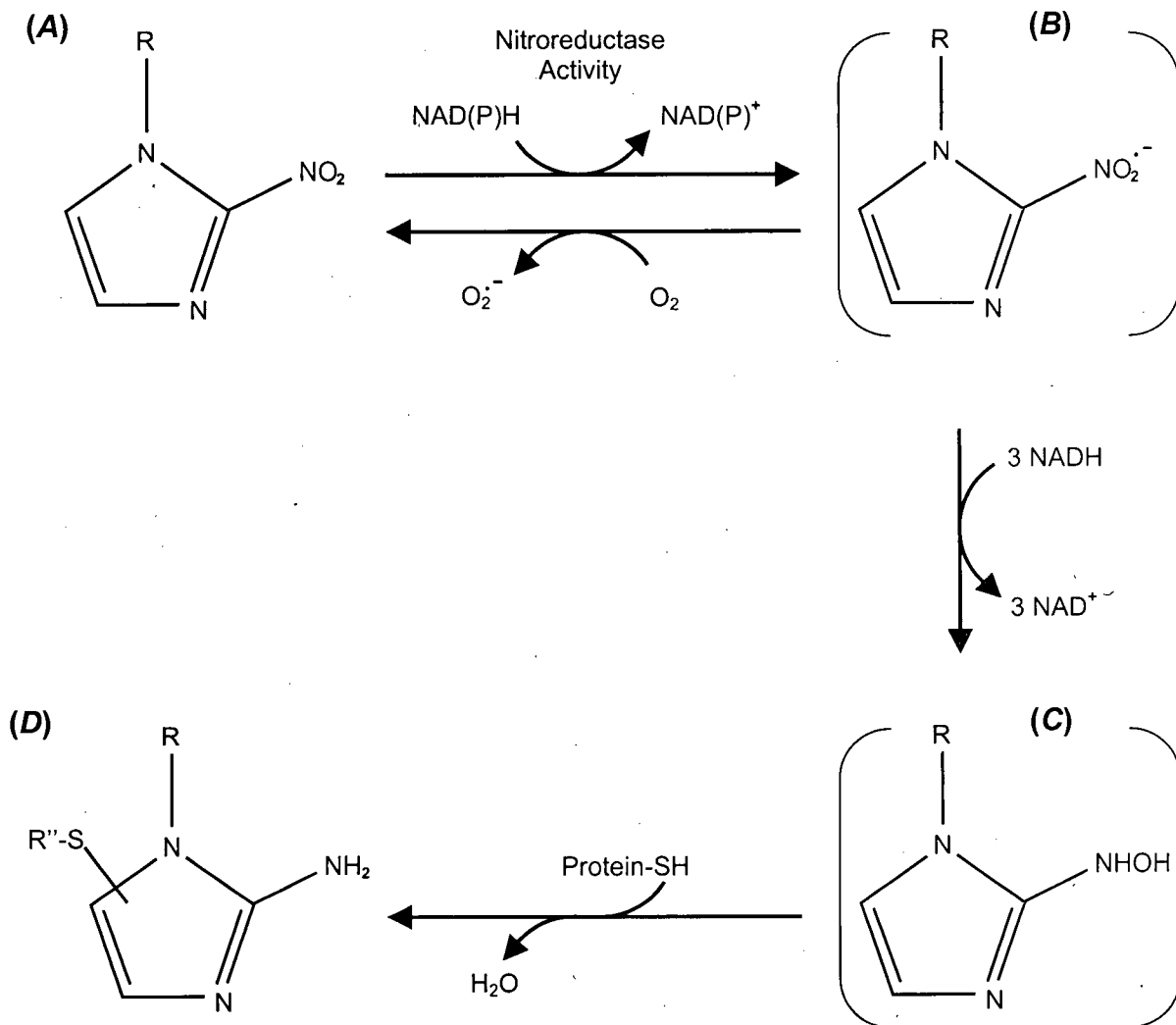


Figure 1.5 Mechanism of 2-nitroimidazole binding in hypoxic cells.

(A) 2-nitroimidazole derivative; R = side chain (see Figure 1.4).

(B) Nitro radical anion intermediate. Note the conversion of (A) to (B) is reversible in the presence of oxygen.

(C) Hydroxylamine intermediate.

(D) 2-nitroimidazole adduct bound to intracellular thiol-containing protein (S-R'').

Figure adapted from Arteel *et al.*, 1998.

intermediate. This reaction is reversible in the presence of oxygen (Perez-Reyes *et al.*, 1980), which is thought to account for the dependence of 2-nitroimidazole binding on low levels of oxygen (Raleigh *et al.*, 1999). The formation of 2-nitroimidazole adducts is dependent on cellular redox state insofar as the conversion of parent drug to bound adduct requires NADH as an electron donor (Moreno *et al.*, 1983). Importantly, neither an increase in the absolute levels of intracellular NADH nor an increase in the pyridine nucleotide redox state (i.e. more NADH relative to NAD^+) changes the oxygen dependence of 2-nitroimidazole binding (Arteel *et al.*, 1998). The rate of formation of the nitro radical anion may increase, but the anion is still rapidly reoxidized in the presence of oxygen. Conversion of the nitro radical anion intermediate into a form that binds to intracellular macromolecules likely occurs through a chemically unstable hydroxylamine intermediate (McClelland *et al.*, 1984). Reductively activated 2-nitroimidazole adducts are formed most efficiently with thiol-containing proteins (Raleigh and Koch, 1990) and peptides such as glutathione (Varghese, 1983; Chacon *et al.*, 1988; Arteel *et al.*, 1997), although the precise physical structure of 2-nitroimidazole adducts bound to macromolecules is presently unknown.

Observations of 2-nitroimidazole adducts bound in some normal tissues *in vivo* (Cobb *et al.*, 1990; Cobb *et al.*, 1992) led to speculation that binding could occur in the presence of oxygen if cells contained high levels of oxygen-sensitive enzymes such as cytochrome P450-dependent nitroreductases (Cobb *et al.*, 1990). However, subsequent studies demonstrated that large differences in P450 nitroreductase levels did not weaken the link between tissue pO_2 and 2-nitroimidazole binding in murine liver tissue (Arteel *et al.*, 1995). High levels of oxygen independent nitroreductases such as NAD(P)H:quinone acceptor oxidoreductase (DT diaphorase) may also influence non-oxygen dependent binding of 2-nitroimidazoles (Cobb *et al.*, 1992), although this effect does not appear to dominate binding patterns in a variety of normal and tumour tissue assessed *in vivo* (Parliament *et al.*, 1992). Thus the binding of 2-nitroimidazoles

generally require low levels of oxygen in the majority of cell types, but the relative number of bound adducts per cell can be influenced by metabolic factors that can vary between different tissue and tumour types (Raleigh *et al.*, 1996).

Other studies with radiolabeled derivatives of misonidazole demonstrated that the side chain of the drug was retained during nitroreduction and intracellular adduct binding (Raleigh *et al.*, 1985; Rasey *et al.*, 1985). These observations led to assessment of a variety of 2-nitroimidazole derivatives as potential hypoxia markers, many of which had been originally tested as alternatives to misonidazole for use as enhancers of radiation sensitivity (Williams *et al.*, 1982). The most prominent agents were 2-nitroimidazole derivatives that differed in their side chain composition, ranging from fluorination (e.g. CCI-103F and EF5) to the addition of more complicated ring structures (e.g. pimonidazole).

1.5.2.3 CCI-103F

Fluorinated 2-nitroimidazole derivatives exhibit similar oxygen-dependent binding characteristics as radiolabeled misonidazole (Raleigh *et al.*, 1987; Rasey *et al.*, 1987). CCI-103F (Figure 1.4B) is a hexafluorinated 2-nitroimidazole derivative originally developed to study tumour hypoxia based on bulk retention of the drug in tumours measured by non-invasive imaging methods (Raleigh *et al.*, 1986; Maxwell *et al.*, 1989; Jin *et al.*, 1990; Kwock *et al.*, 1992). Levels of CCI-103F binding were consistent with the known hypoxic fractions of a variety of tumour types (Maxwell *et al.*, 1989; Jin *et al.*, 1990), and tumour-to-plasma ratios were comparable to those reported for misonidazole (Raleigh *et al.*, 1986). However, non-invasive imaging techniques monitor bulk tumour retention of a drug as an indication of the hypoxic fraction, and therefore do not provide information on the spatial heterogeneity of hypoxia within a tumour and have limited sensitivity for detecting smaller hypoxic fractions (Cline *et al.*, 1990; Kwock *et al.*, 1992).

An important advance in the use of 2-nitroimidazole derivatives for measuring tumour hypoxia was realized with the synthesis of polyclonal antiserum against the hexafluorinated side chain of protein-bound CCI-103F (Raleigh *et al.*, 1987). The antiserum had a much higher affinity for bound CCI-103F adducts than for the free drug (Raleigh *et al.*, 1994), and enabled testing of fluorescence and peroxidase-based immunohistochemical methods for detecting tumour cells containing CCI-103F adducts in tissue sections. Immunohistochemical detection of bound CCI-103F adducts was more efficient than autoradiographic detection of radiolabeled 2-nitroimidazoles, and did not require the administration or handling of radioactive agents (Miller *et al.*, 1989). The binding patterns of CCI-103F and misonidazole were very similar to each other on a microregional level in multicellular spheroids and murine tumours (Raleigh *et al.*, 1987; Miller *et al.*, 1989; Moore *et al.*, 1992), suggesting that the two agents were labeling similar populations of tumour cells.

Automated methods to quantify fractions of CCI-103F-labeled cells in sections derived from canine tumour biopsies (Cline *et al.*, 1994; Cline *et al.*, 1997; Thrall *et al.*, 1997) provided a method for measuring tumour hypoxia with potential clinical applicability. An enzyme-linked immunosorbent assay (ELISA) was also developed to quantify the total concentration of bound CCI-103F adducts found in single cell suspensions produced from tumour biopsies (Raleigh *et al.*, 1992). Despite the loss of positional information obtainable by analyzing tumour sections, the ELISA was thought to be more convenient than automated analyses of tumour sections for repeated tumour hypoxia measurements (Raleigh *et al.*, 1994; Azuma *et al.*, 1997; Thrall *et al.*, 1997). Despite the development of these methods to detect and quantify cells containing bound CCI-103F adducts and the favorable binding pattern comparisons with misonidazole, CCI-103F was not used clinically due to the relative insolubility of the drug (5.3 mM in water; Raleigh *et al.*, 1986). However, the use of other 2-nitroimidazole derivatives with improved water

solubility (pimonidazole and EF5) enabled tumour hypoxia to be studied in the clinic, with much of the detection and quantification methodology derived from pre-clinical work with CCI-103F.

1.5.2.4 Pimonidazole

Pimonidazole (Ro 03-8799) is a 2-nitroimidazole derivative previously used as an alternative to misonidazole as a radiosensitizer. Pimonidazole has a piperidine-containing side chain (Figure 1.4C), and monoclonal antibodies were developed against protein-bound adducts of pimonidazole (Arteel *et al.*, 1995) enabling their detection by immunohistochemistry. Oxygen-dependent inhibition of pimonidazole binding *in vitro* is half-maximal at $\sim 4 \mu\text{M O}_2$ (Arteel *et al.*, 1998) with detectable binding up to $14 \mu\text{M O}_2$ (Arteel *et al.*, 1995). Pimonidazole is highly soluble in saline (400 mM), and is not cytotoxic to human tumour xenograft cells when administered in single doses up to 400 mg/kg (Durand and Raleigh, 1998). Pimonidazole is a weak base ($\text{pK}_a = 8.6$ at 37°C) and intracellular uptake of the drug (and therefore amount of drug available for adduct formation) could potentially be decreased in tumour areas with low extracellular pH. While decreased pimonidazole uptake with lower pH has been observed *in vitro* (Dennis *et al.*, 1985; Watts *et al.*, 1990), any *in vivo* effect appears to be relatively small compared to the large binding differences observed between hypoxic and aerobic cells (Arteel *et al.*, 1995). Moreover, while intra-tumour gradients of oxygen can be steep spatially, pH gradients in the same areas tend to be relatively flat (Helmlinger *et al.*, 1997), suggesting the sharp transitions between labeled and non-labeled cells observed in most tumours is influenced by oxygen more than pH.

A considerable advantage to the use of pimonidazole as a hypoxia marker is that relatively detailed toxicity and pharmacokinetic studies were performed when pimonidazole was used as a clinical radiosensitizer (Saunders *et al.*, 1982; Roberts *et al.*, 1984; Dische *et al.*, 1989). Pimonidazole has a plasma elimination half-life of just over 5 hours in humans, and the drug has been shown to preferentially accumulate in tumours within 30 minutes of administration with a

tumour-to-plasma ratio of 3.4-to-1 (Saunders *et al.*, 1984). Armed with this previous clinical knowledge, pimonidazole was introduced rather quickly into the clinic as a marker of tumour hypoxia (Kennedy *et al.*, 1997; Varia *et al.*, 1998).

Binding patterns of pimonidazole-labeled cells in (spontaneous) clinical tumours (Kennedy *et al.*, 1997) are extremely similar to patterns of CCI-103F labeling in spontaneous canine tumours (Cline *et al.*, 1994). From a functional standpoint, tumour cells that bind pimonidazole have been shown to be clonogenic, providing evidence that pimonidazole is bound in viable, therapeutically relevant hypoxic cells *in vivo* (Durand and Raleigh, 1998). Pimonidazole binding has been correlated with the fraction of Eppendorf pO₂ readings below a given threshold value (either 5 or 10 mmHg; Raleigh *et al.*, 1999), and mean or median pO₂ measurements obtained with Oxylite probes have also correlated well with mean and median fractions of pimonidazole-containing cells in three human tumour xenograft lines (Bussink *et al.*, 2000b). Functionally, pimonidazole binding has been correlated with the radiobiological hypoxic fraction of various murine tumours (Raleigh *et al.*, 1999) and with radiation-induced DNA damage as assessed by the alkaline comet assay (Olive *et al.*, 2000), providing further evidence that hypoxic cells labeled with pimonidazole are therapeutically relevant. Attempts to combine pimonidazole labeling with measures of perfused tumour blood vessels in the clinic are ongoing (Janssen *et al.*, 2002), and may represent a useful vehicle for relating both microenvironmental parameters to clinical therapeutic outcome.

Fluorescent antibodies against bound pimonidazole adducts have enabled quantification of pimonidazole-labeled cells by flow cytometry analysis of single cell suspensions derived from whole experimental tumours (Durand and Raleigh, 1998; Olive *et al.*, 2000) or from clinical biopsies (Durand and Aquino-Parsons, 2001a; Durand and Aquino-Parsons, 2001b). Interestingly, the number of pimonidazole adducts bound in a given hypoxic cell can vary between tumours, and even within different regions of the same tumour. Differences in the

numbers of bound pimonidazole adducts may be due to transient perfusion (and thus non-constant drug exposure and oxygenation status), different nitroreductase activities in some cells, or variations in the ratio of intracellular protein thiol to non-protein thiol concentrations (Raleigh and Koch, 1990). However, despite variations in the *absolute* number of bound adducts between pimonidazole-containing cells, the several-fold increase in the *relative* number of bound pimonidazole adducts between labeled and non-labeled cells provides a clear transition within a few cell diameters *in vivo*. Thus the fraction of a tumour section that is hypoxic can be quantified by setting a “threshold” to identify the fraction of tumour area that is “pimonidazole-positive”, without distinguishing between hypoxic cells that contain higher or lower numbers of bound adducts. Similarly, fluorescence intensity thresholds can be set to distinguish between labeled and non-labeled cells in flow cytometry analyses. This methodology is analogous to citing the fraction of Eppendorf pO_2 measurements below a given threshold of oxygen tension, and will be discussed further in Section 1.5.2.6.

1.5.2.5 EF5

EF5 is a pentafluorinated derivative of etanidazole (Figure 1.4D) that has been shown to display less non-oxygen dependent binding than misonidazole (Lord *et al.*, 1993). Monoclonal antibody synthesized against bound EF5 adducts has facilitated analysis of the hypoxic content of spheroids and tumours by image analysis and flow cytometry (Evans *et al.*, 1995; Koch *et al.*, 1995). EF5 has been used to study hypoxia in normal (murine) tissues (Bergeron *et al.*, 1999) and to measure tumour hypoxia in the clinic (Evans *et al.*, 2000; Evans *et al.*, 2001), albeit with different quantification principles than are typically used for pimonidazole (see Section 1.5.2.6). EF5 binding correlates with resistance to ionizing radiation in tumours (Evans *et al.*, 1996; Lee *et al.*, 1996) and in subpopulations of spheroid cells derived from different spheroid cell layers (Woods *et al.*, 1996). Interestingly, the best correlations of EF5 and radiobiological hypoxic fraction were found when only considering cells with intermediate binding intensities (Evans *et*

al., 1996), which may represent cells at intermediate levels of steady-state oxygenation. EF5 binding correlates weakly with Eppendorf pO₂ readings; which has been attributed to differences in detection volumes, the influence of necrosis, and the measurement duration of each technique (Evans *et al.*, 2000; Jenkins *et al.*, 2000). Detailed clinical pharmacokinetic studies have been performed with EF5, highlighting the *in situ* stability of the drug and a plasma elimination half-life that is approximately twice that of either the parent compound (etanidazole) or pimonidazole (Koch *et al.*, 2001). This body of work has made EF5 a suitable alternative to pimonidazole for measuring tumour hypoxia in the clinic, and may eventually lead to analyses involving sequential administration of the two markers to measure changes in hypoxia over time (see Chapters 3, 4, and 6).

1.5.2.6 Quantification of pimonidazole and EF5

Differences in the absolute numbers of hypoxia marker adducts bound in hypoxic cells from different tumours has led to a substantial debate over the appropriate method to quantify tumour hypoxia using exogenous markers. Proponents of EF5 typically view hypoxia marker binding as a continuum that parallels the continuum of steady-state tumour cell oxygenation. A cell containing more bound adducts is more intensely fluorescent after contact with appropriate antibody, and is therefore considered more hypoxic than a cell containing fewer bound adducts in a given tumour. Since the absolute fluorescence intensity can vary between tumours, EF5 binding is “calibrated” *in vitro* using excised tumour tissue exposed to the hypoxia marker under defined oxygen levels. The maximal binding intensity of the *in vitro* tissue sample is then compared to that obtained *in situ*, and an estimate for the oxygenation level of cells in the tumour are determined. The assumption is that the primary variables determining binding intensity are the concentration of marker in the cell, the degree of cellular hypoxia, and the duration of binding allowed between hypoxia marker administration and tumour biopsy. While these may be the primary variables when labeling hypoxic cells *in vitro*, comparison to hypoxia marker

binding *in vivo* assumes constant tumour perfusion (i.e. marker delivery and therefore intracellular concentration) and cellular oxygenation (i.e. ability to bind hypoxia marker) over time. Thus the *delivery* of hypoxia marker and the *duration of hypoxia in situ* are not taken into account with this method, both of which likely constitute very important determinants of hypoxia marker binding intensity.

As discussed in Section 1.2.1.2, tumour perfusion can be quite variable over time in a variety of tumour types. Delivery of exogenous hypoxia markers to tumour cells may not be a limitation if the goal is for a given cell to receive enough marker to be detectable above some threshold value (e.g. for image or flow cytometry analysis). Exogenous hypoxia markers are typically freely diffusible, even to relatively poorly perfused tumour regions provided the circulation lifetimes are sufficiently long. However, since delivery of the drug may not be constant over time, the *absolute* number of bound adducts would be variable in areas of varying perfusion. It is worth noting that this is not a problem if the goal were to determine the fraction of tumour cells labeled with a concentration of marker sufficient to distinguish between labeled and non-labeled cells (i.e. to produce sufficient binding *relative* to non-hypoxic cells).

The duration of cellular hypoxia is an even more complex variable that may affect absolute levels of hypoxia marker binding. Since changes in tumour oxygenation can occur over time in a variety of tumour types (Section 1.2.1.2), the intensity of hypoxia marker binding may also be affected by the fraction of time that a given cell is below the appropriate oxygen tension. Clearly a cell that was able to bind hypoxia marker adducts for 3 hours would have a higher absolute binding intensity than a cell that was only hypoxic enough to bind marker for 30 minutes (with a given marker concentration). Again, this issue is avoided by using a quantification method that expresses hypoxia as a fraction of tumour cells labeled with (detectable) levels of hypoxia marker, without distinguishing between lightly and heavily labeled cells. This method for

quantifying hypoxic tumour cells will therefore be used for the flow cytometry analyses of tumour cells containing exogenous hypoxia markers presented in Chapters 3 and 4.

1.5.3 Endogenous Hypoxia Markers

Recently, there has been an increasing movement toward the use of hypoxia responsive proteins as endogenous “markers” of tumour hypoxia (Sutherland *et al.*, 1996). Endogenous gene products that are up-regulated in response to hypoxia represent less inconvenient and invasive “markers” of hypoxia when compared to exogenous agents (that must be administered), such as pimonidazole and EF5. The expression of endogenous markers can also be measured in archival biopsy material, allowing retrospective assessments of endogenous marker expression with therapeutic outcome. This feature of endogenous hypoxia markers has led to a large number of studies in a relatively short period of time, primarily involving hypoxia inducible factor-1 α and carbonic anhydrase 9.

1.5.3.1 Hypoxia inducible factor-1 α

As outlined in Section 1.4.1, the expression of a variety of hypoxia inducible genes is regulated by the hypoxia inducible factor-1 (HIF-1) transcription factor (Semenza, 2003). The α -subunit of HIF-1 is rapidly degraded in the presence of oxygen, and relative protein levels therefore increase below a given level of oxygenation. Antibodies have been developed for immunohistochemical detection of HIF-1 α , and correlations observed between fractions of cells containing high levels of HIF-1 α and cell fractions labeled with the exogenous hypoxia markers EF5 (Vukovic *et al.*, 2001) or pimonidazole (Vordermark and Brown, 2003) in human tumour xenografts. However, HIF-1 α co-localized relatively poorly with either exogenous marker, and image analysis identified HIF-1 α -containing cells located closer to tumour vasculature than EF5-labeled cells. These data can be reconciled by the differences in oxygen dependency for increased levels of HIF-1 α protein (half-maximal at 1.5-2% O₂; Jiang *et al.*, 1996) compared to EF5 binding (half-maximal at ~1% O₂). Thus with respect to the diffusion-limited model of

tumour hypoxia, HIF-1 α protein levels are increased in cells that are closer to tumour vasculature and not hypoxic enough to bind significant levels of exogenous hypoxia marker.

Degradation of HIF-1 α is rapid in the presence of oxygen with a half-life of only a few minutes (Wang *et al.*, 1995; Jiang *et al.*, 1996; Jewell *et al.*, 2001; Vordermark *et al.*, 2004), and tumour samples must therefore be rapidly fixed or frozen upon excision to prevent loss of detectable protein. This characteristic of HIF-1 α is not commonly discussed in the literature and may preclude its use as an endogenous marker for archival material, particularly in the (common) situation where the time between tumour biopsy and tissue fixation is unknown.

In terms of prognostic ability, increased HIF-1 α protein levels have been correlated with decreased overall survival after treatment of oligodendrogliomas (Birner *et al.*, 2001) and cancers of the esophagus (Koukourakis *et al.*, 2001b), lung (Giatromanolaki *et al.*, 2001b), and breast (Bos *et al.*, 2003). Increased HIF-1 α levels also correlated with decreased overall survival and disease free survival after radiation treatment of cancers of the cervix (Birner *et al.*, 2000) and of the head and neck (Aebersold *et al.*, 2001; Koukourakis *et al.*, 2002). Observations that HIF-1 α protein levels can be increased by non-oxygen dependent mechanisms in some cases (Maxwell *et al.*, 1999; Semenza, 2003) may influence its prognostic utility, particularly in spontaneous clinical tumours that typically have increased genetic heterogeneity compared to tumour cell lines used for *in vitro* or *in vivo* experimental work. Indeed, correlations between HIF-1 α protein levels and *in vitro* radiobiological hypoxic fractions indicate a relationship that is dependent on tumour cell type (Vordermark *et al.*, 2004). Other studies have shown poor correlations between HIF-1 α protein levels and pimonidazole in a small series of head and neck tumours (Janssen *et al.*, 2002), or disease free survival in cervix carcinomas (Haugland *et al.*, 2002). Interestingly, HIF-1 α has also been shown to correlate with *improved* disease free survival and overall survival in head and neck tumours treated by surgical resection (Beasley *et al.*, 2002). These latter observations oppose the relatively common belief that hypoxic tumours

tend to be more aggressive, and suggest further work is required relating HIF-1 α levels to outcome from various treatment regimens before HIF-1 α can be used as a reliable prognostic indicator (Brown and Le, 2002; Begg, 2003).

Gene products that are transcriptionally regulated by HIF-1 may represent attractive alternatives to HIF-1 α as endogenous hypoxia markers, particularly since HIF-1 transcriptional activity requires oxygen-dependent hydroxylation by the co-repressor FIH-1 (Jiang *et al.*, 1997; Pugh *et al.*, 1997; Mahon *et al.*, 2001). Thus the transcription of HIF-1 regulated genes provides a second oxygen-dependent step which may alleviate some of the issues associated with non-oxygen dependent increases in HIF-1 α protein levels (Begg, 2003). HIF-1 regulated gene products that have been used as endogenous markers of tumour hypoxia include the transmembrane protein carbonic anhydrase 9.

1.5.3.2 Carbonic anhydrase 9

As indicated in Section 1.4.2, carbonic anhydrase 9 (CAIX) has a major role in maintaining intracellular pH homeostasis (Potter and Harris, 2004), and is transcriptionally regulated by HIF-1 (Wykoff *et al.*, 2000). The expression of CAIX has been demonstrated in a variety of tumour cell types, indicating its potential utility as a prognostic marker of tumour hypoxia (Beasley *et al.*, 2001; Ivanov *et al.*, 2001; Swinson *et al.*, 2003). CAIX is expressed primarily in viable, hypoxic tumour cells (Olive *et al.*, 2001a) and is stable *in vitro*, with protein levels remaining unchanged for up to 72 hours after up-regulation by hypoxia (Turner *et al.*, 2002). The remarkable stability of CAIX has made it a popular endogenous hypoxia marker for retrospective studies of tumour hypoxia in archival clinical tissue. CAIX expression has been correlated with low pO₂ measurements (Loncaster *et al.*, 2001), and decreased overall survival (Giatromanolaki *et al.*, 2001a; Koukourakis *et al.*, 2001a) and/or disease free survival (Chia *et al.*, 2001; Loncaster *et al.*, 2001; Hui *et al.*, 2002; Hoskin *et al.*, 2003) in a variety of tumour types. However, other groups have reported contradictory results in the same tumour types, with no

significant correlations between CAIX expression and low pO_2 measurements (Hedley *et al.*, 2003) or disease free survival (Kaanders *et al.*, 2002; Turner *et al.*, 2002; Hedley *et al.*, 2003). It remains to be determined whether these discrepancies represent actual differences in the prognostic value of CAIX expression levels, or technology-based differences associated with tumour section image analyses used to quantify CAIX expressing cells (Airley *et al.*, 2003).

Qualitative comparisons between cells expressing CAIX and cells labeled with exogenous pimonidazole indicate a relatively large degree of overlap (Wykoff *et al.*, 2000; Hoskin *et al.*, 2003), although CAIX expressing cells are typically observed closer to tumour vasculature (Olive *et al.*, 2001a; Kaanders *et al.*, 2002). Since CAIX expression is controlled by HIF-1, these observations are consistent with the differences in oxygen dependencies between HIF-1 α protein levels and exogenous hypoxia marker binding cited in the previous Section. Quantitatively, CAIX expression has been found to correlate to varying degrees with pimonidazole binding (Kaanders *et al.*, 2002; Airley *et al.*, 2003; Hoskin *et al.*, 2003), HIF-1 α protein expression (Hui *et al.*, 2002), and expression of the HIF-1 regulated glucose transporter-1 (Glut-1; Airley *et al.*, 2003; Hoskin *et al.*, 2003).

For studying variations in tumour hypoxia over time, the expression of CAIX is less responsive than HIF-1 α to temporal changes in cellular hypoxic status. CAIX is stable once expressed in a hypoxic cell, and therefore theoretically indicates the hypoxic "history" of cells. Tumour cells that were hypoxic enough for long enough over the previous several days will express CAIX, without distinguishing between cells that were hypoxic for all or part of that time. Conversely, HIF-1 α is rapidly degraded in the presence of oxygen and therefore cells containing high levels of HIF-1 α were hypoxic within a few minutes of tumour biopsy for analysis. Similarly, HIF-1 α protein levels increase rapidly in response to hypoxia, particularly when compared to the increased expression of CAIX protein that requires HIF-1 induced up-regulation of CAIX mRNA and subsequent protein synthesis. Different endogenous hypoxia markers

therefore provide disparate information pertaining to the dynamics of tumour hypoxia, and it is unknown which estimate of tumour hypoxia is more relevant for therapy. Furthermore, it would appear that no single method of estimating tumour hypoxia is readily applicable to measuring transient tumour hypoxia, but the combination of multiple hypoxia markers into a single assay may provide insights into the dynamic tumour microenvironment (Chapters 3-4).

1.6 RESEARCH OBJECTIVES

The working hypothesis for this thesis is that tumour hypoxia is a dynamic process, and that tumour cells with a temporally changing hypoxic status differ from tumour cells with more steady-state hypoxia in terms of response to perfusion modification, proximity to tumour vasculature, and gene expression profiles. Judicious selection and development of methods designed to identify and quantify transiently hypoxic tumour cells represents a therapeutically relevant goal, particularly for the further assessment of the presence and potential therapeutic impact of transient hypoxia in the clinic.

1.6.1 Specific Aims

- I. To determine how drug-induced changes in tumour blood flow influence tumour radiosensitivity through improved oxygenation of different tumour cell subpopulations. Work in this aim will help to establish the therapeutic relevance of different populations of hypoxic tumour cells.
- II. To develop a method for quantifying transiently hypoxic tumour cells and to use this method to characterize transient hypoxia in human tumour xenografts. Work in this aim will highlight the importance of selecting appropriate methodology for measuring hypoxic cells in tumours with different transient hypoxia kinetics, and will introduce the concept of hypoxic fractions that are “integrated” over time.
- III. To evaluate an alternate route of exogenous hypoxia marker administration for labeling hypoxic tumour cells. Work in this aim is concerned with extending “integrated” hypoxia measurements to include tumour cells with a hypoxic status that changes over periods of many days, and to establish the therapeutic relevance of these cells.
- IV. To identify differences in gene expression induced by hypoxia between tumour cells grown in disparate microenvironments *in vitro*. Work in this aim may lead to novel endogenous markers to distinguish between chronically and transiently hypoxic tumour cells *in vivo*.

1.6.2 Thesis Overview

The subsequent Chapters of this thesis will deal with each of the Specific Aims listed above. Chapter 2 will focus on drug-induced changes in tumour blood flow to reduce tumour hypoxia. Two drugs with established mechanisms of action were used as tools to modify net tumour perfusion and the distribution of tumour blood flow in different tumour regions. The influence of these perfusion changes on the radiosensitivity of various tumour cell subpopulations indicate the therapeutic relevance of different hypoxic tumour cells.

Chapter 3 will involve the development of a method for identifying and quantifying transiently hypoxic cells in solid tumours. Two sequentially administered exogenous hypoxia markers were used to differentially label cells that were hypoxic over different periods of time, with quantification by flow cytometry. Estimates for the transiently hypoxic fractions of two tumour types will be presented, along with indications of the kinetics of transient hypoxia in these tumours and the importance of “time-integrated” tumour hypoxia measurements. The potential clinical applicability and relevance of the method will also be discussed. Chapter 4 will describe oral administration of the exogenous hypoxia marker pimonidazole to label hypoxic tumour cells. Oral pimonidazole was combined with injection of a second hypoxia marker or a proliferation marker to provide insights into the fractions of tumour cells with long-term changes in hypoxic status, and the therapeutic relevance of these cells.

Chapter 5 presents gene expression patterns from cells exposed to a transient hypoxic episode after being grown in different microenvironments *in vitro*. Candidate gene products to potentially differentiate between hypoxic cells in different growth conditions *in vivo* will be identified, along with preliminary data for using a selected gene product as a potential endogenous marker of transiently hypoxic tumour cells. Chapter 6 will include a thesis summary and will present suggestions for future work, with particular reference to the potential clinical applicability of the data, methods, and concepts discussed in this thesis.

CHAPTER 2: MODIFYING TUMOUR PERFUSION TO IMPROVE TUMOUR RADIOSENSITIVITY

This Chapter has been adapted from the following published manuscript:

Bennewith, KL and Durand, RE (2001) Drug-induced alterations in tumour perfusion yield increases in tumour cell radiosensitivity. *Br J Cancer* **85**(10): 1577-1584.

2.1 INTRODUCTION

As outlined in Section 1.3.1, many solid tumours contain poorly oxygenated cells that are less sensitive to treatment with ionizing radiation. The presence of diffusion-limited hypoxic cells is well-established in a variety of tumour types, and was traditionally thought to represent the primary barrier to effective radiation therapy. However, the radiation response of tumour cells not only depends on their oxygenation level at the time of irradiation (Gray *et al.*, 1953), but also on their nutrient status insofar as it influences DNA repair capacity (Ling *et al.*, 1988; Gerweck *et al.*, 1993; Denekamp and Dasu, 1999). Tumour cells that have a higher nutrient status and are at intermediate levels of oxygenation (i.e. cells situated along the oxygen diffusion gradient) are therefore thought to represent important limitations to radiation therapy (Wouters and Brown, 1997; Evans *et al.*, 1997; Olive *et al.*, 2002). Moreover, tumour cells that experience changes in hypoxic status over time (i.e. transiently hypoxic cells) have also been postulated to influence tumour response to radiation therapy, despite inadequate methodology to detect these tumour cells in the clinic. Transiently hypoxic tumour cells are thought to have improved DNA repair capacity relative to diffusion-limited hypoxic cells (Denekamp and Dasu, 1999), and have been shown to retain some capacity to proliferate during temporary decreases in oxygenation (Durand and Raleigh, 1998).

One strategy for improving tumour response to radiation therapy is to improve the oxygenation of tumour cells at the time of irradiation. For example, increasing the oxygen content of systemic blood through breathing high oxygen content gas would be thought to increase the delivery and the diffusion distance of oxygen in a tumour, thereby targeting diffusion-limited hypoxic cells (Chaplin *et al.*, 1986). Conversely, modifying tumour perfusion may increase oxygen delivery to tumour regions that are normally transiently hypoxic, without necessarily influencing oxygen delivery to diffusion-limited hypoxic cells. The hemorrheologic drug pentoxifylline was used as a tool to study how changing tumour perfusion to favor

increased delivery of oxygen prior to a dose of radiation could influence the radiosensitivity of different subpopulations of tumour cells.

Pentoxifylline has been shown to increase the deformability of red blood cells and leukocytes *in vitro* (Ehrly, 1978; Armstrong *et al.*, 1990; Arcuri *et al.*, 1998). As discussed in Section 1.2.1.2, chaotic tumour vasculature can contribute to the formation of a hypoxic tumour microenvironment (Vaupel *et al.*, 1989). The buildup of cellular waste products and CO₂ in poorly vascularized tumour tissue decreases tumour extracellular pH, which may also decrease the pH of some tumour microvasculature containing sluggish blood flow. Lower pH can increase the rigidity of blood cells and increase blood viscosity (Van Nueten and Vanhoutte, 1980; Hakim and Macek, 1988), further impairing blood flow through tumour blood vessels. Pentoxifylline is thought to counteract microenvironment-induced increases in blood cell rigidity, decrease blood viscosity, and improve blood flow through narrow tumour vasculature. Pentoxifylline has been shown to decrease interstitial fluid pressure and increase net tumour perfusion, oxygenation, and radiosensitivity in a variety of experimental tumour systems (Lee *et al.*, 1992; Song *et al.*, 1992; Honess *et al.*, 1993; Lee *et al.*, 1993; Lee *et al.*, 1994; Song *et al.*, 1994; Honess *et al.*, 1995; Kelleher *et al.*, 1998).

Pentoxifylline was used to induce changes in tumour perfusion on a whole tumour and a microregional scale in two different human tumour xenografts. Net tumour perfusion was measured by quantifying tumour uptake of the radioisotope rubidium-86 (Rb⁸⁶; Sapirstein, 1958; Gullino and Grantham, 1961), while changes in microregional tumour perfusion were assessed by quantifying tumour areas that were differentially stained with two sequentially administered fluorescent perfusion dyes (Trotter *et al.*, 1989). These methods indirectly measure drug-induced changes in tumour cell oxygenation, and the oxygenation status can be functionally evaluated using an *in vivo-in vitro* assay of tumour cell sensitivity to ionizing radiation. Fluorescence-activated cell sorting based on intracellular content of a fluorescent perfusion dye

was used in conjunction with the radiosensitivity assay to isolate the radiation responses of different subpopulations of tumour cells. These data therefore provide information on tumour cells that are preferentially radiosensitized by pentoxifylline-induced changes in tumour perfusion, and indicate the relevance of these cells in tumour response to ionizing radiation.

2.2 MATERIALS AND METHODS

The materials and methods outlined in Sections 2.2.1, 2.2.4, and 2.2.5 are central to this thesis and will be used in subsequent Chapters; the methods will therefore be discussed in some detail.

2.2.1 Tumours

Tumours derived from SiHa, a human cervical squamous cell carcinoma (Friedl *et al.*, 1970), and WiDr, a human colon adenocarcinoma (Noguchi *et al.*, 1979), were used for all experiments in this Chapter and in Chapters 3-4. Both were obtained as cultured cell lines (American Type Culture Collection, Rockville, MD), grown in severe combined immunodeficient (SCID) mice and maintained by intramuscular transplant. Experimental tumours were grown as dorsal subcutaneous implants in 7-8 week old SCID mice (typically male; bred in-house), and were used 3-4 weeks after implantation at an average weight of ~500 mg. All procedures were performed in accordance with the ethical standards of the University of British Columbia Committee on Animal Care and the Canadian Council on Animal Care.

2.2.2 Reagents

Diltiazem hydrochloride (ICN Biomedicals, Costa Mesa, CA) and pentoxifylline (Sigma-Aldrich Canada Ltd., Oakville, ON) were dissolved in Dulbecco's PBS (Gibco Invitrogen Corp., Burlington, ON) for intraperitoneal (i.p.) injection at the cited concentrations in an approximate volume of 0.01 ml/g mouse body weight. Rubidium-86 chloride (Rb^{86}Cl ; Amersham Pharmacia Biotech, Buckinghamshire, UK) was diluted in PBS to an activity of ~3.7 MBq of Rb^{86} per 0.1 ml injection.

2.2.3 Rubidium-86 (Rb^{86}) Extraction

Tissue uptake of Rb^{86} after a bolus intravenous (i.v.) injection of Rb^{86}Cl is proportional to the fraction of the cardiac output (CO) flowing through that tissue (Sapirstein, 1958). This method of estimating tissue perfusion has also been validated for measuring net blood flow in implanted

tumours (Gullino and Grantham, 1961), however each blood flow measurement is terminal since the detection of Rb^{86} is performed on excised tissue. A modified Rb^{86} extraction method was developed to enable multiple tumour blood flow measurements in the same mouse (e.g. before and after treatment with a blood flow modifying drug); each animal (and tumour) was therefore used as its own control.

The method involved a solid-state radiation detection probe positioned over the implanted tumour during each of two sequential i.v. injections of Rb^{86}Cl (Figure 2.1), with i.p. administration of a blood flow modifying drug before the second Rb^{86}Cl injection. Activity from the tumour area was measured for 90 seconds after each isotope injection, which has previously been established as the time in which tumour uptake of Rb^{86} is at a plateau (Zanelli and Fowler, 1974). The activity remaining from the first Rb^{86}Cl injection was used as the background signal for the second injection, and the radioactivity of the tail was measured after each injection in order to correct for any solution remaining at the injection site. Mice were excluded from analysis if the activity remaining in the tail from either Rb^{86}Cl injection was more than 10% of the injected activity (suggesting poor injection technique).

Animals were terminated 90 seconds after the second isotope injection, and the tumour and overlying skin were excised, weighed, and monitored for radioactivity in a Cobra II Auto Gamma well-type radiation counter (Packard Instrumentals, Meriden, CT). The external radioactivity signal from the tumour area was normalized for the skin overlying the tumour to provide a radioactivity estimate for the tumour alone. Data are expressed in terms of % injected activity per gram of tumour tissue, which is proportional to the % cardiac output per gram of tissue (% CO/g).

2.2.4 Dual Stain Mismatch

Changes in regional tumour perfusion over time can be assessed using two sequentially administered fluorescent perfusion dyes (Trotter *et al.*, 1989). Tumour areas stained more

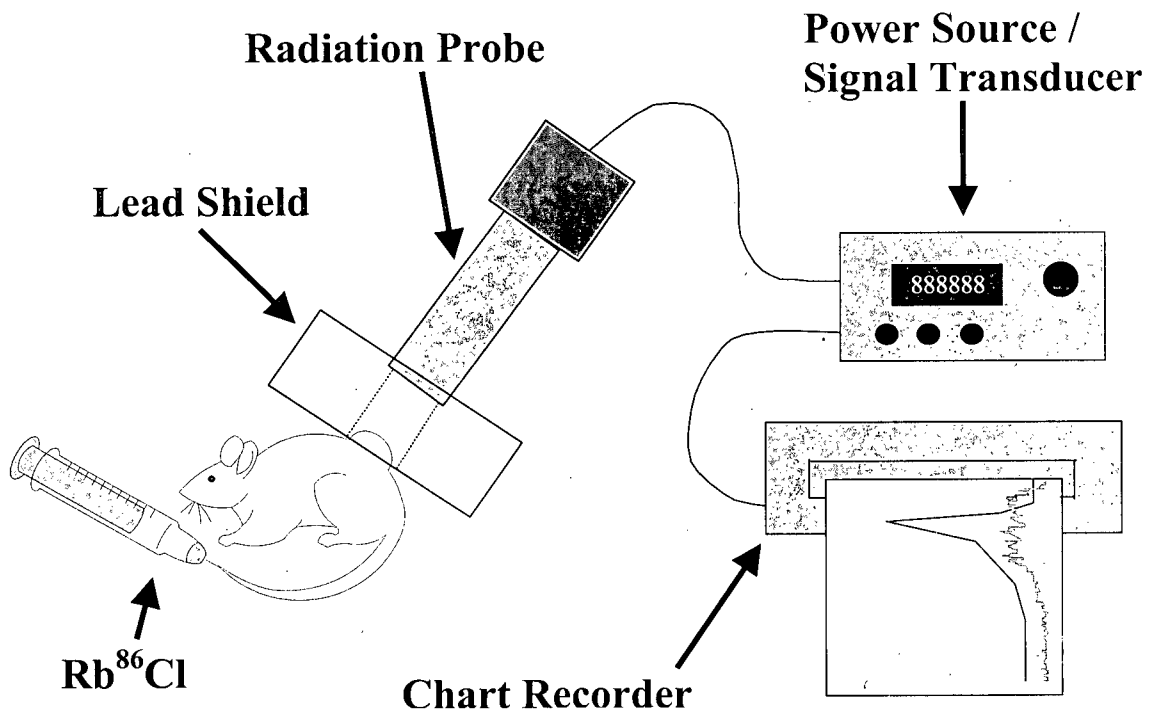


Figure 2.1 Diagram of the Rb^{86} extraction method.

The lead shield was designed with an aperture so the radioactivity signal from the tumour area could be isolated from the overall radioactivity of the animal. The signal from the tumour area is normalized for activity from the skin overlying the tumour (see text).

intensely with one dye relative to the other indicate regions that experienced a relative increase or decrease in perfusion during the time between dye injections (Figure 2.2).

The fluorescent bisbenzimidazole dye Hoechst 33342 (0.5 mg per mouse delivered in 0.05 ml PBS; Sigma-Aldrich Canada Ltd.) was administered by i.v. injection to tumour-bearing mice, followed 35 minutes later by i.v. injection of the carbocyanine derivative DiOC₇ (0.1 mg per mouse in 0.05 ml of 75% DMSO; Sigma-Aldrich Canada Ltd.). Pentoxifylline was injected i.p. 15 or 30 minutes before carbocyanine injection, and 5 minutes later the tumours were excised, embedded, frozen, and sectioned. Representative microscopic images of the tumour sections were digitized and analyzed by locally developed software that enabled quantitative assessment of the differential relative fluorescence intensities of each stain (Durand and LePard, 1994; Durand and LePard, 1995). Ten images were collected for each tumour and the data were averaged to include perfusion changes from various tumour regions.

Differences in staining profiles were quantified using a multistep algorithm to facilitate statistical analysis. Briefly, the fluorescence intensity of each stain was normalized against the maximal and background stain intensities found in each set of ten images (for a given tumour). Each image was then analyzed on a pixel-by-pixel basis, and when the fluorescence intensity of either stain exceeded background, the relative intensity of the carbocyanine staining (green) was compared with the Hoechst staining (blue). Relative staining intensities that varied by less than a factor of 2 were defined as "matched" staining and assigned a value of "0% change". A 2- to 3-fold increase in carbocyanine staining relative to Hoechst staining (green > blue) indicated areas of increased relative perfusion over the time interval and were defined as "+100% change". Similarly, a 3- to 4-fold increase in relative staining intensity was defined as a "+200% change", etc. Areas of decreased carbocyanine intensity relative to Hoechst intensity (green < blue) were expressed as negative percentage changes. Percentage changes exceeding $\pm 300\%$ (i.e. > 4-fold

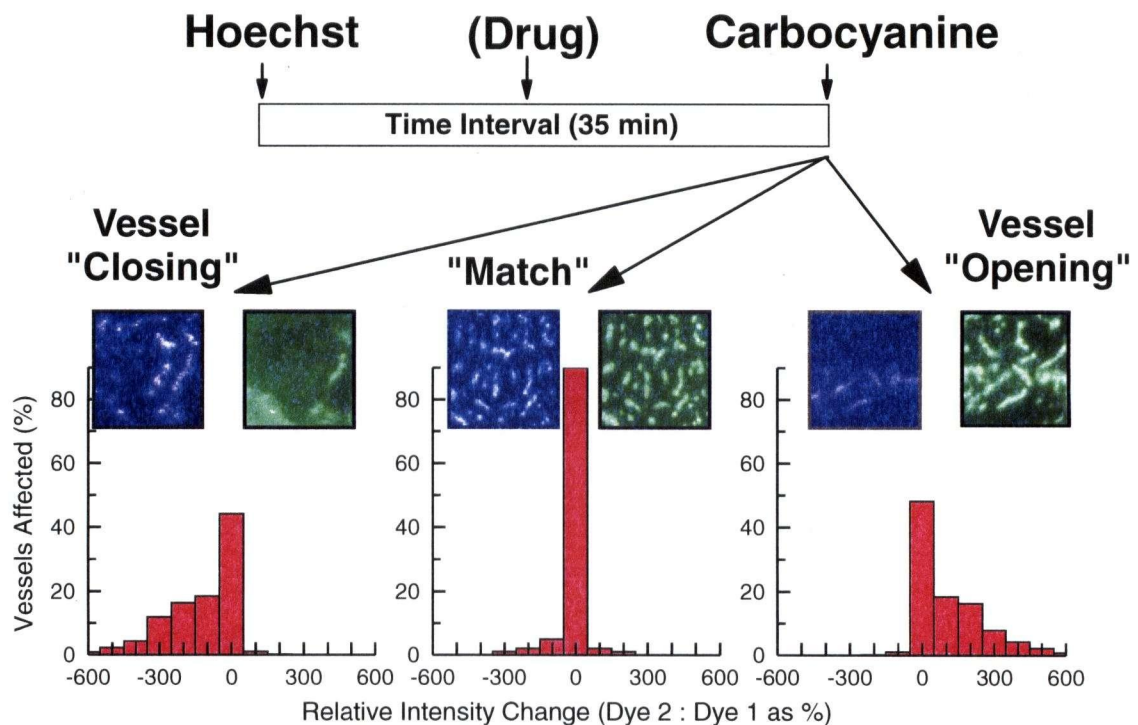


Figure 2.2 Illustration of dual stain mismatch experiments.

Tumour areas that stained more brightly with carbocyanine relative to Hoechst (i.e. positive intensity changes) were adjacent to blood vessels that became more functional (“opened”) during the time interval. Tumour areas that stained less brightly with carbocyanine relative to Hoechst (i.e. negative intensity changes) were adjacent to blood vessels that became less functional (“closed”) during the time interval. Tumour areas that had “matched” staining patterns were adjacent to blood vessels that did not increase or decrease perfusion by more than 2-fold during the time between dye injections.

changes in relative staining intensity) roughly corresponded to previous visual criteria for stain “mismatch” (Trotter *et al.*, 1989).

2.2.5 Fluorescence Activated Cell Sorting

Fluorescence-activated cell sorting is a method to subdivide a tumour into a number of fractions based on intracellular content of the fluorescent dye Hoechst 33342. Hoechst administered i.v. to tumour-bearing animals demarcates cells at varying distances from functional tumour blood vessels (and therefore at varying levels of oxygenation; see Chapter 3).

Tumour-bearing animals were treated with either diltiazem or pentoxifylline before whole body 250 keV X-irradiation with a dose rate of 3 Gy/min. Immediately post-irradiation, animals were given an i.v. injection of Hoechst 33342 (1 mg in 0.05 ml double-distilled water), and 20 minutes later the tumours were excised and washed in ice-cold PBS. Hoechst at this concentration is not toxic to host animals or tumour cells.

Single-cell suspensions were prepared from excised experimental tumours by finely mincing with crossed scalpels and agitating the resulting brie for 40 minutes in an enzyme suspension containing 0.5% trypsin and 0.08% collagenase in PBS. After incubation, 0.06% DNase was added and the cell suspension gently vortexed and filtered through 30 μ m nylon mesh to remove clumps. Monodispersed cells were washed by centrifugation and resuspended in minimal essential medium (MEM; Gibco Invitrogen Corp.) containing 10% fetal bovine serum (FBS; HyClone, Logan, UT) for cell sorting (Durand, 1982; Durand, 1986).

Viable tumour cells were sorted using a dual laser FACS 440 flow cytometer (Becton Dickinson, Mountainview, CA). Cells were distinguished from cellular debris on the basis of forward light scatter (cell size); sort windows were automatically set to subdivide the cell population into eight fractions of differing intracellular Hoechst concentrations (Durand, 1986). In general, the brightest Hoechst-stained cells, designated fraction 1, were proximal to functional vasculature while the dimmest Hoechst-stained cells, designated fraction 8, were most distant

from functional vasculature at the time of Hoechst injection (Chaplin *et al.*, 1985; Olive *et al.*, 1985; Chaplin *et al.*, 1986). The primary assumption of the method is that the Hoechst staining profile mimics the oxygenation profile during irradiation, which is valid provided the time between irradiation and Hoechst injection is sufficiently short so that significant changes in tumour perfusion do not occur (Chaplin *et al.*, 1985). Predetermined numbers of cells were sorted into tubes containing MEM with 10% fetal bovine serum (M10), and 1% penicillin-streptomycin containing 0.1% Fungizone (Gibco Invitrogen Corp.).

2.2.6 *In Vivo-In Vitro* Cloning Assay

In vivo-in vitro cloning assays are used to determine the efficacy of a particular cytotoxic treatment. Tumour-bearing mice are treated (in this case with drug prior to radiation) and the tumour is excised, disaggregated, and known numbers of cells are added to Petri dishes for growth *in vitro*. Clonogenic tumour cells that survived the cytotoxic treatment will proliferate to form colonies that can be subsequently stained and counted. Data are typically presented in terms of tumour cell "survival" and expressed as a fraction of the number of cells plated for a given dose of treatment.

Sorting the tumour cells into different subpopulations based on their relative proximity to perfused vasculature prior to plating provides information on the survival of different subpopulations of tumour cells (Chaplin *et al.*, 1985; Olive *et al.*, 1985; Durand, 1986). Tubes containing sorted tumour cells (obtained as described in Section 2.2.5) were poured and rinsed into 100 mm tissue culture dishes and incubated at 37°C in 94% air with 6% CO₂ for two weeks to allow colony formation. No special additives were used for tumour cell culture, nor were feeder cells, gel cultures, or low oxygen tensions found to improve cell growth or viability of these cell lines (note that these human tumour cell lines were initially selected in tissue culture). For all clonogenicity data, the ratio of observed colonies to cells plated is presented without correcting for control plating efficiencies (which were in the 20-30% range).

2.2.7 Statistics

Statistical tests were conducted using SPSS software (SPSS Inc., Chicago, IL). Two-sample student's t-tests (two-tailed) were used to analyze the dual stain mismatch and radiosensitivity data.

2.3 RESULTS

2.3.1 Drug-Induced Changes in Net Tumour Perfusion

The Rb^{86} extraction method was used to determine the pentoxifylline dose required to increase net tumour blood flow 15 minutes after administration. Net SiHa tumour perfusion did not significantly change 15 minutes after administration of 5-50 mg/kg pentoxifylline (Figure 2.3A). Net WiDr tumour perfusion increased linearly with pentoxifylline dose up to $130\% \pm 40\%$ (mean \pm s.e.m.) 15 minutes after administration of 50 mg/kg (Figure 2.3A). Changes in net tumour perfusion were also determined at varying times after administration of the drug dose that provided the largest increases in net tumour perfusion after 15 minutes. Interestingly, the increase in net WiDr tumour perfusion observed 15 minutes after pentoxifylline administration returned to control levels within 30 minutes (Figure 2.3B).

2.3.2 Pentoxifylline-Induced Changes in Microregional Tumour Perfusion

Changes in tumour blood flow on a microregional level were studied 15 and 30 minutes after administration of pentoxifylline in both tumour types. In the absence of drug treatment, SiHa tumours demonstrate fewer large-scale changes in perfusion over a 35 minute period than WiDr tumours (this will be discussed further in Chapter 3). Microregional SiHa tumour perfusion was not significantly affected 15-30 minutes after administration of 5 mg/kg pentoxifylline (Figure 2.4A). A redistribution of microregional WiDr tumour perfusion was observed 15 and 30 minutes after 50 mg/kg pentoxifylline compared to untreated tumours (Figure 2.4B). Specifically, the fraction of WiDr tumour blood vessels normally exposed to increased perfusion over a 35 minute interval (positive relative intensity changes) increased with pentoxifylline treatment. These data suggest that 50 mg/kg pentoxifylline increased blood flow through WiDr tumour vasculature that would not normally experience perfusion changes over a 35 minute period.

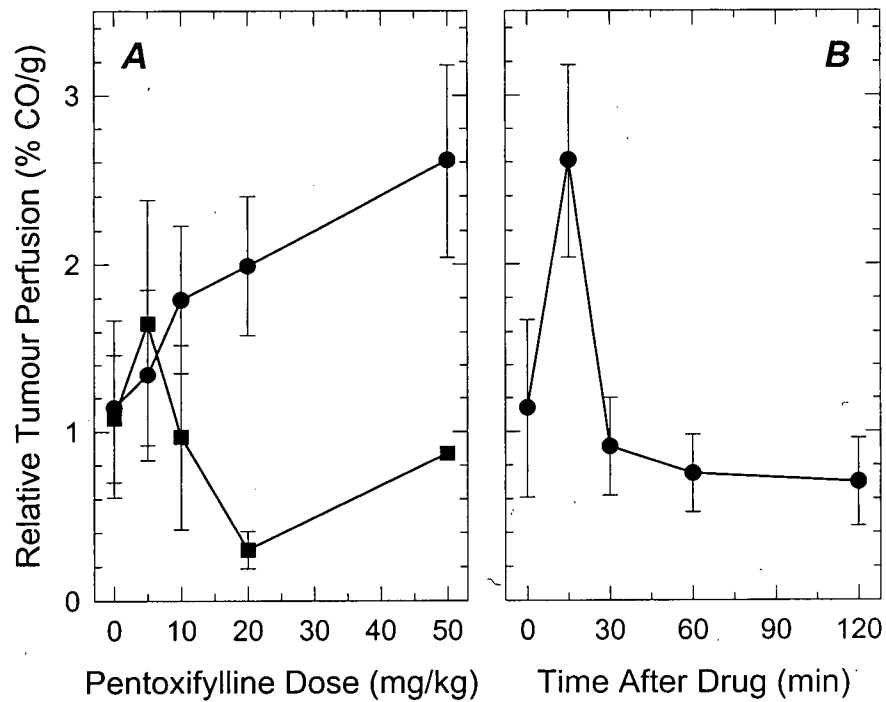


Figure 2.3 Relative net tumour perfusion measured by Rb^{86} extraction.

(A) Net tumour perfusion measured 15 minutes after administration of pentoxifylline. SiHa tumour perfusion (■) did not change significantly over the doses studied, while WiDr tumour perfusion (●) increased linearly with increasing pentoxifylline dose. Data are mean \pm s.e.m.; $n = 3-5$ animals per data point.

(B) Net perfusion of WiDr tumours after administration of 50 mg/kg pentoxifylline. The increase in net WiDr perfusion observed after 15 minutes returned to control levels by 30 minutes. Data are mean \pm s.e.m.; $n = 3-5$ animals per data point.

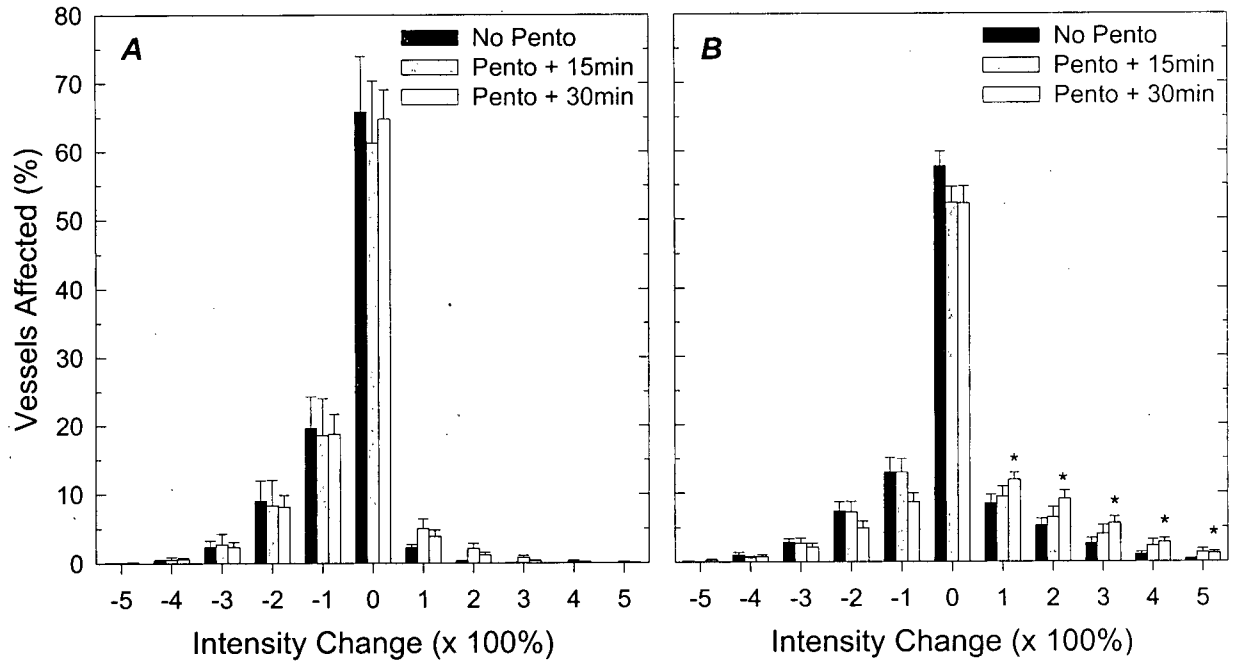


Figure 2.4 Dual stain mismatch data showing changes in the microregional distribution of tumour blood flow 15 and 30 minutes after administration of pentoxifylline (Pento).

(A) SiHa tumours did not demonstrate statistically significant alterations in microregional perfusion after administration of 5 mg/kg pentoxifylline. Data are mean + s.e.m.; $n = 6$ animals per group.

(B) WiDr tumours demonstrated statistically significant increases ($*p < 0.05$) in microregional tumour perfusion 30 minutes after administration of 50 mg/kg pentoxifylline. Data are mean + s.e.m.; $n = 8-10$ animals per group .

2.3.3 Impact of Tumour Perfusion Modification on Tumour Cell Radiosensitivity

Mice bearing SiHa or WiDr tumours were given 5 mg/kg and 50 mg/kg pentoxifylline at various times prior to single irradiation doses of 5 Gy or 10 Gy respectively. The different radiation doses are reflective of the inherent radiosensitivity differences between these two tumour types. Drug concentrations were chosen based on the maximal increases in net tumour perfusion observed by Rb⁸⁶ extraction presented in Figure 2.3. No significant changes in tumour cell radiosensitivity were observed when SiHa tumour-bearing mice were given 5 mg/kg pentoxifylline 15 minutes to 2 hours prior to a single radiation dose of 5 Gy (Figure 2.5A).

Increases in the radiosensitivity of some WiDr tumour cell subpopulations were observed when 50 mg/kg pentoxifylline was administered 15-30 minutes prior to a radiation dose of 10 Gy (Figure 2.5B). The cells that corresponded to intermediate levels of Hoechst intensity exhibited statistically significant increases in radiosensitivity (i.e. decreased survival) with pentoxifylline treatment prior to irradiation ($p < 0.05$). Increased tumour cell radiosensitivity was also observed in the most brightly Hoechst-stained tumour cells, while no significant radiosensitivity increase was observed in the dimmest Hoechst-stained tumour cells. These data suggest that pentoxifylline had no observable radiosensitizing effect on diffusion-limited hypoxic cells (dim sort fractions; distant from functional tumour vasculature).

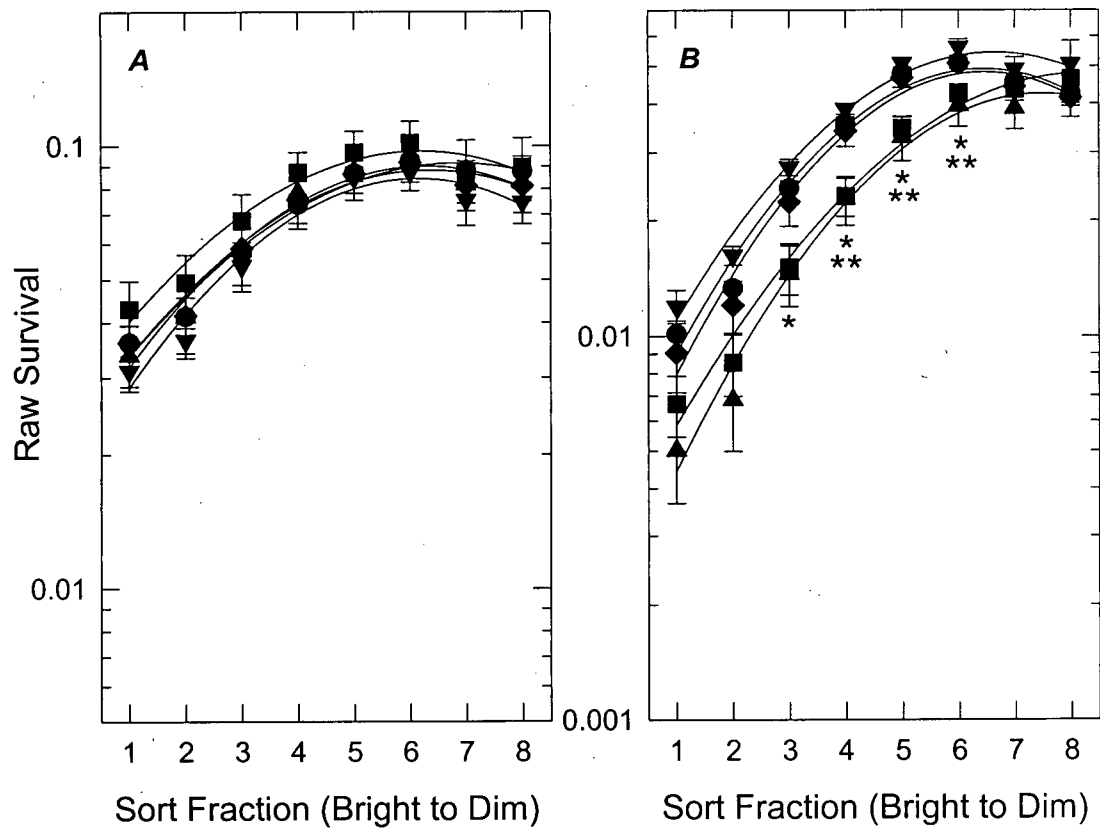


Figure 2.5 Radiosensitivity data for SiHa and WiDr tumours with pentoxifylline (Pento) administered prior to tumour irradiation.

Tumour cells were sorted based on Hoechst 33342 content prior to the *in vitro* cloning assay. Pentoxifylline was administered 15 min (■), 30 min (▲), 1 h (▼), and 2 h (◆) prior to tumour irradiation (●).

(A) SiHa tumour cell radiosensitivity was not significantly affected by 5 mg/kg pentoxifylline prior to 5 Gy irradiation. Data are mean \pm s.e.m.; $n = 4-6$ animals per curve.

(B) WiDr tumour cell radiosensitivity was significantly increased in sort fractions 3-6 (* $p < 0.05$) and sort fractions 4-6 (** $p < 0.05$) when 50 mg/kg pentoxifylline was administered 15 and 30 minutes prior to 10 Gy irradiation respectively. Data are mean \pm s.e.m.; $n = 4-8$ animals per curve.

2.4 DISCUSSION

Tumours that have been derived from different cell lines can have very different characteristics in terms of their hypoxic fractions, intrinsic radiosensitivity, and propensity to undergo changes in hypoxia over time. SiHa tumours demonstrate little evidence of transient perfusion over relatively short periods of time, while WiDr tumours typically demonstrate relatively large-scale perfusion changes over periods of 30 minutes or less (Durand and Aquino-Parsons, 2001a) and have a higher fraction of hypoxic cells (Durand and Raleigh, 1998). In addition, qualitative microscopic examination of tumour sections indicates that SiHa tumours tend to contain larger diameter blood vessels than WiDr tumours. Thus the narrower vasculature and increased transient perfusion in WiDr tumours may suggest higher levels of transient hypoxia compared to SiHa tumours.

In terms of drug-induced changes in perfusion, the mechanism of action of a given drug may prove more efficacious in modifying tumour perfusion of different tumour types. Importantly, the activity of pentoxifylline does not require delivery to tumour cells and is therefore not limited by areas of poor tumour perfusion. The accepted mechanism of pentoxifylline-induced changes in tumour perfusion (i.e. by affecting blood cell deformability and increasing blood flow through narrow tumour vasculature) suggests that this drug may be more effective in tumours containing tortuous vasculature and/or intermittent perfusion. Thus when combined with the features of WiDr tumours described above, pentoxifylline would likely be more effective in increasing perfusion in WiDr tumours relative to SiHa tumours. Indeed, pentoxifylline did not significantly increase the net perfusion of SiHa tumours (Figure 2.3A), or the radiosensitivity of tumour cell subpopulations (Figure 2.5A). It is worth noting that these data indicate pentoxifylline was ineffective at increasing the oxygenation (and hence the radiosensitivity) of diffusion-limited hypoxic cells (furthest from functional vasculature; sort fractions 7-8).

Pentoxifylline increased the net perfusion of WiDr tumours (Figure 2.3A) 15 minutes after administration of 50 mg/kg, a dose that agrees with other published data (Song *et al.*, 1992; Honess *et al.*, 1993; Song *et al.*, 1994; Kelleher *et al.*, 1998) although the maximal increases in tumour perfusion varies between tumour systems. The increase in net tumour perfusion after 15 minutes coincided with an increase in blood flow through tumour blood vessels that did not normally experience increases in functionality over that time interval (Figure 2.4B). Interestingly, the redistribution of tumour perfusion on a microregional level lasted for 30 minutes despite no observable increase in net tumour perfusion at that time. These data suggest that changes in tumour blood flow on a microregional scale may not necessarily be associated with changes in net blood flow to a tumour, and would therefore not be detectable using the Rb⁸⁶ extraction method.

The *in vivo-in vitro* cloning assay data indicate increases in the radiosensitivity of WiDr tumour cells at intermediate levels of Hoechst intensity when pentoxifylline was given 15 and 30 minutes prior to tumour irradiation (Figure 2.5B). In a tumour displaying temporally constant blood flow, the intermediate sort fractions contain cells that were presumably intermediately oxygenated, receiving intermediate levels of stain due to their distance from functional vasculature. However, in tumours with perfusion changes on the order of minutes such as WiDr tumours, the intermediate sort fractions can also contain cells with a perfusion status that changed during the lifetime of the Hoechst in the circulation ($t_{1/2} = 110$ seconds; Olive *et al.*, 1985). Thus intermediate sort fractions are potentially enriched with transiently hypoxic tumour cells, although methods to directly identify transiently hypoxic cells were not available at the time of these experiments (see Chapter 3).

When taken with the known mechanism of pentoxifylline-induced changes in tumour perfusion and the dual stain mismatch data 30 minutes after drug administration, the radiosensitivity assay therefore suggests pentoxifylline-induced oxygenation of transiently

hypoxic tumour cells. The increase in WiDr radiosensitivity after 30 minutes was of comparable magnitude to the increased radiosensitivity associated with the net perfusion increase after 15 minutes. These data suggest both the microregional redistribution of tumour blood flow to increase oxygen delivery to transiently hypoxic cells and the increase in net tumour blood flow were capable of increasing WiDr tumour cell radiosensitivity. However, this argument relies on two indirect measurements and one functional assessment of tumour oxygenation (by measuring tumour perfusion and radiosensitivity respectively), and would benefit from a method to directly measure transiently hypoxic tumour cells on a cell-by-cell basis (see Chapters 3 and 4).

It is worth emphasizing at this point that WiDr and SiHa tumours display different microenvironmental characteristics despite being implanted in the same SCID murine host strain. Tumour cells are therefore capable of influencing the characteristics and functionality of host vasculature (including response to blood flow modification) in a tumour-type specific fashion. These observations imply that further study of the microenvironment associated with different human tumour xenografts provides information with potential clinical relevance, without the necessary technical limitations associated with studying tumours in the clinic.

The influence of various tumour cell subpopulations on tumour response to radiation is difficult to directly assess clinically, largely due to limitations in methodology and current definitions of tumour “response” to therapy. In the clinic, tumours are generally considered “responsive” to treatment if the tumour decreases in size with continued therapy, indicating a majority of tumour cells have both died and disappeared from the tumour. However, when considering the goal of tumour “cure”, kinetics studies in experimental tumours suggest that killing tumour cells that are maximally resistant to treatment is critical since even a relatively small number of cells surviving treatment can cause tumour regrowth (Durand, 1993; Durand, 1994). Defining a radiotherapy intervention that affects a minority of (maximally resistant) tumour cells is therefore difficult in the clinic, particularly since the response of the majority of

tumour cells is the easiest to directly observe. Thus the further refinement of pre-clinical and clinical methods designed to elucidate the responses of specific tumour cell subpopulations to various therapeutic interventions is warranted.

Determining the identity of cells that respond to a particular therapeutic intervention has important implications for the advancement of clinical therapy. Various populations of tumour cells likely have different influences on tumour response to therapy, and more work is necessary to determine which tumour cells are primarily responsible for treatment failure. Tumour cells at intermediate levels of oxygenation are thought to affect tumour response to radiation (Wouters and Brown, 1997; Evans *et al.*, 1997; Olive *et al.*, 2002), and pre-clinical work has suggested the potential importance of transiently hypoxic tumour cells on clinical cancer therapy (Durand and Raleigh, 1998; Denekamp and Dasu, 1999). The data presented in this Chapter also support the potential therapeutic relevance of transient tumour hypoxia in that drug-induced changes in tumour blood flow to favor increased oxygen delivery to cells normally exposed to transient perfusion yielded increases in tumour cell sensitivity to radiation. Despite these pre-clinical observations, further characterization of tumour hypoxia in the clinic is necessary before strategies for targeting specific tumour cell subpopulations can be effectively utilized.

There is, however, a lack of methodology available to study (dynamic) tumour hypoxia in the clinic. In particular, there are no satisfactory methods to distinguish between diffusion-limited hypoxic, intermediately oxygenated, and transiently hypoxic cells in experimental tumours, let alone in the more technically and ethically limiting clinical situation. The development of methods to distinguish between hypoxic cells derived from different oxygen deprivation mechanisms is therefore a worthwhile endeavor, particularly if the methods could potentially be applied to the clinic for use in improving cancer therapy.

CHAPTER 3: QUANTIFYING TRANSIENT TUMOUR HYPOXIA BY FLOW CYTOMETRY

This Chapter has been adapted from the following published manuscript:

Bennewith, KL and Durand, RE (2004) Quantifying transient hypoxia in human tumor xenografts by flow cytometry. *Cancer Res* **64**(17): 6183-6189.

3.1 INTRODUCTION

Many solid tumours contain subpopulations of cells that are poorly oxygenated, and the presence of these cells has been shown to limit the outcome of cancer therapy by radiation, chemotherapy, and even surgery (Hockel and Vaupel, 2001). The oxygenation status of a tumour is thought to have potential prognostic value in cancer treatment, and many methods for measuring tumour oxygenation have been developed (Section 1.5). Exogenous markers, such as pimonidazole (Arteel *et al.*, 1995) and EF5 (Lord *et al.*, 1993), have been used clinically to label poorly oxygenated tumour cells for subsequent image analysis of tumour sections obtained by excision biopsy (Raleigh *et al.*, 2001), for flow cytometry analysis of cells from excision or fine needle aspirate biopsies (Olive *et al.*, 2000; Durand and Aquino-Parsons, 2001a; Durand and Aquino-Parsons, 2001b), or for visual scoring of tumour cell smears (Olive *et al.*, 2001b). However, while exogenous markers are useful tools to identify poorly oxygenated cells in both experimental and clinical tumours, a single injection or infusion of a marker (as is typically performed) only provides information on tumour oxygenation during the circulation lifetime of the marker. Moreover, only those cells that are at sufficiently low levels of oxygen for sufficient time intervals will bind measurable quantities of a given marker. Thus there are inevitable questions as to the therapeutic relevance of the labeled cells in terms of both the degree and duration of their oxygen deprivation.

As discussed in Section 1.2, the terms “hypoxic” or “hypoxia” in this thesis denote oxygen deprivation that is sufficient to result in decreased cellular sensitivity to ionizing radiation. Operationally, exogenous hypoxia markers specifically label such cells (Evans *et al.*, 1996; Raleigh *et al.*, 1999), and “thresholds” used to distinguish labeled from non-labeled cells in flow cytometry analyses (Hodgkiss *et al.*, 1995; Durand and Raleigh, 1998) provide tumour hypoxic fractions that are consistent with other functional assays such as the paired radiation survival curve technique (Moulder and Rockwell, 1984). However, even though radiation survival curves

provide unequivocal data regarding tumour radiosensitivity (and oxygenation indirectly), these parameters are again assessed over the relatively short duration of the radiation exposure and therefore do not take into account changes in hypoxia that occur over time.

Tumour hypoxia was originally thought to arise exclusively in tumour cells situated at a substantial distance from functional tumour blood vessels (100-150 μm), beyond which there is limited oxygen delivery due to the high oxygen consumption of the intervening cells (Section 1.2.1). This diffusion-limited hypoxia has been extensively characterized in both animal and human tumour systems, and its impact on cancer therapy is well understood. However, observations in animal tumours over two decades ago (Brown, 1979) led to suggestions of a more dynamic form of hypoxia, which has more recently been discussed as a potential factor impacting clinical cancer therapy (Denekamp and Dasu, 1999; Durand, 2001; Durand and Aquino-Parsons, 2001a; Durand and Aquino-Parsons, 2001b). This transient or intermittent hypoxia is poorly understood, and there are many unanswered questions regarding its presence and potential influence in the treatment of solid tumours. Transient hypoxia is thought to occur in tumour cells that are dependent on tumour blood vessels that are subject to partial and/or intermittent decreases in functionality, thereby reducing oxygen (and nutrient) delivery and availability (Section 1.2.2). Importantly, as the oxygenation status of these cells increases or decreases over time, there are concomitant changes in their sensitivity to radiation (Denekamp and Dasu, 1999) or chemotherapy (Durand, 2001). Moreover, a portion of transiently hypoxic cells are capable of retaining some proliferative capacity during the temporary reduction (or absence) of oxygen (Durand and Raleigh, 1998), and therefore could potentially proliferate upon reoxygenation of a tumour region. Thus although their presence in clinical tumours has been difficult to demonstrate conclusively so far (largely due to inadequate methodology), transiently hypoxic tumour cells are potentially important players in limiting tumour response to therapy.

Efforts to better understand the mechanism of transient hypoxia generation have primarily involved monitoring changes in tumour oxygen tension (pO_2) over time by the insertion of one (or two) oxygen detection probes (with the presumption that the probe is positioned in a region of tumour containing viable cells). Oxygen tensions have been monitored continuously in murine tumours using recessed-tip oxygen microelectrodes (Kimura *et al.*, 1996; Dewhirst *et al.*, 1998; Braun *et al.*, 1999) and in human melanoma xenografts using Oxylite fibre-optic microprobes (Brurberg *et al.*, 2003; Brurberg *et al.*, 2004). These studies have provided real-time evidence that significant, yet highly heterogeneous changes in tumour blood flow and pO_2 can occur with different periodicities and magnitudes in different tumour types, and in different regions of the same tumour. However, these data also reconfirm the spatial and temporal heterogeneity of the tumour microenvironment, suggesting the need for multiple measurements to more accurately depict the tumour as a whole. Moreover, the functional significance of temporally fluctuating tumour pO_2 observed in this way is largely inferential since the overall fraction of viable tumour cells displaying a dynamic hypoxic status is not directly queried.

In Chapter 2, the effect of drug-induced blood flow modification on transient hypoxia in human tumour xenografts was indirectly studied using dual stain mismatch analyses of tumour sections, and the functional significance of the observed changes in tumour perfusion were demonstrated by a radiosensitivity assay. The dual stain mismatch method was originally designed to observe (non-induced) microregional fluctuations in tumour blood flow, and differences between the relative staining intensities of two i.v. injected fluorescent dyes indicate tumour areas that were subject to perfusion changes during the time between stain injections (Trotter *et al.*, 1989; Trotter *et al.*, 1991; Durand and LePard, 1995). Presumably, regions of a tumour that are subject to fluctuations in blood flow (and thus oxygen delivery) may also exhibit changes in hypoxia depending on the degree and duration of the perfusion fluctuations. While this technique is adequate for quantifying transient tumour perfusion in animal systems, there are

technical and ethical limitations to extending the method to tumours in the clinic. Since information regarding the presence and duration of intermittent hypoxia episodes in clinical tumours would improve our understanding of the microenvironmental limitations of current cancer therapy protocols, an approach for potentially measuring changes in tumour hypoxia in the clinic is needed.

To quantify changes in hypoxia over time and essentially over an entire tumour, the hypoxia markers pimonidazole and CCI-103F (Raleigh *et al.*, 1987) were sequentially administered to mice bearing human tumour xenografts. Since hypoxia markers are bound and retained in hypoxic cells during the circulation lifetime of the agent, multiple hourly injections of pimonidazole were used to estimate a tumour hypoxic fraction that was “integrated” over time. Fractions of pimonidazole-labeled cells were then compared to the more “typical” hypoxic fraction determined with a single subsequent injection of CCI-103F, and those cells that contained one hypoxia probe and not the other indicated cells that were hypoxic at one point in time and “oxic” at another (Franko, 1986; Iyer *et al.*, 1998; Ljungkvist *et al.*, 2000). Importantly, the use of flow cytometry allowed quantification of transient hypoxia on a cell-by-cell basis, which provided an improvement in resolution when compared to the “local” insertion of probes (Kimura *et al.*, 1996; Dewhirst *et al.*, 1998; Braun *et al.*, 1999; Brurberg *et al.*, 2003; Brurberg *et al.*, 2004) or the analysis of tumour sections for changes in microregional perfusion (Trotter *et al.*, 1989; Trotter *et al.*, 1991; Durand and LePard, 1995) or hypoxia (Ljungkvist *et al.*, 2000; Raleigh *et al.*, 2001). Moreover, flow cytometry analysis provides hundreds of thousands of data points for a single tumour, while also allowing the exclusion of necrosis and host cells from the measurements. Information on the proximity of transiently hypoxic cells relative to tumour vasculature that was functional just before tumour excision was obtained by sorting the tumour cells based on Hoechst 33342 perfusion (Chaplin *et al.*, 1985; Olive *et al.*, 1985) prior to hypoxia marker analysis.

Using an 8 hour observation window and two xenografted tumour systems, the data clearly indicate time and tumour-dependent variation in the number of transiently hypoxic cells and the proximity of these cells to functional tumour vasculature. Furthermore, it was found that hypoxia measurements that are “integrated” over time enable the inclusion of transiently hypoxic cells into estimates of tumour hypoxic fractions, and application of similar approaches in the clinic would allow assessment of the therapeutic relevance of these estimates.

3.2 MATERIALS AND METHODS

3.2.1 Tumours and Reagents

SiHa and WiDr human tumour xenografts were used as described in Section 2.2.1. Pimonidazole hydrochloride was supplied as Hydroxyprobe-1 (Natural Pharmaceuticals International, Inc., Belmont, MA), and CCI-103F was a generous gift from Dr. James A. Raleigh from the University of North Carolina. Pimonidazole was dissolved at a concentration of 20 mg/ml in double-distilled water and CCI-103F was dissolved in 10% DMSO and 90% peanut oil, also at 20 mg/ml. Both hypoxia probes were injected i.p. at a dose of 100 mg/kg mouse body weight. Pimonidazole and CCI-103F are conducive to combined assays for hypoxia since they have similar abilities to discriminate hypoxic cells, and neither inhibition of labeling nor cross-reactivity between primary antibodies has been observed in flow cytometry or tumour section analyses (Ljungkvist *et al.*, 2000).

3.2.2 Fluorescence Activated Cell Sorting

Single-cell suspensions were prepared from excised tumours and sorted into fractions based on intracellular concentration of Hoechst 33342 i.v. injected by the lateral tail vein 20 minutes before host sacrifice and tumour excision as described in Section 2.2.5. In this case, the tumours were sorted into six fractions for subsequent flow cytometry analysis. In general, the brightest Hoechst-stained cells, designated fraction 1, were proximal to functional vasculature while the dimmest Hoechst-stained cells, designated fraction 6, were most distant from functional vasculature at the time of Hoechst injection (Chaplin *et al.*, 1985; Olive *et al.*, 1985; Chaplin *et al.*, 1986).

Hoechst 33342 has a high avidity for DNA and slowly diffuses away from functional vasculature after i.v. injection, thereby establishing a marked gradient of staining intensity with increasing depth into tissue (Durand, 1982; Chaplin *et al.*, 1985). A 20 minute interval between Hoechst injection and tumour excision provides an optimal Hoechst intensity gradient between

brightly staining and dimly staining tumour cells with increasing distance from functional tumour blood vessels, thereby facilitating sorting based on the relative intracellular Hoechst intensity (Chaplin *et al.*, 1985; Olive *et al.*, 1985; Chaplin *et al.*, 1986). The presence of cellular debris in the most dimly staining Hoechst fractions provides (indirect) evidence that the lower end of the Hoechst intensity gradient includes cells adjacent to tumour necrosis.

3.2.3 Antibodies

Fractions of tumour cells obtained by fluorescence activated cell sorting were fixed in chilled 70% ethanol and stored at -20°C for a minimum of 24 hours. Detection of intracellular hypoxia marker adducts was achieved by incubation with appropriate antibodies before analysis by flow cytometry (Durand and Raleigh, 1998). Intracellular protein-bound adducts of pimonidazole were identified by an unconjugated IgG1 mouse monoclonal (clone 4.3.11.3) primary antibody (Arteel *et al.*, 1995) and a goat anti-mouse Alexa 594 (red) fluorescent secondary antibody (Molecular Probes Inc., Eugene, OR). Intracellular CCI-103F adducts were visualized with anti-CCI-103F rabbit antisera (Raleigh *et al.*, 1987) supplied by Dr. James A. Raleigh, and a polyclonal goat anti-rabbit Alexa 488 (green) fluorescent secondary antibody (Molecular Probes Inc.). DNA was counterstained with 4', 6-diamidino-2-phenylindole dihydrochloride hydrate (DAPI; Sigma-Aldrich Canada Ltd., Oakville, ON) at a concentration of 2 µg/ml prior to flow cytometry analysis. All antibodies were diluted in a solution containing 4% calf serum (HyClone, Logan, UT) and 0.1% Triton X-100 in Dulbecco's PBS (Gibco Invitrogen Corp., Burlington, ON).

3.2.4 Flow Cytometry

Flow cytometry analyses were performed using a dual laser Epics Elite-ESP flow cytometer (Beckman Coulter Corp., Hialeah, FL). Data were obtained in the form of list mode files that were subsequently reprocessed for analysis using the WINLIST software package (Verity Software House Inc., Topsham, ME). Cells were identified based on forward light scatter (cell

size) and time-of-flight (cell doublet discrimination) to exclude cellular debris and cell doublets from further analysis. The diploid DNA content of host (murine) normal cells enabled their exclusion from analysis of the hyperdiploid human tumour cells.

The fluorescent antibodies described in Section 3.2.3 enable identification of cells containing protein-bound hypoxia marker adducts by flow cytometry, and the *absolute* fluorescence intensity of a given cell (at the appropriate emission wavelength) is proportional to the *absolute* number of bound hypoxia marker adducts in that cell. Bivariate plots of absolute fluorescence intensity vs DNA content on a cell-by-cell basis enable a fluorescence intensity threshold to be set to distinguish between cells that are “labeled” with hypoxia marker *relative* to cells that are “non-labeled”. A considerable advantage to setting relative intensity thresholds is realized by sorting the tumour cells prior to analysis. Since the brightest Hoechst-stained cells were closest to functional vasculature and contain the fewest hypoxic cells, relative fluorescence intensity thresholds can be set based on profiles from this sort fraction (for a given tumour) and kept relatively constant for the analysis of the remaining sort fractions for that tumour.

Cells identified as “pimonidazole-positive” or “CCI-103F-positive” were quantified and the data were normalized to the expected profile for simultaneous administration of the two markers (i.e. close to 100% concordance between pimonidazole- and CCI-103F-labeled cells). This normalization provided more conservative estimates of the fraction of cells labeled only with CCI-103F or only with pimonidazole.

3.2.5 Statistics

Statistical tests were conducted using SPSS software (SPSS Inc., Chicago, IL). Two-sample student's t-tests (two-tailed) were used to analyze the flow cytometry data from the unsorted tumour samples.

3.3 RESULTS

3.3.1 "Time-Integrated" Pimonidazole Labeling in SiHa Tumours

Plasma pimonidazole levels were maintained at a high level over time by repetitively administering the hypoxia marker via hourly injections; hypoxic cells were therefore labeled over a 1-8 hour period (Figure 3.1). For SiHa tumours, there was a statistically significant ($p < 0.05$) increase in the fraction of total tumour cells labeled with pimonidazole from 37% after a 1 hour period of pimonidazole labeling to 56% after 5-8 hours of exposure to pimonidazole (Figure 3.1A). It is important to note that the presence of bound pimonidazole adducts in a particular cell is an indication only that the cell had been hypoxic enough for long enough at some point during the labeling interval to bind sufficient quantities of the marker. Thus cells labeled with pimonidazole were not necessarily hypoxic *at the time of tumour excision*.

Pimonidazole labeling within subpopulations of SiHa tumour cells located at increasing distance from functional tumour blood vessels was also examined by sorting the cells based on Hoechst 33342 perfusion prior to flow cytometry analysis (Figure 3.1B). As expected, there were increasing numbers of pimonidazole-labeled cells as the distance from tumour vasculature increased (decreased Hoechst staining intensity; higher sort fraction number). For example, with a single injection of pimonidazole (1 hour of labeling in Figure 3.1A) and the tumour cells sorted into six fractions (open circles in Figure 3.1B), pimonidazole labeling was observed in ~4% of the tumour cells staining most brightly with Hoechst (fraction 1 of 6; closest to functional vasculature). These cells correspond to ~0.7% of the total number of sorted tumour cells ($4\% \times 1/6$ of total tumour cells per sort fraction). Similarly, 72% of the cells furthest from functional tumour blood vessels were labeled with pimonidazole (fraction 6 of 6; 12% of the total number of tumour cells). Therefore, the increase in the total number of pimonidazole-labeled cells with time observed in Figure 3.1A was primarily due to an increase in the number of pimonidazole-labeled cells found in sort fractions of intermediate to dim Hoechst intensity (fractions 3-6).

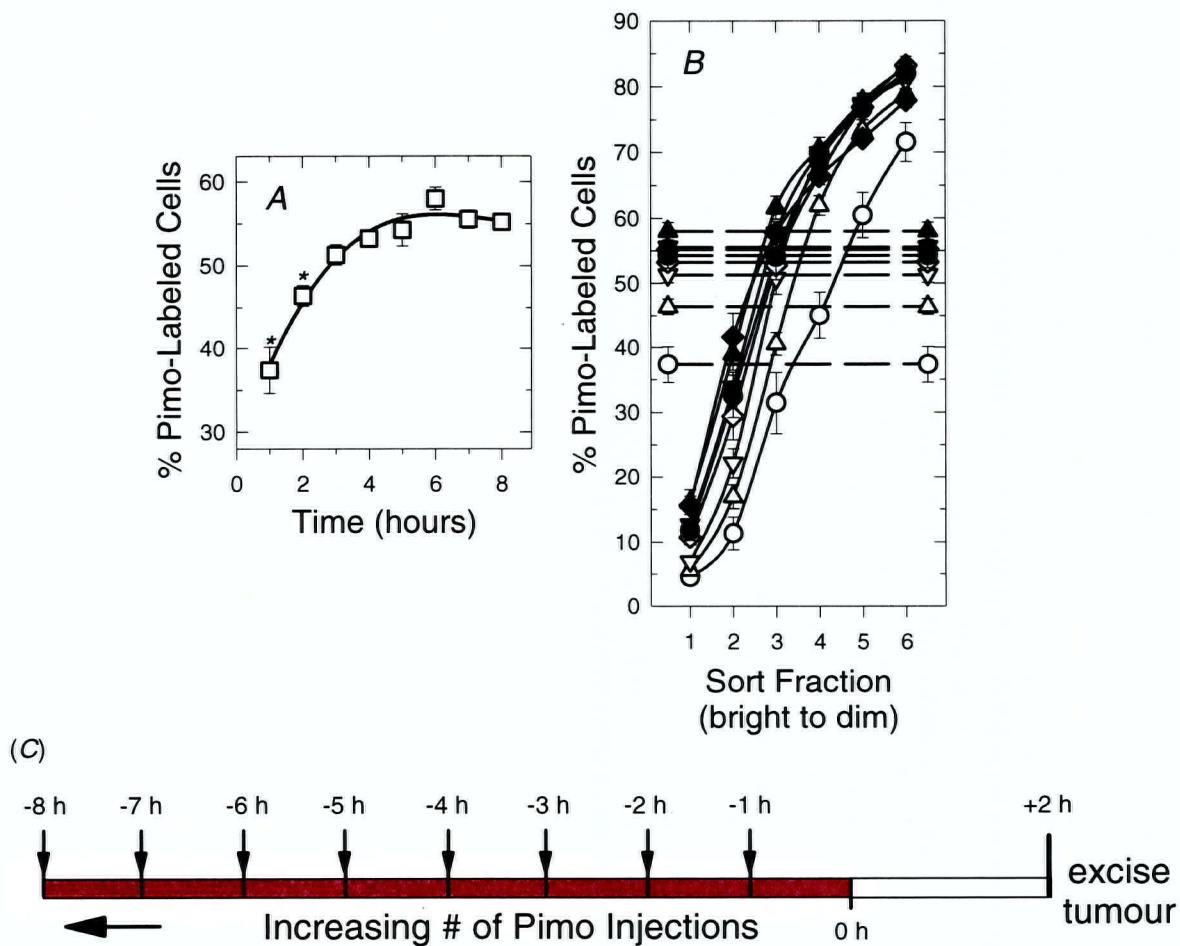


Figure 3.1 SiHa tumour cells labeled with pimonidazole (Pimo).

(A) Percentage of Pimo-labeled tumour cells (□) after tumour-bearing mice were given hourly i.p. Pimo injections prior to tumour excision. *Statistically significant difference with each subsequent time point ($p < 0.05$).

(B) Same data with tumour cells sorted before Pimo analysis based on cellular content of the fluorescent perfusion dye Hoechst 33342. Dashed lines indicate percentage of Pimo-labeled cells from whole tumours. Mice were given hourly Pimo injections for 1 h (○), 2 h (△), 3 h (▽), 4 h (◇), 5 h (●), 6 h (▲), 7 h (▼), or 8 h (◆). Data are mean \pm s.e.m.; $n = 4-9$ tumours per curve.

(C) Experimental protocol. Each red box represents a 1 hour pimonidazole labeling interval resulting from a single pimonidazole injection. The white box indicates the 2 hour period prior to tumour excision used for administration of a second hypoxia marker (see Section 3.3.2).

3.3.2 Evidence of Transient Hypoxia in SiHa Tumours

A second hypoxia marker, CCI-103F, was injected 1 hour after the final pimonidazole injection and 2 hours prior to tumour excision for each of the tumours (Figure 3.2A). It is worth noting that these data represent *all* CCI-103F-labeled cells detected in each sample, and that a portion of these cells may or may not have been labeled previously with pimonidazole. Similarly, the data presented in Figure 3.1 indicated *all* tumour cells labeled with pimonidazole, without distinguishing between cells that may or may not have been labeled with subsequent CCI-103F. Importantly, the degree of hypoxia as assessed by CCI-103F labeling did not increase with increased pimonidazole administration, indicating that labeling hypoxic cells with multiple injections of pimonidazole over time did not affect tumour oxygenation (Raleigh *et al.*, 1999). On a cellular level, these data also indicate that differences in the numbers of intracellular pimonidazole adducts (even after multiple injections of pimonidazole) did not limit subsequent binding of CCI-103F in the same cells. This was largely expected, since the number of bound intracellular pimonidazole adducts has been shown to increase linearly with time and dose (Durand and Raleigh, 1998).

The fractions of tumour cells that were labeled with *both* pimonidazole (red) and subsequent CCI-103F (green) are shown in Figure 3.2B. These cells were therefore sufficiently hypoxic at some point during the circulation lifetimes of each hypoxia probe to label with both markers, although labeled cells may or may not have been hypoxic for the entire labeling duration of either marker. Again, the presence of bound intracellular hypoxia marker adducts does not necessarily indicate cells that were hypoxic *at the time of tumour excision*.

Figures 3.2C and 3.2D indicate the percentage of tumour cells in each sort fraction that were *exclusively* labeled with CCI-103F (green only) or pimonidazole (red only) respectively. Importantly, the determination of whether or not a particular cell is “pimonidazole-positive” or “CCI-103F-positive” (i.e. is above a given threshold of relative fluorescence intensity) is

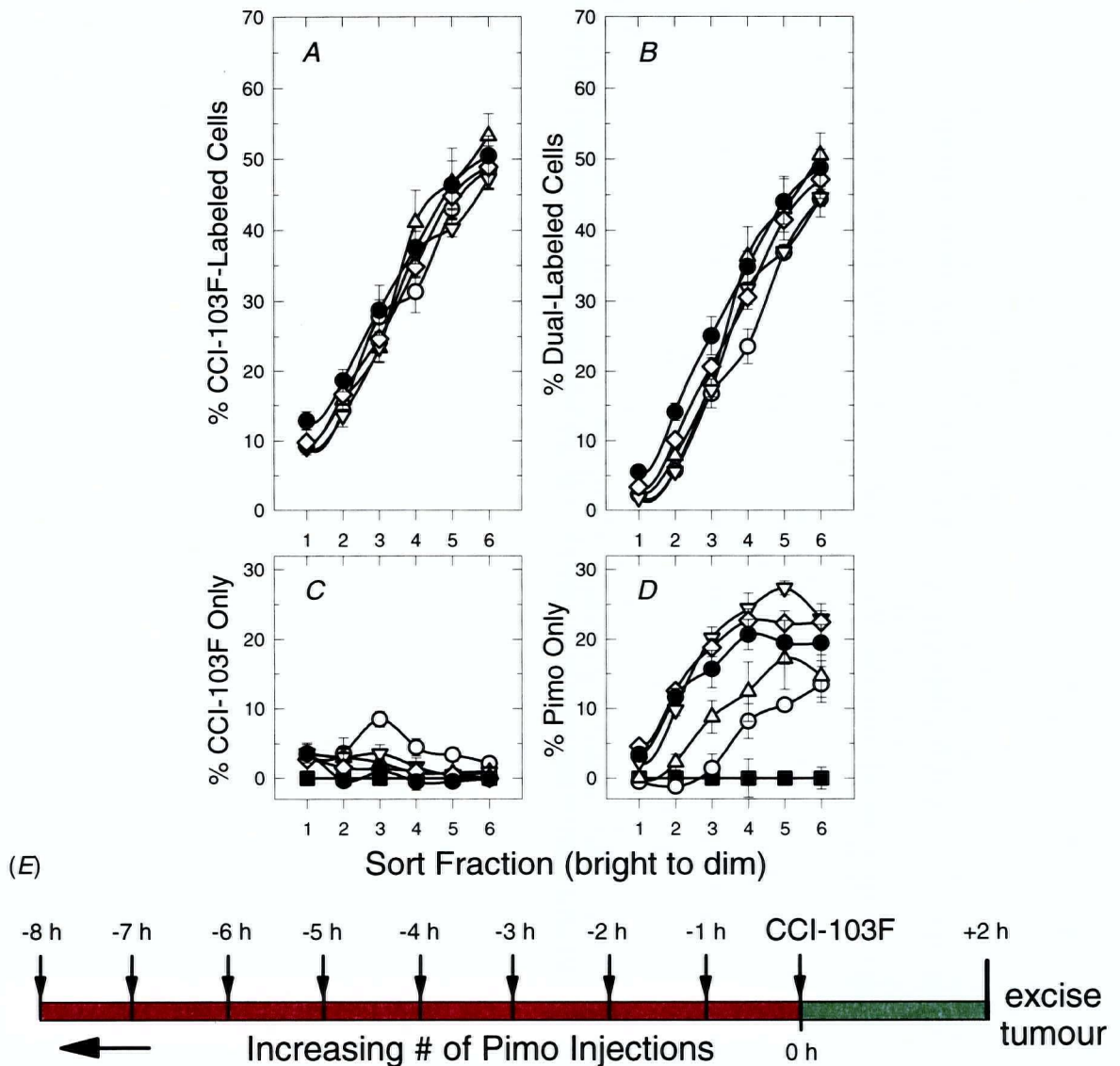


Figure 3.2 Sorted SiHa tumour cells labeled with CCI-103F and/or pimonidazole (Pimo).

(A) Percentage of tumour cells labeled with CCI-103F 2 h after i.p. injection of the marker.

(B) Percentage of tumour cells labeled with both Pimo and subsequent CCI-103F.

(C) Percentage of tumour cells labeled with CCI-103F, but not previously labeled with Pimo.

(D) Percentage of tumour cells labeled with Pimo, but not labeled with subsequent CCI-103F.

Mice were given hourly Pimo injections 1 h (○), 2 h (△), 3 h (▽), 4 h (◇), or 5 h (●) prior to CCI-103F injection, or a single Pimo injection simultaneously with CCI-103F (■). Curves for 6-8 hourly Pimo injections were not significantly different than the 5 h curve and were omitted for clarity. Data are mean \pm s.e.m.; $n = 4-6$ tumours per curve.

(E) Experimental protocol. Red boxes represent 1 hour pimonidazole labeling intervals from single pimonidazole injections; green box indicates the CCI-103F labeling interval.

performed independently for each marker. Thus while the relative fluorescence intensity of cells containing bound pimonidazole adducts increases with increasing pimonidazole dose administered over time, the ability to identify cells labeled with CCI-103F is not affected.

The profiles in Figure 3.2D represent cells that were hypoxic enough during the pimonidazole exposure to label with that marker, but were not hypoxic enough during the subsequent exposure to CCI-103F to label with that marker. As the duration of pimonidazole labeling was increased, there was an increase in the fraction of cells that labeled only with pimonidazole. These data suggest that the increase in total pimonidazole-labeled cells with time observed in Figure 3.1A was due to the detection of cells that were hypoxic only transiently. The number of cells that were transiently hypoxic during the 1-5 hour period of pimonidazole labeling ranged from 5-20% of the total number of tumour cells. Interestingly, the majority of cells that demonstrated changes in hypoxia over this time period were located at an intermediate to large distance from tumour vasculature that was functional just prior to tumour excision (sort fractions 3-6).

Typical flow cytometry profiles are presented in Figure 3.3 for comparison of a SiHa tumour in which pimonidazole and CCI-103F were administered simultaneously (Figures 3.3A and 3.3B), and a SiHa tumour with 5 hourly injections of pimonidazole followed by an injection of CCI-103F (Figures 3.3C and 3.3D). Tumour cells were sorted based on Hoechst 33342 perfusion prior to flow cytometry analysis, and profiles for the brightest and the dimmest Hoechst-stained sort fractions are shown in each case. For all plots, pimonidazole-positive cells (red) are above the horizontal threshold and CCI-103F-positive cells (green) are to the right of the vertical threshold; the dashed diagonal line is included as an approximate slope of the population of dual-labeled cells. The majority of hypoxic tumour cells in Figures 3.3A and 3.3B are dual-labeled (red and green), with few cells labeled only with pimonidazole or CCI-103F. Cells labeled only with pimonidazole (i.e. red and not green) are observed in Figures 3.3C and

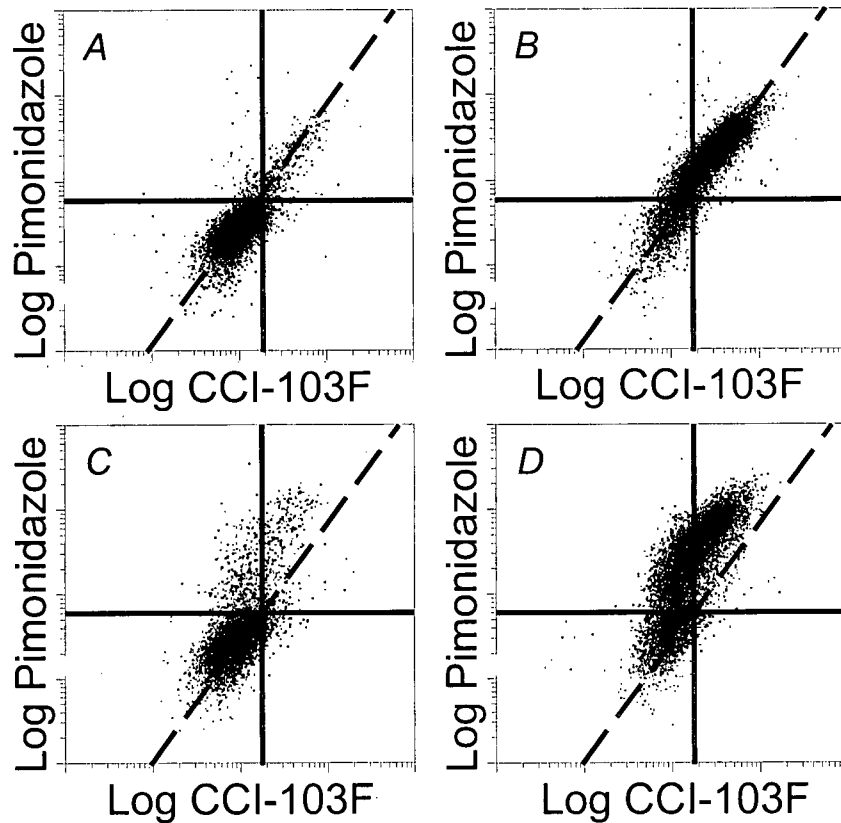


Figure 3.3 Representative flow cytometry dot plots showing hypoxic SiHa tumour cells labeled with pimonidazole and CCI-103F.

The threshold (solid) lines on each plot are for illustration purposes only; actual thresholds used for analysis were set using linear distributions of each hypoxia marker vs DNA content, with additional gating on multivariate plots.

(A) Sort fraction 1 (brightest Hoechst) and (B) sort fraction 6 (dimmiest Hoechst) for SiHa tumour with pimonidazole and CCI-103F administered simultaneously 2 h prior to tumour excision.

(C) Sort fraction 1 and (D) sort fraction 6 for SiHa tumour with 5 hourly injections of pimonidazole followed by a single CCI-103F injection 2 h prior to tumour excision. Note the distribution of labeled cells has a distinctly different shape (upward shift relative to the dashed line) due to the increased fraction of cells labeled only with pimonidazole.

3.3D as upward shifts of the dual-labeled populations from the unlabeled cells, due to an increase in the fraction of cells above the (horizontal) threshold for being considered pimonidazole-positive, and to the left of the (vertical) threshold and therefore CCI-103F-negative.

Figure 3.3 also effectively illustrates the benefits of flow cytometry for quantifying the continuum of hypoxic status for tens of thousands of tumour cells simultaneously. Flow cytometry provided a vastly increased number of discrete measurements and an improved resolution when compared to regional pO_2 detection with solid probes (Kimura *et al.*, 1996; Dewhirst *et al.*, 1998; Braun *et al.*, 1999; Brurberg *et al.*, 2003; Brurberg *et al.*, 2004) or microregional hypoxia marker detection in tumour sections (Ljungkvist *et al.*, 2000; Raleigh *et al.*, 2001). Moreover, the different flow cytometry profiles between cells of differing intracellular Hoechst intensities visually reinforces the relative rarity of observing hypoxic cells directly adjacent to tumour blood vessels that were functional just prior to analysis (which would be indicative of relatively large-scale changes in vascular functionality).

3.3.3 Transient Hypoxia in WiDr Tumours

For WiDr tumours, there was a statistically significant ($p < 0.05$) increase in the fraction of total tumour cells labeled with pimonidazole from 44% after 1-3 hours to 52% by 5-8 hours (Figure 3.4A). As with the SiHa experiments, tumour cells were sorted based on Hoechst 33342 perfusion prior to flow cytometry analysis (Figure 3.4B), and a less dramatic increase in pimonidazole-labeled cells with time was observed. Interestingly, there was a decrease in pimonidazole labeling in the most dimly Hoechst-stained cells (sort fraction 6) for all WiDr curves relative to the preceding sort fraction that was not observed in SiHa tumours. Since pimonidazole preferentially labels viable hypoxic cells (Durand and Raleigh, 1998), this disparity may be due to a decrease in WiDr tumour cell viability at a large distance from tumour vasculature. Indeed, these tumours typically contain relatively large areas of necrosis away from tumour blood vessels and a large amount of cellular debris, suggesting a high degree of cell

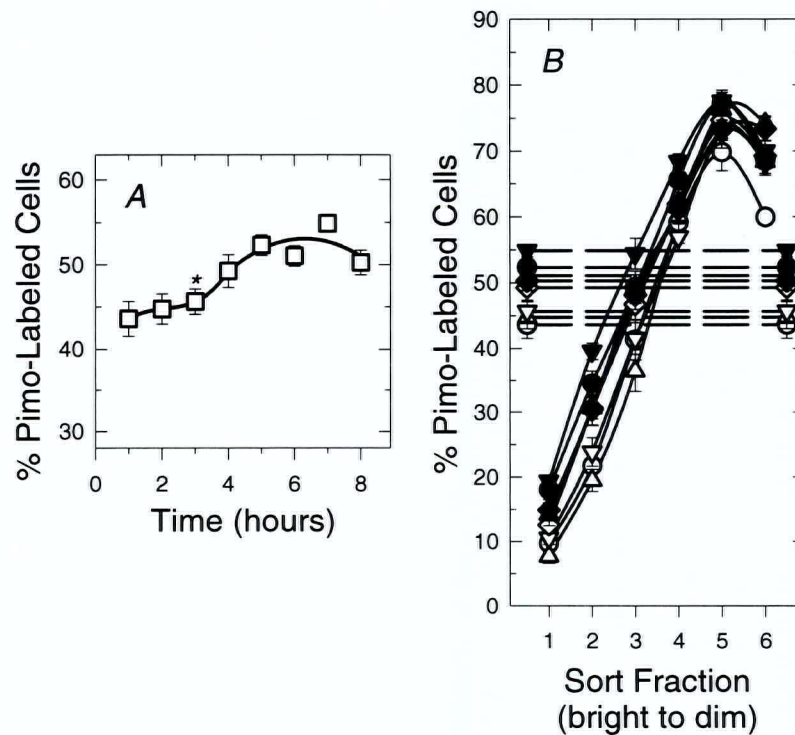


Figure 3.4 WiDr tumour cells labeled with pimonidazole (Pimo).

(A) Percentage of Pimo-labeled tumour cells (□) after tumour-bearing mice were given hourly i.p. Pimo injections prior to tumour excision. *Statistically significant differences between each preceding time point and the 5 h point ($p < 0.05$).

(B) Same data with tumour cells sorted before Pimo analysis. Dashed lines indicate percentage of Pimo-labeled cells from whole tumours. Mice were given hourly Pimo injections for 1 h (○), 2 h (△), 3 h (▽), 4 h (◇), 5 h (●), 6 h (▲), 7 h (▼), or 8 h (◆). Data are mean \pm s.e.m.; $n = 4-8$ tumours per curve.

(C) Experimental protocol. Each red box represents a 1 hour pimonidazole labeling interval resulting from a single pimonidazole injection. The white box indicates the 2 hour period prior to tumour excision used for CCI-103F labeling.

mortality in these regions. Conversely, SiHa tumours tend to contain far less cellular debris, and a larger fraction of viable SiHa cells are typically recoverable per gram of tumour when compared to WiDr tumours.

When CCI-103F was administered to WiDr tumours 1 hour after the final pimonidazole injection and 2 hours prior to tumour excision (Figure 3.5A), the decrease in pimonidazole labeling in the most dimly Hoechst-stained fraction was also observed for CCI-103F. This is consistent with the previous explanation (e.g. decreased cell viability), independent of the individual hypoxia marker used. Additionally, there was a relatively high level of CCI-103F labeling in the brightest Hoechst staining fraction (sort fraction 1) compared to the pimonidazole labeling in Figure 3.4B for the same subpopulation of cells.

Tumour cells that were labeled with *both* pimonidazole (red) and subsequent CCI-103F (green) are indicated in Figure 3.5B, and tumour cells that either labeled only with CCI-103F or only with pimonidazole in Figures 3.5C and 3.5D respectively. Although there is an observable increase in the fraction of cells labeled only with pimonidazole (red only) over time (Figure 3.5D), the differences between the curves are much less distinct than for the SiHa data (Figure 3.2D). Up to 8% of the total number of unsorted WiDr tumour cells were transiently hypoxic over the 5 hour period, with an approximately equal contribution from cells in each sort fraction for the 3-5 hour curves.

Typical flow cytometry profiles for two WiDr tumours are presented in Figure 3.6, where pimonidazole and CCI-103F were administered simultaneously 2 hours before tumour excision (Figures 3.6A and 3.6B), or 5 hourly injections of pimonidazole were given with a subsequent CCI-103F injection 2 hours prior to tumour excision (Figures 3.6C and 3.6D). There was an observable upward shift of the dual-labeled population from the unlabeled cells with 5 hourly injections of the marker in Figures 3.6C and 3.6D, however the shift was diminished relative to that observed in SiHa tumours (Figures 3.3C and 3.3D).

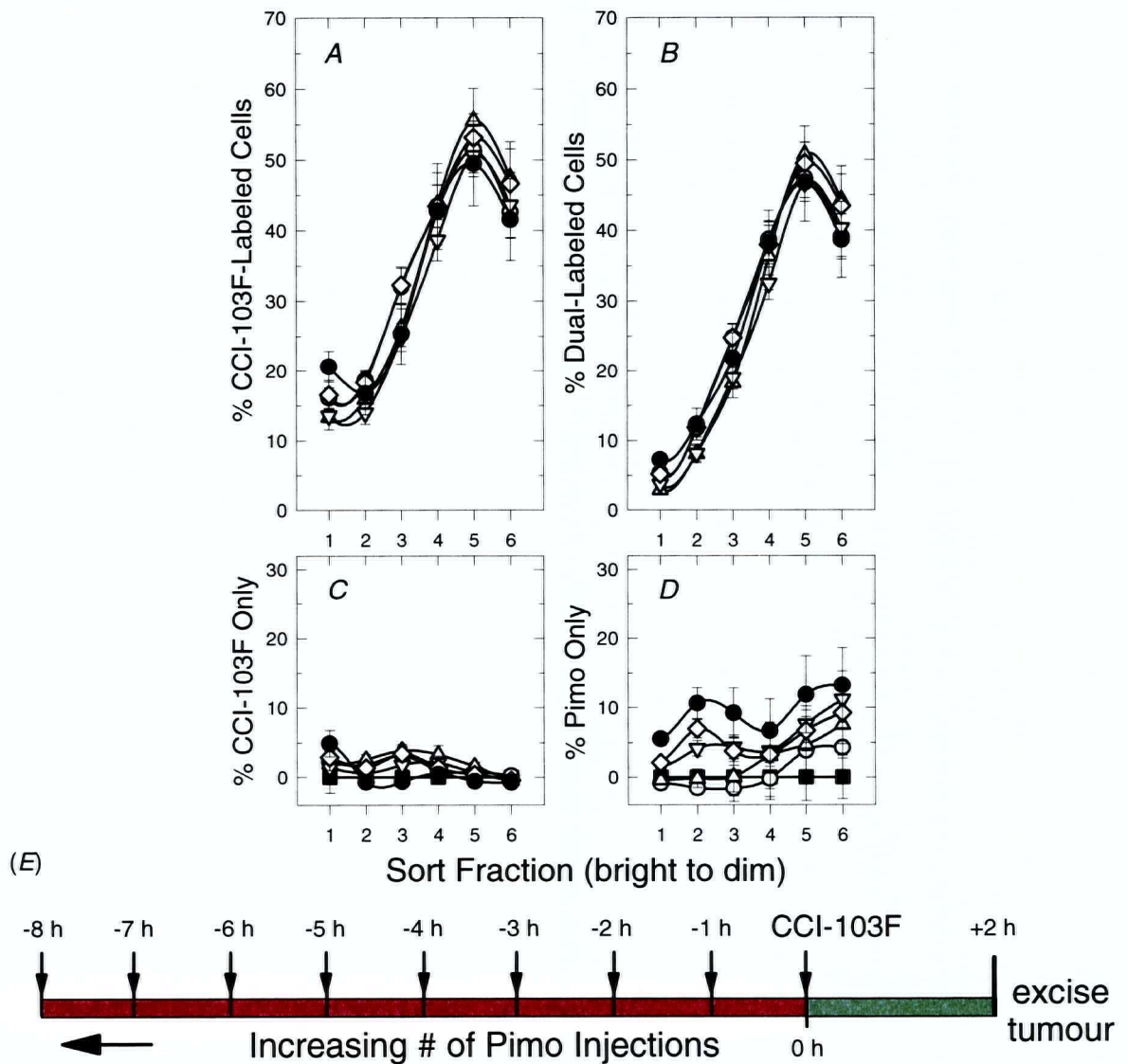


Figure 3.5 Sorted WiDr tumour cells labeled with CCI-103F and/or pimonidazole (Pimo).

(A) Percentage of tumour cells labeled with CCI-103F 2 h after i.p. injection of the marker.

(B) Percentage of tumour cells labeled with both Pimo and subsequent CCI-103F.

(C) Percentage of tumour cells labeled with CCI-103F, but not previously labeled with Pimo.

(D) Percentage of tumour cells labeled with Pimo, but not labeled with subsequent CCI-103F.

Mice were given hourly Pimo injections for 1 h (○), 2 h (△), 3 h (▽), 4 h (◇), or 5 h (●) prior to CCI-103F injection, or a single Pimo injection simultaneously with CCI-103F (■). Curves for 6-8 hourly Pimo injections were not significantly different than the 5 h curve and were omitted for clarity. Data are mean \pm s.e.m.; $n = 4-8$ tumours per curve.

(E) Experimental protocol. Red boxes represent 1 hour pimonidazole labeling intervals from single pimonidazole injections; green box indicates the CCI-103F labeling interval

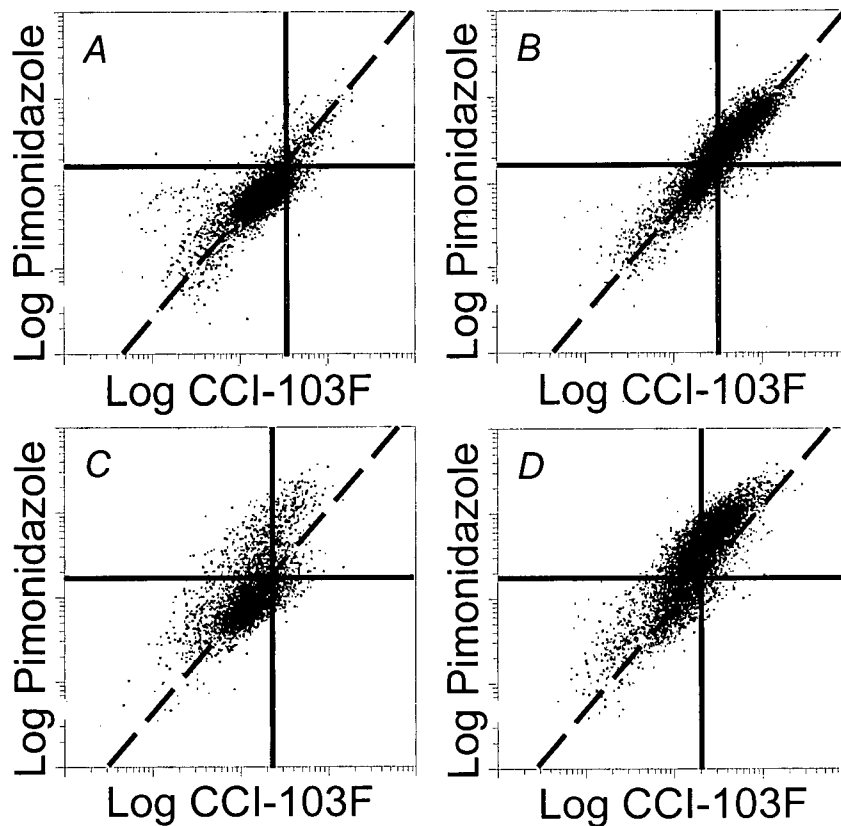


Figure 3.6 Representative flow cytometry dot plots showing hypoxic WiDr tumour cells labeled with pimonidazole and CCI-103F.

(A) Sort fraction 2 and (B) sort fraction 6 for WiDr tumour with pimonidazole and CCI-103F administered simultaneously 2 h prior to tumour excision.

(C) Sort fraction 2 and (D) sort fraction 6 for WiDr tumour with 5 hourly injections of pimonidazole followed by a single CCI-103F injection 2 h prior to tumour excision. Note the distribution of labeled cells has a slightly different shape due to a fraction of cells labeled only with pimonidazole, although the difference is not as marked as was observed in SiHa tumours (Figure 3.3).

3.4 DISCUSSION

While dividing tumour cells into either “hypoxic” or “non-hypoxic” fractions is a simplistic representation of tumour cell oxygenation *in vivo*, it is a necessary step in quantifying tumour hypoxia when one considers the myriad of absolute fluorescence intensities observed in a population of tumour cells. As discussed in Sections 1.5.2.4 and 1.5.2.6, the *absolute* fluorescence intensity of hypoxia marker-containing tumour cells varies within a given tumour due to microregional and cellular differences in the degree of hypoxia, the duration of hypoxia, the concentration of hypoxia marker delivered over time, and the intracellular nitroreductase levels and activities. Furthermore, technical aspects of the flow cytometric data collection (e.g. detector voltage, sheath fluid flow rate, sample pressure, etc.) can produce marked differences in the apparent fluorescence intensities of tumour cell samples, even if every effort is made to reproduce and maintain the numerical flow cytometer settings. Fortunately, despite these variations in measured cellular fluorescence intensities, there remains a several-fold difference in the fluorescence intensity of “labeled” cells *relative* to “non-labeled” cells (i.e. cells that accumulated sufficient quantities of bound hypoxia marker adducts during the labeling interval *relative* to the population of cells that did not).

For the experiments reported in this Chapter, multiple hourly injections of pimonidazole were used to label cells over increasing intervals of time. Thus tumour cells were essentially exposed to larger cumulative doses of pimonidazole with increasing numbers of injections, although the plasma concentration of pimonidazole at any point in time was limited by continued clearance of the marker (elimination $t_{1/2} = 30$ minutes; Walton *et al.*, 1989). As the total cumulative pimonidazole dose increased, the *absolute* fluorescence intensity increased for *all* tumour cells (since even “oxic” tumour cells are capable of binding small quantities of hypoxia markers). Thus if an *absolute* (i.e. fixed) fluorescence intensity threshold were to be set for a given tumour after a single 100 mg/kg injection, then increasing the total cumulative

pimonidazole dose administered would lead to erroneously high estimates of “labeled” cells (due to the inclusion of cells that are clearly “oxic”). However, a *relative* fluorescence intensity threshold is set *independently* for each tumour (and for each hypoxia marker concentration) based on the data obtained in the analysis of *that* tumour. The method therefore remains valid over a range of hypoxia marker concentrations, provided the hypoxia marker dose is not so high as to induce changes in tumour blood flow, hypoxia, cellular metabolism, or toxicity (as can occur after administration of pimonidazole in larger single doses). The non-linear binding kinetics of pimonidazole as a function of oxygenation are particularly helpful when determining an appropriate fluorescence intensity threshold, as a significant increase in binding occurs only in “hypoxic” cells (Figure 3.7).

One important consideration with the “time-integrated” pimonidazole data is that the increase in pimonidazole-labeled cells observed over time was not due solely to the increase in total cumulative pimonidazole dose from the multiple pimonidazole injections. Importantly, previously published data indicate a linear increase in relative fluorescence intensity of hypoxic cells with increasing single doses of pimonidazole up to 400 mg/kg, whereas the fraction of pimonidazole-labeled SiHa tumour cells is approximately the same 3 hours after single injections of 200-400 mg/kg (Durand and Raleigh, 1998). These data indicate that increasing the administered dose of pimonidazole increases the fluorescence intensity of hypoxic cells (Figure 3.7), without significantly increasing the labeling of cells identified as “oxic” at lower administered doses (assuming no pimonidazole-induced increases in tumour hypoxia with increasing dose as discussed above).

Previously published dual stain mismatch data (Figure 3.8) indicate that SiHa and WiDr tumour xenografts have very different propensities to undergo fluctuations in tumour perfusion over a 30 minute period. Changes in WiDr perfusion (and likely hypoxia) typically occur with a frequency of less than an hour, and these perfusion changes can be quite dramatic in some

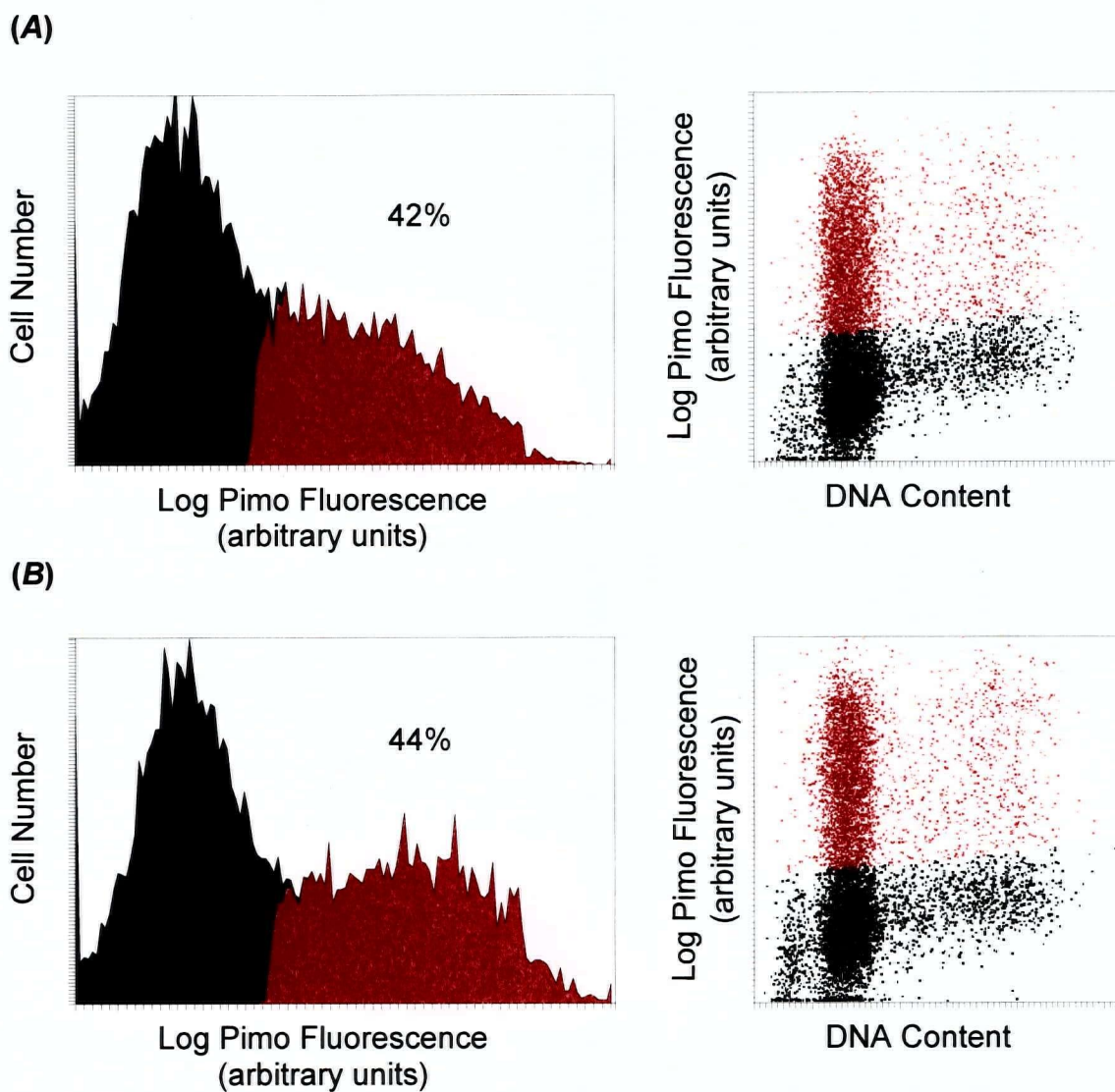


Figure 3.7 Comparison of different pimonidazole doses on the relative fluorescence intensity of pimonidazole-labeled cells and the fraction of pimonidazole-labeled cells.

(A) SiHa tumour cells labeled 3 hours after a single injection of 100 mg/kg pimonidazole. The histogram illustrates the relative fluorescence intensity of labeled (red) vs non-labeled (black) tumour cells. The flow cytometry dot plot is a more “typical” representation of the data; thresholds are set based on linear distributions of fluorescence intensity vs DNA content.

(B) SiHa tumour cells labeled 3 hours after a single injection of 300 mg/kg pimonidazole. Note the increased fluorescence intensity of the pimonidazole-labeled cells (i.e. increased width of red histogram or height of red dots) compared to the relatively static fluorescence intensity of the non-labeled cells. Despite the 3-fold increase in pimonidazole dose, the area of the red histogram and the number of red dots (i.e. the fraction of pimonidazole-labeled cells) were virtually equivalent to those in (A).

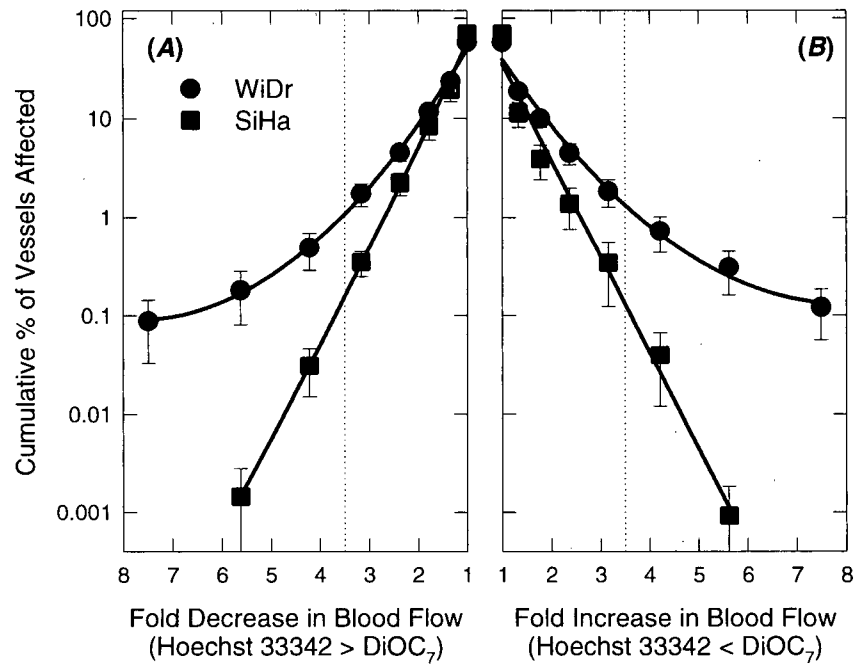


Figure 3.8 Dual stain mismatch data for untreated WiDr and SiHa human tumour xenografts. Plots indicate cumulative fractions of blood vessels exhibiting (A) decreases or (B) increases in the normalized intensity ratio of carbocyanine (DiOC₇) relative to Hoechst 33342 over a 30 minute period (see Section 2.2.4 and Figure 2.2). Vertical dotted lines indicate qualitative (visual) identification of stain "mismatch" (Trotter, *et al.*, 1989). Note the greater fraction of WiDr tumour blood vessels that demonstrate larger scale changes in perfusion during the time interval. Data are mean \pm s.e.m.; $n = 15$ tumours per tumour type. Figure adapted from Durand and Aquino-Parsons, 2001a.

tumour regions, representing up to 8-fold differences in the delivery of two sequentially administered fluorescent perfusion dyes. Conversely, SiHa perfusion tends to be much more stable over relatively short time intervals and perfusion changes (when present) are typically of a lesser magnitude. These observations had initially suggested that SiHa tumour blood flow was fairly constant, and that there was little transient hypoxia in these tumours. While this statement remains true when considered on the order of minutes, the data reported herein suggest that significant changes in the hypoxic status of SiHa tumour cells can occur over several hours.

Hypoxia probes such as pimonidazole “integrate” tumour hypoxia over the circulation time of the agent (murine plasma elimination $t_{1/2} = 30$ minutes; Walton *et al.*, 1989). Thus a single 100 mg/kg injection of pimonidazole would label cells that were hypoxic enough (for long enough) during a ~1-1.5 hour period without distinguishing between cells that were hypoxic for all or part of this time. For experimental tumours that exhibit changes in tumour perfusion (and likely hypoxia) over periods of less than an hour such as WiDr tumours, pimonidazole labeling would not detect minor or short-lived changes in hypoxia that occurred within this time frame. This is important insofar as the estimates for the fraction of transiently hypoxic cells included in this Chapter should be viewed as conservative (particularly for WiDr tumours) since they do not take into consideration changes in tumour hypoxia that may have occurred with a duration of less than an hour. Similarly, previously published data indicating changes in SiHa tumour hypoxia over many days using “time-integrated” orally administered pimonidazole (Bennewith *et al.*, 2002) should also be viewed as conservative (where the shortest interval of hypoxia marker labeling was 6-12 hours; see Chapter 4).

While no attempts were made to shorten the interval of hypoxia measurement with pimonidazole, the labeling interval was increased by performing multiple hourly injections of the marker. SiHa tumours demonstrated distinct hypoxia marker “mismatch” when pimonidazole exposure was maintained, indicating the number of hypoxic tumour cells increased over times up

to at least 5 hours. Importantly, the fraction of SiHa tumour cells that were hypoxic over a 1 hour period was 37% (determined by a single pimonidazole injection as is typically performed in rodents), but increased significantly to 56% when considered over a longer period of time! This increase in the total fraction of hypoxic cells was due to the inclusion of cells that were not labeled with subsequent CCI-103F, and were therefore transiently hypoxic. Thus the “time-integrated” administration of pimonidazole over a 5 hour period provided an estimate for the hypoxic fraction of SiHa tumours that included cells that were transiently hypoxic.

WiDr tumours demonstrated a large degree of concordance between the two hypoxia markers over the same time frame. Indeed, the fraction of hypoxic cells increased only marginally from 44% to 52% from 1-5 hours of pimonidazole exposure, indicating a lesser propensity for WiDr tumours to undergo changes in hypoxia over this time period. When combined with the dual stain mismatch data indicating a large degree of perfusion fluctuation in WiDr tumours over a 30 minute interval (Figure 3.8), these data suggest that the bulk of intermittent hypoxia episodes in WiDr tumours likely occur with a frequency of less than an hour. Therefore, a single pimonidazole injection appears to provide a hypoxic fraction that already includes the majority of transiently hypoxic cells in WiDr tumours. A more accurate representation of transient hypoxia (specifically) in WiDr tumours would involve assessing differences in tumour hypoxia over shorter time intervals, perhaps combining “time-integrated” pimonidazole labeling with differential quantification of a short-lived endogenous hypoxia “marker” such as HIF-1 α (Semenza, 2001; Begg, 2003; Vordermark and Brown, 2003).

The intra-tumoural proximity of transiently hypoxic cells relative to vasculature that was perfused just prior to tumour excision was also determined. Transiently hypoxic cells in SiHa tumours were found primarily at an intermediate to large distance from functional tumour vasculature, which is an observation that has important mechanistic implications. With earlier dual stain mismatch data indicating relatively large perfusion changes in (some) tumour blood

vessels (Trotter *et al.*, 1989), it was tempting to assume that transient hypoxia was largely a result of complete stoppages of flow through tumour blood vessels. While larger-scale changes in perfusion are the most impressive to observe, they have perhaps taken attention away from more modest (and more frequently observed) changes in perfusion that may also impact tumour hypoxia (Trotter *et al.*, 1991; Durand and LePard, 1995). Indeed, studies monitoring erythrocyte flux through tumour blood vessels in murine tumours have shown that modest changes in flux are more common than complete stoppages in tumour blood flow (Dewhirst *et al.*, 1996).

The location of transiently hypoxic cells at an intermediate to large distance from tumour vasculature also makes intuitive sense when one considers the location of the boundary between “oxygenated” (i.e. radiosensitive) and radiobiologically hypoxic cells in relation to functional blood vessels. In order for changes in tumour perfusion to impact the oxygenation of cells directly adjacent to a functional blood vessel, the vessel would have to experience a drastic decrease in flow (i.e. complete collapse or obstruction). However, a much less drastic decrease in blood vessel functionality could conceivably shift the boundary between “oxic” and hypoxic cells toward the vessel by a few cell diameters. The oxygenation of cells at an intermediate distance from tumour blood vessels should therefore be more responsive to modest blood flow changes than the cells directly adjacent to tumour vasculature. Due to the radial geometry of tumour cords surrounding tumour blood vessels, the number of cells that could potentially be affected by modest changes in tumour perfusion could conceivably be quite large. Thus the number of tumour cells affected by (relatively infrequent) large-scale changes in tumour perfusion is likely small relative to the number of cells potentially affected by more modest perfusion changes. Measuring changes in tumour hypoxic status on a cellular level using flow cytometry analysis provides a means to detect and quantify these cells, with a resolution that is not possible with regional pO_2 observation (Kimura *et al.*, 1996; Dewhirst *et al.*, 1998; Braun *et*

al., 1999; Brurberg *et al.*, 2003; Brurberg *et al.*, 2004) or microregional hypoxia marker detection (Ljungkvist *et al.*, 2000; Raleigh *et al.*, 2001).

It is worth noting that SiHa tumour cells that demonstrated changes in their hypoxic status over time were present in a similar proximity to tumour blood vessels as cells inferred to be at a static level of intermediate oxygenation (Wouters and Brown, 1997; Evans *et al.*, 1997; Olive *et al.*, 2002). Further work is required to resolve these two conceptually different (though possibly related) types of hypoxic cell, although both are potentially important limitations of cancer therapy.

Quantification of transiently hypoxic cells in solid tumours has a number of practical implications for the clinic. Of primary importance is the ability to detect these cells, and to address whether the presence of intermittent hypoxia correlates with poor clinical prognosis. From a therapy standpoint, the presence and fraction of transiently hypoxic cells in a tumour could conceivably dictate the type of treatment strategy that is employed (Chaplin *et al.*, 1986). For example, strategies that improve tumour perfusion (Chaplin *et al.*, 1998; Bennewith and Durand, 2001) or that involve repeated low doses of radiation (Denekamp and Dasu, 1999) or drugs (Durand, 2001) would be expected to target cells with changing perfusion and hypoxic status. Ideally, quantification of the intermittently hypoxic content of a tumour could be used to individualize treatments designed to target hypoxic tumour cells.

Since some tumour cells are hypoxic only intermittently, assessing tumour hypoxia over relatively short periods of time likely underestimates the (potentially therapeutically relevant) hypoxic fraction of a tumour. Thus the administration of hypoxia markers such as pimonidazole by a single i.p. injection in experimental animals or by i.v. infusion in patients (plasma half-lives of 30 minutes (Walton *et al.*, 1989) and 5.1 hours (Saunders *et al.*, 1984) respectively), may not provide an accurate picture of tumour hypoxia when considered over a period of many hours in rodents or a day or more in patients. Changes in hypoxia over longer time intervals may not be

considered important when administering a single dose of therapy, but could potentially have a significant impact on tumour response to multi-fractionated radiotherapy (Denekamp and Dasu, 1999) or chemotherapy (Durand, 2001). Changes in tumour hypoxia over time may also affect the regrowth potential of a tumour as formerly hypoxic cells may suddenly find themselves in an environment that is better oxygenated and more favorable for proliferation (Durand and Raleigh, 1998; Durand and Aquino-Parsons, 2001b). An additional complexity arises when one considers changes in tumour hypoxia that may be induced by the tumour response to therapy itself, a factor that has not been adequately studied in the clinic to this point. Thus a method for measuring changes in tumour hypoxia over time may have application to determining treatment-induced changes in tumour hypoxia, while “time-integrated” hypoxia measurements may provide more therapeutically relevant estimates of hypoxia prior to therapy.

By using two sequentially administered hypoxia markers with subsequent analysis by flow cytometry, the presence of intermittent hypoxia episodes on a whole-tumour scale was established over several hours, enabling estimation of the transiently hypoxic fractions of two human tumour xenografts. A similar method (e.g. using pimonidazole and EF5) would be applicable to detecting transiently hypoxic cells in biopsies obtained from human tumours, which would enable the presence and influence of these cells to be studied in the clinic. Once these critical clinical questions have been addressed, it follows that re-evaluation of methods used to measure hypoxia in the clinic may be necessary. Overall, improved understanding of transient hypoxia will aid in the design of cancer therapy protocols to take advantage of the dynamic nature of the solid tumour microenvironment.

CHAPTER 4: ORALLY ADMINISTERED PIMONIDAZOLE TO LABEL HYPOXIC TUMOUR CELLS

This Chapter has been adapted from the following published manuscript:

Bennewith, KL, Raleigh, JA, and Durand, RE (2002) Orally administered pimonidazole to label hypoxic tumor cells. *Cancer Res*, **62**(23): 6827-6830.

4.1 INTRODUCTION

It is well accepted that poorly oxygenated tumour cells have a negative impact on tumour response to therapy, and considerable effort has been devoted to developing techniques for quantifying tumour hypoxia in the clinic. However, many of the current methods are inconvenient, requiring the insertion of a polarographic probe (Kallinowski *et al.*, 1990), or injection of a hypoxia marker with non-invasive regional imaging (Koh *et al.*, 1992) or biopsy if microregional information is desired (Kennedy *et al.*, 1997; Evans *et al.*, 2000; Olive *et al.*, 2000). Furthermore, these techniques only provide information about tumour hypoxia during the time that the electrode is in place or over the circulation lifetime of the injected hypoxia marker. Each method is therefore typically used for measuring hypoxia during a fixed time interval, without consideration of hypoxia that may change over time.

Chapter 3 introduced a novel method for estimating transient tumour hypoxia using flow cytometry analysis of hypoxic cells differentially labeled with one of two sequentially administered exogenous hypoxia markers. Multiple injections of the hypoxia marker pimonidazole increased the interval of hypoxic cell labeling and generated a “time-integrated” measurement of tumour hypoxia. However, the duration of pimonidazole labeling was limited to 8 hours or less for the sake of convenience, practicality, and tolerance of the animals to multiple *i.p.* injections. With these limitations in mind, it was discovered that pimonidazole administered in the drinking water of tumour-bearing mice could effectively label hypoxic tumour cells, and that tumour hypoxia could therefore be measured over much longer periods of time than was possible with multiple *i.p.* injections.

Using a principle similar to that discussed in Chapter 3, hypoxic cells labeled with oral pimonidazole (i.e. by a hypoxia measurement that was “integrated” over time) were compared to cells labeled with a second hypoxia marker, CCI-103F (Raleigh *et al.*, 1987), providing a means to study the long-term dynamics of tumour hypoxia. Subsequent determination of the

proliferative capacity of tumour cells labeled with oral pimonidazole provided indications of the potential therapeutic relevance of these cells, while pharmacokinetic investigations were conducted to monitor plasma pimonidazole concentrations over time. Consequently, the use of orally administered pimonidazole not only adds convenience and versatility to the measurement of tumour hypoxia, but also has the potential to provide new insights into transient tumour hypoxia and the dynamic tumour microenvironment.

4.2 MATERIALS AND METHODS

4.2.1 Common Materials and Methods

SiHa and WiDr tumour xenografts were used as described in Section 2.2.1. Pimonidazole and CCI-103F were used as described in Section 3.2.1, except that pimonidazole was dissolved at a concentration of 1 mg/ml in sterilized water for oral administration. Fluorescence activated cell sorting based on intracellular Hoechst 33342 intensity was performed as described in Section 3.2.2. Intracellular adducts of pimonidazole and CCI-103F were labeled with the appropriate antibodies as outlined in Section 3.2.3, and cells containing bound hypoxia marker adducts were identified and quantified by flow cytometry as described in Section 3.2.4.

4.2.2 Iododeoxyuridine

In order to label cells actively synthesizing DNA, iododeoxyuridine (IdUrd; Sigma-Aldrich Canada Ltd., Oakville, ON, Canada) was injected i.p. 30 minutes prior to tumour excision at a dose of 90 mg/kg (6 mg/ml stock solution in 40 mM Tris buffer, pH 10). IdUrd incorporates into DNA during DNA synthesis, and (alcohol-fixed) tumour cell samples were therefore denatured in 2N HCl containing 0.5% Triton X-100 for 20 minutes before antibody contact to allow the antibody access to the incorporated IdUrd. Tumour cells were washed three times with minimal essential medium (MEM) to neutralize the acid prior to contact with a B44 clone-conjugated FITC antibody (Becton Dickinson Biosciences, San Jose, CA). Goat anti-mouse IgG R-phycoerythrin fluorescent secondary antibody (Sigma-Aldrich Canada Ltd.) was used in conjunction with the monoclonal anti-pimonidazole primary antibody identified in Section 3.2.3. Again, each antibody was diluted in a solution containing 4% calf serum (HyClone, Logan, UT) and 0.1% Triton X-100 in Dulbecco's PBS (Gibco Invitrogen Corp., Burlington, ON).

4.2.3 Pimonidazole Pharmacokinetics

Blood samples were taken from the lateral tail vein of mice at various times after the initiation of *ad libitum* pimonidazole consumption or i.p. injection of pimonidazole. Plasma was

obtained by centrifugation, and the samples were subsequently treated with 0.5 ml methanol, vortexed, and centrifuged. The supernatant was removed and evaporated to dryness under vacuum with gentle warming (45°C) prior to reconstitution in deionized water. Concentrations of pimonidazole were quantified using Waters modular high-precision liquid chromatography (HPLC) equipment (Waters Assoc., Milford, MA) including model 510 HPLC pumps, a model 712 Waters Intelligent Sample Processor (WISP), and a model 996 photodiode array detector. Separations were performed on a Waters reversed-phase octadecylsilane (C18) Symmetry column (15 cm x 3.9 mm i.d., 5 µm beads) and eluted isocratically with 11% acetonitrile in 50 mM ammonium dihydrogen orthophosphate containing 5 mM hexane sulfonic acid at a flow rate of 1 ml/min. Absorbance was monitored at 324 nm, and pimonidazole was quantified based on chromatograph peak area with reference to same-day standard curves (derived from spiked mouse plasma standards) that were linear over the range 0.05-50 µg/ml. The lower limit of detection was < 0.05 µg/ml with an on-column detection of < 1 ng for a 20 µl injection volume; run times were < 7 minutes.

4.3 RESULTS

4.3.1 SiHa Tumour Cells Labeled with Oral Pimonidazole

Pimonidazole was administered orally (*ad libitum*) to SiHa tumour-bearing mice for 3-96 hours, and the fractions of tumour cells that had incorporated the marker over time are indicated in Figure 4.1A. The apparent rapid increase in the fraction of pimonidazole-labeled cells from 3-6 hours (dashed line) is an indication of pimonidazole consumption that was inadequate to allow discrimination of hypoxic tumour cells by flow cytometry. Interestingly, an increase in the fraction of pimonidazole-labeled cells was observed between 6 and 48 hours of continued pimonidazole consumption, followed by a further gradual increase in labeling up to 96 hours (solid line). Increased resolution of the shorter labeling intervals would be required to determine if the labeling pattern could be described as asymptotically increasing over time (as was the case with the hourly pimonidazole injections used in Chapter 3).

Tumour cells labeled with oral pimonidazole were also evaluated at increasing distance from functional tumour blood vessels by sorting the cells into subpopulations based on intracellular content of Hoechst 33342 prior to flow cytometry analysis (Figure 4.1B). By essentially “breaking down” tumours into subpopulations of cells from regions of differing blood flow (at the time of Hoechst administration), substructure in the pimonidazole labeling patterns could be observed. Specifically, there was an increased percentage of pimonidazole-labeled cells with increasing distance from functional tumour vasculature (decreased Hoechst staining intensity; dimmer sort fraction). Moreover, the increased total number of pimonidazole-labeled cells observed beyond 6 hours in Figure 4.1A was largely due to increased labeling of cells at a distance from tumour blood vessels that were functional just before tumour excision.

4.3.2 Relative Fluorescence Intensity of Oral Pimonidazole-Labeled Tumour Cells

Tumour cells are scored as “positive” for pimonidazole labeling when the intensity of anti-pimonidazole antibody fluorescence is above a threshold value, allowing labeled cells to be

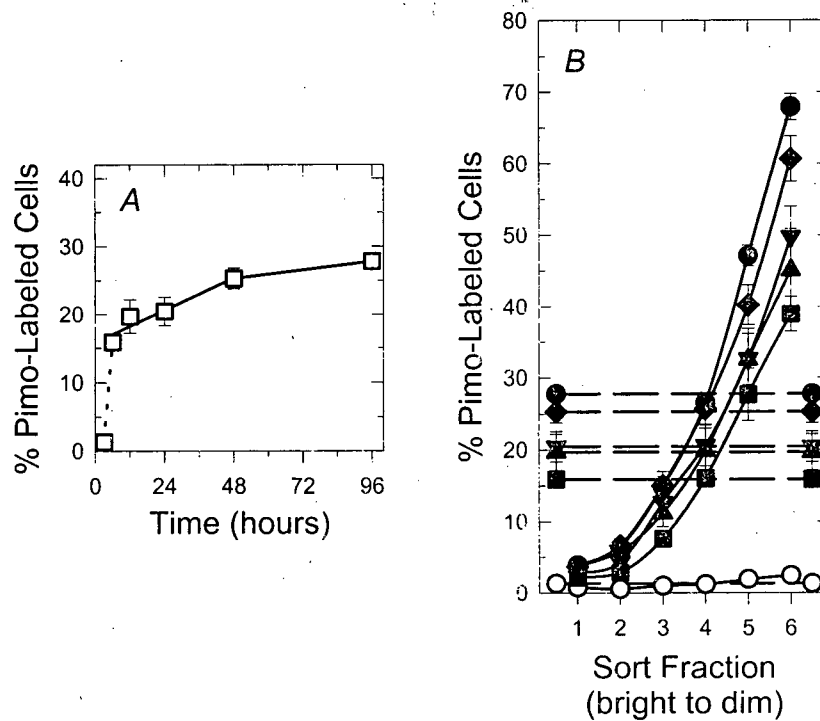


Figure 4.1 SiHa tumour cells labeled with oral pimonidazole (Pimo).

(A) Percentage of tumour cells labeled with oral Pimo after tumour-bearing mice consumed Pimo-containing water *ad libitum* for 3-96 h (□).

(B) Same data with tumour cells sorted prior to Pimo analysis based on Hoechst 33342. Dashed lines indicate percentage of Pimo-labeled cells from whole tumours.

Mice were allowed to drink Pimo-containing water for 3 h (○), 6 h (■), 12 h (▲), 24 h (▼); 48 h (◆), or 96 h (●) prior to tumour excision. Data are mean \pm s.e.m.; $n = 10-12$ tumours per curve (except for 3 h and 6 h; see Section 4.3.3).

distinguished from non-labeled cells. Information about the relative number of pimonidazole adducts bound per hypoxic cell can be obtained by expressing the fluorescence intensity of pimonidazole-“positive” (hypoxic) cells relative to the fluorescence intensity of pimonidazole-“negative” (non-labeled) cells. Figure 4.2A illustrates the relative fluorescence intensity of pimonidazole-labeled cells with increasing duration of pimonidazole consumption as a function of their proximity to functional vasculature (sort fraction). For example, the fluorescence of hypoxic cells in sort fraction 6 (distant from functional blood vessels) was 4- to 7-fold more intense than the fluorescence of non-labeled cells with increasing duration of pimonidazole consumption (also shown in Figure 4.2B; triangles). When the relative fluorescence intensity of pimonidazole labeling in the least well-perfused cells was compared to the estimated cumulative pimonidazole dose based on the volume of water consumed (Figure 4.2B; diamonds), the amount of incorporated pimonidazole per labeled cell progressively increased with time, essentially paralleling pimonidazole exposure. Thus, both the percentage of pimonidazole-labeled cells (Figure 4.1B) and the number of bound pimonidazole adducts per labeled cell (Figure 4.2B) increased with increasing duration of pimonidazole consumption in this sort fraction.

Interestingly, for all tumour cells that incorporated pimonidazole (recognizing that many fewer pimonidazole-labeled cells were in fact near blood vessels), it was found that cells at an intermediate radial distance from functional tumour vasculature contained the least number of bound pimonidazole adducts. This presumably reflects, in part, that cells nearer tumour blood vessels are typically larger, more likely to be proliferating, and are more metabolically active than cells that are further from functional blood vessels. Therefore, cells closer to tumour blood vessels (when hypoxic) tended to be more intensely labeled with pimonidazole than smaller, less metabolically active cells. With sustained hypoxia however, cells that were more distant from tumour vasculature became more intensely labeled than the intermediate cells. Taken together,

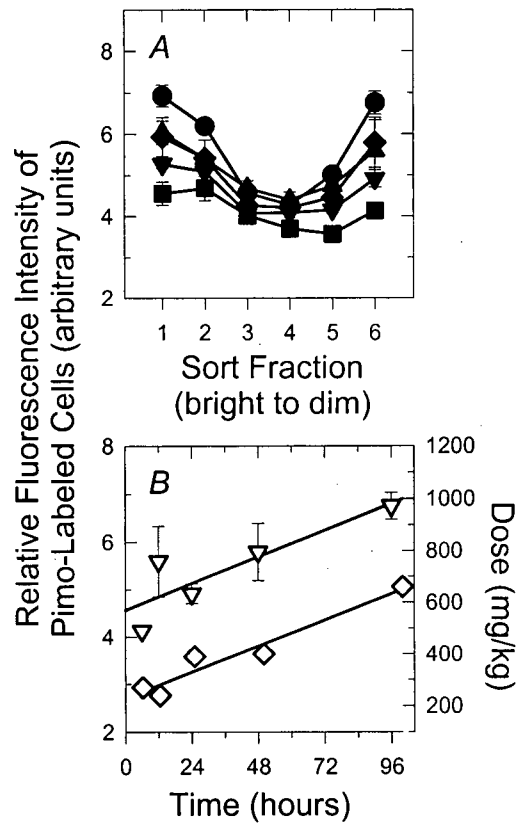


Figure 4.2 Relative fluorescence intensity of SiHa tumour cells labeled with oral pimonidazole (Pimo).

(A) Fluorescence intensity of Pimo-labeled cells relative to the fluorescence intensity of non-labeled cells. Mice were allowed to drink Pimo-containing water for 6 h (■), 12 h (▲), 24 h (▼), 48 h (◆), or 96 h (●) prior to tumour excision; tumour cells were sorted prior to Pimo analysis.

(B) Relative fluorescence intensity of Pimo-labeled cells for the most hypoxic tumour cells (sort fraction 6; ▽), plotted on left axis. Cumulative pimonidazole dose ingested by tumour-bearing mice over time (◇), plotted on right axis. Data are mean \pm s.e.m.; $n = 4$ tumours per curve.

these data illustrate a rather complex interplay between the delivery and retention of pimonidazole with tumour cell proximity to functional vasculature.

4.3.3 Oral Pimonidazole and Transiently Hypoxic SiHa Tumour Cells

The fraction of tumour cells labeled with oral pimonidazole over time was also compared to tumour cells labeled with an i.p. injection of CCI-103F administered 3 hours prior to tumour excision. The CCI-103F binding represented a relative “snapshot” of tumour hypoxia over 3 hours, while oral pimonidazole provided a hypoxia measurement that was “integrated” over 6-96 hours. Similar fractions of cells were labeled with CCI-103F over a 3 hour period in a number of SiHa tumours and, of particular importance, ingestion of pimonidazole did not adversely affect tumour oxygenation (Raleigh *et al.*, 1999) or cell viability (Durand and Raleigh, 1998) as assessed by CCI-103F binding (Figure 4.3A).

Tumour cells labeled with *both* oral pimonidazole (red) and subsequent i.p. CCI-103F (green) are indicated in Figure 4.3B. During a simultaneous 3 hour exposure to oral pimonidazole (1 mg/ml) and CCI-103F, tumour hypoxia was detectable by CCI-103F but only minimally by pimonidazole binding, indicating inadequate pimonidazole consumption over 3 hours to discriminate hypoxic from non-hypoxic tumour cells by flow cytometry analysis. After 6 hours, oral pimonidazole produced very similar information to that obtained from the 3 hour exposure to CCI-103F. Importantly, these results argue that the differences in labeling observed between 6 and 96 hours of oral pimonidazole consumption shown in Figure 4.1 were not due to inadequate pimonidazole ingestion or binding over the shorter time intervals.² The fractions of tumour cells labeled with pimonidazole (red), but not with subsequent CCI-103F (i.e. not green) are shown in Figure 4.3C, indicating cells that were subject to changes in their hypoxic status over time. These tumour cells were sufficiently hypoxic during the long-term exposure to oral

² While this statement remains true for these data, a caveat became evident with further study of oral pimonidazole to label hypoxic tumour cells over a 6 hour period. These observations will be discussed in Section 4.3.5 as they apply to the WiDr tumour data.

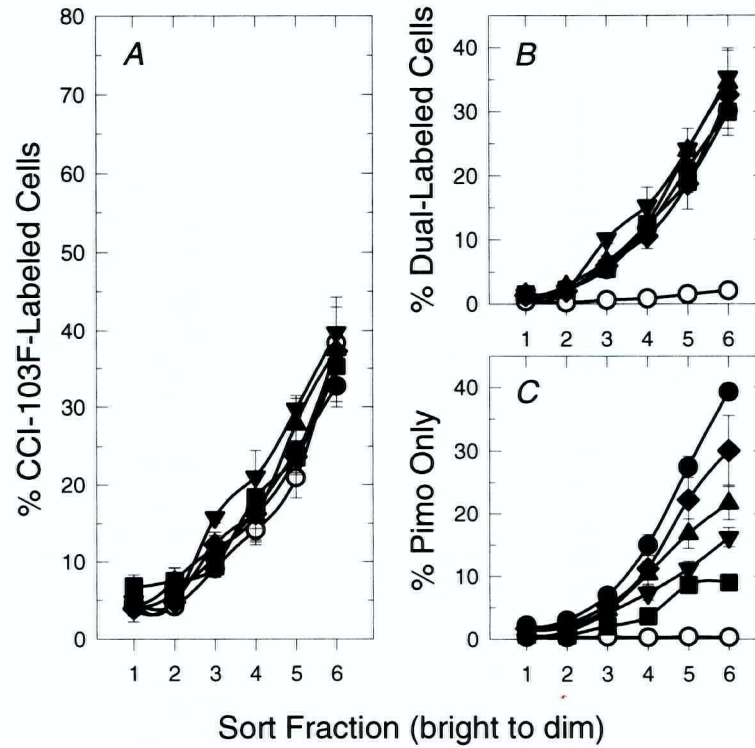


Figure 4.3 Sorted SiHa tumour cells labeled with CCI-103F and/or oral pimonidazole (Pimo).

(A) Percentage of tumour cells labeled with CCI-103F 3 h after i.p. injection of the marker.

(B) Percentage of tumour cells labeled with both oral Pimo and subsequent i.p. CCI-103F.

(C) Percentage of tumour cells labeled with oral Pimo, but not with subsequent CCI-103F.

Mice were allowed to drink Pimo-containing water for 3 h (○), 6 h (■), 12 h (▲), 24 h (▼), 48 h (◆), or 96 h (●) prior to tumour excision. Data are mean \pm s.e.m.; $n = 4$ tumours per curve.

pimonidazole to incorporate that marker, yet were not hypoxic enough to incorporate CCI-103F during the 3 hours just prior to analysis. Interestingly, most tumour cells demonstrating a changing hypoxic status over this relatively long timeframe were located in sort fractions of the poorest perfusion status prior to tumour excision.

4.3.4 Oral Pimonidazole and Proliferative Capacity of SiHa Tumour Cells

SiHa tumour cells actively synthesizing DNA 30 minutes prior to tumour excision (labeled with iododeoxyuridine; IdUrd) are indicated in Figure 4.4A for mice consuming oral pimonidazole for 6-96 hours. The fractions of S-phase tumour cells decreased with increasing distance from tumour blood vessels that were functional 10 minutes later (i.e. the time difference between IdUrd and Hoechst 33342 injections). While there was some degree of scatter in the IdUrd data (likely due to different SiHa tumour implant generations used for various experiments), there was no consistent trend of changing tumour cell proliferative capacity with increasing pimonidazole consumption.

Cells labeled with *both* oral pimonidazole (red) and subsequent IdUrd (green) are shown in Figure 4.4B. These data indicate that a relatively small, but therapeutically relevant, fraction of cells that were hypoxic enough to label with oral pimonidazole during the previous 6-96 hours were sufficiently well-oxygenated to be capable of synthesizing DNA just prior to analysis.

4.3.5 Oral Pimonidazole to Label Hypoxic WiDr Tumour Cells

WiDr tumour cells labeled with oral pimonidazole after 6-96 hours of *ad libitum* consumption are indicated in Figure 4.5. The increase in pimonidazole-labeled cells between 6 and 12 hours (dashed line) is indicative of inadequate consumption and/or binding of pimonidazole over this time period, particularly when compared to the CCI-103F profiles in Figure 4.6A. Since the SiHa tumour data presented in Figure 4.1 indicated adequate labeling of hypoxic tumour cells over a 6 hour period, the contradictory observations in WiDr tumours would suggest some form of tumour type-specific differences in pimonidazole labeling with 6

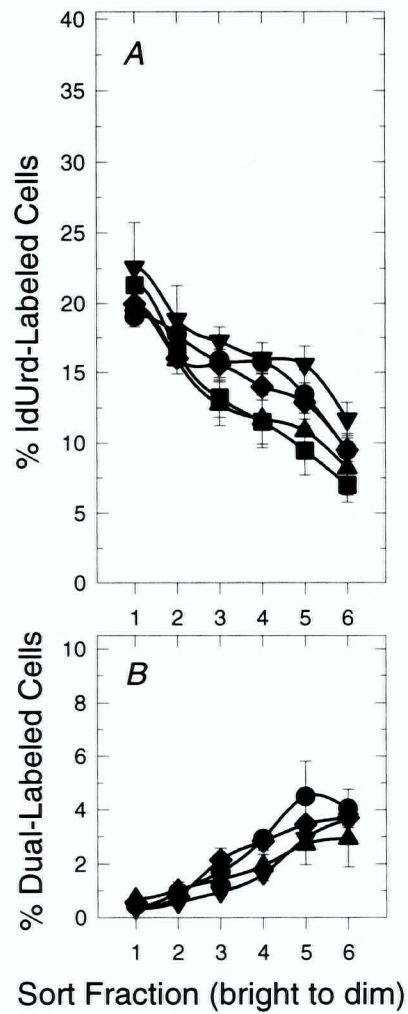


Figure 4.4 Sorted SiHa tumour cells labeled with IdUrd and/or oral pimonidazole (Pimo).

(A) Percentage of tumour cells labeled with IdUrd 30 min after i.p. injection of the marker.

(B) Percentage of tumour cells labeled with both oral Pimo and subsequent i.p. IdUrd.

Mice were allowed to drink Pimo-containing water for 6 h (■), 12 h (▲), 24 h (▼), 48 h (◆), or 96 h (●) prior to tumour excision. Data are mean \pm s.e.m.; $n = 4-6$ tumours per curve.

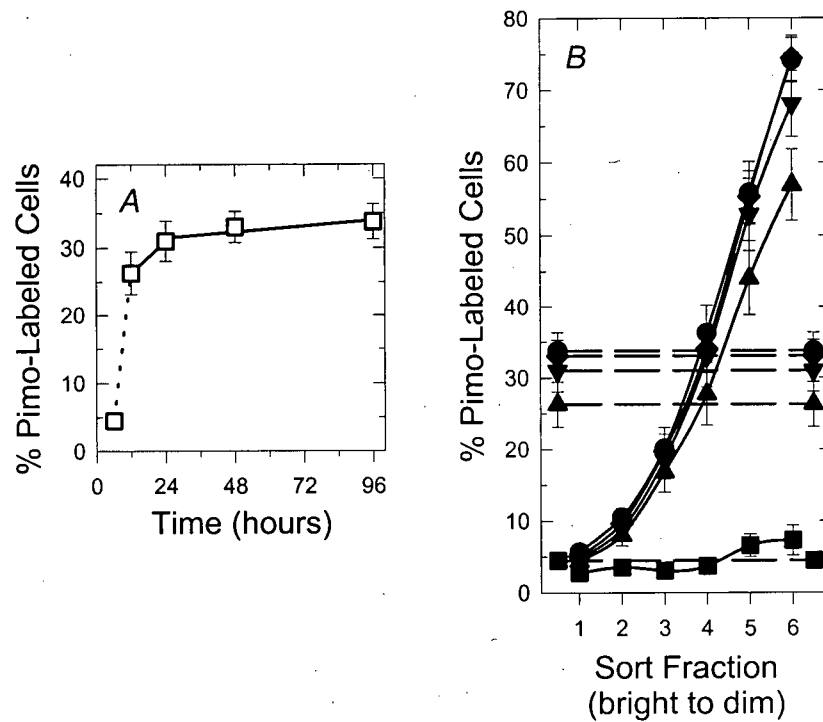


Figure 4.5 WiDr tumour cells labeled with oral pimonidazole (Pimo).

(A) Percentage of tumour cells labeled with oral Pimo after tumour-bearing mice consumed Pimo-containing water *ad libitum* for 6-96 h (□).

(B) Same data with tumour cells sorted prior to Pimo analysis based on Hoechst 33342. Dashed lines indicate percentage of Pimo-labeled cells from whole tumours.

Mice were allowed to drink Pimo-containing water for 6 h (■), 12 h (▲), 24 h (▼), 48 h (◆), or 96 h (●) prior to tumour excision. Data are mean \pm s.e.m.; $n = 10-12$ tumours per curve.

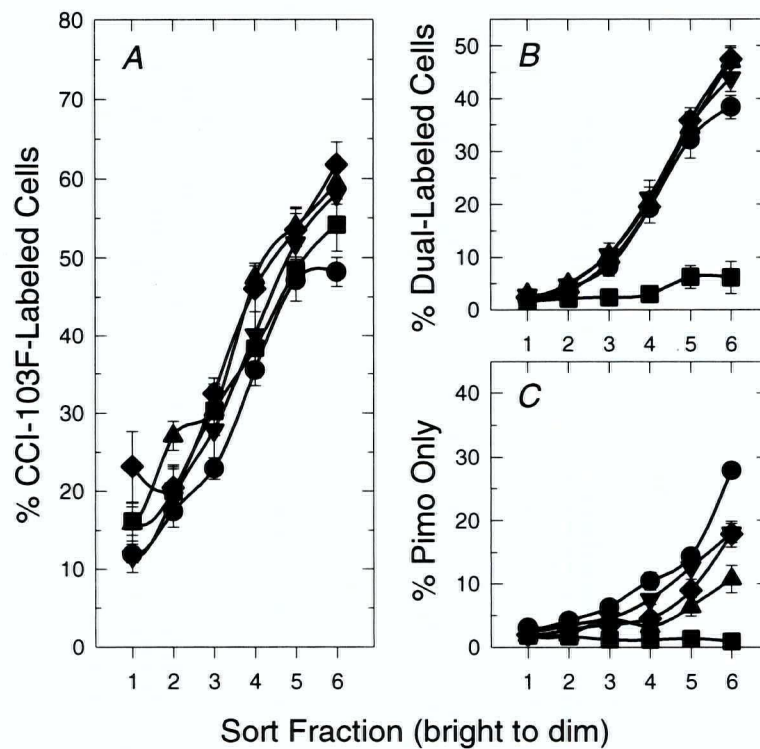


Figure 4.6 Sorted WiDr tumour cells labeled with CCI-103F and/or oral pimonidazole (Pimo).

(A) Percentage of tumour cells labeled with CCI-103F 3 h after i.p. injection of the marker.

(B) Percentage of tumour cells labeled with both oral Pimo and subsequent i.p. CCI-103F.

(C) Percentage of tumour cells labeled with oral Pimo, but not with subsequent CCI-103F.

Mice were allowed to drink Pimo-containing water for 6 h (■), 12 h (▲), 24 h (▼), 48 h (◆), or 96 h (●) prior to tumour excision. Data are mean \pm s.e.m.; $n = 6$ tumours per curve.

hours of consumption. Indeed, hypoxic SiHa and WiDr tumour cells typically bind different absolute numbers of pimonidazole adducts *in vivo* over a given period of time, suggesting differences in intracellular nitroreductase levels and/or activities (Durand and Raleigh, 1998). While this could conceivably impair the discrimination of labeled from non-labeled cells at low concentrations of pimonidazole depending on the tumour-type, this was not likely a major factor in the binding differences observed after 6 hours of oral pimonidazole consumption. Subsequent experiments with oral pimonidazole in SiHa tumours showed a similar low level of binding over a 6 hour period and, in hindsight, these observations could be reconciled through the differences in murine activity at various times of day. Mice are largely nocturnal, and the 6 hour time point indicated in Figure 4.1 was initiated at 5:00 AM (i.e. the mice were still active), while the 6 hour time points in all subsequent oral pimonidazole experiments were initiated at 7:00-9:00 AM. Therefore, caution is warranted when using oral pimonidazole to label hypoxic tumour cells over periods of 6 hours or less to ensure adequate mouse activity for sufficient *ad libitum* pimonidazole consumption.

In terms of the increase in pimonidazole-labeled WiDr tumour cells over time relative to SiHa tumour cells, Figure 4.5A indicates a sharper increase between 12 and 24 hours and a more gradual increase from 24 to 96 hours (solid line). Again, improved resolution of the shorter labeling intervals would be required before the labeling patterns could be accurately described as either "multi-phasic" or "asymptotic". The increase in pimonidazole-labeled WiDr tumour cells over time were primarily in the more poorly perfused sort fractions (Figure 4.5B), and the percentage of pimonidazole-labeled (hypoxic) cells was greater in WiDr tumours than in SiHa tumours for a given duration of pimonidazole consumption. The CCI-103F data presented in Figure 4.6 suggest that 12 hours of oral pimonidazole consumption provided a hypoxia profile that was comparable to that obtained from 3 hours of CCI-103F labeling. Moreover, the fractions of cells labeled only with oral pimonidazole were less than that obtained for SiHa

tumours, suggesting WiDr tumour cells have a lesser propensity to undergo long-term changes in their hypoxic status.

Figure 4.7A illustrates WiDr tumour cells labeled with a 30 minute "pulse" of IdUrd, indicating a larger range of proliferation between tumour cells with increasing distance from functional tumour blood vessels when compared to SiHa tumours over the same time period. Cells labeled with *both* oral pimonidazole (red) and IdUrd (green) are shown in Figure 4.7B, with a relatively higher fraction of formerly hypoxic cells synthesizing DNA compared to SiHa tumours, and a relative maximum of these cells at an intermediate distance from functional tumour vasculature.

4.3.6 Pimonidazole Pharmacokinetics

Plasma levels of pimonidazole after 6-96 hours of oral consumption are shown in Figure 4.8A. Plasma pimonidazole levels were variable between mice after 6 hours of pimonidazole consumption, again highlighting the influence of mouse activity on *ad libitum* water consumption over relatively short time intervals. As consumption of pimonidazole-containing water continued over many days, plasma concentration of the marker remained relatively constant, suggesting a continual elimination of drug from the bloodstream. This occurred independently of pimonidazole uptake and retention in hypoxic tumour cells since pharmacokinetic profiles of mice without tumours were indistinguishable from mice that had either SiHa or WiDr tumour implants. Moreover, neither the tumour types, tumour sizes, nor the mouse weights consistently influenced plasma pimonidazole concentrations.

Typical profiles for consumption of pimonidazole-containing water over time are shown in Figure 4.8B (open circles), along with single-mouse profiles for unusually high (open squares) and low (open triangles) levels of consumption. Interestingly, the relatively high pimonidazole consumption observed in the single mouse corresponded with a relatively large (> 1.5 g) increase in body weight over the 96 hour period, but did not produce noticeably increased plasma

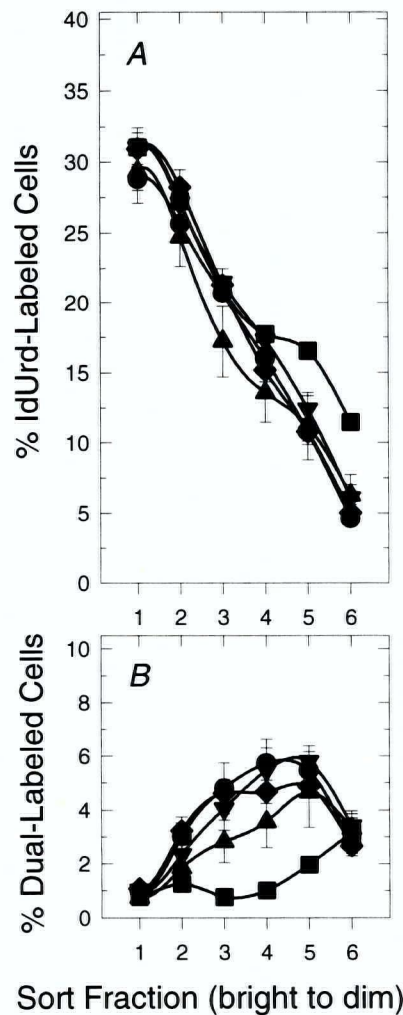


Figure 4.7 Sorted WiDr tumour cells labeled with IdUrd and/or oral pimonidazole (Pimo). (A) Percentage of tumour cells labeled with IdUrd 30 min after i.p. injection of the marker. (B) Percentage of tumour cells labeled with both oral Pimo and subsequent i.p. IdUrd. Mice were allowed to drink Pimo-containing water for 6 h (■), 12 h (▲), 24 h (▼), 48 h (◆), or 96 h (●) prior to tumour excision. Data are mean \pm s.e.m.; $n = 6-8$ tumours per curve.

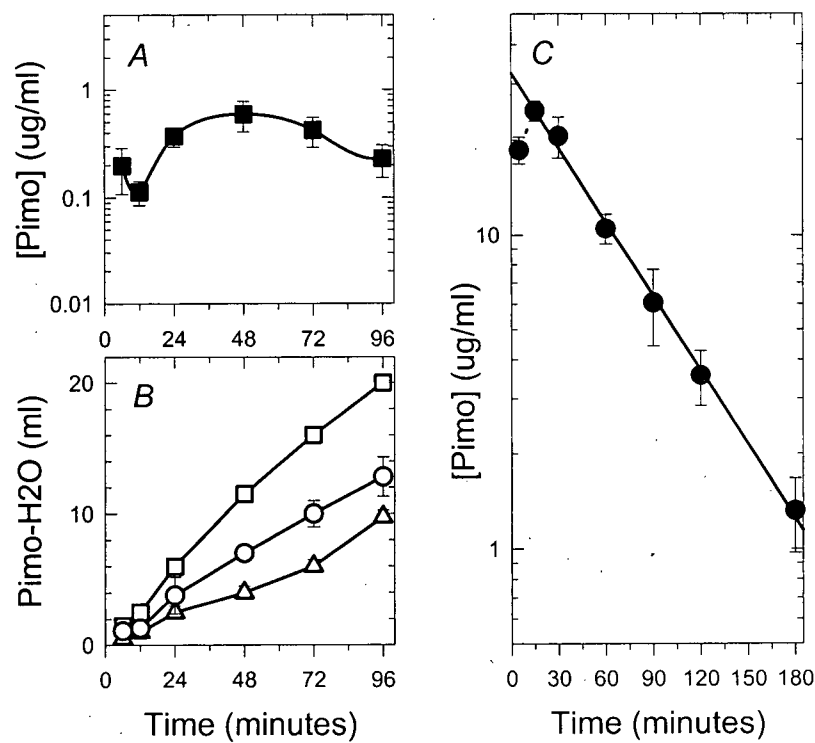


Figure 4.8 Pimonidazole pharmacokinetics.

(A) Concentration of pimonidazole in mouse plasma after *ad libitum* consumption of pimonidazole-containing water for 6-96 h. Data are mean \pm s.e.m.; $n = 9$ mice.

(B) Cumulative consumption of pimonidazole-containing water over 6-96 h (\circ). Data are mean \pm s.e.m.; $n = 7$ mice. Single mice with abnormally high (\square) or low (\triangle) consumption rates are shown separately.

(C) Concentration of pimonidazole in mouse plasma after a single i.p. injection of 100 mg/kg pimonidazole. The least-squares fit regression line (solid) was used for calculation of the plasma half-life of pimonidazole. Data are mean \pm s.e.m.; $n = 9$ mice.

pimonidazole levels. The mouse that consumed unusually low levels of pimonidazole-containing water lost > 1.5 g of body weight over the 96 hour period, and also had low plasma pimonidazole levels.

For comparison, pharmacokinetic data for a single i.p. injection of 100 mg/kg pimonidazole are presented in Figure 4.8C. The plasma elimination half-life was 37 ± 3 minutes, and was similar for mice with or without implanted tumours, and mice with different tumour types and tumour sizes.

4.4 DISCUSSION

Orally administered pimonidazole enables tumour hypoxia to be measured over longer periods of time than was possible with the multiple pimonidazole injections used in Chapter 3. However, there are important differences inherent to each route of pimonidazole administration in terms of the hypoxia measurement integration times and the sensitivity to changes in cellular hypoxic status. A single injection of pimonidazole will label hypoxic tumour cells over a few circulation half-lives of the drug, without distinguishing between cells that were hypoxic for all or part of this time. A particular cell will be labeled with pimonidazole provided it is hypoxic enough for long enough to bind detectable quantities of the marker while there is sufficient concentration of drug in the circulation. This principle also applies to orally administered pimonidazole, with the caveat that the concentration of pimonidazole obtainable in the circulation during *ad libitum* consumption is less than that observed after i.p. injection (Figure 4.8). Cells must therefore be hypoxic enough to bind pimonidazole for relatively long periods of time in order to accumulate detectable quantities of the marker, and the minimum labeling duration for oral pimonidazole is 6-12 hours (Figure 4.1 and 4.5). The longer integration time of oral pimonidazole is therefore less sensitive to changes in hypoxia that occur over periods of less than about 6 hours, but is amenable to studying longer-term changes in tumour hypoxia.

An interesting extension of these observations arises when considering cells that *are* labeled with pimonidazole during the minimum labeling duration (e.g. <6 hours in the SiHa experiments shown in Figure 4.1). Since cells only retain and accumulate pimonidazole when hypoxic, any cells with a hypoxic status that changed significantly during the minimum labeling duration would not bind detectable quantities of the marker. This implies that the tumour cells labeled with pimonidazole after 6 hours of low dose oral pimonidazole consumption exhibited minimal changes in their hypoxic status over this time period. Thus cells that are initially labeled with oral pimonidazole were the most hypoxic for the largest proportion of the minimum labeling

duration, although further work would be required to justify describing these cells as “chronically” hypoxic over the minimum labeling interval.

As the labeling interval was increased with continued pimonidazole consumption over a few days, cells displaying a dynamic hypoxic status were included in the measurement as indicated by the increased differential labeling when compared to CCI-103F (Figure 4.3C). These data suggest changes in tumour hypoxia that occurred over a period of days in SiHa tumours, while WiDr tumours typically contained cells with a hypoxic status that changed over shorter periods of time (Figure 4.6C). Interestingly, increasing fractions of hypoxic cells labeled with oral pimonidazole over time were found primarily in the more dimly staining Hoechst fractions for both tumour types. When taken with the results presented in Chapter 3, these data suggest that tumour cells with a hypoxic status that changes over a period of days are generally located further from functional tumour vasculature than cells with a hypoxic status that changes on the order of a few hours.

Importantly, tumour cells labeled with oral pimonidazole were subsequently able to synthesize DNA (Figure 4.4B and 4.7B) as measured with a 30 minute “pulse”-label of IdUrd. The presence of cells labeled with IdUrd and oral pimonidazole indicate the potential therapeutic relevance of formerly hypoxic tumour cells, but also should be interpreted as a conservative estimate of the fraction of pimonidazole-labeled cells that may potentially be capable of subsequent proliferation. The relatively short IdUrd exposure limited the number of tumour cells labeled, and the 24-26 hour cell cycle time of WiDr and SiHa tumours (Durand and Sham, 1998) suggests a much larger fraction of tumour cells would traverse S-phase over longer IdUrd labeling intervals. Estimates of the near-maximal proliferative potential of tumour cells that were hypoxic *in vivo* can be obtained using *in vitro* IdUrd labeling of tumour cells post-excision (Durand and Aquino-Parsons, 2001a). This method effectively increases the cellular oxygen and nutrient status of formerly hypoxic tumour cells while also ensuring sufficient delivery of IdUrd

(i.e. without *in vivo* perfusion or diffusion limitations). Modifying the IdUrd labeling method would therefore enable the determination of less conservative estimates of the proliferative capacity of tumour cells labeled with oral pimonidazole, further highlighting the therapeutic importance of these cells.

Clinical evidence is emerging to support the pre-clinical notion that solid tumours can contain temporally changing microregional blood flow (Hill *et al.*, 1996; Pigott *et al.*, 1996) and cellular oxygenation status (Durand and Aquino-Parsons, 2001a). However, current methodology to detect tumour hypoxia in the clinic does not typically consider tumour cells that may exhibit an intermittent hypoxic status over the course of a few days. Changes in tumour hypoxia over these timeframes may not be considered important when administering a single dose of therapy (e.g. radiation delivered over a few minutes), but may have a significant impact on tumour response to multi-fractionated radiotherapy (Wouters and Brown, 1997; Denekamp and Dasu, 1999) or chemotherapy (Durand, 2001). As discussed above, formerly hypoxic tumour cells are capable of subsequent proliferation (Durand and Raleigh, 1998), suggesting these cells may represent important contributors to tumour regrowth after (or during) treatment (Denekamp and Dasu, 1999; Durand and Aquino-Parsons, 2001a; Durand and Aquino-Parsons, 2004). This raises the (probably alarming) suggestion that methods of assessing tumour hypoxia over relatively short periods of time may underestimate the therapeutically relevant hypoxic fraction of a tumour. Thus the generation of "time-integrated" tumour hypoxia measurements (that include transiently hypoxic cells) through the use of oral pimonidazole may provide estimates of tumour hypoxia that are more physiologically and therapeutically relevant over a course of therapy.

Oral administration of pimonidazole offers the primary advantages of versatility and convenience in the determination of tumour hypoxia. Implicit in this statement is the potential to determine the hypoxic fraction of a tumour not only *prior* to clinical therapy, but also *during*

treatment in hopes of identifying those tumours that are responding poorly. Pimonidazole is more convenient to administer orally rather than by infusion, and quantification of hypoxia in clinical tumours can be minimally invasive with analysis of fine needle aspirate biopsies by flow cytometry (Olive *et al.*, 2000; Durand and Aquino-Parsons, 2001a). Of particular importance, oral delivery of pimonidazole in the clinic, when combined with administration of a second hypoxia marker such as EF5 (Lord *et al.*, 1993) or with a proliferation marker, may finally allow questions regarding the presence and potential therapeutic impact of transiently hypoxic cells in clinical tumours to be addressed. Data generated in this regard would aid in the development of therapeutic strategies designed to exploit the dynamic tumour microenvironment.

CHAPTER 5: MICROENVIRONMENT-INDUCED DIFFERENTIAL GENE EXPRESSION

This Chapter has been adapted from the following manuscript:

Bennewith, KL, Marra, MA, Khattrra, J and Durand, RE. CD151 may be an endogenous marker of transient tumor hypoxia. (*in preparation*)

5.1 INTRODUCTION

Quantifying transiently hypoxic tumour cells using exogenous hypoxia markers and flow cytometry as outlined in Chapters 3 and 4 may prove useful for studying tumour hypoxia in the clinic. However, since exogenous hypoxia markers must be administered (whether by injection, infusion, or orally), hypoxia measurements are limited to prospective clinical studies. The identification of a variety of intracellular proteins with expression levels that are influenced by cellular oxygenation levels has stimulated the use of these gene products as endogenous hypoxia “markers”. The primary advantage of endogenous hypoxia markers is their potential application to archival biopsy material for retrospective studies into the relationship between marker expression and therapeutic outcome.

As outlined in Section 1.5.3, endogenous hypoxia markers typically consist of gene products regulated by the hypoxia-inducible factor-1 (HIF-1) transcription factor, such as carbonic anhydrase 9 (CAIX; Beasley *et al.*, 2001; Ivanov *et al.*, 2001; Olive *et al.*, 2001a; Swinson *et al.*, 2003), although a subunit of the HIF-1 heterodimer (HIF-1 α) has also been used (Brown and Le, 2002; Begg, 2003). As with other measures of tumour hypoxia, the expression levels of endogenous hypoxia markers have typically been used to estimate tumour hypoxia at a single point in time, without consideration of potential temporal variations in tumour hypoxic status. CAIX is a relatively stable protein once expressed, and therefore provides a “history” of tumour hypoxia. Cells containing CAIX may be hypoxic at the time of tumour sampling (i.e. experimental tumour excision or clinical tumour biopsy), or may have been hypoxic at some point during the previous few days. Conversely, the post-translational regulation of HIF-1 α is rapidly responsive to changes in cellular oxygenation; HIF-1 α protein levels increase relatively quickly in the absence of oxygen, and the protein is also degraded rapidly in the presence of oxygen (Jiang *et al.*, 1996; Jewell *et al.*, 2001). Tumour cells containing increased levels of HIF-1 α therefore represent cells that were hypoxic within a few minutes of tumour sampling.

For specifically studying changes in tumour hypoxia over time, neither CAIX nor HIF-1 α are adequate alone since there is limited information on the expression of either marker under conditions of transient hypoxia *in vivo*. Comparing the differential expression of CAIX and HIF-1 α as an indication of transiently hypoxic cells is one possibility, although the uncertainties associated with the duration of hypoxia indicated by increased CAIX expression would make quantification difficult. Differential expression of HIF-1 α with binding of an exogenous hypoxia marker such as pimonidazole (where the initiation time for the hypoxia measurement is known) may be a more useful alternative, depending on the duration of transient hypoxia in question (see Chapter 6).

An alternative approach to studying transient tumour hypoxia involves the identification of gene products that may be preferentially up-regulated (or down-regulated) under specific microenvironmental conditions. Tumour cells that are exposed to fluctuating blood flow, and the concomitant changes in oxygen and nutrient availability, may adapt to the adverse environment through expression of specific hypoxia-inducible genes. Similarly, cells that are subjected to chronically low oxygen or nutrient status may express certain genes in order to (temporarily) survive the poor growth conditions. Thus by analyzing global gene expression profiles for tumour cells exposed to different growth conditions, candidate genes that are differentially expressed under conditions of transient (or diffusion-limited) hypoxia may be identified. Ideally, products of differentially expressed genes could be used to distinguish between cells exposed to different microenvironmental conditions *in vivo* and, by extension, to assess the clinical presence and therapeutic impact of transiently hypoxic tumour cells.

We chose to conduct these studies using tumour cells grown *in vitro* as multicellular spheroids (Sutherland, 1988), which are tumour cell aggregates that contain a natural gradient of oxygen and nutrients between the outer and the inner cell layers (see Figure 5.1). Thus under typical growth conditions, the cells on the outside of spheroids are well-nourished, well-

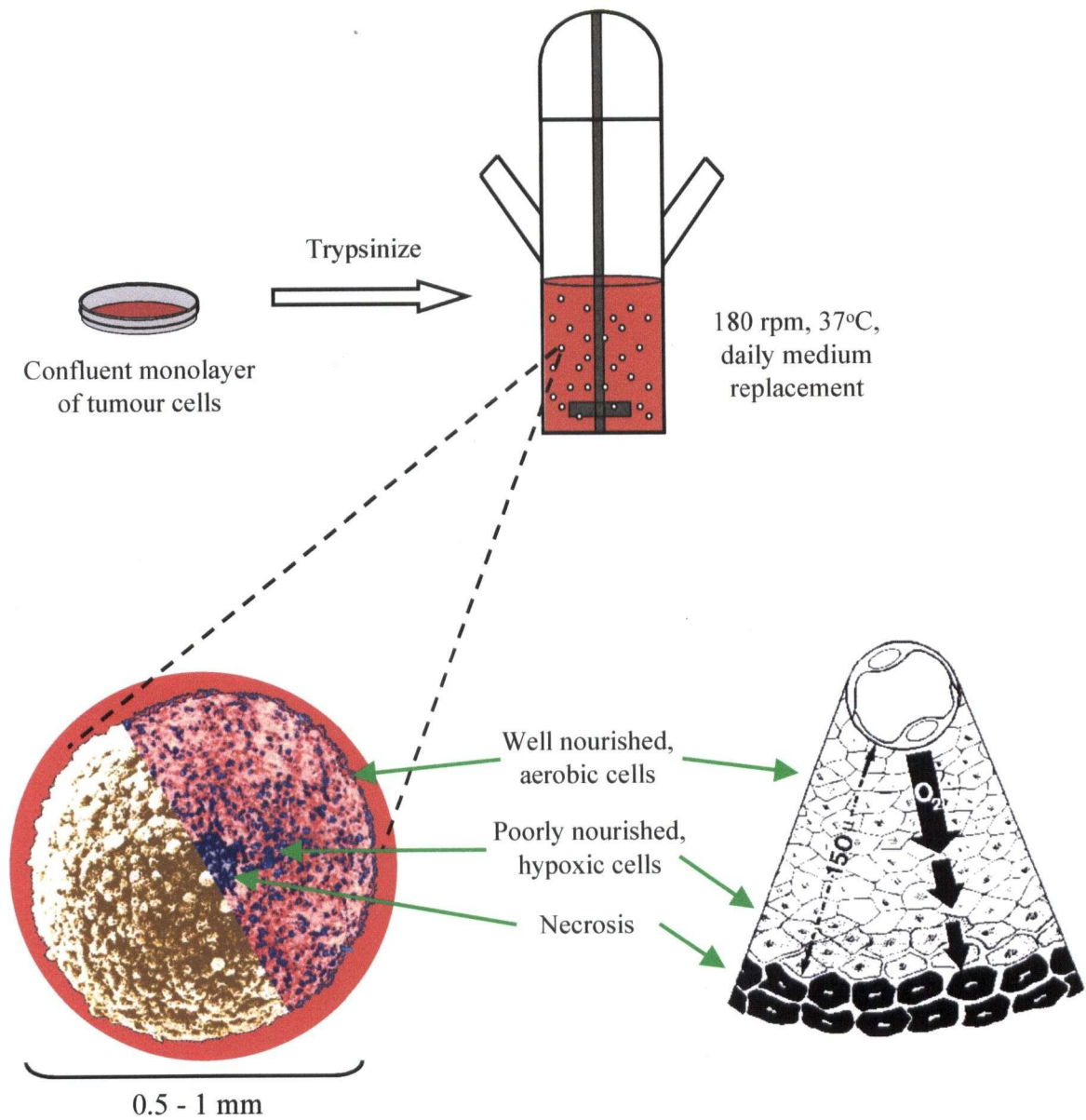


Figure 5.1 Multicellular spheroid model.

Exponentially growing tumour cells are inoculated into glass spinner culture flasks and maintained as indicated in the text. Also shown is a one-quarter cross-section of a spheroid illustrating the different growth conditions with increasing spheroid depth. Note the similarities to a diffusion-limited tumour microenvironment.

oxygenated, and have a high proliferative fraction (similar to cells located adjacent to functional tumour blood vessels). The inner spheroid cell layers contain cells that are more poorly nourished and oxygenated, have a lower fraction of proliferating cells, and larger spheroids even have necrotic centers suggesting a microenvironment with similarities to diffusion-limited hypoxia.

The multicellular spheroid system therefore enables more relevant modeling of the *in vivo* tumour microenvironment than is possible with cells grown in monolayer culture, and tumour cells from varying depths in the spheroids can be selectively recovered using fluorescence activated cell sorting based on Hoechst 33342 diffusion. While the ability to sort spheroid cells into subpopulations is a considerable advantage, disaggregating spheroids into a single cell suspension is a prerequisite step that may affect cellular gene expression profiles. Moreover, the pO_2 of individual spheroid cell layers with increasing depth is unknown, although it can be estimated (e.g. by labeling with exogenous hypoxia markers at different ambient oxygen tensions). The extent of the oxygen diffusion gradient between the outer and the inner cell layers also produces sorted cell populations that are not "pure" from an absolute oxygenation standpoint. This is particularly the case when sorting is based on spheroid volume, where the spheroid geometry dictates that increased numbers of contiguous cell layers are included in the inner sort fractions compared to the outer sort fractions to obtain the same number of cells. The use of tumour cells grown in monolayer culture would have avoided concerns over absolute oxygenation values and cell sorting methodology, however spheroids are the only system in which spontaneous, chronic hypoxia can be easily differentiated from acute oxygen deprivation, and were therefore considered the most useful and relevant model for these studies.

The spheroid system also has important advantages over human tumour xenografts, particularly since the experimental conditions (e.g. oxygenation, glucose, pH, etc.) can be varied easily and independently to more readily study their respective roles in tumour cell gene

expression. Furthermore, contamination of the tumour cell population with host (murine) normal tissue cells is not a concern with cells grown *in vitro*.

Serial analysis of gene expression (SAGE) was used to study the differential gene expression of tumour cells from different spheroid subpopulations under conditions of oxygen-deprivation. SAGE is a method to compare global gene expression patterns between populations of cells (Velculescu *et al.*, 1995), and does not require any previous knowledge of the genes under study (e.g. unlike probe-based methods such as gene expression arrays). SAGE has been used for comparing gene expression profiles between a variety of cell types including tumour cells versus normal cells (Zhang *et al.*, 1997), endothelial cells derived from normal versus tumour tissue (St Croix *et al.*, 2000), or cells at varying stages of tumour progression or metastasis (Parle-McDermott *et al.*, 2000; Porter *et al.*, 2001).

Thus, multicellular spheroids were used to simulate conditions of diffusion-limited and transient hypoxia in the inner and outer spheroid cell layers respectively, and SAGE was performed to identify differentially expressed genes between tumour cells grown in the different microenvironments. Candidate gene products were identified that may have potential to distinguish between diffusion-limited and transiently hypoxic tumour cells *in vivo*. If protein levels of selected genes are also differentially responsive to hypoxia in cells under disparate growth conditions, then probes against these gene products may represent a relatively untapped resource for studying tumour microenvironment dynamics.

5.2 MATERIALS AND METHODS

5.2.1 Multicellular Spheroids

Multicellular spheroids were grown from SiHa cells (Friedl *et al.*, 1970), the human cervical squamous cell carcinoma cell line used for human tumour xenograft studies in Chapters 2-4. SiHa cells were obtained as a cultured cell line (American Type Culture Collection, Rockville, MD) and were maintained by propagation as monolayers in 100 mm plastic Petri dishes with weekly subcultivation in M10 (minimal essential medium containing 10% fetal bovine serum).

To initiate spheroid growth, asynchronous cells were removed from a confluent Petri dish with 0.1% trypsin and added to a 250 ml glass spinner culture flask (Bellco, Vineland, NJ) containing 200 ml of M10. The spinner flask was pre-gassed with 5% CO₂ in air prior to inoculation, maintained at 37°C, and stirred at 180 rpm for the duration of spheroid formation and growth. Medium was initially changed 3 days after flask inoculation, and then daily thereafter.

Spheroids were 21-23 days old at the time of experimentation (corresponding to a mean size of ~500 µm). Approximately 100-200 spheroids were transferred into two separate 75 ml glass spinner flasks, each containing 50 ml of M10 pre-treated with a gas mixture of 5% CO₂ and either 1% or 10% O₂ respectively. Both 75 ml flasks were maintained at 37°C and treated with either the 1% O₂ or the 10% O₂ gas mixture for 3 hours. Single cell suspensions were prepared from the spheroids in each flask by harvesting the spheroids and agitating them for 8 minutes with 0.25% trypsin in Dulbecco's PBS. Monodispersed cells were suspended in ice cold M10, and the cell suspensions remained on ice for cell sorting (Durand, 1982; Durand, 1986).

5.2.2 Fluorescence Activated Cell Sorting

Fluorescence activated cell sorting was based on the distribution of 0.2 mg Hoechst 33342 (0.01 ml from a 20 mg/ml stock solution) added to the medium 20 minutes before spheroid harvest (Durand, 1982). Single cell suspensions derived from spheroids treated with either 1%

or 10% O₂ were sorted in a similar fashion as outlined in Section 2.2.5, except in this case each cell suspension was divided into only two fractions based on intracellular Hoechst concentration. The brightest Hoechst-stained cells were from the outer half of the spheroids while the dimmest Hoechst-stained cells were from the inner half of the spheroids (based on spheroid volume). Approximately 5 x 10⁶ cells were collected in each sort fraction, and the tumour cells were then treated with TRIzol Reagent (Invitrogen Corp., Carlsbad, CA) for RNA extraction.

RNA quality was assessed using an Agilent 2100 Bioanalyzer (Agilent Technologies, Palo Alto, CA) that compared the quality and quantity of mRNA for the 18S and 28S ribosomal protein subunits. Importantly, the presence of residual Hoechst 33342 in cell lysates did not appear to adversely affect the quality or integrity of the extracted RNA. The enzymatic dissociation of spheroids into a single cell suspension is a necessary prerequisite to sorting different spheroid cell subpopulations, and could conceivably have influenced cellular transcript levels. However, the enzyme contact time was minimized while still allowing for sufficient spheroid dissociation, and samples from either spheroid flask were treated identically to minimize *differential* effects on gene expression patterns.

5.2.3 Modeling Tumour Hypoxia with Spheroids

Three SAGE libraries were constructed, each one representing cell populations obtained from different experimental conditions (Figure 5.2). Cells from the outer half of spheroids treated with 10% O₂ for 3 hours had been exposed to “aerobic” conditions. Note that this level of oxygenation could more accurately be described as *hyperoxic* relative to the maximally oxygenated cells typically found in SiHa tumour xenografts (Olive *et al.*, 2002), but well oxygenated cells were desired for comparison with the hypoxia-treated cells. Cells from the outer half of spheroids treated with 1% O₂ for 3 hours were derived from conditions of “transient” hypoxia. That is, these cells were grown under well-nourished, well-oxygenated conditions and were exposed to a low level of oxygen for a relatively short period of time. Cells

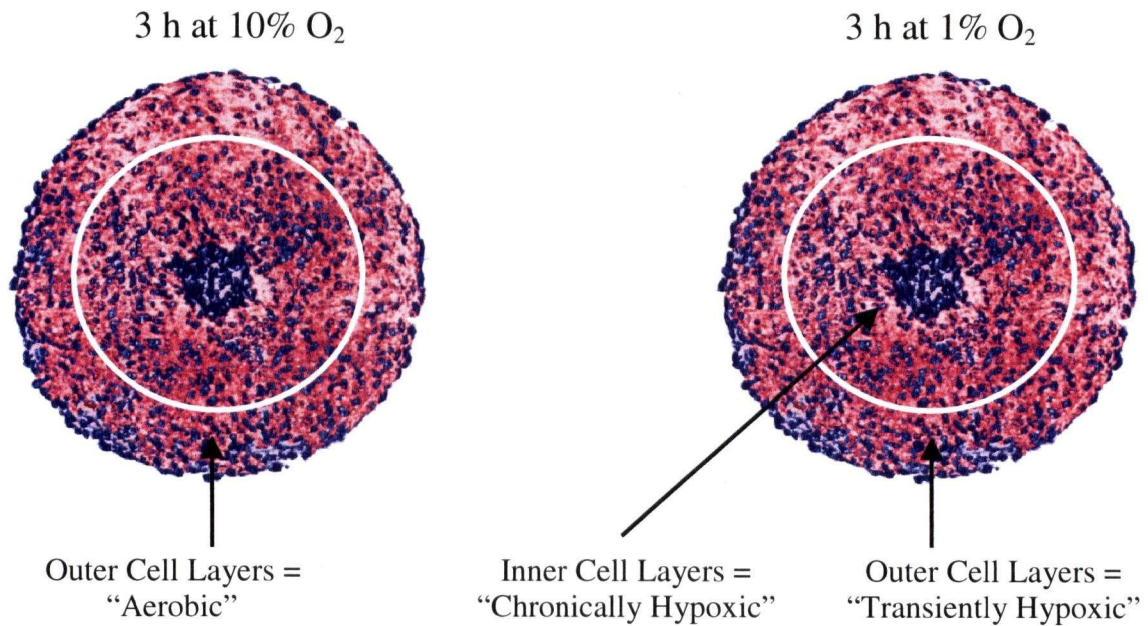


Figure 5.2 Illustration of different subpopulations of cells within multicellular spheroids. Flasks of spheroids were treated with either 10% O₂ or 1% O₂ for 3 hours. Two subpopulations of cells were isolated from spheroids in each flask (indicated by the regions on either side of the white circles); three of these cell subpopulations were retained and used for construction of serial analysis of gene expression (SAGE) libraries. The SAGE libraries therefore represented populations of tumour cells taken from different regions of a continuous oxygen and nutrient gradient between the outside and the inside of the spheroids.

from the inner half of spheroids treated with 1% O₂ for 3 hours were derived from conditions of “chronic” hypoxia. These cells were located at a distance from the supply of nutrients and oxygen (i.e. the media) for a significant period of time leading up to the date of the experiment (on the order of days), and therefore simulated a diffusion-limited tumour microenvironment.

5.2.4 Serial Analysis of Gene Expression

Serial analysis of gene expression (SAGE) libraries were constructed using the I-SAGE kit (Invitrogen Corp.) in collaboration with Dr. Marco A. Marra, Director of Canada’s Michael Smith Genome Sciences Centre. A diagram of the SAGE method is presented in Figure 5.3.

Briefly, mRNA from a cell population of interest is bound to magnetic beads (or some sort of solid phase medium) containing oligo deoxythymidine (dT) chains. Double stranded cDNA is generated and restriction digested with the “anchoring” enzyme (Nla III in this case); the cDNA of interest remains bound to the solid phase beads, and therefore represents sequence that is downstream of the 3’-most restriction enzyme site (CATG in this case). The cDNA pool is divided in half and ligated to one of two linkers, each containing a restriction site for the tagging enzyme and unique PCR primer binding sites. Each pool is restriction digested with the tagging enzyme (Bsm FI in this case) that cleaves the cDNA downstream of the enzyme binding site in a sequence independent fashion, creating “tags” with 10 base pairs (bp) of unique sequence. The cDNA pools are recombined and the tags are ligated together to form “ditags”, which are subsequently PCR amplified and the linkers removed by restriction digestion with the anchoring enzyme. The ditags are ligated together and the resultant concatemers (consisting of 20-50 tags each) are cloned into sequencing vectors, and transformed by electroporation into *E. coli* bacteria for subsequent colony formation. Resultant colonies are chosen at random and the concatemer-containing vectors undergo automated sequencing.

Since SAGE tags are derived from sequence that is downstream of the 3’-most CATG site in the original mRNA transcript, these sequences tend to be unique to specific genes. Thus the

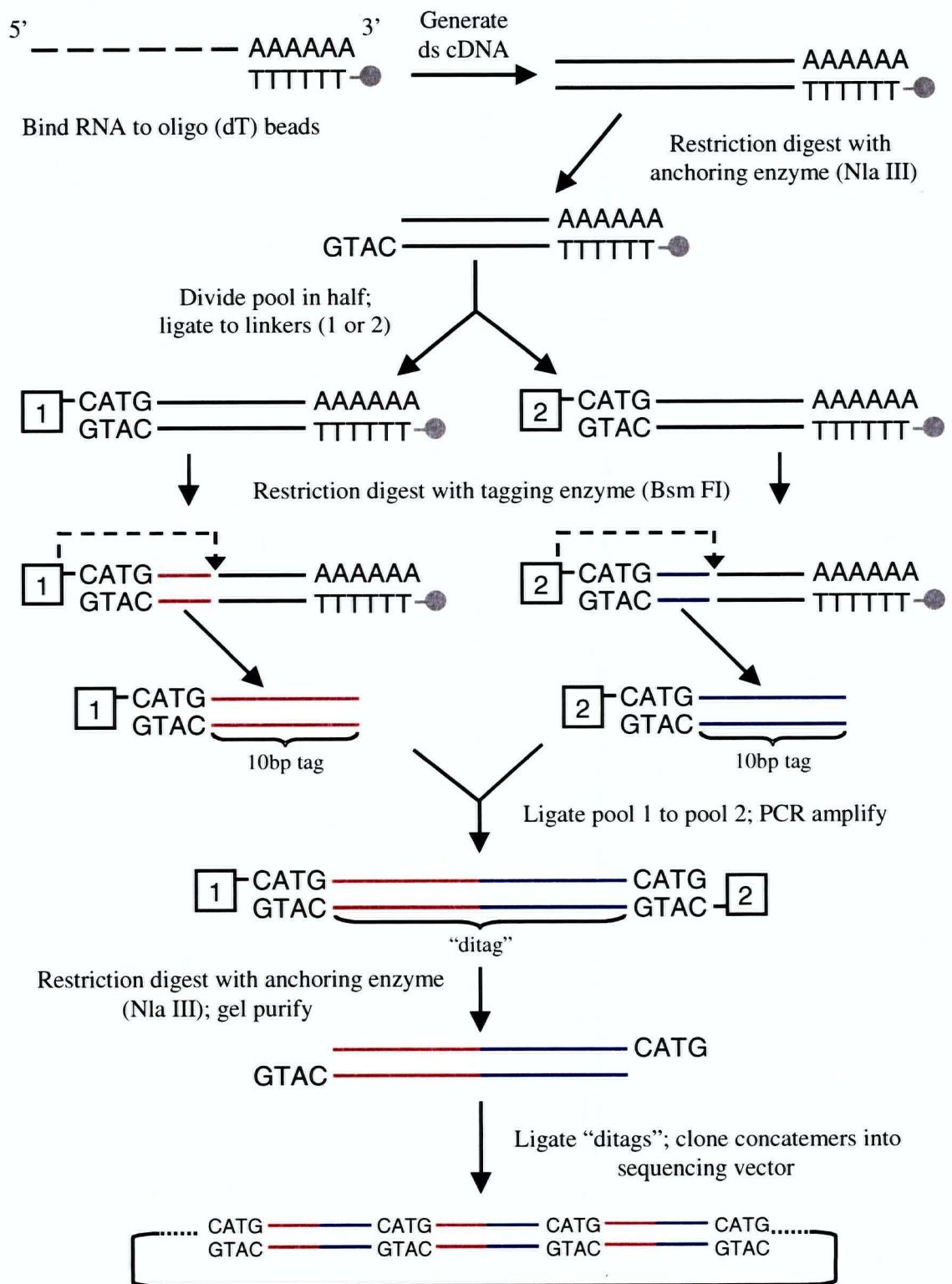


Figure 5.3 Diagram of serial analysis of gene expression (SAGE).

Dashed line indicates mRNA; solid lines indicate cDNA. Nla III digests DNA at CATG sequences and Bsm FI digests DNA at a fixed distance downstream of the enzyme recognition sequence, irrespective of the intervening sequence.

sequence of a given tag can be used to identify the original gene transcript expressed under the experimental conditions. Moreover, the relative number of a given SAGE tag with a particular sequence provides an indication of the relative expression level of the corresponding gene in the original population of cells.

The Nla III anchoring enzyme digests DNA at CATG sequences (typically occurring every ~256 bp), and therefore mRNA transcripts that do not contain a CATG sequence will not be included in the analysis. It is also worth noting that the Bsm FI tagging enzyme produces 10 bp of unique sequence in each SAGE tag, although other enzymes have been used to create longer tags containing 17 bp of unique sequence (Saha *et al.*, 2002). Longer tag sequences are more specific for a given gene, and this “LongSAGE” method therefore decreases the number of ambiguous tags (i.e. tag sequences that may correspond to more than one gene). However, this advantage is somewhat offset by the fewer number of (longer) ditags possible per concatemer in the sequencing vectors, and the resultant increase in the number of total sequencing reactions necessary to sequence a given number of tags. Overall, longer SAGE tags were not used for the studies reported herein since the methodology was not fully validated in-house at the time of SAGE library construction.

5.2.5 DISCOVERYspace

Approximately 100,000 tags were sequenced for each of the three SAGE libraries (i.e. for cells derived from each experimental condition), with 66,000-75,000 tag sequences of sufficient quality to warrant inclusion in the analysis, and 17,000-22,000 unique tag sequences (Table 5.1). Comparison of the different SAGE libraries was facilitated using “DISCOVERYspace”, a locally developed program that calculates statistics for comparing multiple SAGE libraries (Audic and Claverie, 1997) and enables automated mapping of SAGE tag sequences to their corresponding genes by querying publicly available databases.

Abundance Classes for Aerobic Cells

Level of Expression	1	2-4	5-9	10-99	100-999	1000+	Total
# of Unique Tag Sequences	10159	4198	1482	1180	75	1	17095
Cumulative # of Tags	10159	10966	9587	26287	16648	1110	74757

Abundance Classes for Chronically Hypoxic Cells

Level of Expression	1	2-4	5-9	10-99	100-999	1000+	Total
# of Unique Tag Sequences	13952	5069	1554	966	44	2	21587
Cumulative # of Tags	13952	13132	9960	21686	9164	2782	70676

Abundance Classes for Transiently Hypoxic Cells

Level of Expression	1	2-4	5-9	10-99	100-999	1000+	Total
# of Unique Tag Sequences	12062	4727	1467	963	51	1	19271
Cumulative # of Tags	12062	12220	9406	21556	9959	1157	66360

Table 5.1 Summary of abundance classes for SAGE libraries.

The number of unique tag sequences (first row) for given levels of expression (columns) are indicated; the cumulative number of tags represent the number of unique tag sequences multiplied by the respective level of expression of each unique tag sequence. The rightmost column indicates the total number of unique tag sequences and the total number of (high quality) tags sequenced for each library.

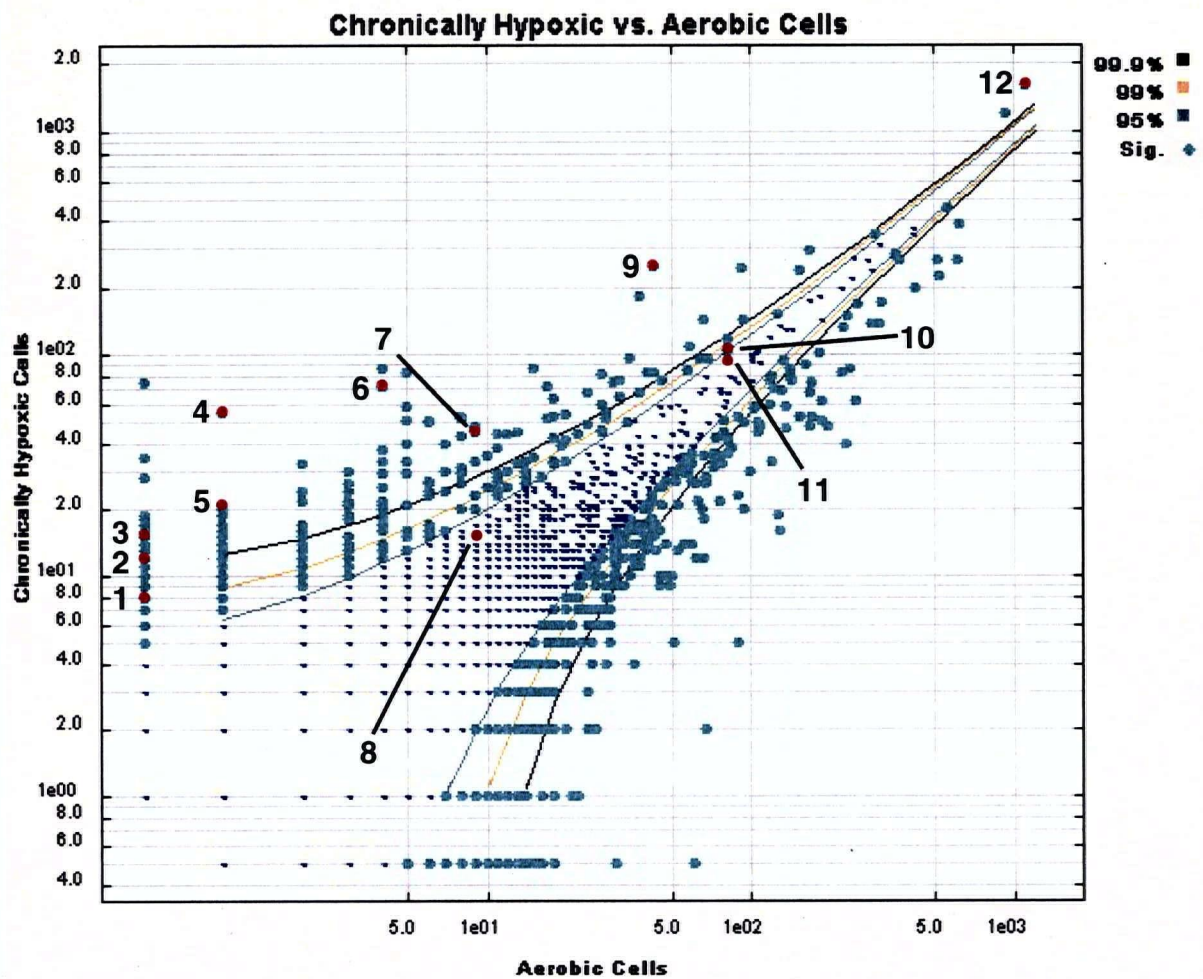
5.3 RESULTS

5.3.1 Summary of SAGE Data

Tags differentially expressed between “chronically hypoxic” and “aerobic” conditions are indicated in Figure 5.4, while Figure 5.5 illustrates tags differentially expressed between “transiently hypoxic” and “aerobic” conditions. Summary statistics for each comparison are included with the respective Figure. Of the tags that were significantly ($> 99.9\%$ CI) differentially expressed between either hypoxic condition and the aerobic cells: 56-71% mapped unambiguously to genes, 8-13% mapped ambiguously to multiple genes, and 21-35% did not map to any known sequence in the public (*Homo sapiens*) sequence databases queried (Mammalian Gene Collection and RefSeq). Selected tags that corresponded to genes of interest are labeled numerically in Figures 5.4 and 5.5, with the gene identifications provided in Table 5.2. Of particular note were tags representing genes previously known to be regulated by HIF-1, including VEGF (gene #2), CAIX and CAXII (genes #1, 10; see Section 1.4.3), Glut-1 (gene #8), and a variety of glycolytic enzymes (genes #3-6, 11-12; see Section 1.4.2 and Figure 1.3). Importantly, these data indicate the experimental conditions were sufficient to induce HIF-1 α -regulated transcription, and suggest that the spheroid trypsinization and cell sorting procedures did not (severely) decrease the relative expression levels of these genes. Protein levels of a few of these genes have previously been used as endogenous markers of hypoxia *in vitro* and *in vivo* (genes #1, 8; see Section 1.5.3.2).

5.3.2 SAGE Tags Differentially Expressed Between Chronic and Transient Hypoxia

SAGE libraries for the chronically hypoxic and transiently hypoxic cells are compared in Figure 5.6. While a few genes may have potential as general indicators of tumour hypoxia (genes #7, 9; see Section 5.4.1), the majority of HIF-1 regulated genes identified in Figures 5.4 and 5.5 did not demonstrate significant differential expression *between* chronically and transiently hypoxic conditions in the model spheroid system.

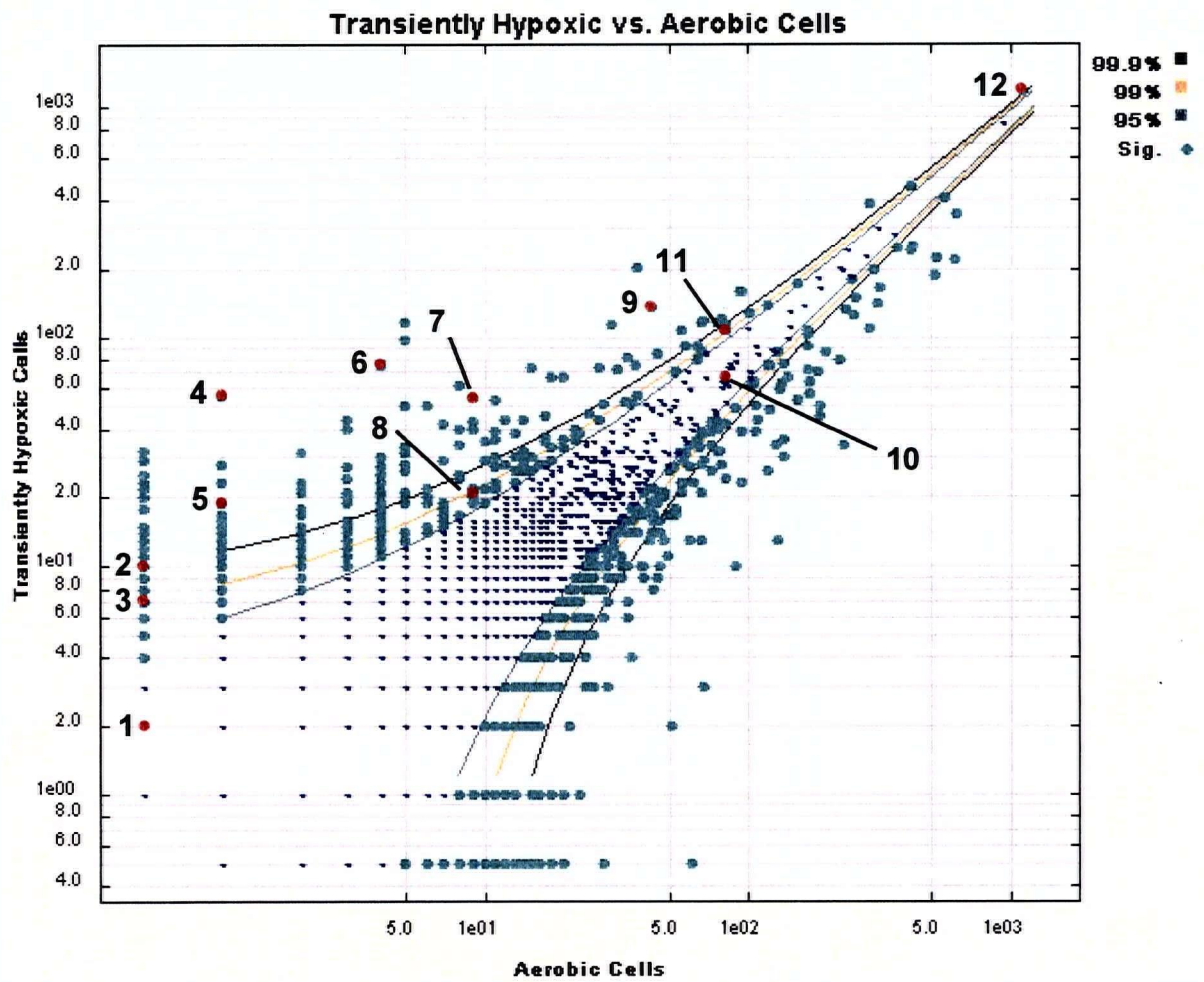


Tags Beyond Confidence Intervals for Comparison	99.9%		99%		95%	
	#	%	#	%	#	%
Chronically Hypoxic > Aerobic	138	0.45	275	0.90	572	1.88
Chronically Hypoxic < Aerobic	143	0.47	286	0.94	611	2.00

Total # of Unique Tag Sequences Compared = 30,492

Figure 5.4 SAGE tags differentially expressed between chronically hypoxic and aerobic cells.

Each data point indicates the relative expression level of one or more unique tag sequences under the specified experimental conditions (on a logarithmic scale). The contour lines delineate calculated confidence intervals, and (light blue) data points outside each set of lines indicate relative expression differences that are statistically significant to the respective confidence interval. The linear collection of data points closest to the abscissa and ordinate represent tags that were not detected in the other library. Selected genes of interest are indicated in red; see Table 5.2 for number designations.



Tags Beyond Confidence Intervals for Comparison	99.9%		99%		95%	
	#	%	#	%	#	%
Transiently Hypoxic > Aerobic	152	0.53	294	1.03	802	2.82
Transiently Hypoxic < Aerobic	111	0.39	236	0.83	561	1.97

Total # of Unique Tag Sequences Compared = 28,414

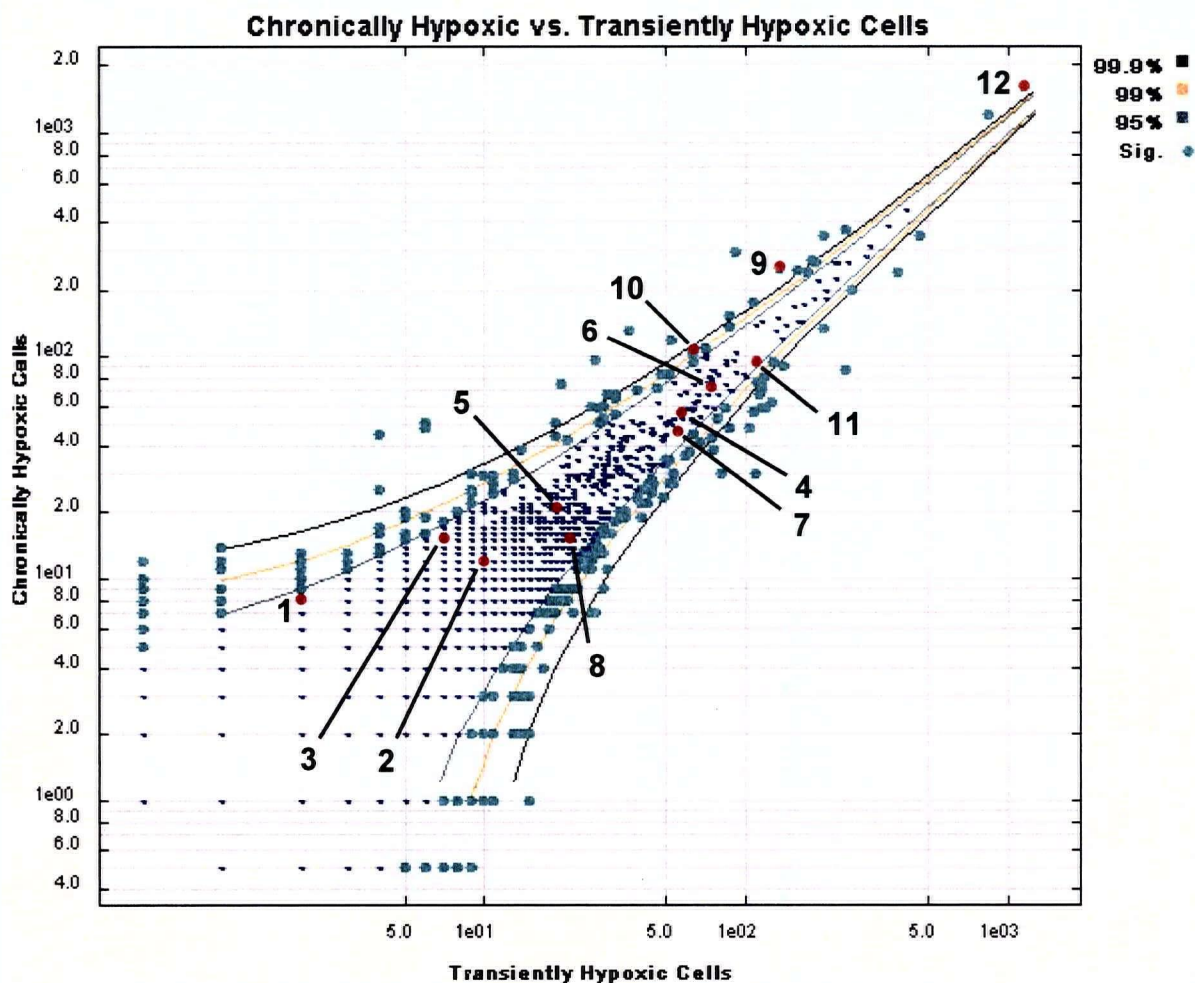
Figure 5.5 SAGE tags differentially expressed between transiently hypoxic and aerobic cells. Selected genes of interest are indicated in red; numbers correspond to the same genes as indicated in Figure 5.4.

Gene #	Absolute # of Tags in Each Condition			Relative Increase in # of Tags Between Each Condition				Gene Identification
	Chr	Tr	Air	Chr > Air	Tr > Air	Chr > Tr	Tr > Chr	
1	8	2	0	(8)	(2)	3.8	-	Carbonic Anhydrase 9 (CAIX)
2	12	10	0	(12)	(10)	1.1	-	Vascular Endothelial Growth Factor (VEGF)
3	15	7	0	(15)	(7)	2.0	-	Phosphofructokinase L
4	55	56	1	58	63	-	1.1	Pyruvate Kinase M
5	21	19	1	22	21	1.0	-	6-Phosphofructo-2-Kinase
6	72	75	4	19	21	-	1.1	Aldolase A / Fructose Biphosphate
7	46	55	9	5.4	6.9	-	1.3	Metallothionein IIA
8	15	21	9	1.8	2.6	-	1.5	Glucose Transporter-1 (Glut-1)
9	254	135	43	6.2	3.5	1.8	-	"Hypothetical Protein" RTP801
10	110	67	82	1.4	-	1.5	-	Carbonic Anhydrase 12 (CAXII)
11	94	103	80	1.2	1.5	-	1.2	Lactate Dehydrogenase A
12	1592	1157	1110	1.5	1.2	1.3	-	Glyceraldehyde-3-Phosphate Dehydrogenase

Table 5.2 Identification of selected tags from Figures 5.4-5.6.

Tag numbers are presented as fold-increases in expression between the cited conditions, and have been normalized for the total number of (high quality) tags sequenced for each library. Numbers in parentheses indicate comparison to a library that did not contain a tag of that sequence (and are not normalized).

'Chr' = chronically hypoxic, 'Tr' = transiently hypoxic, 'Air' = aerobic.



Tags Beyond Confidence Intervals for Comparison	99.9%		99%		95%	
	#	%	#	%	#	%
Chronically > Transiently Hypoxic	24	0.08	52	0.16	190	0.60
Chronically < Transiently Hypoxic	24	0.08	71	0.22	234	0.74

Total # of Unique Tag Sequences Compared = 31,624

Figure 5.6 SAGE tags differentially expressed between chronically hypoxic and transiently hypoxic cells.

Selected genes of interest are indicated in red; numbers correspond to the same genes as indicated in Figures 5.4 and 5.5. Note the majority of these genes are found within the contour lines (i.e. no significant differential expression).

Interestingly, the data in Figure 5.6 also indicate the presence of tag sequences that *were* differentially expressed between cells in the chronically and transiently hypoxic conditions. Figure 5.7 presents the same data from Figure 5.6 including indications of tag ambiguity, unknown tag sequences, and tags that corresponded to a few notable genes (genes #13-16) with the gene identifications provided in Table 5.3. Importantly, if differential expression of the identified transcripts translate to similar differences at the protein level, the gene products may represent potential targets for antibodies to distinguish between diffusion-limited and transiently hypoxic tumour cells. These genes will be discussed further in Sections 5.4.2-5.4.3.

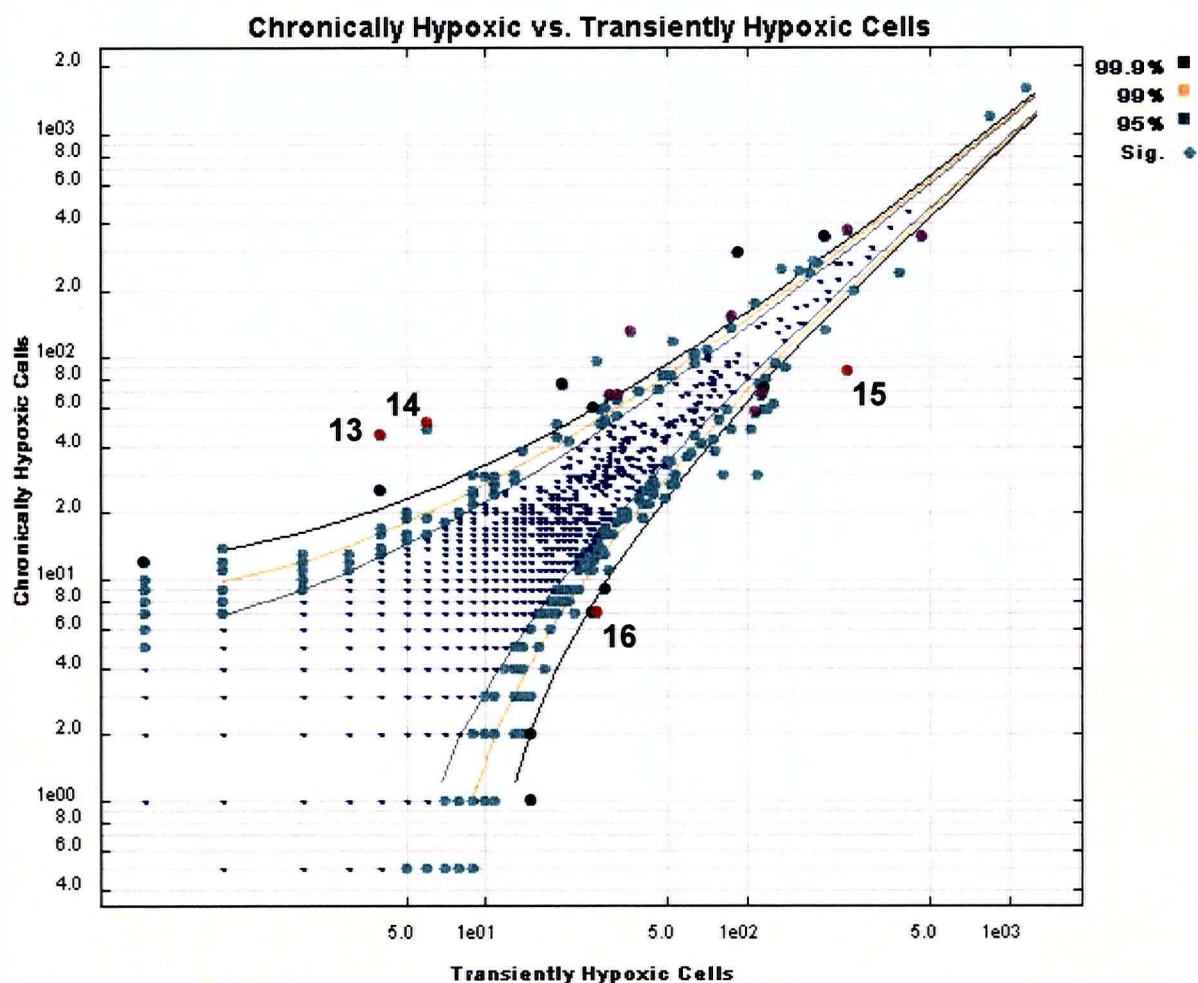


Figure 5.7 Selected genes of interest significantly differentially expressed between chronically and transiently hypoxic cells (> 99.9% CI).

Black data points represent ambiguous tags, pink data points indicate unknown tag sequences, and genes of interest specific to this comparison are indicated in red. Number designations are identified in Table 5.3.

Gene #	Absolute # of Tags in Each Condition			Relative Increase in # of Tags Between Each Condition				Gene Identification
	Chr	Tr	Air	Chr > Air	Tr > Air	Chr > Tr	Tr > Chr	
13	45	4	9	5.3	-	11	-	Stearoyl-CoA (Delta-9) Desaturase
14	51	6	6	9.0	-	8.0	-	Diphosphomevalonate Decarboxylase
15	87	242	240	-	1.1	-	3.0	S100 Calcium Binding Protein P
16	7	27	17	-	1.8	-	4.1	CD151 Antigen

Table 5.3 Identification of selected tags from Figure 5.7.

Tag numbers are presented as fold-increases in expression between the cited conditions, and have been normalized for the total number of (high quality) tags sequenced for each library.

'Chr' = chronically hypoxic, 'Tr' = transiently hypoxic, 'Air' = aerobic.

5.4 DISCUSSION

It is important to reiterate that SAGE provides information on relative gene expression at the mRNA transcript level, and there are a variety of potential applications for these data. If one is interested in gene expression specifically, the relative expression levels for selected genes indicated by SAGE are typically confirmed with subsequent (cost-effective) alternatives, such as quantitative real-time RT-PCR with subsequent Northern blot analysis. Further molecular studies into the mechanisms of gene regulation and the identification and characterization of novel genes could then be pursued as desired.

However, the studies reported herein did not involve gene expression *per se*, and SAGE was merely used as a means to identify potential candidate genes that may be capable of distinguishing between cells growing in different microenvironmental conditions. Thus the preliminary experiments performed following SAGE data analysis were directed toward probing tumour cell populations for detectable differences in candidate gene products, without attempting to further validate or quantify the transcript expression differences observed by SAGE. Moreover, in order to utilize existing in-house methodology and expertise, detection of gene products in tumour cell populations was implemented at the protein level (in favor of a transcript-based probing method such as *in situ* hybridization). While there is an obvious and significant leap from the serial analysis of relative transcript expression levels to the detection of the resultant protein(s), the latter endpoint was deemed more relevant to the (initial) project goal of identifying potential endogenous markers of transient hypoxia. Extensions of these studies will be discussed in Chapter 6.

A relatively efficient and cost-effective means of probing tumour cell populations for the expression of (a small number of) candidate gene products at the protein level is to preferentially select genes for further study that have commercial antibodies readily available. Fluorescent secondary antibodies could then be used for image analysis of tissue sections or for flow

cytometry analysis of single cell suspensions, thereby providing qualitative and quantitative information on hypoxia-induced alterations in protein levels under various *in vitro* and *in vivo* conditions. Preliminary data for one of the more promising gene products (CD151; gene #16) will be presented in Section 5.4.3, where differential gene expression at the mRNA level was observed between chronically hypoxic and transiently hypoxic conditions, and levels of the associated protein provided some intriguing labeling patterns *in vivo*. However, before these data are presented, other potential markers of tumour hypoxia will be discussed.

5.4.1 Metallothionein IIA and RTP801

Expression of metallothionein IIA mRNA (gene #7) was increased 5- to 7-fold under either hypoxic condition relative to aerobic spheroid cells. Metallothioneins are a heavily thiolated endogenous family of polypeptides that have been shown to increase the resistance of mammalian cells to radiotherapy and chemotherapy (Bakka *et al.*, 1982; Satoh *et al.*, 1994; Shibuya *et al.*, 1997), and metallothionein IIA is the predominant form of the protein (Skroch *et al.*, 1993). Up-regulation of metallothionein IIA mRNA has been observed after hypoxia and reoxygenation *in vitro* (Murphy *et al.*, 1994), qualitatively confirming the hypoxia-induction observed in Figures 5.4 and 5.5. However, the potential use of metallothionein IIA as a marker of hypoxia *in vivo* requires further study since metallothionein protein expression increases rapidly in murine tumours with hypoxia induction by hydralazine (Raleigh *et al.*, 1998), but does not localize well with pimonidazole labeling in clinical biopsies (Raleigh *et al.*, 2000).

SAGE tags corresponding to the “hypothetical protein” RTP801 (gene #9) were significantly differentially expressed between all three experimental conditions. RTP801 is ubiquitously expressed at low levels in a variety of human tissues, and is up-regulated rapidly in response to hypoxia *in vitro* and *in vivo* (Shoshani *et al.*, 2002), again confirming the observations in Figures 5.4 and 5.5. RTP801 is thought to play a role in enhancing oxidative stress-induced cell death (Kim *et al.*, 2003; Lee *et al.*, 2004), although the intracellular signaling mechanism is largely

unknown. Conversely, in some cell types the presence of RTP801 prior to hypoxia *in vitro* is thought to suppress the generation of reactive oxygen species and protect cells from oxidative stress-induced cell death (Shoshani *et al.*, 2002).

RTP801 may represent a useful marker of tumour hypoxia in some tumour types, and the statistically significant differential expression and high relative tag abundances between hypoxic and aerobic cells (Table 5.2) are favorable characteristics if translatable to the protein level. However, in terms of differentiating between diffusion-limited and transiently hypoxic cells, the difference in absolute tag abundances is less than 2-fold and (if also applicable to protein expression) may not provide a large enough labeling differential to discriminate between hypoxic cells in different microenvironmental conditions.

5.4.2 Indications of Microenvironmentally-Influenced Differential Gene Expression

Stearoyl-CoA desaturase (gene #13) is the rate-limiting enzyme in the synthesis of monounsaturated fatty acids used for membrane phospholipids, triglycerides, and cholesterol esters (Ntambi and Miyazaki, 2004). Increased levels of stearoyl-CoA desaturase mRNA have been found in colonic and esophageal carcinomas, and in hepatocellular adenocarcinomas relative to their normal tissues of origin (Li *et al.*, 1994), although the influence of the tumour microenvironment on gene expression is unknown.

Diphosphomevalonate decarboxylase (gene #14) is an enzyme involved in the synthesis of prenyl-derived lipids and the post-translational prenylation of proteins, including the oncoprotein Ras. Blocking enzyme activity has been shown to inhibit the membrane association of mutant Ras, thereby decreasing mutant Ras-activated cell proliferation *in vitro* (Cuthbert and Lipsky, 1995; Cuthbert and Lipsky, 1997). Thus the enzyme may potentially contribute to tumour progression in some cases by assisting in the activation of oncogenic proteins, although gene expression levels of diphosphomevalonate decarboxylase have not previously been reported in tumours.

S100 calcium binding protein P (S100P; gene # 15) is thought to be involved in mediating intracellular calcium signaling, although the precise signaling pathways are currently unknown. Elevated levels of S100P have been observed following loss of senescence in breast cancer cell lines *in vitro*, implying that overexpression may be an early event in immortalization of human breast epithelial cells (Guerreiro Da Silva *et al.*, 2000). S100P is highly differentially expressed at the mRNA and protein level in a variety of tumours compared to normal tissues including breast (Russo *et al.*, 2001), pancreas (Iacobuzio-Donahue *et al.*, 2002; Crnogorac-Jurcevic *et al.*, 2003; Logsdon *et al.*, 2003), and prostate (Mousses *et al.*, 2002). Expression of S100P protein has also been found to increase with clinical tumour progression in cancers of the breast (Russo *et al.*, 2001) and prostate (Mousses *et al.*, 2002). While these studies suggest a relationship between S100P expression and tumour aggressiveness, there is little information on the influence of the tumour microenvironment on S100P gene expression.

As indicated in Table 5.3, both stearoyl-CoA desaturase and diphosphomevalonate decarboxylase (genes #13 and #14) demonstrated significantly higher levels of expression in cells under poor growth conditions (inner spheroid cell layers; “chronically hypoxic”) relative to better-nourished cells (outer spheroid cell layers; “aerobic” and “transiently hypoxic”). Note that the differential expression occurred irrespective of the 3 hour hypoxia treatment. Similarly, S100 calcium binding protein P (gene #15) was significantly more highly expressed in the outer spheroid cell layers (“aerobic” and “transiently hypoxic”) relative to the inner spheroid cell layers (“chronically hypoxic”) irrespective of the hypoxia treatment. One possible explanation may be that the inner spheroid cell layers experienced a greater degree of hypoxia than the outer layers during treatment (i.e. < 1% O₂ with oxygen diffusion limitations). However, the lack of differential expression between conditions of chronic and transient hypoxia (i.e. inner and outer cell layers) for a variety of known hypoxia-regulated genes argues against this oxygenation difference as a primary determinant of gene expression in this system.

Furthermore, hypoxia-regulated expression of genes #13-15 have not previously been reported, suggesting the different cellular microenvironments (independent of hypoxia) may be involved in the observed differences in relative gene expression. The expression levels of these genes may also be related to the degree of tumour cell proliferation in the different spheroid regions, representing an indirect relationship with cellular oxygenation and/or nutrient status. Thus, while hypoxia is the most commonly studied microenvironmental factor influencing tumour cell gene expression, other characteristics of the tumour microenvironment may also produce specific and exploitable differential gene expression patterns.

Overall, more work is necessary with genes #13-15 to further characterize mRNA and protein expression patterns; with particular attention to regulation by the tumour microenvironment, relationship to cellular proliferative status, and assessment of gene product levels as potential indicators of specific microenvironmental conditions.

5.4.3 CD151

One of the more interesting differentially expressed tags mapped to the gene for CD151 (gene #16), a member of the tetraspanin family of transmembrane proteins. CD151 (or platelet-endothelial tetraspan antigen-3; PETA-3) is expressed in a variety of cell types (Sincock *et al.*, 1997; Funakoshi *et al.*, 2003), and is able to form complexes with a number of different integrins involved in cell motility (Yauch *et al.*, 1998; Berditchevski and Odintsova, 1999; Sincock *et al.*, 1999). In tumour cells, CD151 protein concentrates along tumour cell-endothelial cell borders during *in vitro* transendothelial invasion (Longo *et al.*, 2001), and over-expression of CD151 has been found to enhance tumour cell motility, invasion, and metastasis (Testa *et al.*, 1999; Kohno *et al.*, 2002). In the clinic, tumours containing high levels of CD151 protein correlate with decreased survival in non-small cell lung cancer (Tokuhara *et al.*, 2001) and colon cancer (Hashida *et al.*, 2003), which has been attributed to increased formation of metastases. The

influence of the tumour microenvironment on CD151 expression has not previously been reported.

As indicated in Table 5.3, CD151 mRNA levels were found to be 4-fold higher in transiently hypoxic cells compared to chronically hypoxic cells from the same population of spheroids. The availability of a commercial antibody to CD151 protein facilitated the detection of CD151 in frozen tissue sections of SiHa spheroids and SiHa tumour xenografts (Figure 5.8). Based on the work reported in Chapter 3, transiently hypoxic tumour cells are typically located at an intermediate distance from functional tumour vasculature in SiHa tumours, and the presence of CD151 expressing cells in this region is intriguing. These preliminary observations warrant more detailed studies into the influence of hypoxia and the tumour microenvironment on the expression of CD151 mRNA and protein. Of particular interest is the degree and duration of hypoxia required to induce changes in CD151 expression, the kinetics of CD151 up-regulation (and down-regulation), and the potential influence of other microenvironmental factors on CD151 expression levels.

As evidenced by the (relatively brief) descriptions of selected genes in Sections 5.4.1-5.4.3, a great many questions have been generated by the SAGE data regarding the role of the tumour microenvironment in influencing the expression of a variety of genes. While elucidating the specific mechanism(s) of gene regulation was not a direct goal of the work presented in this Chapter, identification of a number of genes that were differentially expressed between the experimental conditions indicates a rather large area for further study. Of particular relevance to this thesis was the identification of a number of genes that were significantly differentially expressed between cells grown under different microenvironmental conditions *in vitro* and exposed to a relatively short-term hypoxic episode. Differential expression of the products of these genes may enable the use of probes for selectively identifying cells exposed to different microenvironments *in vivo*.

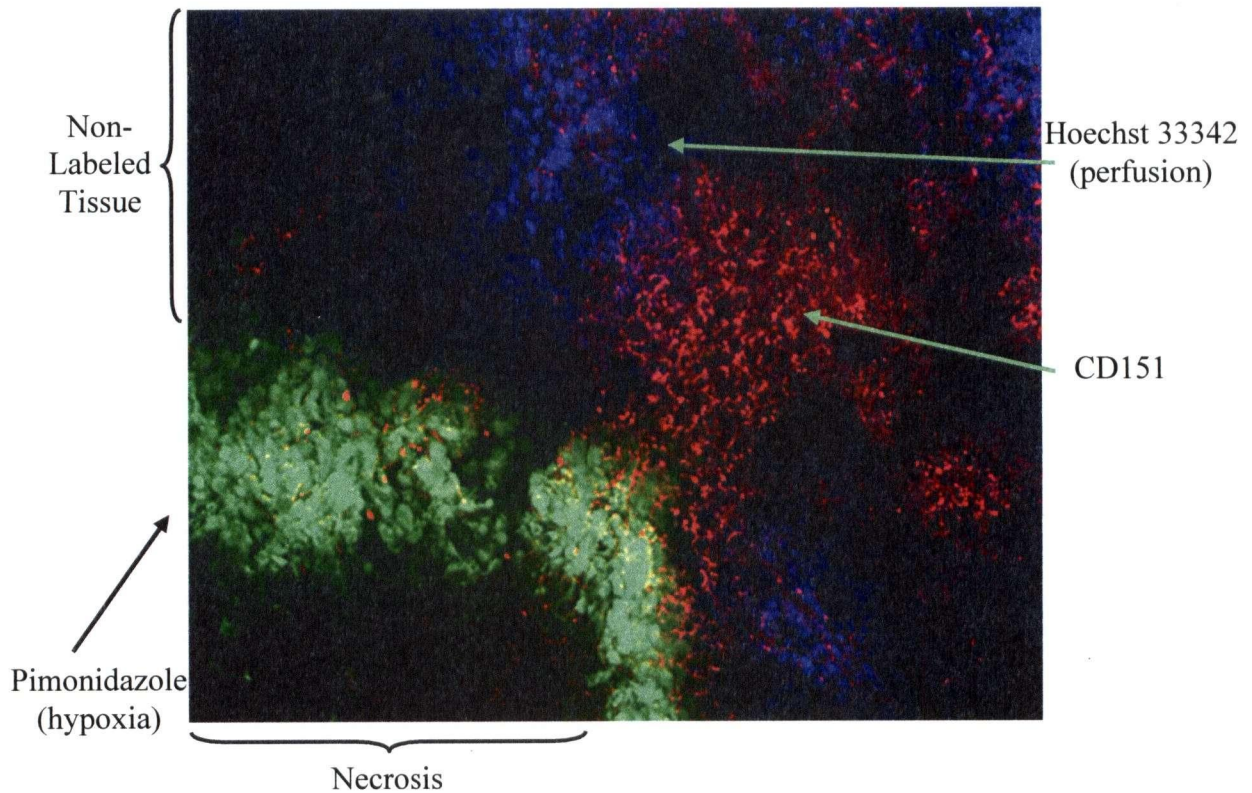


Figure 5.8 Section of SiHa human tumour xenograft showing proximity of CD151 to perfused blood vessels and diffusion-limited hypoxia.

Pimonidazole (100 mg/kg) was administered 1 hour prior to tumour excision and Hoechst 33342 was administered 20 minutes prior to tumour excision. Previous work in Chapter 3 indicated that transiently hypoxic SiHa tumour cells are typically located closer to tumour blood vessels than cells labeled with a single injection of pimonidazole. Blue = Hoechst 33342 (perfusion), green = pimonidazole (diffusion-limited hypoxia), red = CD151.

Ultimately, the detection of genes differentially expressed in specific subpopulations of tumour cells would facilitate further studies into both the physiological mechanisms associated with tumour hypoxia, and the therapeutic relevance of various features of the tumour microenvironment. A rapid and relatively non-invasive method to identify and quantify tumour cells that are potentially more relevant for therapeutic outcome would also aid in the assignment of treatment strategies to take advantage of the dynamic solid tumour microenvironment. Thus by exploiting the specific gene expression profiles of transiently (or chronically) hypoxic tumour cells, it may be possible to address some fundamental questions about tumour physiology and to improve clinical cancer therapy strategies targeting tumour hypoxia.

CHAPTER 6: SUMMARY AND FUTURE DIRECTIONS

6.1 SUMMARY

The tumour microenvironment is increasingly being appreciated as a dynamic entity with potentially far-reaching therapeutic implications, although surprisingly little is known about tumour physiology in the clinic. This lack of knowledge stems, in part, from inadequate methodology to detect and study various tumour microenvironmental parameters in the necessarily restrictive realm of clinical cancer research. Since tissue oxygenation is considered the most easily measurable characteristic of the tumour microenvironment, and since poorly oxygenated tumours typically correlate with poor clinical outcome, a variety of methods have been developed for measuring tumour oxygenation. Each method has its own unique advantages and disadvantages in terms of invasiveness, resolution, detection sensitivity, and functional relevance of the oxygenation levels measured. However, none of the currently used methods for measuring tumour oxygenation consider potential changes in oxygenation status that may occur over time. A number of pre-clinical studies suggest that temporal fluctuations in tumour blood flow and regional oxygenation can be common and inter-related phenomena in experimental tumour systems, but their presence and influence in clinical tumours is largely unknown. Of particular importance is the lack of methodology available for detecting changes in the hypoxic status of individual tumour cells over time, an aspect of the tumour microenvironment that may represent a significant barrier to effective cancer therapy. Using novel methods to measure intermittent tumour hypoxia on a cellular level, the studies reported herein revealed rather surprising insights into the dynamic tumour microenvironment.

Two human tumour xenografts (WiDr and SiHa) were studied in this thesis, each with intrinsically different propensities to undergo changes in perfusion over time despite being implanted in the same murine host system. WiDr tumours typically exhibit frequent, large-scale changes in tumour perfusion over periods of 30 minutes or less, while SiHa tumours have much more stable blood flow over the same period of time. Relatively modest drug-induced increases

in net tumour perfusion were capable of significantly changing the microregional distribution of blood flow in WiDr tumours, but not in SiHa tumours. Drug treatment temporarily decreased the level of transient perfusion in WiDr tumours, and increased the oxygenation status of hypoxic tumour cell subpopulations as indicated by increased sensitivity to ionizing radiation. Specifically, fluorescence activated cell sorting prior to an *in vivo-in vitro* cloning assay revealed radiosensitivity increases in subpopulations of WiDr tumour cells at an intermediate distance from functional tumour blood vessels. These data suggest that tumour cells with an oxygenation status that changes over time are therapeutically relevant, highlighting the importance of a method to identify and quantify these transiently hypoxic cells.

Subsequent studies involved assessing transient hypoxia in WiDr and SiHa tumours on a whole-tumour scale by sequentially administering two exogenous hypoxia markers followed by quantification of hypoxic tumour cells by flow cytometry. High levels of the first hypoxia marker (pimonidazole) were maintained in the circulation for up to 8 hours using multiple hourly injections, providing a “time-integrated” measure of tumour hypoxia with an asymptotic increase in the total number of hypoxic cells over time. Subsequent administration of a second hypoxia marker (CCI-103F) showed that substantial numbers of the previously pimonidazole-labeled cells were no longer hypoxic during the circulation lifetime of the second marker. The overall fraction of tumour cells that demonstrated changes in hypoxic status over time increased with different kinetics and by different magnitudes in the two xenograft systems. Surprisingly, up to 20% of the cells in SiHa tumours were intermittently hypoxic over an 8 hour period, despite previous observations of relatively stable tumour perfusion when assessed over 30 minute intervals. Moreover, 8% of the cells in WiDr tumours were intermittently hypoxic over an 8 hour period despite previous observations of frequent, large-scale perfusion changes over 30 minute intervals. These observations indicate the importance of proper definition of “transient”

tumour perfusion or hypoxia since both tumour types displayed transient and relatively steady-state behavior when assessed with different methods and over different periods of time.

Interestingly, the tumour cells that demonstrated a transient hypoxic status were typically *not* adjacent to tumour blood vessels (as had been suggested by previous observations of large-scale changes in tumour perfusion over time). These data indicate that more frequently observed, smaller-scale changes in tumour perfusion may be more relevant sources of transient hypoxia.

During the course of these studies, it was discovered that the exogenous hypoxia marker pimonidazole could label hypoxic tumour cells when administered in the drinking water of tumour-bearing mice. As pimonidazole consumption was maintained for 6–96 hours (*ad libitum*), both the fraction of hypoxic tumour cells and the relative number of pimonidazole adducts bound in those cells increased. Further, the sustained ingestion of pimonidazole revealed a larger (i.e. “time-integrated”) hypoxic fraction compared to a single injection of a second hypoxia marker (CCI-103F). The numbers of hypoxic cells observed with longer-term oral pimonidazole administration also increased with different kinetics and by different magnitudes in SiHa and WiDr tumours, reflecting the inclusion of transiently hypoxic tumour cells into the tumour hypoxia estimates. Moreover, a proportion of cells labeled with oral pimonidazole were subsequently sufficiently well-oxygenated to synthesize DNA, indicating the potential therapeutic relevance of tumour cells with a changing oxygenation status. Thus in addition to its convenience and versatility when compared to hypoxia marker injection, oral administration of pimonidazole identified physiologically and therapeutically relevant hypoxic tumour cells assessed over relatively long periods of time.

Importantly, the use of a “time-integrated” measure of tumour hypoxia (with either multiple injections or oral administration of pimonidazole) combined with a subsequent “snapshot” of tumour hypoxia with a second hypoxia marker (e.g. EF5) is a strategy with potential clinical applicability. In particular, the use of flow cytometry to identify and quantify cells in fine needle

aspirate biopsies that are differentially labeled with either hypoxia marker would provide invaluable information on the presence of transient tumour hypoxia in the clinic. Further clinical application of this method would allow studies into the duration of intermittent hypoxia episodes and the fractions of transiently hypoxic cells in clinical tumours which would, in turn, have important implications for the strategic improvement of cancer therapy.

An additional method to study transiently hypoxic tumour cells with potential clinical applicability could be realized by identifying gene products that are more highly expressed under conditions of transient (or diffusion-limited) hypoxia. The influence of reduced cellular oxygenation on the expression of various genes *in vitro* is well-established, and increased levels of select hypoxia-inducible genes have been used as endogenous indicators of hypoxic cells *in vivo*. However, little is known about gene expression differences between hypoxic cells in the disparate tumour microenvironments typically associated with either transient or diffusion-limited hypoxia. Serial analysis of gene expression was used to identify genes differentially expressed between subpopulations of cells grown in multicellular spheroids exposed to a relatively short-term period of hypoxia. The outer and inner spheroid cell layers contained cells in different growth conditions, and selective recovery of specific cell subpopulations allowed construction of global gene expression profiles from *in vitro* conditions of transient or diffusion-limited hypoxia respectively. Notably, the multicellular spheroid system largely reflects the solid tumour microenvironment *in vivo*, enabling more relevant modeling of tumour hypoxia than is possible with tumour cells grown in monolayer culture. Genes that were differentially expressed between conditions of transient and diffusion-limited hypoxia were identified, representing a potentially valuable resource for the future development of methods to selectively identify and quantify similar cells *in vivo*. However, more work is required before the potential of these data can be fully realized.

6.2 FUTURE DIRECTIONS

A number of additional studies can be envisaged as extensions to this thesis, particularly from the data and concepts presented in Chapters 3-5.

With the method for quantifying transient tumour hypoxia in experimental tumours outlined in Chapter 3, directly assessing the therapeutic efficacy of various cytotoxic treatments on transiently hypoxic cells would be valuable. This could perhaps be accomplished by analyzing half of a tumour (or one of two tumours from the same animal) for transient hypoxia while plating the other half in an *in vivo-in vitro* survival assay after treatment. Additional experiments using various hypoxia modification strategies (e.g. carbogen gas, nicotinamide, etc.) could be used to quantify the effects of tumour hypoxia modification on transient hypoxia and treatment response.

To study the mechanisms of transient hypoxia generation, differential pimonidazole and CCI-103F labeling could be combined with the dual stain mismatch method to compare regions of transient hypoxia with regions of transient perfusion over various periods of time. The perfusion dyes would necessitate image analysis for quantification rather than flow cytometry, but useful information could be obtained, particularly with hypoxia modification.

The concept of “time-integrated” hypoxia measurements using an exogenous marker could also be combined with endogenous hypoxia marker expression to quantify changes in tumour hypoxia over time. Using pimonidazole and a rapidly responsive endogenous marker such as HIF-1 α may represent a useful method to study changes in hypoxia that occur over relatively short periods of time (on the order of minutes) in some tumour types (e.g. WiDr). Due to the instability of HIF-1 α , this method would likely require quantification by image analysis after rapid tissue fixation, although quantifying HIF-1 α levels by flow cytometry may also be possible (Vordermark and Brown, 2003).

Extensions of the studies presented in Chapter 4 regarding oral pimonidazole to label hypoxic tumour cells are necessary, particularly for improving the labeling of hypoxic cells over shorter labeling intervals (< 6-12 hours). Preliminary attempts to increase the dose of oral pimonidazole consumed over time involved using up to a 4-fold higher pimonidazole concentration in the drinking water. However, the mice had an aversion to water containing higher concentrations of pimonidazole, even when glucose was added as a sweetener. Pre-clinical studies involving pimonidazole administration by forced oral dosing would facilitate the generation of more in-depth oral pimonidazole pharmacokinetic data, particularly since an escalating series of pimonidazole doses could be used. While oral dosing in this way would get away from the concept of "time-integrated" hypoxia measurements, the data would prove beneficial for studying the plasma clearance rate of orally administered pimonidazole. In the clinic, administering pimonidazole orally to label hypoxic tumour cells should be tested to determine if this represents a feasible (and more convenient) alternative to pimonidazole administered by intravenous infusion.

From a methodological standpoint, the concepts of "time-integrated" hypoxia measurements and differential labeling of hypoxic cells with two exogenous hypoxia markers could be directly applied to the clinic with flow cytometry analysis of tumour biopsies (Durand and Aquino-Parsons, 2001a; Olive *et al.*, 2001b). Pimonidazole and EF5 are already used clinically to measure tumour hypoxia, and pharmacokinetic data are available for each marker (Saunders *et al.*, 1984; Koch *et al.*, 2001). Moreover, pharmacokinetics studies of pimonidazole combined with the parent compound of EF5 (etanidazole; SR-2508) have previously been conducted when these agents were under study as clinical radiosensitizers (Newman *et al.*, 1988; Bleehen *et al.*, 1989). While the pharmacokinetics of etanidazole and EF5 are different, the earlier work suggests that administering both pimonidazole and an etanidazole-derivative at different points in time may be clinically feasible. Unfortunately, considerable "philosophical differences"

between proponents of either EF5 or pimonidazole regarding the “correct” method for quantifying fractions of hypoxic tumour cells labeled with either marker may delay these types of experiments.

The SAGE data presented in Chapter 5 represent a rather large resource for future work. A number of tag sequences were identified with significant differential expression between the model conditions of chronic and transient hypoxia, any of which could be pursued for further study. Repeating the spheroid experiments is necessary to validate the relative expression levels of selected genes using a more cost-effective method such as quantitative real-time RT-PCR. A number of tag sequences did not match any known sequence in the RefSeq or MGC (*Homo sapiens*) databases, and RT-PCR using a primer derived from the tag sequence and a poly-T primer may help in isolating a partial sequence of the unknown genes. Other tags matched multiple genes in the databases, and RT-PCR using commercial primers specific to these genes would identify the gene(s) represented by an ambiguous SAGE tag sequence.

The kinetics of hypoxia-induced gene expression can be studied in spheroids by varying the degree and duration of the *in vitro* hypoxic episode. Repeated hypoxic exposures over varying lengths of time could be used to simulate intermittent hypoxia (Cairns *et al.*, 2001; Cairns and Hill, 2004), and the multicellular spheroid model is also conducive to independently studying the effects of other tumour microenvironmental parameters (e.g. glucose, pH, etc.) on levels of mRNA or protein expression. Once the expression behavior of a particular gene of interest is characterized, studies into the mechanism(s) of induction could be conducted as desired.

Using the expression level of a particular gene of interest (e.g. CD151) as an indication of microenvironmental conditions *in vivo* could be tested in human tumour xenografts at the transcript level (using *in situ* hybridization) or the protein level (using flow cytometry or Western blots). Expression levels of genes such as CD151 should also be combined with quantification

of hypoxia, transient hypoxia, and tumour cell proliferation in the same system to identify potential relationships.

Lastly, for membrane-bound proteins such as CD151, it may be possible to sort cells based on the level of CD151 expression, as has been done previously with CAIX (Olive *et al.*, 2001a). Provided the disaggregation of human tumour xenografts for cell sorting could be managed without perturbing CD151 protein levels, cells with varying levels of CD151 expression could be plated in an *in vivo-in vitro* cloning assay to determine the relationship between CD151 and response to radiation or chemotherapy treatment.

In summary, this thesis constitutes a body of work with potentially important methodological and therapeutic implications, and also represents a starting point for continued pre-clinical and clinical studies into the relationship between tumour perfusion, tumour hypoxia, and microenvironment-induced differential gene expression. As such, the data and concepts presented in this thesis provide both a foundation and an impetus for directed studies to improve clinical cancer therapy through enhanced understanding of the dynamic tumour microenvironment.

REFERENCES

- Aebersold DM, Burri P, Beer KT, Laissue J, Djonov V, Greiner RH, and Semenza GL (2001) Expression of hypoxia-inducible factor-1 α : a novel predictive and prognostic parameter in the radiotherapy of oropharyngeal cancer. *Cancer Res* **61**: 2911-2916
- Airley RE, Loncaster J, Raleigh JA, Harris AL, Davidson SE, Hunter RD, West CM, and Stratford IJ (2003) GLUT-1 and CAIX as intrinsic markers of hypoxia in carcinoma of the cervix: relationship to pimonidazole binding. *Int J Cancer* **104**: 85-91
- Arcuri LB, Fredrickson MK, and Ziegler KM. (1998). Pentoxifylline. In *AHFS Drug Information*, McEvoy GK (ed) pp. 1238-1242. American Society of Health-System Pharmacists: Bethesda.
- Armstrong M, Jr., Needham D, Hatchell DL, and Nunn RS (1990) Effect of pentoxifylline on the flow of polymorphonuclear leukocytes through a model capillary. *Angiology* **41**: 253-262
- Arteel GE, Iimuro Y, Yin M, Raleigh JA, and Thurman RG (1997) Chronic enteral ethanol treatment causes hypoxia in rat liver tissue *in vivo*. *Hepatology* **25**: 920-926
- Arteel GE, Raleigh JA, Bradford BU, and Thurman RG (1996) Acute alcohol produces hypoxia directly in rat liver tissue *in vivo*: role of Kupffer cells. *Am J Physiol* **271**: G494-500
- Arteel GE, Thurman RG, and Raleigh JA (1998) Reductive metabolism of the hypoxia marker pimonidazole is regulated by oxygen tension independent of the pyridine nucleotide redox state. *Eur J Biochem* **253**: 743-750
- Arteel GE, Thurman RG, Yates JM, and Raleigh JA (1995) Evidence that hypoxia markers detect oxygen gradients in liver: pimonidazole and retrograde perfusion of rat liver. *Br J Cancer* **72**: 889-895
- Audic S and Claverie JM (1997) The significance of digital gene expression profiles. *Genome Res* **7**: 986-995
- Azuma C, Raleigh JA, and Thrall DE (1997) Longevity of pimonidazole adducts in spontaneous canine tumors as an estimate of hypoxic cell lifetime. *Radiat Res* **148**: 35-42
- Baish JW, Gazit Y, Berk DA, Nozue M, Baxter LT, and Jain RK (1996) Role of tumor vascular architecture in nutrient and drug delivery: an invasion percolation-based network model. *Microvasc Res* **51**: 327-346
- Bakka A, Johnsen AS, Endresen L, and Rugstad HE (1982) Radioresistance in cells with high content of metallothionein. *Experientia* **38**: 381-383
- Beasley NJ, Leek R, Alam M, Turley H, Cox GJ, Gatter K, Millard P, Fuggle S, and Harris AL (2002) Hypoxia-inducible factors HIF-1 α and HIF-2 α in head and neck cancer: relationship to tumor biology and treatment outcome in surgically resected patients. *Cancer Res* **62**: 2493-2497
- Beasley NJ, Wykoff CC, Watson PH, Leek R, Turley H, Gatter K, Pastorek J, Cox GJ, Ratcliffe P, and Harris AL (2001) Carbonic anhydrase IX, an endogenous hypoxia marker, expression in head and neck squamous cell carcinoma and its relationship to hypoxia, necrosis, and microvessel density. *Cancer Res* **61**: 5262-5267
- Begg AC (2003) Is HIF-1 α a good marker for tumor hypoxia? *Int J Radiat Oncol Biol Phys* **56**: 917-919
- Behrooz A and Ismail-Beigi F (1997) Dual control of glut1 glucose transporter gene expression by hypoxia and by inhibition of oxidative phosphorylation. *J Biol Chem* **272**: 5555-5562
- Bennewith KL and Durand RE (2001) Drug-induced alterations in tumour perfusion yield increases in tumour cell radiosensitivity. *Br J Cancer* **85**: 1577-1584
- Bennewith KL, Raleigh JA, and Durand RE (2002) Orally administered pimonidazole to label hypoxic tumor cells. *Cancer Res* **62**: 6827-6830
- Berditchevski F and Odintsova E (1999) Characterization of integrin-tetraspanin adhesion complexes: role of tetraspanins in integrin signaling. *J Cell Biol* **146**: 477-492
- Bergeron M, Evans SM, Sharp FR, Koch CJ, Lord EM, and Ferriero DM (1999) Detection of hypoxic cells with the 2-nitroimidazole, EF5, correlates with early redox changes in rat brain after perinatal hypoxia-ischemia. *Neuroscience* **89**: 1357-1366
- Berry RJ, Hall EJ, and Cavanagh J (1970) Radiosensitivity and the oxygen effect for mammalian cells cultured *in vitro* in stationary phase. *Br J Radiol* **43**: 81-90
- Birner P, Gatterbauer B, Oberhuber G, Schindl M, Rossler K, Prodinger A, Budka H, and Hainfellner JA (2001) Expression of hypoxia-inducible factor-1 α in oligodendrogliomas: its impact on prognosis and on neoangiogenesis. *Cancer* **92**: 165-171
- Birner P, Schindl M, Obermair A, Plank C, Breitenecker G, and Oberhuber G (2000) Overexpression of hypoxia-inducible factor 1 α is a marker for an unfavorable prognosis in early-stage invasive cervical cancer. *Cancer Res* **60**: 4693-4696
- Bleehen NM, Newman HF, Maughan TS, and Workman P (1989) A multiple dose study of the combined radiosensitizers Ro 03-8799 (pimonidazole) and SR 2508 (etanidazole). *Int J Radiat Oncol Biol Phys* **16**: 1093-1096

- Bos R, van der Groep P, Greijer AE, Shvarts A, Meijer S, Pinedo HM, Semenza GL, van Diest PJ, and van der Wall E (2003) Levels of hypoxia-inducible factor-1 α independently predict prognosis in patients with lymph node negative breast carcinoma. *Cancer* **97**: 1573-1581
- Braun RD, Lanzen JL, and Dewhirst MW (1999) Fourier analysis of fluctuations of oxygen tension and blood flow in R3230Ac tumors and muscle in rats. *Am J Physiol* **277**: H551-568
- Braun RD, Lanzen JL, Snyder SA, and Dewhirst MW (2001) Comparison of tumor and normal tissue oxygen tension measurements using OxyLite or microelectrodes in rodents. *Am J Physiol Heart Circ Physiol* **280**: H2533-2544
- Brizel DM, Dodge RK, Clough RW, and Dewhirst MW (1999) Oxygenation of head and neck cancer: changes during radiotherapy and impact on treatment outcome. *Radiother Oncol* **53**: 113-117
- Brizel DM, Scully SP, Harrelson JM, Layfield LJ, Bean JM, Prosnitz LR, and Dewhirst MW (1996) Tumor oxygenation predicts for the likelihood of distant metastases in human soft tissue sarcoma. *Cancer Res* **56**: 941-943
- Brizel DM, Sibley GS, Prosnitz LR, Scher RL, and Dewhirst MW (1997) Tumor hypoxia adversely affects the prognosis of carcinoma of the head and neck. *Int J Radiat Oncol Biol Phys* **38**: 285-289
- Brown JM (1979) Evidence for acutely hypoxic cells in mouse tumours, and a possible mechanism of reoxygenation. *Br J Radiol* **52**: 650-656
- Brown JM (1993) SR 4233 (tirapazamine): a new anticancer drug exploiting hypoxia in solid tumours. *Br J Cancer* **67**: 1163-1170
- Brown JM and Giaccia AJ (1998) The unique physiology of solid tumors: opportunities (and problems) for cancer therapy. *Cancer Res* **58**: 1408-1416
- Brown JM and Le QT (2002) Tumor hypoxia is important in radiotherapy, but how should we measure it? *Int J Radiat Oncol Biol Phys* **54**: 1299-1301
- Brown JM and Siim BG (1996) Hypoxia-specific cytotoxins in cancer therapy. *Semin Radiat Oncol* **6**: 22-36
- Bruick RK and McKnight SL (2001) A conserved family of prolyl-4-hydroxylases that modify HIF. *Science* **294**: 1337-1340
- Brurberg KG, Graff BA, Olsen DR, and Rofstad EK (2004) Tumor-line specific pO₂ fluctuations in human melanoma xenografts. *Int J Radiat Oncol Biol Phys* **58**: 403-409
- Brurberg KG, Graff BA, and Rofstad EK (2003) Temporal heterogeneity in oxygen tension in human melanoma xenografts. *Br J Cancer* **89**: 350-356
- Bussink J, Kaanders JH, Strik AM, and van der Kogel AJ (2000a) Effects of nicotinamide and carbogen on oxygenation in human tumor xenografts measured with luminescence based fiber-optic probes. *Radiother Oncol* **57**: 21-30
- Bussink J, Kaanders JH, Strik AM, Vojnovic B, and van Der Kogel AJ (2000b) Optical sensor-based oxygen tension measurements correspond with hypoxia marker binding in three human tumor xenograft lines. *Radiat Res* **154**: 547-555
- Bussink J, Kaanders JH, and van der Kogel AJ (2003) Tumor hypoxia at the micro-regional level: clinical relevance and predictive value of exogenous and endogenous hypoxic cell markers. *Radiother Oncol* **67**: 3-15
- Cairns RA and Hill RP (2004) Acute hypoxia enhances spontaneous lymph node metastasis in an orthotopic murine model of human cervical carcinoma. *Cancer Res* **64**: 2054-2061
- Cairns RA, Kalliomaki T, and Hill RP (2001) Acute (cyclic) hypoxia enhances spontaneous metastasis of KHT murine tumors. *Cancer Res* **61**: 8903-8908
- Cater DB and Silver IA (1960) Quantitative measurements of oxygen tension in normal tissues and in the tumours of patients before and after radiotherapy. *Acta Radiol* **53**: 233-256
- Chacon E, Morrow CJ, Leon AA, Born JL, and Smith BR (1988) Regioselective formation of a misonidazole-glutathione conjugate as a function of pH during chemical reduction. *Biochem Pharmacol* **37**: 361-363
- Chao CF, Subjeck JR, Brody H, Shen J, and Johnson RJ (1984) The effect of nitroimidazoles on glucose utilization and lactate accumulation in mouse brain. *Radiat Res* **97**: 87-96
- Chaplin DJ, Durand RE, and Olive PL (1985) Cell selection from a murine tumor using the fluorescent probe Hoechst 33342. *Br J Cancer* **51**: 569-572
- Chaplin DJ, Durand RE, and Olive PL (1986) Acute hypoxia in tumors: implications for modifiers of radiation effects. *Int J Radiat Oncol Biol Phys* **12**: 1279-1282
- Chaplin DJ, Hill SA, Bell KM, and Tozer GM (1998) Modification of tumor blood flow: current status and future directions. *Semin Radiat Oncol* **8**: 151-163
- Chapman JD (1979) Hypoxic sensitizers--implications for radiation therapy. *N Engl J Med* **301**: 1429-1432
- Chapman JD (1984) The detection and measurement of hypoxic cells in solid tumors. *Cancer* **54**: 2441-2449
- Chapman JD (1991) Measurement of tumor hypoxia by invasive and non-invasive procedures: a review of recent clinical studies. *Radiother Oncol* **20**: 13-19

- Chapman JD, Baer K, and Lee J (1983) Characteristics of the metabolism-induced binding of misonidazole to hypoxic mammalian cells. *Cancer Res* **43**: 1523-1528
- Chapman JD, Franko AJ, and Sharplin J (1981) A marker for hypoxic cells in tumours with potential clinical applicability. *Br J Cancer* **43**: 546-550
- Chia SK, Wykoff CC, Watson PH, Han C, Leek RD, Pastorek J, Gatter KC, Ratcliffe P, and Harris AL (2001) Prognostic significance of a novel hypoxia-regulated marker, carbonic anhydrase IX, in invasive breast carcinoma. *J Clin Oncol* **19**: 3660-3668
- Cline JM, Rosner GL, Raleigh JA, and Thrall DE (1997) Quantification of CCI-103F labeling heterogeneity in canine solid tumors. *Int J Radiat Oncol Biol Phys* **37**: 655-662
- Cline JM, Thrall DE, Page RL, Franko AJ, and Raleigh JA (1990) Immunohistochemical detection of a hypoxia marker in spontaneous canine tumours. *Br J Cancer* **62**: 925-931
- Cline JM, Thrall DE, Rosner GL, and Raleigh JA (1994) Distribution of the hypoxia marker CCI-103F in canine tumors. *Int J Radiat Oncol Biol Phys* **28**: 921-933
- Cobb LM, Nolan J, and Butler SA (1990) Distribution of pimonidazole and RSU 1069 in tumour and normal tissues. *Br J Cancer* **62**: 915-918
- Cobb LM, Nolan J, and Hacker T (1992) Retention of misonidazole in normal and malignant tissues: interplay of hypoxia and reductases. *Int J Radiat Oncol Biol Phys* **22**: 655-659
- Cockman ME, Masson N, Mole DR, Jaakkola P, Chang GW, Clifford SC, Maher ER, Pugh CW, Ratcliffe PJ, and Maxwell PH (2000) Hypoxia inducible factor- α binding and ubiquitylation by the von Hippel-Lindau tumor suppressor protein. *J Biol Chem* **275**: 25733-25741
- Coleman CN, Mitchell JB, and Camphausen K (2002) Tumor hypoxia: chicken, egg, or a piece of the farm? *J Clin Oncol* **20**: 610-615
- Colleoni M, Rocca A, Sandri MT, Zorzino L, Masci G, Nole F, Peruzzotti G, Robertson C, Orlando L, Cinieri S, de Braud F, Viale G, and Goldhirsch A (2002) Low-dose oral methotrexate and cyclophosphamide in metastatic breast cancer: antitumor activity and correlation with vascular endothelial growth factor levels. *Ann Oncol* **13**: 73-80
- Collingridge DR, Young WK, Vojnovic B, Wardman P, Lynch EM, Hill SA, and Chaplin DJ (1997) Measurement of tumor oxygenation: a comparison between polarographic needle electrodes and a time-resolved luminescence-based optical sensor. *Radiat Res* **147**: 329-334
- Cowan DS, Hicks KO, and Wilson WR (1996) Multicellular membranes as an *in vitro* model for extravascular diffusion in tumours. *Br J Cancer* **74**: S28-31
- Craighead PS, Pearcey R, and Stuart G (2000) A phase I/II evaluation of tirapazamine administered intravenously concurrent with cisplatin and radiotherapy in women with locally advanced cervical cancer. *Int J Radiat Oncol Biol Phys* **48**: 791-795
- Crnogorac-Jurcevic T, Missiaglia E, Blaveri E, Gangeswaran R, Jones M, Terris B, Costello E, Neoptolemos JP, and Lemoine NR (2003) Molecular alterations in pancreatic carcinoma: expression profiling shows that dysregulated expression of S100 genes is highly prevalent. *J Pathol* **201**: 63-74
- Cuthbert JA and Lipsky PE (1995) Suppression of the proliferation of Ras-transformed cells by fluoromevalonate, an inhibitor of mevalonate metabolism. *Cancer Res* **55**: 1732-1740
- Cuthbert JA and Lipsky PE (1997) Regulation of proliferation and Ras localization in transformed cells by products of mevalonate metabolism. *Cancer Res* **57**: 3498-3505
- Dasu A and Denekamp J (1998) New insights into factors influencing the clinically relevant oxygen enhancement ratio. *Radiother Oncol* **46**: 269-277
- Denekamp J and Dasu A (1999) Inducible repair and the two forms of tumour hypoxia--time for a paradigm shift. *Acta Oncol* **38**: 903-918
- Dennis MF, Stratford MR, Wardman P, and Watts ME (1985) Cellular uptake of misonidazole and analogues with acidic or basic functions. *Int J Radiat Biol* **47**: 629-643
- Dewhirst MW (1998) Concepts of oxygen transport at the microcirculatory level. *Semin Radiat Oncol* **8**: 143-150
- Dewhirst MW, Braun RD, and Lanzen JL (1998) Temporal changes in pO₂ of R3230AC tumors in Fischer-344 rats. *Int J Radiat Oncol Biol Phys* **42**: 723-726
- Dewhirst MW, Kimura H, Rehmus SW, Braun RD, Papahadjopoulos D, Hong K, and Secomb TW (1996) Microvascular studies on the origins of perfusion-limited hypoxia. *Br J Cancer Suppl* **27**: S247-251
- Dewhirst MW, Klitzman B, Braun RD, Brizel DM, Haroon ZA, and Secomb TW (2000) Review of methods used to study oxygen transport at the microcirculatory level. *Int J Cancer* **90**: 237-255
- Dewhirst MW, Ong ET, Braun RD, Smith B, Klitzman B, Evans SM, and Wilson D (1999) Quantification of longitudinal tissue pO₂ gradients in window chamber tumours: impact on tumour hypoxia. *Br J Cancer* **79**: 1717-1722

- Dewhirst MW, Ong ET, Klitzman B, Secomb TW, Vinuya RZ, Dodge R, Brizel D, and Gross JF (1992) Perivascular oxygen tensions in a transplantable mammary tumor growing in a dorsal flap window chamber. *Radiat Res* **130**: 171-182
- Dewhirst MW, Secomb TW, Ong ET, Hsu R, and Gross JF (1994) Determination of local oxygen consumption rates in tumors. *Cancer Res* **54**: 3333-3336
- Dische S, Bennett MH, Orchard R, Stratford MR, and Wardman P (1989) The uptake of the radiosensitizing compound Ro 03-8799 (Pimonidazole) in human tumors. *Int J Radiat Oncol Biol Phys* **16**: 1089-1092
- Durand RE (1982) Use of Hoechst 33342 for cell selection from multicell systems. *J Histochem Cytochem* **30**: 117-122
- Durand RE (1986) Use of a cell sorter for assays of cell clonogenicity. *Cancer Res* **46**: 2775-2778
- Durand RE (1989) Distribution and activity of antineoplastic drugs in a tumor model. *J Natl Cancer Inst* **81**: 146-152
- Durand RE (1991) Keynote address: the influence of microenvironmental factors on the activity of radiation and drugs. *Int J Radiat Oncol Biol Phys* **20**: 253-258
- Durand RE (1993) Cell kinetics and repopulation during multifraction irradiation of spheroids: implications for clinical radiotherapy. *Sem Radiat Oncol* **3**: 105-114
- Durand RE (1994) The influence of microenvironmental factors during cancer therapy. *in vivo* **8**: 691-702
- Durand RE (2001) Intermittent blood flow in solid tumours--an under-appreciated source of 'drug resistance'. *Cancer Metastasis Rev* **20**: 57-61
- Durand RE and Aquino-Parsons C (2001a) Clinical relevance of intermittent tumour blood flow. *Acta Oncol* **40**: 929-936
- Durand RE and Aquino-Parsons C (2001b) Non-constant tumour blood flow: implications for therapy. *Acta Oncol* **40**: 862-869
- Durand RE and Aquino-Parsons C (2004) Predicting response to treatment in human cancers of the uterine cervix: sequential biopsies during external beam radiotherapy. *Int J Radiat Oncol Biol Phys* **58**: 555-560
- Durand RE and LePard NE (1994) Modulation of tumor hypoxia by conventional chemotherapeutic agents. *Int J Radiat Oncol Biol Phys* **29**: 481-486
- Durand RE and LePard NE (1995) Contribution of transient blood flow to tumour hypoxia in mice. *Acta Oncol* **34**: 317-324
- Durand RE and Raleigh JA (1998) Identification of nonproliferating but viable hypoxic tumor cells *in vivo*. *Cancer Res* **58**: 3547-3550
- Durand RE and Sham E (1998) The lifetime of hypoxic human tumor cells. *Int J Radiat Oncol Biol Phys* **42**: 711-715
- Ebert BL, Gleadle JM, O'Rourke JF, Bartlett SM, Poulton J, and Ratcliffe PJ (1996) Isoenzyme-specific regulation of genes involved in energy metabolism by hypoxia: similarities with the regulation of erythropoietin. *Biochem J* **313**: 809-814
- Ehrly AM (1978) The effect of pentoxifylline on the flow properties of human blood. *Curr Med Res Opin* **5**: 608-613
- Epstein AC, Gleadle JM, McNeill LA, Hewitson KS, O'Rourke J, Mole DR, Mukherji M, Metzen E, Wilson MI, Dhanda A, Tian YM, Masson N, Hamilton DL, Jaakkola P, Barstead R, Hodgkin J, Maxwell PH, Pugh CW, Schofield CJ, and Ratcliffe PJ (2001) *C. elegans* EGL-9 and mammalian homologs define a family of dioxygenases that regulate HIF by prolyl hydroxylation. *Cell* **107**: 43-54
- Evans SM, Hahn S, Pook DR, Jenkins WT, Chalian AA, Zhang P, Stevens C, Weber R, Weinstein G, Benjamin I, Mirza N, Morgan M, Rubin S, McKenna WG, Lord EM, and Koch CJ (2000) Detection of hypoxia in human squamous cell carcinoma by EF5 binding. *Cancer Res* **60**: 2018-2024
- Evans SM, Hahn SM, Magarelli DP, and Koch CJ (2001) Hypoxic heterogeneity in human tumors: EF5 binding, vasculature, necrosis, and proliferation. *Am J Clin Oncol* **24**: 467-472
- Evans SM, Jenkins WT, Joiner B, Lord EM, and Koch CJ (1996) 2-Nitroimidazole (EF5) binding predicts radiation resistance in individual 9L s.c. tumors. *Cancer Res* **56**: 405-411
- Evans SM, Jenkins WT, Shapiro M, and Koch CJ (1997) Evaluation of the concept of "hypoxic fraction" as a descriptor of tumor oxygenation status. *Adv Exp Med Biol* **411**: 215-225
- Evans SM, Joiner B, Jenkins WT, Laughlin KM, Lord EM, and Koch CJ (1995) Identification of hypoxia in cells and tissues of epigastric 9L rat glioma using EF5 [2-(2-nitro-1H-imidazol-1-yl)-N-(2,2,3,3,3-pentafluoropropyl) acetamide]. *Br J Cancer* **72**: 875-882
- Franko AJ (1985) Hypoxic fraction and binding of misonidazole in EMT6/Ed multicellular tumor spheroids. *Radiat Res* **103**: 89-97
- Franko AJ (1986) Misonidazole and other hypoxia markers: metabolism and applications. *Int J Radiat Oncol Biol Phys* **12**: 1195-1202

- Franko AJ and Chapman JD (1982) Binding of ¹⁴C-misonidazole to hypoxic cells in V79 spheroids. *Br J Cancer* **45**: 694-699
- Franko AJ, Chapman JD, and Koch CJ (1982) Binding of misonidazole to EMT6 and V79 spheroids. *Int J Radiat Oncol Biol Phys* **8**: 737-739
- Franko AJ and Koch CJ (1984) Binding of misonidazole to V79 spheroids and fragments of Dunning rat prostatic and human colon carcinomas *in vitro*: diffusion of oxygen and reactive metabolites. *Int J Radiat Oncol Biol Phys* **10**: 1333-1336
- Franko AJ, Koch CJ, Garrecht BM, Sharplin J, and Hughes D (1987) Oxygen dependence of binding of misonidazole to rodent and human tumors *in vitro*. *Cancer Res* **47**: 5367-5376
- Friedl F, Kimura I, Osato T, and Ito Y (1970) Studies on a new human cell line (SiHa) derived from carcinoma of uterus. I. Its establishment and morphology. *Proc Soc Exp Biol Med* **135**: 543-545
- Fukuda R, Hirota K, Fan F, Jung YD, Ellis LM, and Semenza GL (2002) Insulin-like growth factor 1 induces hypoxia-inducible factor 1-mediated vascular endothelial growth factor expression, which is dependent on MAP kinase and phosphatidylinositol 3-kinase signaling in colon cancer cells. *J Biol Chem* **277**: 38205-38211
- Fukuda R, Kelly B, and Semenza GL (2003) Vascular endothelial growth factor gene expression in colon cancer cells exposed to prostaglandin E2 is mediated by hypoxia-inducible factor 1. *Cancer Res* **63**: 2330-2334
- Funakoshi T, Tachibana I, Hoshida Y, Kimura H, Takeda Y, Kijima T, Nishino K, Goto H, Yoneda T, Kumagai T, Osaki T, Hayashi S, Aozasa K, and Kawase I (2003) Expression of tetraspanins in human lung cancer cells: frequent downregulation of CD9 and its contribution to cell motility in small cell lung cancer. *Oncogene* **22**: 674-687
- Fyles A, Milosevic M, Hedley D, Pintilie M, Levin W, Manchul L, and Hill RP (2002) Tumor hypoxia has independent predictor impact only in patients with node-negative cervix cancer. *J Clin Oncol* **20**: 680-687
- Fyles AW, Milosevic M, Wong R, Kavanagh MC, Pintilie M, Sun A, Chapman W, Levin W, Manchul L, Keane TJ, and Hill RP (1998) Oxygenation predicts radiation response and survival in patients with cervix cancer. *Radiation Oncol* **48**: 149-156
- Gerweck LE and Seetharaman K (1996) Cellular pH gradient in tumor versus normal tissue: potential exploitation for the treatment of cancer. *Cancer Res* **56**: 1194-1198
- Gerweck LE, Seneviratne T, and Gerweck KK (1993) Energy status and radiobiological hypoxia at specified oxygen concentrations. *Radiat Res* **135**: 69-74
- Giatromanolaki A, Koukourakis MI, Sivridis E, Pastorek J, Wykoff CC, Gatter KC, and Harris AL (2001a) Expression of hypoxia-inducible carbonic anhydrase-9 relates to angiogenic pathways and independently to poor outcome in non-small cell lung cancer. *Cancer Res* **61**: 7992-7998
- Giatromanolaki A, Koukourakis MI, Sivridis E, Turley H, Talks K, Pezzella F, Gatter KC, and Harris AL (2001b) Relation of hypoxia inducible factor 1 α and 2 α in operable non-small cell lung cancer to angiogenic/molecular profile of tumours and survival. *Br J Cancer* **85**: 881-890
- Gray LH, Conger AD, Ebert M, Hornsey S, and Scott OC (1953) The concentration of oxygen dissolved in tissues at the time of irradiation as a factor in radiotherapy. *Br J Radiol* **26**: 638-648
- Griffiths JR (1991) Are cancer cells acidic? *Br J Cancer* **64**: 425-427
- Griffiths JR and Robinson SP (1999) The OxyLite: a fibre-optic oxygen sensor. *Br J Radiol* **72**: 627-630
- Groebe K, Erz S, and Mueller-Klieser W (1994) Glucose diffusion coefficients determined from concentration profiles in EMT6 tumor spheroids incubated in radioactively labeled L-glucose. *Adv Exp Med Biol* **361**: 619-625
- Guerreiro Da Silva ID, Hu YF, Russo IH, Ao X, Salicioni AM, Yang X, and Russo J (2000) S100P calcium-binding protein overexpression is associated with immortalization of human breast epithelial cells *in vitro* and early stages of breast cancer development *in vivo*. *Int J Oncol* **16**: 231-240
- Gullino PM and Grantham FH (1961) Studies on the exchange of fluids between host and tumor. II. The blood flow of hepatomas and other tumors in rats and mice. *J Natl Cancer Inst* **27**: 1465-1491
- Hakim TS and Macek AS (1988) Effect of hypoxia on erythrocyte deformability in different species. *Biorheology* **25**: 857-868
- Hall EJ, Bedford JS, and Oliver R (1966) Extreme hypoxia; its effect on the survival of mammalian cells irradiated at high and low dose-rates. *Br J Radiol* **39**: 302-307
- Hashida H, Takabayashi A, Tokuhara T, Hattori N, Taki T, Hasegawa H, Satoh S, Kobayashi N, Yamaoka Y, and Miyake M (2003) Clinical significance of transmembrane 4 superfamily in colon cancer. *Br J Cancer* **89**: 158-167
- Hashizume H, Baluk P, Morikawa S, McLean JW, Thurston G, Roberge S, Jain RK, and McDonald DM (2000) Openings between defective endothelial cells explain tumor vessel leakiness. *Am J Pathol* **156**: 1363-1380

- Haugland HK, Vukovic V, Pintilie M, Fyles AW, Milosevic M, Hill RP, and Hedley DW (2002) Expression of hypoxia-inducible factor-1 α in cervical carcinomas: correlation with tumor oxygenation. *Int J Radiat Oncol Biol Phys* **53**: 854-861
- Hedley DW, Pintilie M, Woo J, Morrison A, Birl D, Fyles A, Milosevic M, and Hill RP (2003) Carbonic anhydrase IX expression, hypoxia, and prognosis in patients with uterine cervical carcinomas. *Clin Cancer Res* **9**: 5666-5674
- Helmlinger G, Sckell A, Dellian M, Forbes NS, and Jain RK (2002) Acid production in glycolysis-impaired tumors provides new insights into tumor metabolism. *Clin Cancer Res* **8**: 1284-1291
- Helmlinger G, Yuan F, Dellian M, and Jain RK (1997) Interstitial pH and pO₂ gradients in solid tumors *in vivo*: high-resolution measurements reveal a lack of correlation. *Nat Med* **3**: 177-182
- Hewitson KS, McNeill LA, Riordan MV, Tian YM, Bullock AN, Welford RW, Elkins JM, Oldham NJ, Bhattacharya S, Gleadle JM, Ratcliffe PJ, Pugh CW, and Schofield CJ (2002) Hypoxia-inducible factor (HIF) asparagine hydroxylase is identical to factor inhibiting HIF (FIH) and is related to the cupin structural family. *J Biol Chem* **277**: 26351-26355
- Hill SA, Pigott KH, Saunders MI, Powell ME, Arnold S, Obeid A, Ward G, Leahy M, Hoskin PJ, and Chaplin DJ (1996) Microregional blood flow in murine and human tumours assessed using laser Doppler microprobes. *Br J Cancer Suppl* **27**: S260-263
- Hirst DG, Hazlehurst JL, and Brown JM (1985) Changes in misonidazole binding with hypoxic fraction in mouse tumors. *Int J Radiat Oncol Biol Phys* **11**: 1349-1355
- Hockel M, Knoop C, Schlenger K, Vorndran B, Baussmann E, Mitze M, Knapstein PG, and Vaupel P (1993) Intratumoral pO₂ predicts survival in advanced cancer of the uterine cervix. *Radiother Oncol* **26**: 45-50
- Hockel M, Schlenger K, Aral B, Mitze M, Schaffer U, and Vaupel P (1996a) Association between tumor hypoxia and malignant progression in advanced cancer of the uterine cervix. *Cancer Res* **56**: 4509-4515
- Hockel M, Schlenger K, Knoop C, and Vaupel P (1991) Oxygenation of carcinomas of the uterine cervix: evaluation by computerized O₂ tension measurements. *Cancer Res* **51**: 6098-6102
- Hockel M, Schlenger K, Mitze M, Schaffer U, and Vaupel P (1996b) Hypoxia and radiation response, in human tumors. *Semin Radiat Oncol* **6**: 3-9
- Hockel M and Vaupel P (2001) Tumor hypoxia: definitions and current clinical, biologic, and molecular aspects. *J Natl Cancer Inst* **93**: 266-276
- Hodgkiss RJ, Stratford MR, Dennis MF, and Hill SA (1995) Pharmacokinetics and binding of the bioreductive probe for hypoxia, NITP: effect of route of administration. *Br J Cancer* **72**: 1462-1468
- Honess DJ, Andrews MS, Ward R, and Bleehen NM (1995) Pentoxifylline increases RIF-1 tumour pO₂ in a manner compatible with its ability to increase relative tumour perfusion. *Acta Oncologica* **34**: 385-389
- Honess DJ, Dennis IF, and Bleehen NM (1993) Pentoxifylline: Its pharmacokinetics and ability to improve tumour perfusion and radiosensitivity in mice. *Radiother Oncol* **28**: 208-218
- Horsman MR (1998) Measurement of tumor oxygenation. *Int J Radiat Oncol Biol Phys* **42**: 701-704
- Hoskin PJ, Sibtain A, Daley FM, and Wilson GD (2003) GLUT1 and CAIX as intrinsic markers of hypoxia in bladder cancer: relationship with vascularity and proliferation as predictors of outcome of ARCON. *Br J Cancer* **89**: 1290-1297
- Huang Q, Shan S, Braun RD, Lanzen J, Anyrhambatla G, Kong G, Borelli M, Corry P, Dewhirst MW, and Li CY (1999) Noninvasive visualization of tumors in rodent dorsal skin window chambers. *Nat Biotechnol* **17**: 1033-1035
- Hui EP, Chan AT, Pezzella F, Turley H, To KF, Poon TC, Zee B, Mo F, Teo PM, Huang DP, Gatter KC, Johnson PJ, and Harris AL (2002) Coexpression of hypoxia-inducible factors 1 α and 2 α , carbonic anhydrase IX, and vascular endothelial growth factor in nasopharyngeal carcinoma and relationship to survival. *Clin Cancer Res* **8**: 2595-2604
- Iacobuzio-Donahue CA, Maitra A, Shen-Ong GL, van Heek T, Ashfaq R, Meyer R, Walter K, Berg K, Hollingsworth MA, Cameron JL, Yeo CJ, Kern SE, Goggins M, and Hruban RH (2002) Discovery of novel tumor markers of pancreatic cancer using global gene expression technology. *Am J Pathol* **160**: 1239-1249
- Ivan M, Kondo K, Yang H, Kim W, Valiando J, Ohh M, Salic A, Asara JM, Lane WS, and Kaelin Jr WG (2001) HIF α targeted for VHL-mediated destruction by proline hydroxylation: implications for O₂ sensing. *Science* **292**: 464-468
- Ivanov S, Liao SY, Ivanova A, Danilkovitch-Miagkova A, Tarasova N, Weirich G, Merrill MJ, Proescholdt MA, Oldfield EH, Lee J, Zavada J, Waheed A, Sly W, Lerman MI, and Stanbridge EJ (2001) Expression of hypoxia-inducible cell-surface transmembrane carbonic anhydrases in human cancer. *Am J Pathol* **158**: 905-919
- Iyer RV, Kim E, Schneider RF, and Chapman JD (1998) A dual hypoxic marker technique for measuring oxygenation change within individual tumors. *Br J Cancer* **78**: 163-169

- Jaakkola P, Mole DR, Tian YM, Wilson MI, Gielbert J, Gaskell SJ, Kriegsheim AV, Hebestreit HF, Mukherji M, Schofield CJ, Maxwell PH, Pugh CW, and Ratcliffe PJ (2001) Targeting of HIF- α to the von Hippel-Lindau ubiquitylation complex by O₂-regulated prolyl hydroxylation. *Science* **292**: 468-472
- Jain RK (1988) Determinants of tumor blood flow: a review. *Cancer Res* **48**: 2641-2658
- Janssen HL, Haustermans KM, Sprong D, Blommestein G, Hofland I, Hoebbers FJ, Blijweert E, Raleigh JA, Semenza GL, Varia MA, Balm AJ, van Velthuysen ML, Delaere P, Sciort R, and Begg AC (2002) HIF-1 α , pimonidazole, and iododeoxyuridine to estimate hypoxia and perfusion in human head-and-neck tumors. *Int J Radiat Oncol Biol Phys* **54**: 1537-1549
- Jenkins WT, Evans SM, and Koch CJ (2000) Hypoxia and necrosis in rat 9L glioma and Morris 7777 hepatoma tumors: comparative measurements using EF5 binding and the Eppendorf needle electrode. *Int J Radiat Oncol Biol Phys* **46**: 1005-1017
- Jewell UR, Kvietikova I, Scheid A, Bauer C, Wenger RH, and Gassmann M (2001) Induction of HIF-1 α in response to hypoxia is instantaneous. *FASEB J* **15**: 1312-1314
- Jiang BH, Semenza GL, Bauer C, and Marti HH (1996) Hypoxia-inducible factor 1 levels vary exponentially over a physiologically relevant range of O₂ tension. *Am J Physiol* **271**: C1172-1180
- Jiang BH, Zheng JZ, Leung SW, Roe R, and Semenza GL (1997) Transactivation and inhibitory domains of hypoxia-inducible factor 1 α . Modulation of transcriptional activity by oxygen tension. *J Biol Chem* **272**: 19253-19260
- Jin GY, Li SJ, Moulder JE, and Raleigh JA (1990) Dynamic measurements of hexafluoromisonidazole (CCI-103F) retention in mouse tumours by 1H/19F magnetic resonance spectroscopy. *Int J Radiat Biol* **58**: 1025-1034
- Kaanders JH, Wijffels KI, Marres HA, Ljungkvist AS, Pop LA, van den Hoogen FJ, de Wilde PC, Bussink J, Raleigh JA, and van der Kogel AJ (2002) Pimonidazole binding and tumor vascularity predict for treatment outcome in head and neck cancer. *Cancer Res* **62**: 7066-7074
- Kallinowski F, Zander R, Hoeckel M, and Vaupel P (1990) Tumor tissue oxygenation as evaluated by computerized-pO₂-histography. *Int J Radiat Oncol Biol Phys* **19**: 953-961
- Kamura T, Sato S, Iwai K, Czyzyk-Krzeska M, Conaway RC, and Conaway JW (2000) Activation of HIF1 α ubiquitination by a reconstituted von Hippel-Lindau (VHL) tumor suppressor complex. *Proc Natl Acad Sci U S A* **97**: 10430-10435
- Kelleher DK, Thews O, and Vaupel P (1998) Regional perfusion and oxygenation of tumors upon methylxanthine derivative administration. *Int J Radiat Oncol Biol Phys* **42**: 861-864
- Kennedy AS, Raleigh JA, Perez GM, Calkins DP, Thrall DE, Novotny DB, and Varia MA (1997) Proliferation and hypoxia in human squamous cell carcinoma of the cervix: first report of combined immunohistochemical assays. *Int J Radiat Oncol Biol Phys* **37**: 897-905
- Kerbel RS, Klement G, Pritchard KI, and Kamen B (2002) Continuous low-dose anti-angiogenic/metronomic chemotherapy: from the research laboratory into the oncology clinic. *Ann Oncol* **13**: 12-15
- Kim JR, Lee SR, Chung HJ, Kim S, Baek SH, Kim JH, and Kim YS (2003) Identification of amyloid β -peptide responsive genes by cDNA microarray technology: involvement of RTP801 in amyloid β -peptide toxicity. *Exp Mol Med* **35**: 403-411
- Kimura H, Braun RD, Ong ET, Hsu R, Secomb TW, Papahadjopoulos D, Hong K, and Dewhirst MW (1996) Fluctuations in red cell flux in tumor microvessels can lead to transient hypoxia and reoxygenation in tumor parenchyma. *Cancer Res* **56**: 5522-5528
- Koch CJ, Evans SM, and Lord EM (1995) Oxygen dependence of cellular uptake of EF5 [2-(2-nitro-1H-imidazol-1-yl)-N-(2,2,3,3,3-pentafluoropropyl)acetamide]: analysis of drug adducts by fluorescent antibodies vs bound radioactivity. *Br J Cancer* **72**: 869-874
- Koch CJ, Hahn SM, Rockwell Jr K, Covey JM, McKenna WG, and Evans SM (2001) Pharmacokinetics of EF5 [2-(2-nitro-1-H-imidazol-1-yl)-N-(2,2,3,3,3-pentafluoropropyl) acetamide] in human patients: implications for hypoxia measurements *in vivo* by 2-nitroimidazoles. *Cancer Chemother Pharmacol* **48**: 177-187
- Koch CJ, Stobbe CC, and Baer KA (1984) Metabolism induced binding of 14C-misonidazole to hypoxic cells: kinetic dependence on oxygen concentration and misonidazole concentration. *Int J Radiat Oncol Biol Phys* **10**: 1327-1331
- Koh WJ, Rasey JS, Evans ML, Grierson JR, Lewellen TK, Graham MM, Krohn KA, and Griffin TW (1992) Imaging of hypoxia in human tumors with [F-18]fluoromisonidazole. *Int J Radiat Oncol Biol Phys* **22**: 199-212
- Kohno M, Hasegawa H, Miyake M, Yamamoto T, and Fujita S (2002) CD151 enhances cell motility and metastasis of cancer cells in the presence of focal adhesion kinase. *Int J Cancer* **97**: 336-343
- Konerding MA, Malkusch W, Klapthor B, van Ackern C, Fait E, Hill SA, Parkins C, Chaplin DJ, Presta M, and Denekamp J (1999) Evidence for characteristic vascular patterns in solid tumours: quantitative studies using corrosion casts. *Br J Cancer* **80**: 724-732

- Koukourakis MI, Giatromanolaki A, Sivridis E, Simopoulos C, Turley H, Talks K, Gatter KC, and Harris AL (2002) Hypoxia-inducible factor (HIF1 α and HIF2 α), angiogenesis, and chemoradiotherapy outcome of squamous cell head-and-neck cancer. *Int J Radiat Oncol Biol Phys* **53**: 1192-1202
- Koukourakis MI, Giatromanolaki A, Sivridis E, Simopoulos K, Pastorek J, Wyckoff CC, Gatter KC, and Harris AL (2001a) Hypoxia-regulated carbonic anhydrase-9 (CA9) relates to poor vascularization and resistance of squamous cell head and neck cancer to chemoradiotherapy. *Clin Cancer Res* **7**: 3399-3403
- Koukourakis MI, Giatromanolaki A, Skarlatos J, Corti L, Blandamura S, Piazza M, Gatter KC, and Harris AL (2001b) Hypoxia inducible factor (HIF-1 α and HIF-2 α) expression in early esophageal cancer and response to photodynamic therapy and radiotherapy. *Cancer Res* **61**: 1830-1832
- Kwock L, Gill M, McMurry HL, Beckman W, Raleigh JA, and Joseph AP (1992) Evaluation of a fluorinated 2-nitroimidazole binding to hypoxic cells in tumor-bearing rats by ¹⁹F magnetic resonance spectroscopy and immunohistochemistry. *Radiat Res* **129**: 71-78
- Lando D, Peet DJ, Gorman JJ, Whelan DA, Whitelaw ML, and Bruick RK (2002a) FIH-1 is an asparaginyl hydroxylase enzyme that regulates the transcriptional activity of hypoxia-inducible factor. *Genes Dev* **16**: 1466-1471
- Lando D, Peet DJ, Whelan DA, Gorman JJ, and Whitelaw ML (2002b) Asparagine hydroxylation of the HIF transactivation domain a hypoxic switch. *Science* **295**: 858-861
- Laughner E, Taghavi P, Chiles K, Mahon PC, and Semenza GL (2001) HER2 (neu) signaling increases the rate of hypoxia-inducible factor 1 α (HIF-1 α) synthesis: novel mechanism for HIF-1-mediated vascular endothelial growth factor expression. *Mol Cell Biol* **21**: 3995-4004
- Lee I, Boucher Y, Demhartner TJ, and Jain RK (1994) Changes in tumour blood flow, oxygenation and interstitial fluid pressure induced by pentoxifylline. *Br J Cancer* **69**: 492-496
- Lee I, Kim JH, Levitt SH, and Song CW (1992) Increases in tumor response by pentoxifylline alone or in combination with nicotinamide. *Int J Radiat Oncol Biol Phys* **22**: 425-429
- Lee I, Levitt SH, and Song CW (1993) Improved tumour oxygenation and radiosensitization by combination with nicotinamide and pentoxifylline. *Int J Radiat Biol* **64**: 237-244
- Lee J, Siemann DW, Koch CJ, and Lord EM (1996) Direct relationship between radiobiological hypoxia in tumors and monoclonal antibody detection of EF5 cellular adducts. *Int J Cancer* **67**: 372-378
- Lee MJ, Kim JY, Suk K, and Park JH (2004) Identification of the hypoxia-inducible factor 1 α -responsive HGTD-P gene as a mediator in the mitochondrial apoptotic pathway. *Mol Cell Biol* **24**: 3918-3927
- Li J, Ding SF, Habib NA, Fermor BF, Wood CB, and Gilmour RS (1994) Partial characterization of a cDNA for human stearyl-CoA desaturase and changes in its mRNA expression in some normal and malignant tissues. *Int J Cancer* **57**: 348-352
- Ling CC, Robinson E, and Shrieve DC (1988) Repair of radiation induced damage--dependence on oxygen and energy status. *Int J Radiat Oncol Biol Phys* **15**: 1179-1186
- Linsenmeier RA and Yancey CM (1987) Improved fabrication of double-barreled recessed cathode O₂ microelectrodes. *J Appl Physiol* **63**: 2554-2557
- Ljungkvist AS, Bussink J, Rijken PF, Raleigh JA, Denekamp J, and Van Der Kogel AJ (2000) Changes in tumor hypoxia measured with a double hypoxic marker technique. *Int J Radiat Oncol Biol Phys* **48**: 1529-1538
- Logsdon CD, Simeone DM, Binkley C, Arumugam T, Greenson JK, Giordano TJ, Misk DE, Kuick R, and Hanash S (2003) Molecular profiling of pancreatic adenocarcinoma and chronic pancreatitis identifies multiple genes differentially regulated in pancreatic cancer. *Cancer Res* **63**: 2649-2657
- Louca JA, Harris AL, Davidson SE, Logue JP, Hunter RD, Wyckoff CC, Pastorek J, Ratcliffe PJ, Stratford IJ, and West CM (2001) Carbonic anhydrase (CA IX) expression, a potential new intrinsic marker of hypoxia: correlations with tumor oxygen measurements and prognosis in locally advanced carcinoma of the cervix. *Cancer Res* **61**: 6394-6399
- Longo N, Yanez-Mo M, Mittelbrunn M, de la Rosa G, Munoz ML, Sanchez-Madrid F, and Sanchez-Mateos P (2001) Regulatory role of tetraspanin CD9 in tumor-endothelial cell interaction during transendothelial invasion of melanoma cells. *Blood* **98**: 3717-3726
- Lord EM, Harwell L, and Koch CJ (1993) Detection of hypoxic cells by monoclonal antibody recognizing 2-nitroimidazole adducts. *Cancer Res* **53**: 5721-5726
- Mahon PC, Hirota K, and Semenza GL (2001) FIH-1: a novel protein that interacts with HIF-1 α and VHL to mediate repression of HIF-1 transcriptional activity. *Genes Dev* **15**: 2675-2686
- Man S, Bocci G, Francia G, Green SK, Jothy S, Hanahan D, Bohlen P, Hicklin DJ, Bergers G, and Kerbel RS (2002) Antitumor effects in mice of low-dose (metronomic) cyclophosphamide administered continuously through the drinking water. *Cancer Res* **62**: 2731-2735
- Masson N, Willam C, Maxwell PH, Pugh CW, and Ratcliffe PJ (2001) Independent function of two destruction domains in hypoxia-inducible factor- α chains activated by prolyl hydroxylation. *EMBO J* **20**: 5197-5206

- Maxwell PH, Wiesener MS, Chang GW, Clifford SC, Vaux EC, Cockman ME, Wykoff CC, Pugh CW, Maher ER, and Ratcliffe PJ (1999) The tumour suppressor protein VHL targets hypoxia-inducible factors for oxygen-dependent proteolysis. *Nature* **399**: 271-275
- Maxwell RJ, Workman P, and Griffiths JR (1989) Demonstration of tumor-selective retention of fluorinated nitroimidazole probes by 19F magnetic resonance spectroscopy *in vivo*. *Int J Radiat Oncol Biol Phys* **16**: 925-929
- McClelland RA, Fuller JR, Seaman NE, Rauth AM, and Battistella R (1984) 2-Hydroxylaminoimidazoles--unstable intermediates in the reduction of 2-nitroimidazoles. *Biochem Pharmacol* **33**: 303-309
- McDonald DM and Baluk P (2002) Significance of blood vessel leakiness in cancer. *Cancer Res* **62**: 5381-5385
- McDonald DM and Foss AJ (2000) Endothelial cells of tumor vessels: abnormal but not absent. *Cancer Metastasis Rev* **19**: 109-120
- Miller GG, Best MW, Franko AJ, Koch CJ, and Raleigh JA (1989) Quantitation of hypoxia in multicellular spheroids by video image analysis. *Int J Radiat Oncol Biol Phys* **16**: 949-952
- Miller GG, Ngan-Lee J, and Chapman JD (1982) Intracellular localization of radioactively labeled misonidazole in EMT-6-tumor cells *in vitro*. *Int J Radiat Oncol Biol Phys* **8**: 741-744
- Minchinton AI, Wendt KR, Clow KA, and Fryer KH (1997) Multilayers of cells growing on a permeable support. An *in vitro* tumour model. *Acta Oncol* **36**: 13-16
- Moore DH, Rouse MB, Massenbueg GS, and Zeman EM (1992) Description of a spheroid model for the study of radiation and chemotherapy effects on hypoxic tumor cell populations. *Gynecol Oncol* **47**: 44-47
- Moreno SN, Mason RP, Muniz RP, Cruz FS, and Docampo R (1983) Generation of free radicals from metronidazole and other nitroimidazoles by *Trichomonas foetus*. *J Biol Chem* **258**: 4051-4054
- Moulder JE and Rockwell S (1984) Hypoxic fractions of solid tumors: experimental techniques, methods of analysis, and a survey of existing data. *Int J Radiat Oncol Biol Phys* **10**: 695-712
- Mousses S, Bubendorf L, Wagner U, Hostetter G, Kononen J, Cornelison R, Goldberger N, Elkahoul AG, Willi N, Koivisto P, Ferhle W, Raffeld M, Sauter G, and Kallioniemi OP (2002) Clinical validation of candidate genes associated with prostate cancer progression in the CWR22 model system using tissue microarrays. *Cancer Res* **62**: 1256-1260
- Murphy BJ, Laderoute KR, Chin RJ, and Sutherland RM (1994) Metallothionein IIA is up-regulated by hypoxia in human A431 squamous carcinoma cells. *Cancer Res* **54**: 5808-5810
- Newell K, Franchi A, Pouyssegur J, and Tannock IF (1993) Studies with glycolysis-deficient cells suggest that production of lactic acid is not the only cause of tumor acidity. *Proc Natl Acad Sci USA* **90**: 1127-1131
- Newman HF, Ward R, Workman P, and Bleehen NM (1988) The multi-dose clinical tolerance and pharmacokinetics of the combined radiosensitizers, Ro 03-8799 (pimonidazole) and SR 2508 (etanidazole). *Int J Radiat Oncol Biol Phys* **15**: 1073-1083
- Noguchi P, Wallace R, Johnson J, Earley EM, O'Brien S, Ferrone S, Pellegrino MA, Mustein J, Needy C, Browne W, and Petricciani J (1979) Characterization of the WIDR: a human colon carcinoma cell line. *In Vitro* **15**: 401-408
- Nordmark M, Alsner J, Keller J, Nielsen OS, Jensen OM, Horsman MR, and Overgaard J (2001) Hypoxia in human soft tissue sarcomas: adverse impact on survival and no association with p53 mutations. *Br J Cancer* **84**: 1070-1075
- Nordmark M, Overgaard M, and Overgaard J (1996) Pretreatment oxygenation predicts radiation response in advanced squamous cell carcinoma of the head and neck. *Radiother Oncol* **41**: 31-39
- Nozue M, Lee I, Yuan F, Teicher BA, Brizel DM, Dewhirst MW, Milross CG, Milas L, Song CW, Thomas CD, Guichard M, Evans SM, Koch CJ, Lord EM, Jain RK, and Suit HD (1997) Interlaboratory variation in oxygen tension measurement by Eppendorf "Histograph" and comparison with hypoxic marker. *J Surg Oncol* **66**: 30-38
- Ntambi JM and Miyazaki M (2004) Regulation of stearoyl-CoA desaturases and role in metabolism. *Prog Lipid Res* **43**: 91-104
- Ohh M, Park CW, Ivan M, Hoffman MA, Kim TY, Huang LE, Pavletich N, Chau V, and Kaelin Jr WG (2000) Ubiquitination of hypoxia-inducible factor requires direct binding to the β -domain of the von Hippel-Lindau protein. *Nat Cell Biol* **2**: 423-427
- Olive PL, Aquino-Parsons C, MacPhail SH, Liao SY, Raleigh JA, Lerman MI, and Stanbridge EJ (2001a) Carbonic anhydrase 9 as an endogenous marker for hypoxic cells in cervical cancer. *Cancer Res* **61**: 8924-8929
- Olive PL, Banath JP, and Aquino-Parsons C (2001b) Measuring hypoxia in solid tumours--is there a gold standard? *Acta Oncol* **40**: 917-923
- Olive PL, Banath JP, and Durand RE (2002) The range of oxygenation in SiHa tumor xenografts. *Radiat Res* **158**: 159-166
- Olive PL, Chaplin DJ, and Durand RE (1985) Pharmacokinetics, binding and distribution of Hoechst 33342 in spheroids and murine tumours. *Br J Cancer* **52**: 739-746

- Olive PL and Durand RE (1983) Fluorescent nitroheterocycles for identifying hypoxic cells. *Cancer Res* **43**: 3276-3280
- Olive PL, Durand RE, Raleigh JA, Luo C, and Aquino-Parsons C (2000) Comparison between the comet assay and pimonidazole binding for measuring tumour hypoxia. *Br J Cancer* **83**: 1525-1531
- Overgaard J and Horsman MR (1996) Modification of hypoxia-induced radioresistance in tumors by the use of oxygen and sensitizers. *Semin Radiat Oncol* **6**: 10-21
- Parle-McDermott A, McWilliam P, Tighe O, Dunican D, and Croke DT (2000) Serial analysis of gene expression identifies putative metastasis-associated transcripts in colon tumour cell lines. *Br J Cancer* **83**: 725-728
- Parliament MB, Wiebe LI, and Franko AJ (1992) Nitroimidazole adducts as markers for tissue hypoxia: mechanistic studies in aerobic normal tissues and tumour cells. *Br J Cancer* **66**: 1103-1108
- Perez-Reyes E, Kalyanaraman B, and Mason RP (1980) The reductive metabolism of metronidazole and ronidazole by aerobic liver microsomes. *Mol Pharmacol* **17**: 239-244
- Pettersen EO and Wang H (1996) Radiation-modifying effect of oxygen in synchronized cells pre-treated with acute or prolonged hypoxia. *Int J Radiat Biol* **70**: 319-326
- Phillips RM, Loadman PM, and Cronin BP (1998) Evaluation of a novel *in vitro* assay for assessing drug penetration into avascular regions of tumours. *Br J Cancer* **77**: 2112-2119
- Pigott KH, Hill SA, Chaplin DJ, and Saunders MI (1996) Microregional fluctuations in perfusion within human tumours detected using laser Doppler flowmetry. *Radiother Oncol* **40**: 45-50
- Pitson G, Fyles A, Milosevic M, Wylie J, Pintilie M, and Hill RP (2001) Tumor size and oxygenation are independent predictors of nodal diseases in patients with cervix cancer. *Int J Radiat Oncol Biol Phys* **51**: 699-703
- Pogue BW, Paulsen KD, O'Hara JA, Wilmot CM, and Swartz HM (2001) Estimation of oxygen distribution in RIF-1 tumors by diffusion model-based interpretation of pimonidazole hypoxia and eppendorf measurements. *Radiat Res* **155**: 15-25
- Porter DA, Krop IE, Nasser S, Sgroi D, Kaelin CM, Marks JR, Riggins GJ, and Polyak K (2001) A SAGE (serial analysis of gene expression) view of breast tumor progression. *Cancer Res* **61**: 5697-5702
- Potter C and Harris AL (2004) Hypoxia inducible carbonic anhydrase IX, marker of tumour hypoxia, survival pathway and therapy target. *Cell Cycle* **3**: 164-167
- Potter CP and Harris AL (2003) Diagnostic, prognostic and therapeutic implications of carbonic anhydrases in cancer. *Br J Cancer* **89**: 2-7
- Prescott DM, Charles HC, Poulson JM, Page RL, Thrall DE, Vujaskovic Z, and Dewhurst MW (2000) The relationship between intracellular and extracellular pH in spontaneous canine tumors. *Clin Cancer Res* **6**: 2501-2505
- Pugh CW, O'Rourke JF, Nagao M, Gleadle JM, and Ratcliffe PJ (1997) Activation of hypoxia-inducible factor-1; definition of regulatory domains within the α subunit. *J Biol Chem* **272**: 11205-11214
- Raleigh JA, Chou SC, Arteel GE, and Horsman MR (1999) Comparisons among pimonidazole binding, oxygen electrode measurements, and radiation response in C3H mouse tumors. *Radiat Res* **151**: 580-589
- Raleigh JA, Chou SC, Bono EL, Thrall DE, and Varia MA (2001) Semiquantitative immunohistochemical analysis for hypoxia in human tumors. *Int J Radiat Oncol Biol Phys* **49**: 569-574
- Raleigh JA, Chou SC, Calkins-Adams DP, Ballenger CA, Novotny DB, and Varia MA (2000) A clinical study of hypoxia and metallothionein protein expression in squamous cell carcinomas. *Clin Cancer Res* **6**: 855-862
- Raleigh JA, Chou SC, Tables L, Suchindran S, Varia MA, and Horsman MR (1998) Relationship of hypoxia to metallothionein expression in murine tumors. *Int J Radiat Oncol Biol Phys* **42**: 727-730
- Raleigh JA, Dewhurst MW, and Thrall DE (1996) Measuring Tumor Hypoxia. *Semin Radiat Oncol* **6**: 37-45
- Raleigh JA, Franko AJ, Koch CJ, and Born JL (1985) Binding of misonidazole to hypoxic cells in monolayer and spheroid culture: evidence that a side-chain label is bound as efficiently as a ring label. *Br J Cancer* **51**: 229-235
- Raleigh JA, Franko AJ, Treiber EO, Lunt JA, and Allen PS (1986) Covalent binding of a fluorinated 2-nitroimidazole to EMT-6 tumors in Balb/C mice: detection by F-19 nuclear magnetic resonance at 2.35 T. *Int J Radiat Oncol Biol Phys* **12**: 1243-1245
- Raleigh JA and Koch CJ (1990) Importance of thiols in the reductive binding of 2-nitroimidazoles to macromolecules. *Biochem Pharmacol* **40**: 2457-2464
- Raleigh JA, LaDine JK, Cline JM, and Thrall DE (1994) An enzyme-linked immunosorbent assay for hypoxia marker binding in tumours. *Br J Cancer* **69**: 66-71
- Raleigh JA, Miller GG, Franko AJ, Koch CJ, Fuciarelli AF, and Kelly DA (1987) Fluorescence immunohistochemical detection of hypoxic cells in spheroids and tumours. *Br J Cancer* **56**: 395-400
- Raleigh JA, Zeman EM, Rathman M, LaDine JK, Cline JM, and Thrall DE (1992) Development of an ELISA for the detection of 2-nitroimidazole hypoxia markers bound to tumor tissue. *Int J Radiat Oncol Biol Phys* **22**: 403-405

- Rasey JS, Grunbaum Z, Krohn K, Nelson N, and Chin L (1985) Comparison of binding of [3H]misonidazole and [14C]misonidazole in multicell spheroids. *Radiat Res* **101**: 473-479
- Rasey JS, Grunbaum Z, Magee S, Nelson NJ, Olive PL, Durand RE, and Krohn KA (1987) Characterization of radiolabeled fluoromisonidazole as a probe for hypoxic cells. *Radiat Res* **111**: 292-304
- Rischin D, Peters L, Hicks R, Hughes P, Fisher R, Hart R, Sexton M, D'Costa I, and von Roemeling R (2001) Phase I trial of concurrent tirapazamine, cisplatin, and radiotherapy in patients with advanced head and neck cancer. *J Clin Oncol* **19**: 535-542
- Roberts JT, Bleehen NM, Workman P, and Walton MI (1984) A phase I study of the hypoxic cell radiosensitizer Ro-03-8799. *Int J Radiat Oncol Biol Phys* **10**: 1755-1758
- Russo J, Hu YF, Silva ID, and Russo IH (2001) Cancer risk related to mammary gland structure and development. *Microsc Res Tech* **52**: 204-223
- Saha S, Sparks AB, Rago C, Akmaev V, Wang CJ, Vogelstein B, Kinzler KW, and Velculescu VE (2002) Using the transcriptome to annotate the genome. *Nat Biotechnol* **20**: 508-512
- Sapirstein LA (1958) Regional blood flow by fractional distribution of indicators. *Am J Physiol* **193**: 161-168
- Sartorelli AC (1988) Therapeutic attack of hypoxic cells of solid tumors: presidential address. *Cancer Res* **48**: 775-778
- Satoh M, Cherian MG, Imura N, and Shimizu H (1994) Modulation of resistance to anticancer drugs by inhibition of metallothionein synthesis. *Cancer Res* **54**: 5255-5257
- Saunders MI, Anderson PJ, Bennett MH, Dische S, Minchinton A, Stratford MR, and Tothill M (1984) The clinical testing of Ro 03-8799--pharmacokinetics, toxicology, tissue and tumor concentrations. *Int J Radiat Oncol Biol Phys* **10**: 1759-1763
- Saunders MI, Dische S, Fermont D, Bishop A, Lenox-Smith I, Allen JG, and Malcolm SL (1982) The radiosensitizer Ro 03-8799 and the concentrations which may be achieved in human tumours: a preliminary study. *Br J Cancer* **46**: 706-710
- Schneiderman G and Goldstick TK (1978) Oxygen electrode design criteria and performance characteristics: recessed cathode. *J Appl Physiol* **45**: 145-154
- Seagroves TN, Ryan HE, Lu H, Wouters BG, Knapp M, Thibault P, Laderoute K, and Johnson RS (2001) Transcription factor HIF-1 is a necessary mediator of the pasteur effect in mammalian cells. *Mol Cell Biol* **21**: 3436-3444
- Secomb TW, Hsu R, Dewhirst MW, Klitzman B, and Gross JF (1993) Analysis of oxygen transport to tumor tissue by microvascular networks. *Int J Radiat Oncol Biol Phys* **25**: 481-489
- Secomb TW, Hsu R, Ong ET, Gross JF, and Dewhirst MW (1995) Analysis of the effects of oxygen supply and demand on hypoxic fraction in tumors. *Acta Oncol* **34**: 313-316
- Seddon BM, Honess DJ, Vojnovic B, Tozer GM, and Workman P (2001) Measurement of tumor oxygenation: *in vivo* comparison of a luminescence fiber-optic sensor and a polarographic electrode in the p22 tumor. *Radiat Res* **155**: 837-846
- Semenza GL (2001) HIF-1 and mechanisms of hypoxia sensing. *Curr Opin Cell Biol* **13**: 167-171
- Semenza GL (2003) Targeting HIF-1 for cancer therapy. *Nat Rev Cancer* **3**: 721-732
- Semenza GL and Wang GL (1992) A nuclear factor induced by hypoxia via de novo protein synthesis binds to the human erythropoietin gene enhancer at a site required for transcriptional activation. *Mol Cell Biol* **12**: 5447-5454
- Shibuya K, Cherian MG, and Satoh M (1997) Sensitivity to radiation treatment and changes in metallothionein synthesis in a transplanted murine tumor. *Radiat Res* **148**: 235-239
- Shoshani T, Faerman A, Mett I, Zelin E, Tenne T, Gorodin S, Moshel Y, Elbaz S, Budanov A, Chajut A, Kalinski H, Kamer I, Rozen A, Mor O, Keshet E, Leshkowitz D, Einat P, Skaliter R, and Feinstein E (2002) Identification of a novel hypoxia-inducible factor 1-responsive gene, RTP801, involved in apoptosis. *Mol Cell Biol* **22**: 2283-2293
- Shrieve DC and Begg AC (1985) Cell cycle kinetics of aerated, hypoxic and re-aerated cells *in vitro* using flow cytometric determination of cellular DNA and incorporated bromodeoxyuridine. *Cell Tissue Kinet* **18**: 641-651
- Shrieve DC and Harris JW (1985) The *in vitro* sensitivity of chronically hypoxic EMT6/SF cells to X-radiation and hypoxic cell radiosensitizers. *Int J Radiat Biol* **48**: 127-138
- Sincock PM, Fitter S, Parton RG, Berndt MC, Gamble JR, and Ashman LK (1999) PETA-3/CD151, a member of the transmembrane 4 superfamily, is localised to the plasma membrane and endocytic system of endothelial cells, associates with multiple integrins and modulates cell function. *J Cell Sci* **112**: 833-844
- Sincock PM, Mayrhofer G, and Ashman LK (1997) Localization of the transmembrane 4 superfamily (TM4SF) member PETA-3 (CD151) in normal human tissues: comparison with CD9, CD63, and $\alpha 5\beta 1$ integrin. *J Histochem Cytochem* **45**: 515-525

- Skroch P, Buchman C, and Karin M (1993) Regulation of human and yeast metallothionein gene transcription by heavy metal ions. *Prog Clin Biol Res* **380**: 113-128
- Song CW, Hasegawa T, Kwon HC, Lyons JC, and Levitt SH (1992) Increase in tumor oxygenation and radiosensitivity caused by pentoxifylline. *Radiat Res* **130**: 205-210
- Song CW, Makepeace CM, Griffin RJ, Hasegawa T, Osborn JL, Choi I-B, and Nah BS (1994) Increase in tumor blood flow by pentoxifylline. *Int J Radiat Oncol Biol Phys* **29**: 433-437
- Spiro IJ, Kennedy KA, Stickler R, and Ling CC (1985) Cellular and molecular repair of X-ray-induced damage: dependence on oxygen tension and nutritional status. *Radiat Res* **101**: 144-155
- Spiro IJ, Rice GC, Durand RE, Stickler R, and Ling CC (1984) Cell killing, radiosensitization and cell cycle redistribution induced by chronic hypoxia. *Int J Radiat Oncol Biol Phys* **10**: 1275-1280
- St Croix B, Rago C, Velculescu VE, Traverso G, Romans KE, Montgomery E, Lal A, Riggins GJ, Lengauer C, Vogelstein B, and Kinzler KW (2000) Genes expressed in human tumor endothelium. *Science* **289**: 1197-1202
- Stone HB, Brown JM, Phillips TL, and Sutherland RM (1993) Oxygen in human tumors: correlations between methods of measurement and response to therapy. Summary of a workshop held November 19-20, 1992, at the National Cancer Institute, Bethesda, Maryland. *Radiat Res* **136**: 422-434
- Sutherland RM (1988) Cell and environment interactions in tumor microregions: the multicell spheroid model. *Science* **240**: 177-184
- Sutherland RM, Ausserer WA, Murphy BJ, and Laderoute KR (1996) Tumor hypoxia and heterogeneity: challenges and opportunities for the future. *Semin Radiat Oncol* **6**: 59-70
- Swinson DE, Jones JL, Richardson D, Wykoff CC, Turley H, Pastorek J, Taub N, Harris AL, and O'Byrne KJ (2003) Carbonic anhydrase IX expression, a novel surrogate marker of tumor hypoxia, is associated with a poor prognosis in non-small-cell lung cancer. *J Clin Oncol* **21**: 473-482
- Tanimoto K, Makino Y, Pereira T, and Poellinger L (2000) Mechanism of regulation of the hypoxia-inducible factor-1 α by the von Hippel-Lindau tumor suppressor protein. *EMBO J* **19**: 4298-4309
- Tannock IF (1968) The relation between cell proliferation and the vascular system in a transplanted mouse mammary tumour. *Br J Cancer* **22**: 258-273
- Tannock IF, Lee CM, Tunggal JK, Cowan DS, and Egorin MJ (2002) Limited penetration of anticancer drugs through tumor tissue: a potential cause of resistance of solid tumors to chemotherapy. *Clin Cancer Res* **8**: 878-884
- Testa JE, Brooks PC, Lin JM, and Quigley JP (1999) Eukaryotic expression cloning with an antimetastatic monoclonal antibody identifies a tetraspanin (PETA-3/CD151) as an effector of human tumor cell migration and metastasis. *Cancer Res* **59**: 3812-3820
- Thomlinson RH and Gray LH (1955) The histological structure of some human lung cancers and the possible implications for radiotherapy. *Br J Cancer* **9**: 539-549
- Thrall DE, Rosner GL, Azuma C, McEntee MC, and Raleigh JA (1997) Hypoxia marker labeling in tumor biopsies: quantification of labeling variation and criteria for biopsy sectioning. *Radiother Oncol* **44**: 171-176
- Tokuhara T, Hasegawa H, Hattori N, Ishida H, Taki T, Tachibana S, Sasaki S, and Miyake M (2001) Clinical significance of CD151 gene expression in non-small cell lung cancer. *Clin Cancer Res* **7**: 4109-4114
- Trotter MJ, Chaplin DJ, Durand RE, and Olive PL (1989) The use of fluorescent probes to identify regions of transient perfusion in murine tumors. *Int J Radiat Oncol Biol Phys* **16**: 931-934
- Trotter MJ, Chaplin DJ, and Olive PL (1991) Possible mechanisms for intermittent blood flow in the murine SCCVII carcinoma. *Int J Radiat Biol* **60**: 139-146
- Turner KJ, Crew JP, Wykoff CC, Watson PH, Poulson R, Pastorek J, Ratcliffe PJ, Cranston D, and Harris AL (2002) The hypoxia-inducible genes VEGF and CA9 are differentially regulated in superficial vs invasive bladder cancer. *Br J Cancer* **86**: 1276-1282
- Urano M, Chen Y, Humm J, Koutcher JA, Zanzonico P, and Ling C (2002) Measurements of tumor tissue oxygen tension using a time-resolved luminescence-based optical oxylite probe: comparison with a paired survival assay. *Radiat Res* **158**: 167-173
- Urtasun RC, Chapman JD, Raleigh JA, Franko AJ, and Koch CJ (1986a) Binding of 3H-misonidazole to solid human tumors as a measure of tumor hypoxia. *Int J Radiat Oncol Biol Phys* **12**: 1263-1267
- Urtasun RC, Koch CJ, Franko AJ, Raleigh JA, and Chapman JD (1986b) A novel technique for measuring human tissue pO₂ at the cellular level. *Br J Cancer* **54**: 453-457
- Van Nueten JM and Vanhoutte PM (1980) Improvement of tissue perfusion with inhibitors of calcium ion influx. *Biochem Pharm* **29**: 479-481
- Van Os-Corby DJ, Koch CJ, and Chapman JD (1987) Is misonidazole binding to mouse tissues a measure of cellular pO₂? *Biochem Pharmacol* **36**: 3487-3494
- Varghese AJ (1983) Glutathione conjugates of misonidazole. *Biochem Biophys Res Commun* **112**: 1013-1020

- Varghese AJ, Gulyas S, and Mohindra JK (1976) Hypoxia-dependent reduction of 1-(2-nitro-1-imidazolyl)-3-methoxy-2-propanol by Chinese hamster ovary cells and KHT tumor cells *in vitro* and *in vivo*. *Cancer Res* **36**: 3761-3765
- Varghese AJ and Whitmore GF (1980) Binding to cellular macromolecules as a possible mechanism for the cytotoxicity of misonidazole. *Cancer Res* **40**: 2165-2169
- Varia MA, Calkins-Adams DP, Rinker LH, Kennedy AS, Novotny DB, Fowler Jr WC, and Raleigh JA (1998) Pimonidazole: a novel hypoxia marker for complementary study of tumor hypoxia and cell proliferation in cervical carcinoma. *Gynecol Oncol* **71**: 270-277
- Vaupel P, Kallinowski F, and Okunieff P (1989) Blood flow, oxygen and nutrient supply, and metabolic microenvironment of human tumors: a review. *Cancer Res* **49**: 6449-6465
- Vaupel P, Schlenger K, Knoop C, and Hockel M (1991) Oxygenation of human tumors: evaluation of tissue oxygen distribution in breast cancers by computerized O₂ tension measurements. *Cancer Res* **51**: 3316-3322
- Velculescu VE, Zhang L, Vogelstein B, and Kinzler KW (1995) Serial analysis of gene expression. *Science* **270**: 484-487
- von Pawel J, von Roemeling R, Gatzemeier U, Boyer M, Elisson LO, Clark P, Talbot D, Rey A, Butler TW, Hirsh V, Olver I, Bergman B, Ayoub J, Richardson G, Dunlop D, Arcenas A, Vescio R, Viallet J, and Treat J (2000) Tirapazamine plus cisplatin versus cisplatin in advanced non-small-cell lung cancer: A report of the international CATAPULT I study group. Cisplatin and tirapazamine in subjects with advanced previously untreated non-small-cell lung tumors. *J Clin Oncol* **18**: 1351-1359
- Vordermark D and Brown JM (2003) Evaluation of hypoxia-inducible factor-1 α (HIF-1 α) as an intrinsic marker of tumor hypoxia in U87 MG human glioblastoma: *in vitro* and xenograft studies. *Int J Radiat Oncol Biol Phys* **56**: 1184-1193
- Vordermark D, Katzer A, Baier K, Kraft P, and Flentje M (2004) Cell type-specific association of hypoxia-inducible factor-1 α (HIF-1 α) protein accumulation and radiobiologic tumor hypoxia. *Int J Radiat Oncol Biol Phys* **58**: 1242-1250
- Vordermark D, Menke D, and Brown JM (2003) Similar radiation sensitivities of acutely and chronically hypoxic cells in HT 1080 fibrosarcoma xenografts. *Radiat Res* **159**: 94-101
- Vukovic V, Haugland HK, Nicklee T, Morrison AJ, and Hedley DW (2001) Hypoxia-inducible factor-1 α is an intrinsic marker for hypoxia in cervical cancer xenografts. *Cancer Res* **61**: 7394-7398
- Walton MI, Bleehen NM, and Workman P (1985) The reversible N-oxidation of the nitroimidazole radiosensitizer Ro 03-8799. *Biochem Pharmacol* **34**: 3939-3940
- Walton MI, Bleehen NM, and Workman P (1989) Effects of localised tumour hyperthermia on pimonidazole (Ro 03-8799) pharmacokinetics in mice. *Br J Cancer* **59**: 667-673
- Wang GL, Jiang BH, Rue EA, and Semenza GL (1995) Hypoxia-inducible factor 1 is a basic-helix-loop-helix-PAS heterodimer regulated by cellular O₂ tension. *Proc Natl Acad Sci U S A* **92**: 5510-5514
- Watts ME, Dennis MF, and Roberts IJ (1990) Radiosensitization by misonidazole, pimonidazole and azomycin and intracellular uptake in human tumour cell lines. *Int J Radiat Biol* **57**: 361-372
- Whalen WJ, Riley J, and Nair P (1967) A microelectrode for measuring intracellular pO₂. *J Appl Physiol* **23**: 798-801
- Williams KJ, Telfer BA, Airley RE, Peters HP, Sheridan MR, van der Kogel AJ, Harris AL, and Stratford IJ (2002) A protective role for HIF-1 in response to redox manipulation and glucose deprivation: implications for tumorigenesis. *Oncogene* **21**: 282-290
- Williams MV, Denekamp J, Minchinton AI, and Stratford MR (1982) *In vivo* assessment of basic 2-nitroimidazole radiosensitizers. *Br J Cancer* **46**: 127-137
- Woods ML, Koch CJ, and Lord EM (1996) Detection of individual hypoxic cells in multicellular spheroids by flow cytometry using the 2-nitroimidazole, EF5, and monoclonal antibodies. *Int J Radiat Oncol Biol Phys* **34**: 93-101
- Wouters BG and Brown JM (1997) Cells at intermediate oxygen levels can be more important than the "hypoxic fraction" in determining tumor response to fractionated radiotherapy. *Radiat Res* **147**: 541-550
- Wykoff CC, Beasley NJ, Watson PH, Turner KJ, Pastorek J, Sibtain A, Wilson GD, Turley H, Talks KL, Maxwell PH, Pugh CW, Ratcliffe PJ, and Harris AL (2000) Hypoxia-inducible expression of tumor-associated carbonic anhydrases. *Cancer Res* **60**: 7075-7083
- Yamagata M, Hasuda K, Stamato T, and Tannock IF (1998) The contribution of lactic acid to acidification of tumours: studies of variant cells lacking lactate dehydrogenase. *Br J Cancer* **77**: 1726-1731
- Yauch RL, Berditchevski F, Harler MB, Reichner J, and Hemler ME (1998) Highly stoichiometric, stable, and specific association of integrin α 3 β 1 with CD151 provides a major link to phosphatidylinositol 4-kinase, and may regulate cell migration. *Mol Biol Cell* **9**: 2751-2765
- Young WK, Vojnovic B, and Wardman P (1996) Measurement of oxygen tension in tumours by time-resolved fluorescence. *Br J Cancer Suppl* **27**: S256-259

- Yu F, White SB, Zhao Q, and Lee FS (2001) HIF-1 α binding to VHL is regulated by stimulus-sensitive proline hydroxylation. *Proc Natl Acad Sci U S A* **98**: 9630-9635
- Zanelli GD and Fowler JF (1974) The measurement of blood perfusion in experimental tumors by uptake of ⁸⁶Rb. *Cancer Res* **34**: 1451-1456
- Zeman EM, Brown JM, Lemmon MJ, Hirst VK, and Lee WW (1986) SR-4233: a new bioreductive agent with high selective toxicity for hypoxic mammalian cells. *Int J Radiat Oncol Biol Phys* **12**: 1239-1242
- Zhang L, Zhou W, Velculescu VE, Kern SE, Hruban RH, Hamilton SR, Vogelstein B, and Kinzler KW (1997) Gene expression profiles in normal and cancer cells. *Science* **276**: 1268-1272
- Zhong H, Chiles K, Feldser D, Laughner E, Hanrahan C, Georgescu MM, Simons JW, and Semenza GL (2000) Modulation of hypoxia-inducible factor 1 α expression by the epidermal growth factor/phosphatidylinositol 3-kinase/PTEN/AKT/FRAP pathway in human prostate cancer cells: implications for tumor angiogenesis and therapeutics. *Cancer Res* **60**: 1541-1545
- Zolzer F and Streffer C (2002) Increased radiosensitivity with chronic hypoxia in four human tumor cell lines. *Int J Radiat Oncol Biol Phys* **54**: 910-920